2021

Ionic dysregulation in white matter damage

Bulman, Christopher

Copyright Statement:

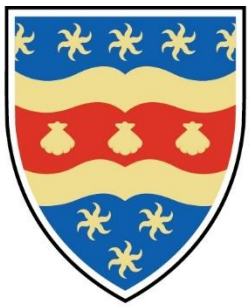

UNIVERSITY OF PLYMOUTH

Ionic dysregulation in white matter damage

By

CHRISTOPHER DAVID BULMAN

A thesis submitted to the University of Plymouth in partial fulfilment for the degree of

DOCTOR OF PHILOSOPHY

Peninsula School of Medicine and Dentistry

March 2021

Acknowledgements:

I would like to thank my supervisor, Prof. Bob Fern, for his guidance and support throughout my research. Thanks also go to all the members of the Fern lab, particularly Drs. Daniel Bloch Hansen, Angelo da Rosa, Sean Doyle and Sarah Ellwood for teaching and advising on lab skills. Thank you to Waldemar Woznica and the Biological Services Unit staff for care of the animals used in my studies.

I am grateful to my friends in the lab for providing much needed entertainment on days of frustration. Thank you to my parents, Steve and Angela, for the love and support throughout this process.

Author's Declaration:

At no time during the registration for the degree of Doctor of Philosophy has the author been registered for any other University award without prior agreement of the Doctoral College Quality Sub-Committee.

Work submitted for this research degree at the University of Plymouth has not formed part of any other degree either at the University of Plymouth or at another establishment.

This study was financed with the aid of a studentship from PUPSMD.

Presentations at conferences:

Oral presentation at the Annual Research Event for Faculty of Medicine & Dentistry, University of Plymouth, 2018.

Poster presentations at the Annual Research Event for Faculty of Medicine & Dentistry, University of Plymouth, 2017 and 2019, and at XIV European Meeting on Glial Cells in Health and Disease.

Word count of main body of thesis: 43,658

Signed:

Date:

Abstract:

Ionic dysregulation in white matter damage

Christopher David Bulman

White matter damage can occur in a variety of neurological diseases where it contributes significantly to impairment of brain function. Dysregulation of ion gradients across membranes is a common phenomenon across many diseases and can be damaging due to increased metabolic demand, oedema and activation of destructive enzyme cascades. Breakdown of ionic gradients can occur under many circumstances. For example, loss of energy supply to ion pumps causes disruption early in stroke progression. Activation of ion channels through voltage or ligand gating contributes greatly to complications such as intracellular calcium overload in many diseases.

This thesis investigated the contribution of different mechanisms of ionic alterations to white matter damage in ischaemic stroke and multiple sclerosis as well as to establish potential treatment options. Particular attention was paid to consequences of glutamate receptor activity. Using the oxygen glucose deprivation model of ischaemia, in the mouse brain slice, it was found that ischaemia-induced potassium release is greater in cortical grey than in corpus callosum white matter. This distinction is dependent on release of vesicular glutamate, as demonstrated by abolition by calcium free media and glutamate receptor antagonists. Variation of ischaemia-induced acidification of grey and white matter was also investigated but no difference between the two tissues was found.

A new acute model of demyelination was established, using direct application of cuprizone to the isolated mouse optic nerve, and protection afforded by glutamate receptor antagonists was determined. Antagonism of AMPA and NMDA receptors acted in synergy to provide greater protection than block of each alone. This effect may allow treatment at lower concentrations to limit adverse side effects. When applied separately, NMDA receptor antagonists provided more protection than AMPA receptor antagonists, suggesting this channel contributed more to the injury progression. The same combination of glutamate antagonists was then investigated in the OGD model of ischaemic stroke but provided no more protection than AMPA receptor antagonist alone.

Table of Contents

List of Figures:

List of Tables:

List of abbreviations:

$[K^+]o$ – extracellular potassium concentration

aCSF – artificial cerebrospinal fluid

AD – anoxic depolarisation

ADP – adenosine diphosphate

AE3 – Anion exchanger 3

AMPA – α-amino-3-hydroxy-5-methyl-4-isoxazolepropionic acid

AMPAR – AMPA receptor

ANOVA – analysis of variance

ASIC – acid sensing ion channel

ATP – adenosine triphosphate

BBB – blood brain barrier

BCS - Bathocuproinedisulfonic acid

BDNF – brain-derived neurotrophic factor

BSK – brain slice keeper

CAE - cuprizone Autoimmune Encephalitis

CAP – compound action potential

CC – corpus callosum

CCAo – common carotid artery occlusion

CICR – calcium induced calcium release

CNP - 2',3'-cyclic nucleotide 3'-phosphodiesterase

CNS – central nervous system

CP 465022 - 3-(2-Chlorophenyl)-2-[2-[6-[(diethylamino)methyl]-2-pyridinyl]ethenyl]-6-fluoro-4(3H)-quinazolinone hydrochloride

Cx43 – connexin 43

D-AP5 - D-2-Amino-5-phosphopentanoic acid

DMSO – dimethyl sulfoxide

EAAT – excitatory amino acid transporter

EAE – experimental autoimmune encephalomyelitis

EGTA – ethylene glycol-bis(β-aminoethyl ether)-N,N,N',N'-tetraacetic acid

E_K – potassium reversal potential

E_{Na} – sodium reversal potential

EPSP – excitatory post-synaptic potential

FDA – food and drug administration

GABA - gamma-aminobutyric acid

GFAP – glial fibrillary acidic protein

GFP – green fluorescent protein

GLUT1 – Glucose transporter 1

GM – grey matter

HEPES – 4-(2-hydroxyethyl)-1-piperazineethanesulfonic acid

IC_{50} – half maximal inhibitory concentration

IP_3 – inositol trisphosphate

ISM – ion-sensitive microelectrode

K2P – Two-pore-domain potassium channel

KCC2 – potassium-chloride cotransporter

K_{ir} – inward rectifying potassium channel

K_v – voltage gated potassium channel

MAG – myelin associated glycoprotein

MAPK – mitogen-activated protein kinase

MBP – myelin basic protein

MCAo – middle cerebral artery occlusion

MCA-CCAo – middle cerebral artery and common carotid artery occlusion

MCT – monocarboxylase transporters

MK-801 – (5S,10R)-(+)-5-methyl-10,11-dihydro-5H-dibenzo[a,d]cyclohepten5,10-imine maleate

MON – mouse optic nerve

MS – multiple sclerosis

NAD+ - nicotinamide adenine dinucleotide

Na_V – voltage gated sodium channel

NBQX – 2,3-dioxo-6-nitro-1,2,3.4-tetrahydrobenzo[*f*]quinoxaline-7-sulfonamide

NCBT – Sodium-coupled bicarbonate transporter

NCX – Na+/Ca2+ exchanger

NGF – nerve growth factor

NHE – sodium hydrogen exchanger

NKCC1 – sodium-potassium-chloride cotransporter 1

NMDA – N-methyl-d-aspartic acid

NMDAR – NMDA receptor

OGD – oxygen/glucose deprivation

OPC – oligodendrocyte precursor cell

PAD – peptidyl arginine deiminase

PBS – phosphate buffered saline

PFA – paraformaldehyde

pH_i – intracellular pH

pH_o – extracellular pH

PIPES – piperazine-N,N'-bis(2-ethanesulfonic acid)

PLC – phospholipase C

PLP – proteolipid protein

PNS – peripheral nervous system

PPMS – primary-progressive multiple sclerosis

PrP^C – cellular prion protein

PrP^{Sc} – scrapie prion protein

QNZ46 – 4-[6-methoxy-2-[(1*E*)-2-(3-nitrophenyl)ethenyl]-4-oxo-3(4*H*)quinazolinyl]benzoic acid

RRMS – relapse-remission multiple sclerosis

TEA – Tetraethylammonium

TIA – transient ischaemic attack

TMA^+ – tetramethylammonium

TMSDMA - N,N-dimethyltrimethylsilylamine

TNF-α – tumour necrosis factor-α

TTC - 2,3,5-triphenyltetrazolium chloride

TTX - tetrodotoxin

V-ATPase – vesicular ATPase

VGCC – voltage gated calcium channel

VGSC – voltage gated sodium channel

WM – white matter

Xc^- - cysteine/glutamate antiporter

Chapter 1:

Introduction

The mammalian brain is composed of two different tissue types with highly distinct structure and function. Grey matter is the tissue containing neuronal cell bodies, short axons and synaptic connections which process synaptic input during interneuronal communication. White matter contains very few neuronal cell bodies and instead comprises of myelinated and unmyelinated nerve fibres essential for transmitting signals between grey matter nuclei and throughout the body. Traditionally, white matter has received less research focus. This is likely due to lack of neurons but also the small proportion of white matter in rodent preclinical models, at around 14% of brain volume, meaning protection will afford less behavioural benefits. However, in humans, white matter occupies close to 50% of the brain and, consequently plays a greater role in human pathology (Goldberg & Ransom, 2003). Therefore, this thesis will focus on mechanisms involved in white matter injury.

1.1. White Matter components

1.1.1. Axons

Axons are long processes, extending from the neuronal cell body, which carry electrical signals for communication. While axons are not exclusive to white matter, they are the major constituent of this tissue. Axons in grey matter tend to be short as they convey signals between nearby neurons as well as to and from white matter tracts (Wen & Chklovskii, 2005). In contrast, axons in the white matter can extend long distances to their effector regions, such as those in the corticospinal tract; these originate in the cerebral cortex and can project up to 1m to the end of the spinal cord, in humans (Blackstone, O'Kane & Reid, 2011).

As cellular components, axons contain a variety of organelles, specialised for axonal function. The cytoskeleton is vital for structural integrity. Actin filaments are closely associated with the axolemma providing a supportive role and allowing axoplasmic transport (Letourneau, 2009). Neurofilaments and microtubules both run longitudinally along the axons, neurofilaments providing structure, while microtubules allow passage of transport proteins and associated organelles (Dale & Garcia, 2012). Mitochondria are abundant within axons and can be transported in either direction along microtubules. These organelles occupy approximately 6% of the myelinated axon (Zambonin *et al.*, 2011). They are oblong in shape and lie longitudinally along the axon (Hollenbeck & Saxton, 2005). Mitochondria are transported along the axon and are fairly evenly distributed, though appear to be sparse at the nodes of Ranvier (Edgar *et al.*, 2008; Perge *et al.*, 2009). However, increase in axonal electrical causes mitochondrial transport to slow in the nodal and paranodal region and increases size of stationary sites for mitochondria, demonstrating a dynamic energy supply (Ohno *et al.*, 2011).

Axons exist in a variety of diameters, from 0.16µm to 9µm in human cortical white matter (Liewald *et al.*, 2014). This dimension is fairly consistent throughout the length of the axon (Friede & Samorajski, 1970). Axonal diameter is highly relevant for function as a wider axon will carry a current with far greater velocity than that of a narrow axon (see section 1.2.4 for detail on this relationship). Diameter is dependent on the number of neurofilaments. Furthermore, diameter is the main determinant of whether an axon is myelinated by oligodendrocyte processes (Hirano & Llena, 1995).

1.1.2. Myelin

Myelin is a good electrical insulator, produced by oligodendrocytes, that ensheathes axons in the vertebrate CNS, in a segmental manner. Between each myelin segment is a

gap known as the node of Ranvier. Myelination functions to greatly increase the conduction velocity of an axon as well as improve metabolic efficiency (see section 1.2.5 for detail) (Trapp & Kidd, 2004). As a result, myelinated axons have a far lesser density of mitochondria compared to unmyelinated counterparts (Andrews *et al.*, 2006).

The myelin sheath forms from a thin sheet of cytoplasm encompassed by lipid membrane that extends from an oligodendrocyte process (Edgar & Griffiths, 2014). The distal end of the sheet has a greater volume of cytoplasm and lines up with an axon to form a ridge. The sheet then forms consecutive wraps around the axon that are densely compacted until the outer sheet which is also more voluminous with cytoplasm. Due to the dense compaction of membranes, mature myelin is highly lipid-rich which produces a high electrical resistance and low capacitance. The inner wrap of myelin is slightly separated from the axon by the periaxonal space, which is usually just 15nm (Peters, 1966). The paranodal edges of the sheet are tightly associated with the axon, in a sequential fashion for each wrap, so as to electrically isolate the periaxonal space from the extracellular space of the nodes. The density of membrane packing at the paranodal ends, known as paranodal loops, is reduced allowing increase in cytoplasmic volume. As a result, the paranodal loops and the inner and outer wrap of myelin are known as non-compact myelin while the main body of myelin wraps is called compact myelin.

Myelin is mostly made of three lipid constituents: cerebrosides, phospholipids and steroids (Wolman, 1968). Together, these make up 70% of the mass of myelin, excluding water. These lipids are vital for the formation and maintenance of the myelin sheath and of the correct structure of the paranodal region (Coetzee *et al.*, 1996; Saher *et al.*, 2005). The remaining mass is composed of proteins vital for myelin function (fig. 1.). Proteolipid protein (PLP) and myelin basic protein (MBP) are both essential for maintaining

compaction of myelin wraps (Duncan, Hammang & Trapp, 1987; Laule *et al.*, 2007; Trapp & Kidd, 2004). PLP binds to cholesterol on the extracellular membrane layer in order to hold sequential wraps together. MBP is located in the intracellular space of compact myelin to ensure the sheet is kept tightly associated. The enzyme 2',3'-cyclic nucleotide 3'-phosphodiesterase (CNP) is responsible for the formation of non-compact myelin and its deletion results in a swollen inner wrap of myelin (Lappe-Siefke *et al.*, 2003). It also plays a role in axonal maintenance alongside myelin-associated glycoprotein (MAG) (Fruttiger *et al.*, 1995; Rasband *et al.*, 2005).

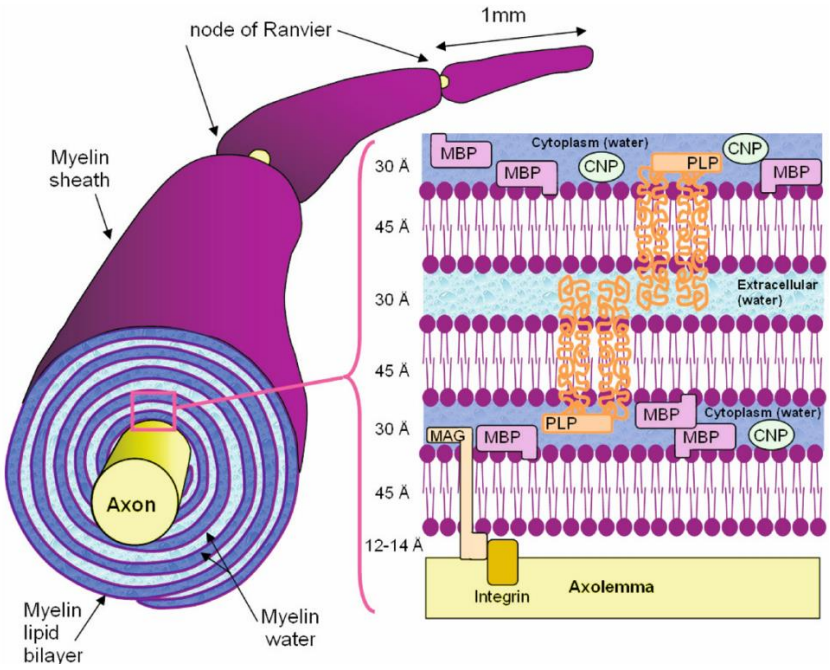

Figure 1. 1. Arrangement of myelin proteins.

Sequential wraps of myelin are held together by PLP which spans the extracellular space to bind cholesterol on the adjacent membrane. The cytoplasm of myelin is bound tight by interactions of intracellular MBP. MAG ensures close coupling on the inner myelin wrap and the axolemma via binding with integrin. CNP is vital for maintenance of myelin, particularly non-compact myelin. Taken from (Laule *et al.*, 2007).

1.1.3. Oligodendrocyte Precursor Cells (OPC)

OPCs, a form of Neuron-glial antigen 2 (NG2) positive cells, exist throughout the CNS, though at greater density within white matter (Dawson *et al.*, 2003). They are the main dividing cells within the brain and are able to differentiate into protoplasmic astrocytes, though more commonly will differentiate to form oligodendrocytes (Zhu, Bergles & Nishiyama, 2008). OPCs consist of an elongated cell body and project many processes radially, some of which extend to the nodes of Ranvier (Butt *et al.*, 1999). These processes form a territory of which there is no overlap with other OPC processes.

OPCs are essential for myelin remodelling. This occurs when a mature oligodendrocyte naturally undergoes death and an OPC will differentiate and replace the lost myelin to maintain proper function of white matter tracts (Rivers *et al.*, 2008). Adult-born oligodendrocytes can also intercalate with existing myelin sheaths, resulting in shorter but increased quantity of internodes, which can cause adaptive changes to conduction (Young *et al.*, 2013). Furthermore, increased neuronal activity within a circuit may act to drive OPC differentiation and myelin production in previously unmyelinated axons (Gibson *et al.*, 2014).

1.1.4. Oligodendrocytes

Oligodendrocytes are the myelinating cells of the CNS. While their PNS counterpart, Schwann cells, will produce one myelin sheath on one axon, oligodendrocytes may ensheath upwards of 50 different axons (Butt & Ransom, 1989; Chong *et al.*, 2012; Ransom, Butt & Black, 1991). Similar to OPCs, oligodendrocytes are found throughout the CNS but in far greater density within the white matter (Edgar & Griffiths, 2014). Oligodendrocytes have a small cell body which consists mostly of a large nucleus with

only a thin layer of surrounding cytoplasm, as reviewed by (Karasek, Swiltoslawski & Zieliniska, 2004).

Early in differentiation, oligodendrocytes increase in complexity and ramification of processes which are guided by growth cone-like structures, extending to pre-myelinated axons (Fox *et al.*, 2006). Once contacted, the process expands laterally to form the inner tongue of the myelin sheath followed by sequential wraps. While the internodes of an individual axon will be very similar in length and thickness, an oligodendrocyte that contacts many different axons can create myelin sheaths of very different dimension (Almeida *et al.*, 2011; Butt, Ibrahim & Berry, 1997).

The cytoskeleton of the oligodendrocyte is formed by a highly dynamic network of microtubules and F-actin microfilaments (Bauer, Richter-Landsberg & Ffrench-Constant, 2009). During process extension, the growth cone-like structure is rich in f-actin with some splayed microtubules interspersed and in greater concentration behind the f-actin (Rumsby *et al.*, 2003). The process body is formed of a dense microtubule arrangement with high acetylation for stability. During myelin expansion, f-actin concentrates to the periphery of the sheet in the non-compact myelin areas, whereas, microtubules are dispersed in dense strands through the main body of myelin (Dyer & Benjamins, 1989a; Dyer & Benjamins, 1989b). However, upon maturation and compaction of the internode, compact myelin loses nearly all of its cytoskeletal structures.

Oligodendrocytes also appear to be involved in the metabolic support of axons by provision of lactate (Butt, Papanikolaou & Rivera, 2019; Lee *et al.*, 2012). Lactate is produced in the oligodendrocyte and released into the periaxonal space through the monocarboxylate transporter, MCT1 (Saab, Tzvetanova & Nave, 2013). Subsequent

uptake into the axon is via MCT2. The activity dependency of this process is explored in section 1.3.3.

1.1.5. Astrocytes

Astrocytes in the white matter are mainly of the fibrous type, as opposed to the protoplasmic astrocytes of the grey matter (Lundgaard *et al.*, 2014). Fibrous astrocytes produce many processes that form contacts with a variety of destinations. Many processes will contact processes from adjacent astrocytes to form astrocyte sheets which partition axons into bundles (Sun *et al.*, 2009). Others will extend to the nodes of Ranvier on nearby axons where they maintain homeostasis as well as modulate axonal activity (Butt, Duncan & Berry, 1994). Astrocyte process end-feet also project to the vasculature where they form the tight blood brain barrier (BBB) and absorb blood nutrients to direct to the cell body. A similar structure is formed by astrocyte end-feet at the parenchymal basal lamina in the form of the glial limitans (Vaughn & Peters, 1967). These processes have very few microtubules and are, instead, dense with glial filaments. Contacts between processes of neighbouring astrocytes or oligodendrocytes are connected by gap junctions, allowing selective passage of ions and other molecules (Abrams & Scherer, 2012). This capability is essential for communication within the astrocyte syncytium via calcium waves as well as dispersion of high concentration of potassium caused by membrane depolarisation (see section 3.1.4).

Astrocyte cytoplasm has a high concentration of glycogen granules. During periods of hypoglycaemia or intense neuronal activity, astrocytes will metabolise the glycogen to form lactate, which may then be transported to axons (Pellerin & Magistretti, 2012). Axons have no glycogen stores and therefore, the supply of lactate allows continued

aerobic respiration when available glucose is insufficient (a similar function is performed by myelin and detailed in section 1.3.3).

Astrocytes are also a fundamental component of the brain's immune system. Upon insult, astrocytes become reactive, increasing in volume and thickening of processes (Norton *et al.*, 1992). Production of glial fibrillary acidic protein (GFAP) is upregulated and cytoskeletal filaments are reduced in density. Reactive astrocytes play a key role in modulating the inflammatory environment of the brain. They are capable of producing a pro- or anti-inflammatory response in microglia depending on location and severity of lesion and time after insult (Rothhammer & Quintana, 2015). Reactive astrocytes will also form a glial scar surrounding an insult; this acts as a physical and chemical barrier to escape of immune cells and infectious agents but also to axonal regeneration.

1.1.6. Microglia

Microglia are the resident immune cells of the CNS, infiltrating from the yolk sac during development; all microglia in the adult CNS derive from those original cells by self-renewal (Ginhoux *et al.*, 2010). In the human CNS, microglia are in greater abundance in the white matter than the grey matter (Mittelbronn *et al.*, 2001). However, this proportion varies between species and is not the case in rodent models.

Microglia are small, elongated cells with very little cytoplasm (Mori & Leblond, 1969). They protrude a network of thin processes with highly complex ramification. These processes are constantly extending and retracting in order to monitor their local environment (Nimmerjahn, Kirchhoff & Helmchen, 2005). In the white matter, the majority of these processes protrude parallel to axon direction (Mori & Leblond, 1969). Processes from neighbouring microglia contact and form gap junctions and hemichannels to create a syncytium similar to that of astrocytes, though the exact

function of this network is yet to be elucidated (Gajardo-Gomez, Labra & Orellana, 2016). Microglia perform a phagocytic function within the CNS. They are able to sense cell debris or markers of dying cells or even tumour cells and act to engulf them (Sierra *et al.*, 2013).

Upon insult to the CNS, microglia undergo a morphological change as they become activated. The cells become larger and the processes lose complexity as they become thicker (Hanisch & Kettenmann, 2007). Proliferation is accelerated to increase number of microglia at the active site as well as release of chemical signals that encourage the migration of nearby microglia to the site (Garden & Moller, 2006). Activated microglia also promote infiltration of peripheral immune cells into the CNS.

1.2. Action Potentials

The primary function of white matter tracts is to propagate action potentials along axons to enable interneuronal communication between different CNS regions and with the periphery. An action potential is a rapid shift and re-establishment of membrane potential caused by flow of electrically charged ions through transmembrane channels. In order for the axonal membrane to be excitable homeostasis of ion concentrations must be maintained with tight control.

1.2.1. Resting potential

The resting potential of a cell is dependent on the relative concentrations of charged particles in the cytoplasm compared to the extracellular space. Across the neuronal membrane, potassium ions are more concentrated in the intracellular compartment compared to extracellular (Wright, 2004). Conversely sodium and chloride ions are at a greater concentration outside the cell compared to within. As the resting cell membrane is almost exclusively permeable to potassium ions, the resting potential sits close to the reversal potential for potassium. The reversal potential of potassium (E_K) is the potential difference at which the electrical gradient becomes sufficient to overcome the flow of K^+ down the concentration gradient out of the cell (Feher, 2017). Consequently, changes in extracellular potassium will have a profound effect on membrane potential. The E_K in neurons is approximately -90mV; however, the resting potential is around -60mV. This is because the membrane is very partially permeable to sodium, which has a reversal potential (E_{Na}) of around +60mV in mammalian neurons. In glial cells, which do not carry action potentials, the resting membrane potential is generally more negative than neurons at around -80 to -90mV (Verkhratsky & Butt, 2013). This is largely due to the abundance of inwardly rectifying potassium channels, K_{ir}, as reviewed in (Butt & Kalsi,

2006). However, there is a degree of heterogeneity in the resting membrane potential of astrocytes, which has been found to range from -82 to -22mV in one study (McKhann, D'Ambrosio & Janigro, 1997).

1.2.2. Ion permeability

As the permeability of the membrane to an ion dictates how much influence this ion will have on the membrane potential, the gating of ion channels can profoundly change the membrane potential. Opening of sodium channels will cause an increase in membrane potential as positive sodium ions enter the cell along their electro-chemical gradient and bring the membrane potential closer to the E_{Na} of ~+60mV. Opening of potassium channels causes hyperpolarisation of the membrane as the permeability of K^+ increases and the net flow of positive ions leaving the cell is accentuated. Opening of non-specific cation channels when the membrane is at rest will cause an increase in the membrane potential. This is because K^+ will leave the cell and Na^+ will enter the cell, causing a neutral exchange and bringing the membrane potential closer to 0mV. In the mature neuron, opening of chloride channels will cause hyperpolarisation of the membrane as negatively charged Cl^- enter the cell. In contrast, in the immature neuron, lack of chloride extrusion by the K^+-Cl^- cotransporter KCC2 results in an accumulation of intracellular chloride (Wang *et al.*, 2002; Watanabe & Fukuda, 2015). Consequently, opening of chloride channels in the developing nervous system causes depolarisation of neuronal membranes.

1.2.3. Voltage gated ion channels in action potentials

An action potential is generated at the axon hillock, which is the thickening of the axon as it joins the neuronal cell body (Palmer & Stuart, 2006). At this point, excitatory post synaptic potentials (EPSPs), generated by synaptic input from other neurons, can

summate to cause a depolarisation of the cell membrane. If this depolarisation is sufficient to surpass a threshold, α-helices in the voltage gated sodium channels will shift causing the channel to undergo conformational change and open (Keynes & Elinder, 1999). Sodium ions are driven into the cell by a combination of concentration gradient and electrical gradient, resulting in a surge of Na^+ entry and consequent depolarisation of the membrane.

As the membrane potential approaches E_{Na}, the drive for entry on sodium into the cell diminishes. Combined with the delayed opening of voltage gated potassium channels, the membrane potential never reaches E_{Na}. Sustained activity of the voltage gated sodium channel will cause the channel-inactivating segment to enter the pore and prevent further passage of ions (Vassilev, Scheuer & Catterall, 1988). This will remain in place until membrane repolarisation and for a short duration after. Permeability to K^+ increases following activation of voltage gated potassium channels causing a delayed efflux of K^+ and a consequent repolarisation and hyperpolarisation of the membrane. This hyperpolarisation is essential for setting the refractory period of an action potential where another cannot be initiated, as well as preventing backwards propagation (Elmslie, 2019). Voltage gated potassium channels will remain open until membrane polarisation is restored. Inactivation of sodium channels and persistence of potassium channels means that, under physiological conditions, depolarisation cannot be sustained which would cause signal block.

1.2.4. Passive action potential propagation

Depolarisation and accumulation of positive charge within the cytosol of the axon causes a repellent force on cations (fig. 1.2), resulting in a spread along the axon (Lodish, 2000). This increase in intracellular positive ions in areas adjacent to the action potential causes

a slight depolarisation in surrounding membrane. Consequently, the threshold for activation of voltage gated sodium channels is met and another action potential is initiated downstream of the previous action potential. However, upstream, hyperpolarisation of the membrane means that the passive spread of ions is likely to not cause threshold depolarisation and inactivation of the sodium channels prevents the influx of Na^+ (Elmslie, 2019).

In axons with a greater diameter, more ions are able to enter the axon and create a larger repellent charge. This results in the spread of positive charge further down the axon and initiates threshold depolarisation and subsequent action potential at a greater distance from the original action potential. As a result, axons with greater diameter are able to propagate an action potential at a faster velocity than those with small diameter.

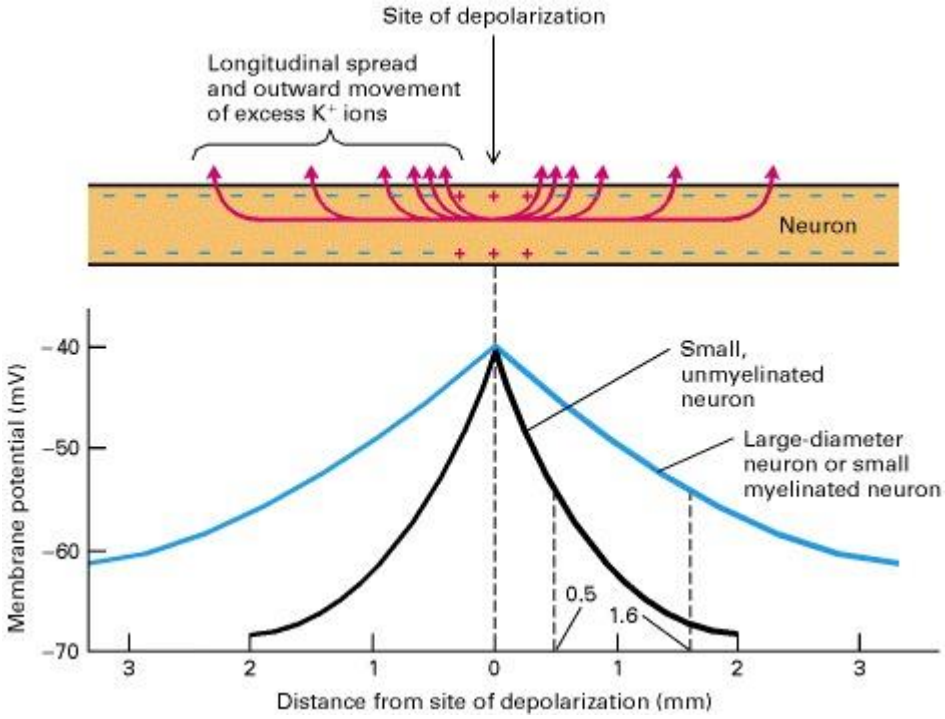

Figure 1. 2. Passive spread of membrane depolarisation.

Repulsion of K^+ from the site of depolarisation causes increase in membrane potential in adjacent areas dependent on distance from depolarisation. This spread is greater in larger diameter axons. Taken from (Lodish, 2000).

1.2.5. Saltatory Conduction

Fast axonal propagation is required for coordinated activity of the CNS. As previously discussed, larger axonal diameter increases conduction velocity but also requires a greater volume of space. Vertebrates have evolved to resolve this issue by myelination of axons which causes dramatic increase in conduction velocity while also maintaining small axon diameter.

In a myelinated axon, voltage gated sodium channels are densely populated in the nodes of Ranvier and very sparse in the internodes (Caldwell *et al.*, 2000). This means action potentials are limited to the nodes. Sodium channel clustering at the node is maintained by association with the scaffolding protein, ankyrin G, and the adhesion protein, neurofascin 186, NF186 (Arancibia-Carcamo & Attwell, 2014). Voltage gated potassium channels are localised to the juxtaparanodal region, with the exception of $K_v3.1b$ and K_v7 which are found in the node (Poliak *et al.*, 2003). Voltage changes experience at this region are minimal due to location under the myelin sheath and electrical isolation from the node by tight paranodal junctions formed by Caspr/Contactin/NF155 complexes (Arancibia-Carcamo & Attwell, 2014). Therefore, it is thought that contribution of membrane repolarisation is limited. These characteristics are depicted in figure 1.3. Recent evidence supports the involvement of nodal clusters of two-pore-domain potassium channels (K2P) in repolarisation of the node following an action potential in myelinated afferent neurons (Kanda *et al.*, 2019). However, whether this mechanism is widespread throughout the CNS is yet to be elucidated.

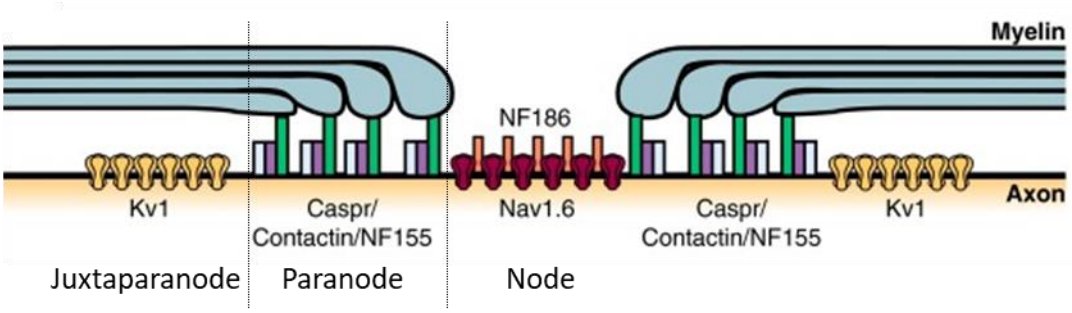

Figure 1. 3. Spatial arrangement of axonal ion channels

Voltage gated sodium channels are maintained clustered at the node of Ranvier by association with NF186. Voltage gated potassium channels are localised in the juxtaparanode and electrically isolated from the node by close association of paranodal proteins. Adapted from (Arancibia-Carcamo & Attwell, 2014).

By increasing the separation between the intracellular and extracellular environment with an electrically insulative lipid composition, myelination is able to reduce the capacitance of the axon. This reduces accumulation of opposing charges across the membrane. As a result, when an action potential causes accumulation of intracellular Na+ at the node, a flow of positive charge along the axon is less impeded by accumulated negative charge and is able to cause depolarisation of the subsequent node. Additionally, myelin increases the resistance of the axon, causing less positive charge to leak while traveling to the subsequent node. Suprathreshold depolarisation of the subsequent node triggers an action potential and, consequently, further signal conduction along the axon. This mode of conduction is known as saltatory and is far faster as it allows the action potential to skip large segments of the axon.

Saltatory conduction is also far more energetically efficient than conduction in unmyelinated axons (Stiefel, Torben-Nielsen & Coggan, 2013). The membrane is only depolarised at the nodes of Ranvier meaning ionic rebalance is only required at these sites. This duty is performed by the Na^+/K^+-ATPase which exports sodium and imports

potassium at the cost of ATP. In a large, unmyelinated axon, far more activity of the Na^+/K^+-ATPase is required due to larger depolarised surface area, resulting in far greater metabolic demand. Interestingly, it has been estimated that energy expenditure on maintenance of myelin structure and the resting potential of oligodendrocytes offsets the energy saved on restoration of axonal membrane potentials in myelinated axons (Harris & Attwell, 2012). Therefore, energy efficiency is likely not the driving factor for myelin evolution.

1.2.6. Sodium-Potassium pump

The sodium-potassium pump, or Na^+/K^+-ATPase, is responsible for maintaining the low intracellular sodium and high intracellular potassium concentrations in all cells (Pivovarov, Calahorro & Walker, 2018). This enzyme is located on the plasma membrane and facilitates the transport of 3 Na^+ into the extracellular space in exchange for 2 K^+. As transport is against concentration gradients and electrogenic in its unbalanced carrying of charge, the process is active and requires energy. For each 3 sodium ions and 2 potassium ions transported, one molecule of ATP is converted to ADP. Indeed, in the CNS, this process is so prevalent that it accounts for 50% of ATP expenditure (Erecinska & Silver, 1994). The electrogenic nature of the pump also contributes to the resting potential of the plasma membrane.

1.3. Axo-Myelinic synapse

Until recently, the myelin sheath was assumed to be a passive structure that undergoes no changes after its formation. However, evidence now points towards chemical communication been axons and myelin that may act to alter functional properties and contribute towards plasticity of white matter activity (Kaller *et al.*, 2017; Stys, 2011).

1.3.1. Glutamate receptors

Glutamate receptors are a broad family of membrane proteins that activate when they bind glutamate. They come in two main forms. Metabotropic glutamate receptors are a form of G-protein coupled receptors that initiate an intracellular signalling pathway upon activation. Ionotropic glutamate receptors are ion channels which undergo conformational change upon glutamate binding and open to allow transmembrane passage of ions to alter membrane electrical potential.

Ionotropic glutamate receptors have a large degree of sequence homology and are composed of four transmembrane subunits that associate to form a pore (Traynelis *et al.*, 2010). However, they can be further subdivided based on structural differences and affinity for synthetic agonists. These categories are mostly named after their synthetic agonists: Kainate, AMPA, NMDA and δ receptors.

Myelin and oligodendrocytes have been shown to express ionotropic glutamate receptors. AMPA receptors containing the subunit GluR4 were the first to be described followed by KA2 subunit-possessing kainate receptors (Brand-Schieber & Werner, 2003; Li & Stys, 2000). NMDA receptors have also been demonstrated in the myelin, particularly those containing NR1 and NR3 and lacking the NR2 subunit (Pina-Crespo *et al.*, 2010). While most NMDA receptors are coactivated by glutamate and glycine, these

receptors are activated by glycine alone. More recently, a fundamental role has been found for NMDAR containing the GluN2D and GluN3A subunits as ablation of these prevents myelinic calcium rise in response to AMPA or NMDA stimulation (Micu *et al.*, 2016). Myelinic NMDA receptors are mainly located on the non-compact myelin of the inner and outer loops (Micu *et al.*, 2006). Functionally, the oligodendrocyte cell body is responsive to AMPA or NMDA application while the myelin membranes are almost solely activated by NMDA (Salter & Fern, 2005).

1.3.2. Axonal glutamate release

Myelinic calcium rise is caused by neurotransmitter release from the axons. This release is dependent on axonal activity as high frequency stimulation of the optic nerve results in a rise in cytoplasmic calcium in the myelin (Micu *et al.*, 2016). This effect is blocked when action potentials are prevented using tetrodotoxin (TTX), revealing membrane depolarisation is required for neurotransmitter release. Furthermore, the release is in a vesicular manner as prevention of vesicular fusion, using tetanus toxin, inhibited stimulation-induced myelin calcium rise. Axonal vesicles are loaded in a similar manner to synaptic vesicles, as evidenced by the inhibition of myelin calcium activity following application of bafilomycin-A1 which prevents action of the H^+-ATPase. This pump is essential for promoting a vesicular environment for loading of neurotransmitter.

For vesicles to fuse and release their contents, intracellular calcium levels must rise. In presynaptic terminals, this occurs by influx of Ca^{2+} through voltage gated calcium channels on the cell membrane. However, in the axon-myelinic synapse, available extracellular calcium is limited by the tiny periaxonal space. The axon has resolved this complication by accessing intracellular stores of calcium in the axoplasmic reticulum (Micu *et al.*, 2016). Proof of this method is that inhibition of either L-type voltage gated

calcium channels or intracellular ryanodine receptors will prevent myelinic calcium rises following electrical stimulation. Therefore, membrane depolarisation causes sufficient calcium influx to activate calcium sensitive calcium channels and allow release of calcium stores from the axoplasmic reticulum.

1.3.3. Function of the axo-myelinic synapse

By eliciting calcium activity in myelin, the axo-myelinic synapse is able to convey information regarding axonal activity to the myelin and oligodendrocyte. This information may be necessary for multiple physiological functions. As axonal mitochondria are largely located within the internode, it is suggested that myelin must provide metabolic support to the axon (Butt, Papanikolaou & Rivera, 2019; Micu *et al.*, 2018). Oligodendrocytes generate pyruvate and lactate which can then be transported to axons via monocarboxylase transporters (MCT) where it is reconverted to pyruvate for metabolism in axonal mitochondria. If myelinic MCT is deleted, the oligodendrocyte is unaffected, but the axon is perturbed (Lee *et al.*, 2012). Activation of oligodendrocyte NMDA receptors causes an upregulation of membrane glucose transporter (GLUT1) expression within minutes (Saab *et al.*, 2016). Increased expression of GLUT1 results in elevated glucose uptake in oligodendrocytes and consequent lactate output to the axons. Therefore, activity dependent signalling from axons to myelin will result in increased metabolic substrate supply.

The dynamic supply of metabolic substrates represents a transient functional effect of axon to myelin signalling. However, there appears to be more persistent changes relating to this form of communication. Deletion of the GluN2D/GluN3A subunit containing NMDA receptor does not result in demyelination, but instead causes decompaction of myelin structure (Micu *et al.*, 2016). This particular NMDA receptor is

known to be highly present in the myelin and largely responsible for axonal activity dependent rises in myelinic calcium. Alterations in myelin microstructure will change its resistance and capacitance, resulting in disturbed conduction velocity of action potentials. Therefore, the functional axo-myelinic synapse may be necessary to maintain correct myelin microstructure. Furthermore, it has been proposed that activity dependent signalling from the axon may regulate paranodal myelin architecture to result in micro-adjustments to conduction velocity in order to correctly time activity spikes in a network (Micu *et al.*, 2018).

1.4. White Matter injury

As white matter is responsible for communication between many different functional regions of the CNS, damage can result in heterogenous deficits. There are many conditions that may cause injury to white matter. Generally, these can be broken down into acute injuries, such as stroke and traumatic brain injury, and degenerative injury, such as multiple sclerosis and vascular dementia. As each component of white matter plays a pivotal function, disruption to any of these will have profound effect on action potential propagation.

1.4.1. Stroke

Stroke is a CNS disease in which blood supply to an area of the brain is perturbed. The CNS has an extremely high metabolic demand; brain blood supply is around a quarter of the cardiac output at rest despite only occupying 2% of the total mass (Engl & Attwell, 2015). Therefore, disturbances result in a deficit of nutrients, mainly oxygen and glucose, in the affected area. Cerebral metabolism mainly occurs via glycolysis and oxidative phosphorylation, meaning supply of oxygen and glucose is imperative. Hence, its cessation will cause extreme metabolic stress. A further consequence of the impaired blood flow is lack of clearance of metabolic products such as CO_2 and lactate. Their accumulation causes additional detriment to the CNS tissue.

Blood supply can be impaired by a blockage in a blood vessel. This is known as an ischaemic stroke and is the cause of 85% of all strokes. Blood supply can also be ceased by rupture of a blood vessel which causes the contents to leak into the brain parenchyma or the meninges. This is a haemorrhagic stroke and accounts for the

remaining 15% of strokes. This thesis will focus on ischaemic stroke, though underlying injury mechanisms are likely to be similar in haemorrhagic stroke.

1.4.1.1. Susceptibility of white matter

Ischaemic stroke results from occlusion of a brain blood vessel and can therefore affect any region of the brain. However, 95% of stroke infarcts will incorporate an area of white matter and on average around 50% of infarct volume will be white matter (Ho *et al.*, 2005).

White matter is less energetically demanding than grey matter and, as a result, has less collateral supply of blood. Consequently, white matter is highly susceptible to ischemic insult as occlusion of supplying blood vessels will result in a greater reduction of blood flow (Wang *et al.*, 2016). Furthermore, the arteries supplying deep subcortical white matter have a high incidence of occlusion resulting in 30% of strokes predominantly affecting white matter (Rosenzweig & Carmichael, 2013).

1.4.1.2. Mechanisms of ischaemic insult to white matter

1.4.1.2.1. Ionic breakdown

One of the earliest events to occur during a stroke is depolarisation of the plasma membrane. As production of ATP is halted by the loss of oxidative phosphorylation, activity of the Na^+/K^+-ATPase is impaired (Yang *et al.*, 1992). The Na^+/K^+-ATPase is responsible for homeostasis of ion gradients across the membrane and as potassium leak channels are persistently open, the extracellular concentration of K^+ begins to rise. Furthermore, the consumption of ATP stores alters the ratio between ATP and ADP and consequently opens ATP sensitive potassium channels, resulting in a further increase in extracellular K^+. The rise in extracellular potassium concentration shifts the reversal

potential for potassium in a positive direction along with the membrane potential. Consequently, voltage gated ion channels are opened, sodium ions enter the axon and the membrane depolarises. Of course, without the functionality of the Na^+/K^+-ATPase, membrane polarisation cannot be re-established. Consequently, subsequent action potentials cannot be propagated and therefore, signals are blocked. While signal blockage has devastating consequences for brain function, this alone does not result in white matter damage.

Membrane depolarisation and alterations of ionic gradients causes further damaging downstream effects. Excessive accumulation of intracellular Na^+ generates an inward drive for Cl^- diffusion across the membrane (Rungta *et al.*, 2015). This ionic build-up within cells causes water to enter the intracellular space via osmosis and results in large-scale swelling (Choi, 1987). Organelles, including mitochondria, also begin to swell and are disrupted, leading to further metabolic stress on the cell (Gwag *et al.*, 1997).

Following failure of the Na^+/K^+-ATPase, astrocytes act to alleviate elevated extracellular potassium by uptake and buffering throughout the syncytium. However, this requires generation of ATP through anaerobic metabolism. As astrocytes absorb more extracellular K^+, they swell up to five times their physiological size until they rupture (Arumugam, Okun & Mattson, 2009). Furthermore, release of potassium from mitochondria through mitochondrial K^+-ATPase channels results in further impairment of oxidative metabolism (Liu *et al.*, 2003).

Depolarisation of the membrane causes activation of voltage gated calcium channels (VGCC) and consequent influx of Ca^{2+} across the plasma membrane (Kristian & Siesjo, 1998). Consequently, increased intracellular calcium and gating of L-type VGCC activates ryanodine receptors on the endoplasmic reticulum (Ouardouz *et al.*, 2006). This acts to

release intracellular stores of Ca^{2+} from the endoplasmic reticulum into the cytoplasm, a process known as calcium induced calcium release (CICR). Excessive entry of calcium into the cytoplasm initiates a deleterious cascade of calcium activated enzymes. Intracellular calcium under physiological conditions is kept in the nanomolar range to keep these enzymes in check (Gleichmann & Mattson, 2011). However, low intracellular calcium is dependent on exportation by Ca^{2+}-ATPase and the Na^{+}/Ca^{2+} exchanger. The first of these is reliant on supply of ATP, which is depleted during ischaemia, in order for activity. The Na^{+}/Ca^{2+} exchanger is driven by an inward concentration and electrical gradient for sodium ions. However, this drive is lost following ischaemia-induced depolarisation (Shenoda, 2015). Consequently, intracellular calcium concentration is allowed to soar to pathological levels. Pathological levels of intracellular calcium cause activation of calcium dependent enzymes such as calpains and caspases, which are cysteine proteases (Chan & Mattson, 1999). These enzymes break down vital cellular components such as the cytoskeleton and metabolic enzymes leading to necrotic cell death. Calpains and caspases can also act to initiate programmed cell death, apoptosis, if necrotic cell death is not reached (Leist *et al.*, 1997).

1.4.1.2.2. Glutamate excitotoxicity

Pathologically high levels of extracellular glutamate cause overactivation of ionotropic glutamate receptors and initiate a cascade leading to cell death (Lewerenz & Maher, 2015). Traditionally, research into this phenomenon has focused on neuronal cell bodies. However, the susceptibility of glial cells, and particularly oligodendrocytes, has now been elucidated. Glutamate application to isolated spinal cords causes death of oligodendrocytes and myelin but not axons (Li & Stys, 2000). This was mediated by

glutamate receptors as their inhibition prevented reduction in compound action potential transmission.

Under physiological conditions, extracellular glutamate is taken up by astrocytes and oligodendrocytes via the glutamate transporters EAAT1 and EAAT2 (Domercq *et al.*, 1999; Mahmoud *et al.*, 2019). These enzymes are cotransporters for sodium and driven by the concentration gradient of Na^+. Therefore, under ischaemic conditions when intracellular sodium levels are elevated, the cotransporters will reverse and export glutamate from the astrocytes and oligodendrocytes into the extracellular space (Li *et al.*, 1999). Extracellular glutamate levels can also rise due to vesicular release from axons, following membrane depolarisation at the axo-myelinic synapse (Doyle *et al.*, 2018). Membrane depolarisation occurs early in ischaemia due to impairment of the Na^+/K^+-ATPase.

Excessive extracellular glutamate and consequent overactivation of glutamate receptors allows dramatic flow of ions across the membrane. The heterogeneity of glutamate receptors results in an increase in an array of ion permeabilities including Na^+, Ca^{2+}, and Cl^- (Huettner, 2015). The increase in intracellular sodium acts to exacerbate membrane depolarisation. However, most importantly, entry of Ca^{2+} causes activation of calcium dependent enzymes that initiate necrotic cell death. Activation of metabotropic glutamate receptors coupled to phospholipase C (PLC) causes production of intracellular inositol-trisphosphate (IP_3), which in turn activates IP_3 receptors on the endoplasmic reticulum (Hartmann & Konnerth, 2005). IP_3 receptor activation acts to mobilise intracellular stores of Ca^{2+}, thereby further increasing intracellular calcium and exacerbating necrotic death mechanics.

Additionally, elevated extracellular glutamate causes splitting and retraction of the paranodal myelin (Fu *et al.*, 2009). This pathological process is attributed to calcium influx through NMDA and kainate receptors as their inhibition attenuates the disruption as well as exclusion of Ca^{2+} from the extracellular fluid. These glutamate-induced anomalies to paranodal myelin structure are caused by degradation of MBP and result in disrupted axo-glial junctions. Consequently, potassium channels, which are highly concentrated in the juxtaparanodal area of the axolemma, become exposed to the extracellular space. Indeed, some voltage gated potassium channels even migrate into the paranodal and nodal axolemma. This exposure of voltage gated potassium channels results in impairment of saltatory conduction and loss of signal propagation. Furthermore, exposure of the paranodal and juxtaparanodal axolemma allows calcium influx into the axon that propagates calcium dependent axonal death.

1.4.2. Multiple Sclerosis

Multiple Sclerosis (MS) is a progressive white matter disease involving autoimmune attack on myelin. It is the world's leading cause of disability in young people, excluding trauma, and can cause profoundly different complications in each case (Kobelt *et al.*, 2017). MS typically presents with an early relapse-remission phase followed by progressive deterioration. However, in around 15% of cases, the disease presents with a primary progressive state, absent of a relapse-remission phase.

1.4.2.1. MS progression profile

During the initial relapse-remission phase, the sufferer will experience periods where function will become impaired over the course of hours or days and remain so for several weeks (Dobson & Giovannoni, 2019). This could be motor, sensory, behavioural or cognitive impairment depending on where the white matter lesion appears. One

example would be impaired vision from a lesion in the optic nerve. Following this relapse period, the function will be restored gradually, though not necessarily to full extent. A relapse in the optic nerve may leave permanent abnormality to any aspect of vision such as colour, contrast or depth perception. This will occur in cycles with accumulating functional impairments and each cycle will result is a steadily worsened remission state with persistent disability. Finally, after approximately 10-15 years, a secondary progressive phase will dominate whereby accruing disability will prevail over remission periods until they are no longer experienced.

1.4.2.2. Demyelination and Remyelination

Functional deficits experienced in MS are a result of plaques of demyelination. Loss of myelin causes disability by slowing or preventing conduction of action potentials along axonal tracts. This results in discoordination of complex signal networks required for proper brain communication.

During the relapse-remission phase of the disease, once the immune insult has been quelled, remyelination of denuded axons can occur (Chari, 2007). Remyelination is initiated by proliferation of oligodendrocyte precursor cells and differentiation into oligodendrocytes (Blakemore & Patterson, 1978). These oligodendrocytes then send forth processes that contact demyelinated axons (Chari, 2007). Oligodendrocytes subsequently mature and produce myelin that wraps around the axons to form a sheath in a similar manner as in development (Franklin & Hinks, 1999). Although remyelination occurs by the same process as developmental myelination, the myelin sheaths produced are thinner and shorter, leaving an enlarged node of Ranvier. However, conduction is not affected by these abnormalities (Smith, Blakemore & McDonald, 1979). Although

axonal conduction is restored, it is unlikely remyelination is responsible for early stages of remission as conduction is still perturbed during this time.

Persistent demyelination of an axon leads to its damage and atrophy (Ferguson *et al.*, 1997). Exposure of the axolemma of a demyelinated axon leads to disorganisation of ion channel distribution which can cause dysfunction (Waxman, Craner & Black, 2004). This can lead to axonal overload of sodium and consequent reversal of the sodium-calcium exchanger. Calcium entry into the axons will lead to a cascade of neurodegeneration via calcium dependent enzymes. Furthermore, oligodendrocytes express trophic factors such as BDNF and NGF that support axonal survival (Byravan *et al.*, 1994). Therefore, remyelination of axons acts to protect them from secondary insult in MS. However, in later stages of MS, remyelination becomes more inconsistent and absent. This is likely to contribute to the neurodegeneration abundant in progressive MS.

1.4.2.3. Outside-in Vs Inside-out

Classically, MS has been considered a primary immune condition in nature whereby immune dysregulation causes an autoreactive attack on myelin. This hypothesis is known as the "outside-in" theory, as the immune abnormalities are initiated from outside the CNS. In this understanding of the disease, preliminary assault of the CNS is initiated by a systemic infection that results in presentation of adhesion molecules on the endothelium of the CNS (Frohman, Racke & Raine, 2006). Consequently, the blood-brain barrier (BBB) is disrupted and circulating lymphocytes may gain access to the CNS parenchyma, to which they are normally prohibited. If pre-existing recognition of myelin antigens are present in the lymphocytes, a cascade of inflammation will occur. CD4+ and CD8+ T cells are thought to mediate inflammatory demyelination, aided by helper T cells,

Th1. Additionally, B cells are thought to mutate once inside the CNS to produce myelin specific antibodies.

The established “outside-in” model of MS has inconsistencies which may be used to validate an “inside-out” model, whereby primary myelin and oligodendrocyte damage act as a catalyst for immune interaction (Stys *et al.*, 2012). Early in lesion development, myelin damage occurs primarily at the inner sheet of the myelin sheath and is demarked with a loss of myelin-associated glycoprotein (MAG) (Aboul-Enein *et al.*, 2003). MAG is expressed on the peri-axonal wraps of myelin and act to bind myelin to the axolemma. An immune insult would not have access to the inner lamellae of myelin and so this observation lends credence to a primary myelin degeneration. Furthermore, these impaired inner myelin wraps can be observed outside of the inflammatory foci (Rodriguez & Scheithauer, 1994). Indeed, degenerating myelin and axons are found throughout white matter in MS brains, even in normal appearing white matter; pathology is far from limited to active inflammatory plaques (Seewann *et al.*, 2009).

Some current treatments of MS focus on suppression of the immune response or even resetting the immune system via haematopoietic stem cell transplants (Mancardi & Saccardi, 2008). While these treatments can be highly effective at preventing inflammation in the relapse-remission phase of MS, they are ineffective during the progressive phase (Molyneux *et al.*, 2000). The abolishment of relapses but continued deterioration of condition and progression of demyelination and axonopathy suggest a non-inflammatory cause to these aspects. However, it is also possible that initial immune insult to the CNS primes the tissue for secondary degeneration that persists irrespective of inflammation.

1.4.2.4. Heterogeneity of MS pathology

There is a high degree of heterogeneity in clinical presentation of multiple sclerosis with most patients presenting relapse-remission MS (RRMS) and others with primary-progressive MS (PPMS). Some patients present with a period of drastic demyelination and axonal loss leading to severe disability that is sudden in onset, known as Marburg's variant. There is also much heterogeneity of plaque pathology (Lucchinetti *et al.*, 2000). This may help to explain the difficulty identifying one unifying disease mechanic. Patients present with four different subclasses of active plaques, as shown by observations from autopsies and biopsies. However, although separate patients will present with different plaque pathology, these will be consistent between plaques of the same patient. All plaques are, however, linked by an infiltration of T lymphocytes and macrophages from the circulatory immune system.

Types I and II plaques are found adjacent to small veins and venules and display high infiltration of T-lymphocytes and macrophages. This suggests inflammation is the prominent destructive mechanism in these classifications of plaques. Further to this, in patients displaying type I or II active plaques, adjacent inactive plaques present with high levels of oligodendrocyte recolonization and remyelination, implicating inflammatory environment for demyelination. Both plaque types display equal loss of all myelin proteins. However, type II plaques display a high reactivity for immunoglobulins specific to myelin as well as macrophages containing myelin degradation products.

The defining features of type III plaques are oligodendrocyte apoptosis accompanied by preferential loss of MAG from myelin. MAG is expressed on the inner lamellae of the myelin sheath, adjacent to the periaxonal space. This may implicate primary demyelination in this form of plaque or demyelination driven by oligodendrocyte

apoptosis. Oligodendrocytes are nearly eradicated in plaques and are even lost in surrounding white matter. Inactive plaques show absence of remyelination. The major inflammatory components are T-lymphocytes, macrophages and, interestingly, activated microglia. These plaques are less venous centred than type I and II plaques, even displaying a rim of preserved myelin around vessels within plaques.

Oligodendrocyte cell death also predominates in type IV plaques with near complete loss in active and inactive plaques, again indicating lack of remyelination; however, cell death is not via apoptosis and the plaque limits are far clearer defined. Furthermore, type IV can be distinguished from type III by the simultaneous loss of all myelin proteins.

These classifications are controversial, however, as there are concerns with the evidence (Disanto *et al.*, 2010). Primarily, many of the samples are from biopsies rather than autopsies which may be less representative of the overall disease (Esiri, 2009).

It has been proposed that heterogeneity of clinical presentation may be representative of the predisposition of a patient's immune system to respond to antigens produced by primary demyelination (Stys *et al.*, 2012). Marburg's variant would demonstrate an individual whose immune system reacts intensely to released myelin debris causing severe inflammation and exacerbated myelin and axonal degeneration. Primary progressive MS would be caused by a weak or absent immune response, allowing the underlying degenerative process to advance unobscured. The more common RRMS would be caused by an intermediate predisposition to react to myelin debris. However, increasing immune senescence with age and disease progress would lead to a quietening of response and onset of secondary progressive degeneration.

1.4.2.5. Glutamate excitotoxicity

Extracellular glutamate concentration in MS plaques has been found to be pathologically elevated and therefore, damage due to excitotoxicity is likely (Srinivasan *et al.*, 2005). There are several potential sources that may contribute toward increased levels of glutamate. Primarily, an abundance of activated microglia and macrophages are recruited to active MS lesions. These cells release glutamate into the extracellular space when exposed to an inflammatory environment such as an MS plaque (Piani *et al.*, 1992). Microglia are capable of producing glutamate from glutamine by glutaminase, which has found to be upregulated in plaques and even correlates to axonal damage (Werner, Pitt & Raine, 2001). Once synthesised, glutamate is released into the extracellular space through uncoupled hemichannels and the glutamate/cystine antiporter; inhibition of either channel reduces neuronal death and improves clinical outcome in the experimental autoimmune encephalomyelitis (EAE) mouse model of MS (Domercq *et al.*, 2007; Shijie *et al.*, 2009). Activated microglia are also capable of stimulating glutamate release from astrocytes, thereby reinforcing elevated extracellular glutamate. Activated microglia release a host of signalling molecules; these include ATP and TNF-α (Bezzi *et al.*, 2001; Pascual *et al.*, 2012). Both molecules are ligands to G-protein coupled receptors on astrocytes, P2Y and TNFR1 respectively, that initiate calcium independent secretion of glutamate from astrocytes. Furthermore, metabotropic glutamate receptors on astrocytes can trigger further secretion of glutamate, thereby amplifying pathological concentrations (Bezzi *et al.*, 1998).

Redistribution of ion channels on demyelinated axons causes accumulation of N-type voltage gated calcium channels and sodium channels ($Na_V1.2$) in the demyelinated internode axolemma (Craner *et al.*, 2004b; Kornek *et al.*, 2001). Redistribution of N-type

calcium channels allows calcium influx into the axon and consequent vesicular release of glutamate. Furthermore, activation of $Na_V1.2$ channels causes intra-axonal elevation of sodium. This, in turn, reduces or reverses drive for the Na^+/Ca^{2+} exchanger and sodium dependent glutamate transporters, resulting in further increased intracellular calcium and reduced glutamate reuptake (Li *et al.*, 1999; Stys, Waxman & Ransom, 1992). It is also possible that chronic overactivation of the axo-myelinic synapse and consequent release of glutamate may cause initial deterioration of the myelin (Micu *et al.*, 2016). This phenomenon may explain why myelin damage often starts on the inner lamellae of the myelin sheath and may result in priming of the immune system as suggested in the "inside-out" model.

Highly calcium permeable NMDA receptors on oligodendrocyte processes would result in particular susceptibility of these components to insult from pathological extracellular glutamate (Karadottir *et al.*, 2005). This could help to explain the advanced demyelination seen in MS followed by axonal degeneration. Oligodendrocytes also express abundance of AMPA receptors on their soma. Depending on subunit composition, calcium permeability is altered along with susceptibility to excitotoxic cell death (Hollmann, Hartley & Heinemann, 1991). AMPA receptors containing GluA2, which is impermeable to calcium, are equally dispersed on oligodendrocytes throughout the brain (Newcombe *et al.*, 2008). However, within MS lesions, oligodendrocytic GluA1 subunits are upregulated meaning AMPA receptors in these regions are less likely to contain GluA2 and are therefore permeable to calcium. This explains the susceptibility of oligodendrocytes in MS lesions to glutamate mediate attack.

Glutamate may also be involved in the disruption of the blood-brain barrier necessary for infiltration of autoreactive immune cells. NMDA receptors are located on endothelial

cells and their antagonism with MK-801 reduces interference with the BBB along with neurological deficits in the EAE model of MS (Bolton & Paul, 1997). Furthermore, kainate receptor subunits GluK1-3 are abundant on endothelial cells in active lesions, supporting a role in BBB disruption (Newcombe *et al.*, 2008).

1.5. Representative white matter tracts

1.5.1. Mouse Corpus Callosum

The corpus callosum (CC) is the largest white matter tract in the mammalian brain and, combined with the characteristic white appearance of myelin, it is easily locatable along the floor of the longitudinal fissure (Fitsiori *et al.*, 2011). The CC is the primary commissural tract, allowing interhemispheric communication via 200-250 million axons in humans. The majority of axons project to homotopical regions in the contralateral hemisphere, permitting coordinated brain activity (Zhou *et al.*, 2013). The projection of axons from the CC is largely dependent on their location within the CC. For example, axons originating from medial cortical regions will be contained in bundles more dorsally within the CC. These axons will then project to medial cortical regions in the contralateral hemisphere. A small proportion of axons project diagonally to different regions in the contralateral hemisphere (Sisti *et al.*, 2012). Though the corpus callosum is a white matter structure, not all axons are myelinated. In fact, in the adult mouse, only a maximum of 28% of CC axons are myelinated (Sturrock, 1980). This is in contrast to around 40% myelination in the human corpus callosum (Tomasch, 1954).

Coronal brain slices containing the corpus callosum are valuable as representative white matter bodies and have been used in the present study. As the largest body of white matter in the mouse brain, it is relatively easy to perform investigations on the CC without contamination from adjacent grey matter structures. On the other hand, the presence of adjacent grey matter does allow for interactions between the two that would be present in situ. This is a particular advantage over preparations such as optic nerves which are entirely isolated white matter. Additionally, coronal brain slices are likely to contain whole cells with the cell body in the grey matter and the axon running

through the corpus callosum (Tekkok & Goldberg, 2001). Therefore, influences from the cell body on the axon, experienced in situ, may be mimicked in the brain slice. Moreover, the presence of grey and white matter in the same preparation allows for direct comparison in observations between the two.

Figure 1. 4. Mouse corpus callosum

Myelin of a coronal mouse brain slice stained in blue with Klüver–Barrera. The corpus callosum is the largest white matter tract of the brain indicated by black arrow. Scale bar = 1mm. Taken from (Mizuno *et al.*, 2014).

1.5.2. Mouse Optic Nerve

The mouse optic nerve (MON) is another representative white matter tract used in this study. The optic nerve is the second cranial nerve and exists as a protrusion of the CNS, meaning it is abundant with CNS glia, such as oligodendrocytes and astrocytes (Butt *et al.*, 2004). Axons of the optic nerve project from retinal ganglion cells in the retina to the optic chiasm, where some cross the midline and others remain ipsilateral (De Moraes, 2013).

The preparation consists purely of a white matter bundle, meaning no neuronal cell bodies are present. Additionally, the mouse optic nerve contains no unmyelinated axons (Gyllensten & Malmfors, 1963). While this means that the optic nerve is not typical of other white matter bundles which contain unmyelinated fibres, the optic nerve is ideal for investigation of interactions between axons and glia as well as disease mechanisms affecting myelin and myelinated axons (Bolton & Butt, 2005). There is no contamination of results from grey matter as the tract is completely separated. The shape and ease with which this tract may be isolated makes it perfect for fitting suction electrodes for stimulation and recording of compound action potentials.

1.6. Overall Research Aims

The difference in mechanisms of injury progression from ischaemia in grey and white matter have lacked in investigation. This deficit in knowledge may have resulted in missed therapeutic opportunity. Furthermore, the emergence of evidence supporting the existence and vital function of the axo-myelinic synapse may offer a crucial prospect for treatment of a variety of white matter diseases, such as stroke and MS.

Chapter 3: This chapter focuses on dysregulation of potassium homeostasis during cerebral ischaemia. Particular interest is concerned with how this may differ in grey and white matter and identifies mechanisms which may lead to these variations. This investigation is novel in its direct comparison of the two tissue types in the same *ex vivo* model of ischaemia.

Chapter 4: Experiments in this chapter investigate any potential variation in accumulation of H^+ during cerebral ischaemia between grey and white matter.

Chapter 5: This chapter examines the dysfunction of glutamatergic signalling in multiple sclerosis and the possibility to combat this using a combination of glutamate receptor antagonists. A new *ex vivo* model of MS is established in order to observe the synergistic capabilities of these drugs.

Chapter 6: Combined glutamate receptor antagonist therapy is tested to combat functional deficits caused by white matter ischaemia. If synergism is present and concentrations may consequently be reduced, side effects caused by the drugs in patients may be prevented.

It is hoped that the knowledge contributed by this thesis will aid in development of treatment for white matter injuries. Some glutamate receptor antagonists tested are

already approved for treatment of other diseases and so, evidence of their efficacy in stroke and MS may lead to swift establishment as a treatment.

Chapter 2:

Methods and Materials

2.1. Animals

All electrophysiology experiments were performed on tissue collected from CD1 mice aged at minimum P30. Procedures were performed according to local ethical guidelines and conformed with the UK Animals (Scientific Procedures) Act 1986. Sacrifice of animals was by schedule 1, with rising levels of CO_2 followed by cervical dislocation for confirmation of death.

2.2. Solutions

All chemicals were purchased from Sigma-Aldrich except where noted otherwise.

2.2.1. Artificial Cerebrospinal Fluid (aCSF) - Sodium Chloride (NaCl) 126mM, Potassium Chloride (KCl) 3mM, Sodium Phosphate Monobasic (NaH_2PO_4) 2mM, Magnesium Chloride ($MgCl_2$) 2mM, Sodium Bicarbonate ($NaHCO_3$) 26mM, Calcium Chloride ($CaCl_2$) 2mM, Glucose 10mM in water. For solution used during oxygen glucose deprivation (OGD aCSF), glucose is replaced with sucrose.

2.2.2. Brain Slice Cutting solution - Sodium Chloride (NaCl) 92mM, Potassium Chloride (KCl) 2.5 mM, Sodium Phosphate Monobasic (NaH_2PO_4) 1.2mM, Sodium Bicarbonate ($NaHCO_3$) 30mM, HEPES 20mM, Glucose 25mM, Sodium Ascorbate 5mM, Thiourea 2mM, Sodium Pyruvate 3mM, Magnesium Sulphate 2mM, Calcium Chloride 2mM in water. Adjusted to pH 7.3-7.4 with Sodium Hydroxide (Ting *et al.*, 2014).

2.3. Drugs

2.3.1. Glutamate receptor antagonists

Throughout this thesis, glutamate receptor antagonists are used to investigate the contribution of glutamate transmission to white matter damage. While some are used for experimental purposes, memantine and perampanel in particular were used with a view to determine therapeutic efficacy.

2.3.1.1. (+)-MK-801 Maleate

Supplier – Tocris (Bio-Techne); Solubility – DMSO; Working concentration – 50µM

MK-801 is a potent, non-competitive NMDA receptor antagonist (Woodruff *et al.*, 1987). The antagonist binds within the ion channel to prevent receptor currents by obstruction of the channel pore and closing of the channel gate (Song *et al.*, 2018). Due to requirement of access to the receptor channel, antagonism is use-dependent and voltage dependent. MK-801 is displaced by ketamine, phencyclidine and SKF 10,047, indicating a similar binding site (Wong *et al.*, 1986). MK-801 is currently not approved for treatment of any disorders due to severe adverse effects including psychotomimetic actions and even neurodegeneration (Bueno *et al.*, 2003; Olney, Labruyere & Price, 1989).

2.3.1.2. NBQX

Supplier – Tocris (Bio-Techne); Solubility – DMSO; Working concentration – 20µM

NBQX is a competitive antagonist of AMPA and kainate receptors, meaning it binds to the same location as glutamate and can be overcome by increasing concentration of agonist (Randle *et al.*, 1992). It has very low affinity for the NMDA receptor. It has not

been approved for use in the clinic due to poor water solubility which has caused nephrotoxicity in trials (Turski *et al.*, 1998). NBQX is sensitive to light and so all experiments were performed in a darkened room with the NBQX solution further shielded.

2.3.1.3. Perampanel

Supplier – Biorbyt Ltd.; Solubility – DMSO; Working concentration 0.2-10µM

Perampanel is a non-competitive selective AMPA receptor antagonist, approved for treatment of partial-onset seizures in the EU, USA and Canada (Hanada, 2014). This was the first treatment inhibiting excitatory post-synaptic function to be approved for this condition. Previous trials had been attempted with experimental competitive AMPA receptor antagonists, such as NBQX (Weiser, 2005). However, although these drugs showed potent binding affinity for AMPA receptors, little effect was shown in the clinic due to meagre access across the blood-brain barrier and poor solubility in neutral solutions. Further high-throughput screenings were employed to find potential drugs that may overcome these issues (Rogawski & Hanada, 2013). To achieve this, potential targets were tested with [^{3}H]AMPA binding assays and inhibition of AMPA induced neuronal cell death. No promising targets were found in the binding assay which tested only for competitive antagonists. However, 2,4-diphenyl-4H-[1,3,4]oxadiazin-5-one showed effective prevention of cell death from AMPA administration. This compound was particularly interesting as it showed little resemblance to classical AMPA receptor antagonists and had potential for chemical modification. Further modifications were made to the structure to improve efficacy, resulting in the creation of perampanel, 1,3,5-triaryl-1H-pyridin-2-one.

Perampanel has a very long terminal half-life in humans, at around 105 hours (Suda & Kimura, 2019). This is advantageous for treatment of chronic illnesses, such as MS, as it allows for a less frequent dosing regimen and a more stable plasma concentration of the drug. Minimalising spikes in drug concentration will lessen the chances of adverse effects from off target receptors (Hanada *et al.*, 2011). A further advantage of perampanel over classical AMPA receptor antagonists is the selectivity for AMPA over kainate receptors, which again reduces off target effects.

2.3.1.4. Memantine Hydrochloride

Supplier – Tocris (Bio-Techne); Solubility – Water; Working concentration – 0.2-10µM

Memantine is the only approved NMDA receptor antagonist for treatment of mild to severe Alzheimer's disease (Alam *et al.*, 2017). The chemical composition results in unique properties that give it significant advantages over other NMDA receptor antagonists and make it acceptable for clinical use. Memantine is an uncompetitive NMDA receptor antagonist; it binds to the Mg^{2+} domain of the open pore of NMDA receptors in a voltage dependent manner unlike early NMDA receptor antagonists which acted competitively at the glutamate binding site on the NR2 subunit. Competitive inhibitors block both pathological and physiological activation of NMDA receptors resulting in adverse psychotomimetic side effects (Lipton, 2004). On the other hand, memantine selectively blocks pathological overactivation of NMDA receptors. This is also due to the moderate binding affinity and fast on-off kinetics of memantine. Other uncompetitive NMDA antagonists, such as MK-801 and PCP, have much greater binding affinities for the Mg^{2+} domain and, as a result, cause continued inactivation for longer than memantine, resulting in impaired physiological activity. Thus, the discovery of

memantine was a breakthrough for treatment of more advanced Alzheimer's disease, where glutamate neurotoxicity plays effect (Rogawski & Wenk, 2003).

2.3.1.5. QNZ46

Supplier – Tocris (Bio-Techne); Solubility – DMSO; Working concentration – 0.2-50µM

QNZ46 is an experimental non-competitive NMDA receptor antagonist that is not currently approved for pharmacological treatment in humans (Hansen & Traynelis, 2011). QNZ46 inhibits NMDA receptors containing GluN2C or GluN2D subunits with greater affinity than those containing GluN2A or GluN2B subunits (Mosley *et al.*, 2010). Myelinic NMDA receptors are known to contain GluN2C/D subunits (Doyle *et al.*, 2018) and therefore, QNZ46 is ideal to investigate their contribution to white matter damage. Furthermore, QNZ46 is use-dependent as it requires glutamate activation of NMDA receptors in order to bind. QNZ46 is sensitive to light and so all experiments were performed in a darkened room with the QNZ46 solution further shielded.

2.3.1.6. CP 465022 hydrochloride

Supplier – Tocris (Bio-Techne); Solubility – DMSO; Working concentration – 0.2-50µM

CP 465022 is an experimental, non-competitive antagonist of AMPA receptors (Lazzaro *et al.*, 2002). Selectivity for AMPA receptors over kainate or NMDA receptors is high with an IC_{50} of just 25nM. This selectivity means CP 465022 is ideal for identifying the contribution of AMPA receptor currents to cuprizone induced injury. Furthermore, the lack of action at kainate receptors may prove beneficial for prevention of adverse effects if the drug were to be used clinically. However, the action of CP 465022 is similar across the spectrum of AMPA receptors which means that the drug will not be specifically targeted towards AMPA receptors expressed by oligodendrocytes.

2.3.2. Potassium channel blockers

2.3.2.1. Tetraethylammonium chloride

Supplier – Sigma-Aldrich; Solubility – Water; Working concentration – 10mM

Tetraethylammonium ions (TEA^+) inhibit voltage gated potassium channel (K_V) currents by occupying the channel pore (Newland *et al.*, 1992). The ions can prevent both influx and efflux by occupying opposite sides of the aqueous pore.

2.3.2.2. Barium chloride

Supplier – Sigma-Aldrich; Solubility – Water; Working concentration – 300µM

Barium ions prevent potassium currents through inwardly rectifying potassium channels (Kir) which are insensitive to TEA^+ blockage (Solessio *et al.*, 2000). Again, the channels have in internal and external pore region which the ions may occupy to prevent ion flow.

2.4. Tissue handling

2.4.1. Dissection

Following cervical dislocation, mice were decapitated, and skin cut along the midline of the back of the head. Incisions were made behind the eye sockets and the optic nerves were severed as close to the eyeball as possible. The top of the skull was then removed with scissors and the brain, with optic nerves attached, carefully extracted into a petri dish of ice cold, oxygenated aCSF. Optic nerves were removed by pulling the optic chiasm from the brain with forceps. For experiments using optic nerves, they were transferred to a Haas-type perfusion interface chamber (Harvard Apparatus Inc.) at this stage. The nerves were then severed from the optic chiasm ensuring no constriction of the nerves occurred. The process took approximately 2 minutes after cervical dislocation.

For experiments involving brain slices, the brain stem and cerebellum were cut off with a scalpel. The forebrains were embedded in cutting solution with 0.5% agarose and stuck to the cutting plate of a Leica VT1200g vibratome along with a stabilising block of 4% agarose, using superglue. The vibratome bath was filled with ice cold, oxygenated cutting solution. Coronal sections of 400µm were cut and those containing the body of the corpus callosum across the midline were collected by floating onto a metal spatula.

2.4.2. Perfusion

For electrophysiology experiments, optic nerves or coronal brain slices were maintained on a nylon mesh in the perfusion interface chamber flowing with aCSF, bubbled with 95% O_2/5% CO_2 and heated to 37^{o}C through the chamber's water bath. Temperature was maintained by a TC-324B or TC-344C (Warner Instruments). A temperature sensor

lay underneath the nylon mesh in the chamber with a feedback loop to the heat coil in the Haas-type perfusion chamber water bath. The chamber was flushed with 95% O_2/5% CO_2 humidified through the heated water bath at a rate of 1.5L/min. Slices and MONs were incubated in this fashion for a minimum of 2h before experimental recordings were taken.

2.5. White matter damage models

2.5.1. Oxygen glucose deprivation

Oxygen glucose deprivation (OGD) is a commonly used model of ischaemic stroke. In this model, isolated tissues or cell cultures are subjected to conditions without oxygen or glucose. Oxygen glucose deprivation was induced by switching the perfusing solution from glucose-containing aCSF to sucrose-containing aCSF (OGD aCSF). This OGD aCSF was bubbled with 95% N_2/5% CO_2, for 1 hour prior to use and throughout, to remove any dissolved atmospheric oxygen. The gas flow through the chamber was also switched to 95% N_2/5% CO_2 to prevent absorption of oxygen from the surroundings. As the solution had to flow through tubing before reaching the chamber, switching the gas flow was delayed, ensuring both sources of oxygen deprivation were applied simultaneously.

Reperfusion of the tissue entailed returning to perfusion with glucose-containing aCSF, oxygenated with 95% O_2/5% CO_2. The gas flow in the chamber was switched back to 95% O_2/5% CO_2, again, delayed for simultaneous oxygenation. Care was taken that perfusion rate should not change when solutions were switched.

2.5.2. *Ex vivo* cuprizone

To make 250mL of 1mM cuprizone aCSF, cuprizone powder was dissolved in 7.5mL of ethanol or DMSO to make 33.3mM solution. To this solution, 17.5mL of aCSF was added and the mixture vortexed until fully dissolved. This was then added to 225mL of aCSF.

To induce cuprizone injury, the perfusion solution was switched to that containing 1mM cuprizone. Special care was taken to ensure unchanged rate of flow. Cuprizone was applied for 100 minutes before return to perfusion with regular aCSF.

2.6. Ion sensitive microelectrodes

2.6.1. Production and setup

Glass borosilicate tubes (1.5mm outer diameter, 0.86mm inner diameter) were pulled to a fine point using P-97 Flaming/Brown Micropipette Puller (Sutter Instruments). Pipettes were placed on a metal holder in a glass petri dish with lid off and baked at 150^{O}C for at least 30 minutes to remove moisture. A glass vial containing 50µL N,N-Dimethyltrimethylsilylamine (TMSDMA) was placed in the glass petri dish and covered with the lid. Baking was continued for a further 30 minutes to allow silinisation. Micropipettes were removed from the oven and allowed to cool before a solution of 100mM NaCl and 5mM KCl was injected into the back. Solution was then forced into the narrowed tip by pressure from a syringe. An ion selective resin membrane, Potassium ionophore I - cocktail B (Sigma-Aldrich), was drawn into the tip by suction using a syringe. For extracellular pH experiments, a hydrogen ionophore was drawn into the tip instead. Reference electrodes were made with the same glass micropipettes and filled with a solution of 100mM NaCl and 5mM KCl only. New electrodes were produced for each experiment.

A silver chloride wire was inserted into the backfilled solution of each electrode and connected to the differential electrometer (World Precision Instruments – FD223a). This in turn was connected to a data acquisition system (iworx – IX/228) which fed data into the computer to be processed in LabScribe2. To prevent the signal being confounded by changes in local field potential, the reference channel was subtracted from the recording channel.

2.6.2. Calibration

Ion sensitive microelectrodes measure the potential difference of an ion in the measuring vicinity (extracellular space), relative to the barrel of the electrode, across the liquid membrane. To convert this value to an ion concentration, the electrodes must be calibrated such that a series of known concentrations equate to measured potential differences. As ISMs were single use, a calibration was performed for every experiment.

2.6.2.1. Potassium

Microelectrodes were calibrated in grounded petri dishes containing 5 solutions of increasing K^+ concentration in bicarbonate buffered aCSF with reduced concentration of Na^+ to maintain osmolarity (Table 1.). Concentrations were chosen to bracket the range of changes seen in tissue. Both the recording and reference electrode were lowered into the calibration solution and recordings were taken until a stable reading was reached. This was usually between 15 and 30 seconds. A mean value for the plateau reached was then determined. A calibration curve was calculated by plotting the voltage recordings against the logarithm base 10 of the concentration of potassium (fig. 2.1). If the relationship were not linear, indicating a non-Nernstian relationship, the electrodes would have been discarded. However, this was never the case. The mean slope of the calibration curve was 52.5±0.5mV (n=45). A recording was also taken from the solution in the perfusion chamber and the curve was adjusted so that the voltage obtained equated to 3mM. This was to account for grounding differences between the chamber and the petri dishes. On occasion, electrode calibration curves were calculated before and after an experiment to establish sensitivity was not altered throughout the duration (fig. 2.1c-d). If the electrode sensitivity were to change throughout the experiment, an accurate calculation of ion concentration could not be interpreted. However, on the

occasions the second calibration was performed, there was no change in slope of the calibration curve. If this were not the case, experiments would be excluded.

Table 2: Constituents of potassium electrode calibration solutions

	Concentration (mM)				
Potassium Chloride	3	6	12	24	48
Sodium Chloride	126	123	117	105	81
Sodium Phosphate Monobasic	2	2	2	2	2
Magnesium Chloride	2	2	2	2	2
Sodium Bicarbonate	26	26	26	26	26
Calcium Chloride	2	2	2	2	2
Glucose	10	10	10	10	10

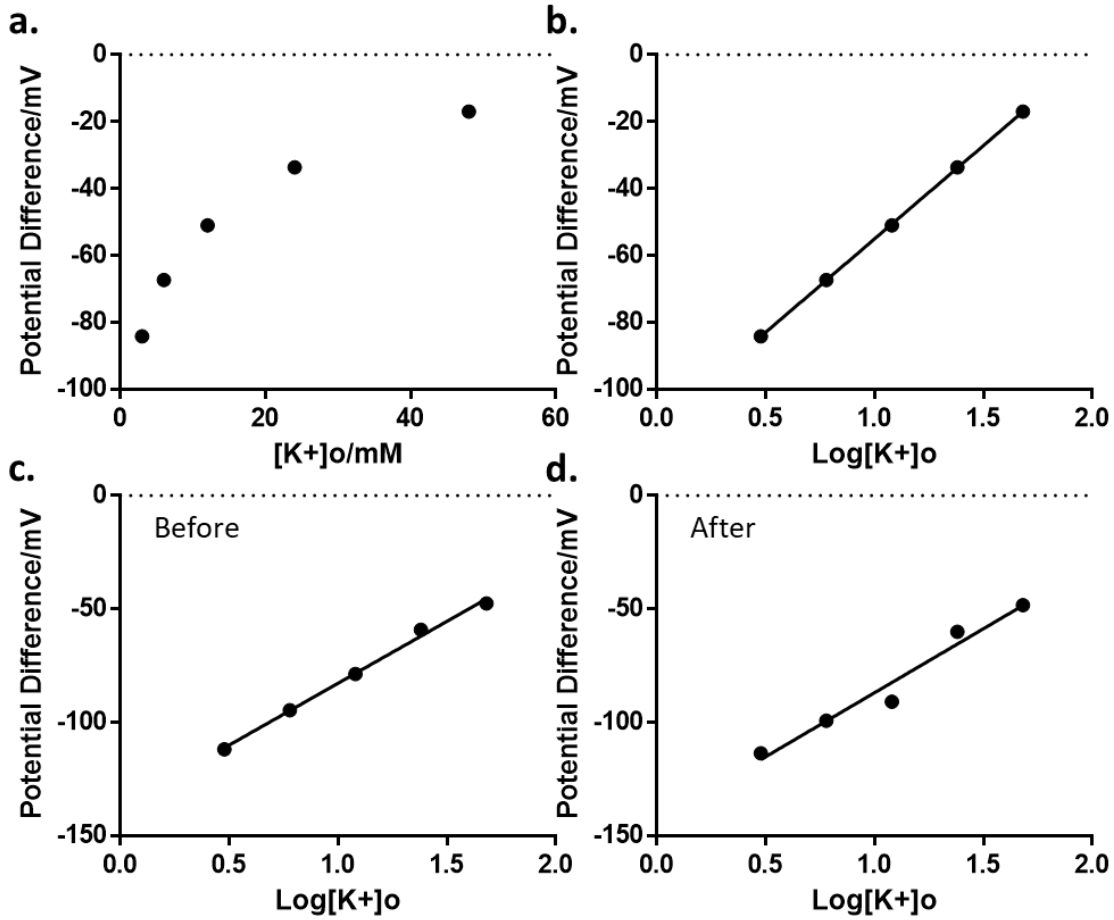

Figure 2. 1. Representative calibrations of potassium selective ISMs.

a. When moved between dishes containing solution with increasing concentration of potassium, potential difference between the dish and electrode solution increased in a logarithmic manner. A mean reading over at least 10 seconds was plotted. **b.** When plotted against the logarithm of potassium concentration, potential difference increase was linear. The slope of this particular electrode was 55.8±0.1mV (R^2=0.9998). This could then be used to determine unknown concentrations of potassium by measuring potential difference. **c-d.** An example of electrode calibration performed before and after an experiment to ensure sensitivity was maintained throughout. Calibration curve slope was 54.6±0.9mV (R^2= 0.9954) before and 56.4±2.6mV (R^2= 0.9634) after experimental use.

2.6.2.2. pH

Microelectrodes were again calibrated in grounded dishes. These contained aCSF of varying pH confirmed using a pH meter. The potential difference recorded by the microelectrodes was plotted against the pH recorded by the pH meter (fig. 2.2). Sensitivity in varying concentrations of confounding ions was not investigated due to the high selectivity of pH-sensitive microelectrode cocktails (Lee, Boron & Parker, 2013). As pH is already a logarithmic scale, a linear regression was fitted to this plot and the slope was used alongside a baseline recording of the grounded perfusion chamber in order to determine pH of the tissue. The mean slope of all electrodes calibrated was -40.9±2.2mV (n=13).

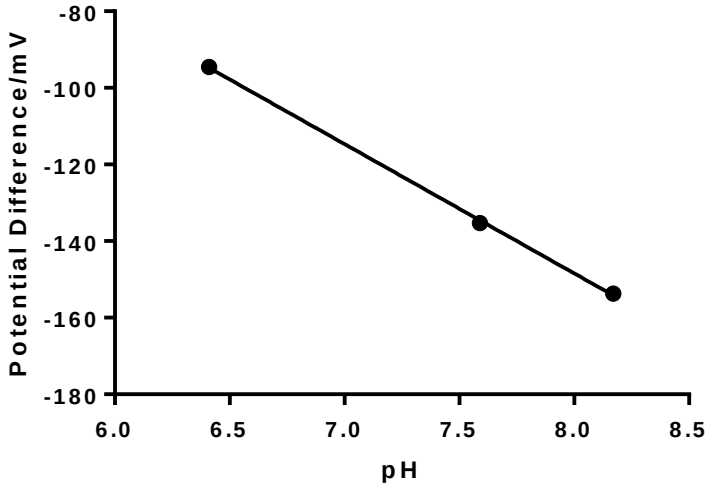

Figure 2. 2. Representative calibration of pH sensitive microelectrodes

The potential difference of three grounded solutions of different pH was recorded and plotted against pH. In this instance, the slope of linear regression was -33.8±0.2mV (R^2=0.9994). This could then be used to determine the pH of brain tissue.

2.6.3. Tissue recording

Electrodes were lowered until touching the tissue and then pushed further as minimally as possible. Recording and reference electrode tips were arranged within 1mm of each other. The entry point for the electrodes into the chamber was made as narrow as possible to limit access of atmosphere. Recordings from the tissue were taken until a stable baseline of at least 10 minutes was achieved before OGD could be initiated. For grey matter (GM) recordings, electrodes were inserted into layer 5 of the secondary motor cortex. White matter recordings were taken from the midline of the corpus callosum. A comparison of grey matter and white matter potassium release mechanics or pH dynamics in equal preparations has not been undertaken before and so findings will be novel and could reveal previously unrealised phenomena.

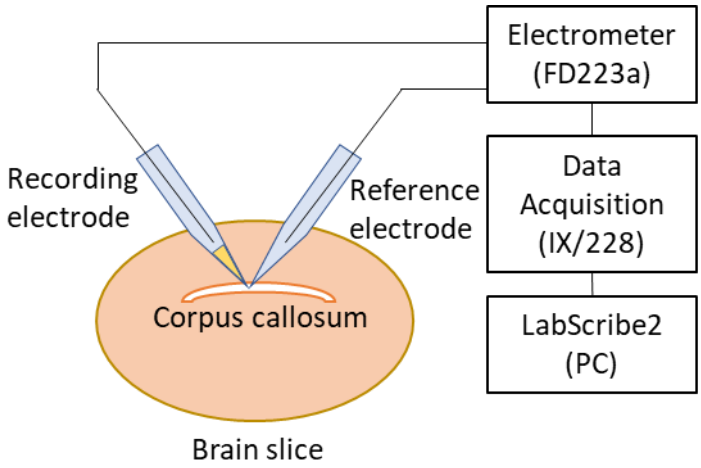

Figure 2. 3. Schematic diagram of ISM recording setup

Recording electrode, with selective ionophore, and reference electrodes were inserted into tissue as close as possible. The differential electrometer observed the potential difference of each electrode which was relayed to the PC via a data acquisition unit. Potential differences were recorded in LabScribe2 and the reference electrode was subtracted from the recording electrode to determine the power of the selected ion.

2.6.4. Data analysis

Raw voltage data were converted to corresponding concentrations in GraphPad Prism 6, using the calibration curve produced for each electrode, to produce a time-course of extracellular ion concentration during and after OGD. Time-courses were compiled for each condition and a mean taken for each time-point.

For potassium, the peak concentration was taken for each time-course and mean for each condition was calculated. This was also performed for the baseline and reperfusion concentrations of potassium. Maximum rate of potassium release was determined by isolating the steepest section of the potassium concentration curve and calculating the slope of a linear regression fit. Half-life of exponential decay values were determined by isolating the period after the peak concentration of potassium and fitting with a decay curve. The half-life of this curve was taken.

For pH, the mean baseline, peak and reperfusion values were calculated as for potassium. The area under the curve during OGD was calculated for each experiment and the mean for grey and white matter were determined.

Graphs are displayed as mean and standard error unless stated. For time-course graphs, points have been pruned by calculating the mean of adjacent points. This is for ease of viewing and care was taken not prune sufficiently to diminish peaks. Significance of difference between the means of selected pairs was performed by one-way ANOVA with Sidak's multiple comparisons. Significance is displayed on the graphs using symbols:

ns	P>0.05
*	0.05≥P>0.01
**	0.01≥P>0.001
***	0.001≥P>0.0001
****	0.0001≥P

2.7. TTC staining

Following an hour of reperfusion after an OGD experiment, brain slices on nylon mesh were transferred to 2% tetrazolium chloride (TTC) in phosphate buffered saline (PBS) at 37°C. Slices were incubated for 15 minutes before transfer to 4% paraformaldehyde (PFA) in PBS. Slices were left to fix overnight and subsequently removed from the mesh and placed in PBS. Slices were imaged using a Leica M80 dissecting microscope with constant settings for each experiment. Images were analysed in Image J. A threshold of red pixel hue was set to distinguish live from dead tissue and this was kept constant for all images. The area of live tissue compared to total tissue was then calculated and mean value determined for each treatment. Statistical significance of treatment groups compared to the control group was established using a one-way ANOVA with Dunnett's multiple comparisons.

2.8. Optic nerve compound action potential recording

2.8.1. Data collection

Nerve tips were put into glass borosilicate suction electrodes filled with aCSF. One end was put into the stimulating electrode which consisted of a single glass tube with one silver chloride wire inside and another wrapped around the base of the tube. These wires were connected to the stimulator (World Precision Instruments – Isostim A320) to produce a bipolar stimulus. The stimulator was in turn connected to a CED – Micro1401-3, which initiated a stimulus pulse upon instruction by the signal6 programme on the computer.

The other end of the nerve was put into one barrel of the recording electrode. This consisted of two glass tubes side by side, each containing a silver chloride wire. These positive and negative wires, along with a ground wire attached to the chamber, were connected to the amplifier (Axon Instruments – CyberAmp 320) in order to boost the recording signal. Signals were then digitised, and subsequently displayed and recorded using Signal 6.

The stimulus amplitude was set supramaximal to that required to achieve the greatest possible action potential throughout the experiment. Compound action potentials were stimulated and recorded every 30 seconds starting 10 minutes before initiating the white matter damage model. Care was taken to ensure constant flow rate of perfusion solution throughout, as changes to this have large effects on the size and shape of compound action potentials.

Upon completion of the experiment, the nerve was crushed using forceps and a final compound action potential was recorded.

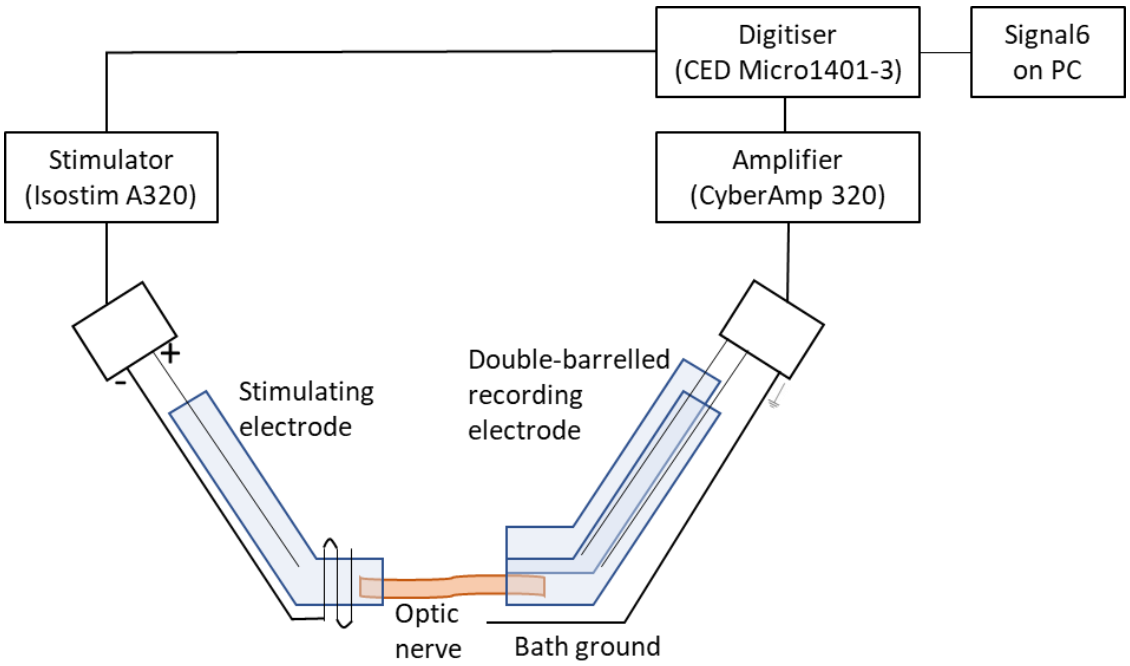

Figure 2. 4. Schematic diagram of CAP recording setup

Optic nerves were stimulated by a bipolar electrode with signals generated by Signal6 software. CAPs were recorded by double barrelled electrodes and amplified before being relayed back to the PC via a digitiser.

2.8.2. Data analysis

For each experiment, the amplitude of each action potential was plotted against time in Signal 6 and then exported to Microsoft excel. In excel, the average CAP amplitude for 10 minutes of baseline recording was calculated. This value was then taken as 1 for normalisation and 0 was set as the amplitude following nerve crush. All CAP amplitudes were normalised, and this was plotted against time. These normalised plots were exported to GraphPad Prism 6 where an average time-course for each treatment could then be plotted. For ease of viewing error bars and to smooth out anomalous spikes, rows were pruned by taking an average of adjacent rows. Furthermore, for each experiment, the mean normalised CAP amplitude for the last 5 minutes of recording was calculated. This was called the endpoint and an average for each treatment group was

established. Mean values were compared to control groups using one-way ANOVA with Dunnett's multiple comparisons. The same symbols were used on graphs as in the ISM experiments.

Chapter 3:

Ischaemia-Induced Potassium Release in Grey and White Matter

Abstract:

Homeostasis of a low concentration of extracellular potassium in the brain is vital to maintain neuronal membrane excitability, prevent destructive enzyme cascades and control cell swelling. During cerebral ischaemia, loss of metabolic supply leads to a breakdown of potassium homeostasis due to failure of the sodium-potassium pump and changes to permeability of some potassium channels. Consequently, extracellular potassium rises dramatically. We investigated whether mechanisms of ischaemia-induced potassium rise differ between grey and white matter of the CNS.

Potassium sensitive microelectrodes were used to measure extracellular potassium concentration in 400µm coronal mouse brain slices, during an hour of oxygen-glucose deprivation. Measurements were taken from the secondary motor cortex in grey matter and the corpus callosum in white matter. The maximum concentration of potassium during ischaemia was found to be higher in grey matter, at 27.1mM, than in white matter, at 16mM. However, when vesicular glutamate transmission was inhibited using a calcium free media or glutamate receptor antagonists, the peak concentration of potassium was significantly reduced in grey matter but not in white matter. Blockade of voltage regulated potassium channels nearly eradicated potassium elevation during ischaemia in both grey and white matter. However, none of these treatments led to increased cell viability as shown by TTC staining. Furthermore, serial exposure to OGD conditions results in a diminished evoked potassium elevation.

Together, the results in this chapter demonstrate that ischaemia induced potassium rise in white matter is not dependent on glutamate transmission as it is in white matter. However, potassium release is likely through voltage dependent potassium channels in both tissues.

3.1. Introduction

3.1.1. Ionic breakdown in ischaemia

One of earliest pathological phenomena of ischaemic stroke is the breakdown of ionic gradients across plasma membranes (Hu & Song, 2017). The negative resting potential of excitable cells is maintained largely by the action of Na^+/K^+-ATPase, which extrudes two K^+ ions in exchange for three Na^+ ions (fig. 3.1). This process is carried out at the expense of dephosphorylating ATP, the energy source for most cellular processes. Thus, in times of extreme energy deprivation, such as ischaemia, the Na^+/K^+-ATPase is prone to failure, impairing the opposition of potassium leak currents. The maintenance of ionic gradients is necessary for structured brain activity and so, this failure is coupled with loss of coordination followed by unconsciousness early on in stroke development.

Increase in extracellular potassium concentration is seen very early on in ischaemia. Prolonged elevation of extracellular potassium concentration can have devastating effects on neural tissue due to its ability to depolarise cell membranes and cause increased intracellular sodium and calcium as well as glutamate release (Krnjevic, 2008). In the rat neocortex, this potassium increase occurs in a three-tiered fashion (Hansen, 1978). A sudden burst of potassium release up to a concentration of around 70mM (fig. 3.1) is preceded by a much slower rise in extracellular potassium activity from a baseline of around 3mM (Somjen, 1979). The duration and threshold of this slow rise appears to be dependent on energy state prior to ischaemic onset. Following the rapid extrusion of potassium, another phase of gradual increase continues until an extracellular concentration of 90mM is reached.

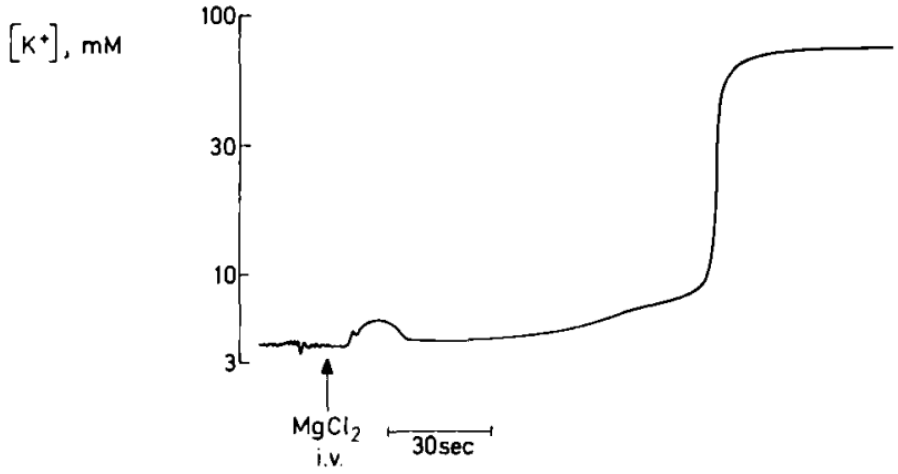

Figure 3. 1. Profile of ischaemia-induced rise in extracellular potassium

Cessation of systemic blood flow by $MgCl_2$ injection causes a gradual increase in extracellular potassium followed by a rapid rise and eventual plateau in the rat cortex. Adapted from (Hansen, 1978).

The initial gradual rise in extracellular concentration is as a result of increased potassium conductance and evokes a hyperpolarisation of the plasma membrane and suppression of spontaneous activity (Krnjevic, 2008). Impaired ATP supply leads to a shift in the ATP/ADP ratio, causing increased potassium current through the K_{ATP} channel (Szeto *et al.*, 2018). K_{ATP} mediated hyperpolarisation of the membrane is thought to be neuroprotective in times of energy deprivation by delaying the onset of anoxic depolarisation (Sun & Feng, 2013; Sun *et al.*, 2006). The subsequent rapid release increase in extracellular potassium is accompanied by an abrupt and stark depolarisation of membrane potential. Depolarisation can be delayed by increasing energy stores with hyperglycaemia prior to ischaemic onset (Hansen, 1978). This is likely the result of synaptic glutamate release, evidenced by increased frequency of miniature excitatory post-synaptic potentials (EPSPs), due to release of intracellular calcium stores (Katchman & Hershkowitz, 1993). This release of intracellular calcium stores is in response to calcium influx via the reversal of the $Na^+/Ca2^+$ exchanger (NCX) which occurs when intracellular sodium levels rise (Lee & Kim, 2015).

Elevated extracellular glutamate concentration can have devastating effects on neural tissue due to sustained activation of NMDA receptors with further depolarisation and a resultant catastrophic influx of calcium ions (Lau & Tymianski, 2010). Pathological intracellular calcium-dependent processes are activated, leading to necrotic and apoptotic cell death. Furthermore, depolarisation-induced cation and anion influx forms an osmotic drive and causes cell swelling and shrinkage of the extracellular space (Rothman, Thurston & Hauhart, 1987), further increasing dangerous extracellular concentrations of glutamate and potassium. Cell swelling itself can also be highly cytotoxic causing blebbing and rupture of the cell membrane (Simard *et al.*, 2007).

3.1.2. Ionic breakdown in white matter

Ischaemia-induced potassium elevation in white matter has been measured to be lower than that seen in grey matter. For example, in the isolated rat optic nerve, a maximum concentration of 14mM was seen during *in vitro* anoxic conditions (Ransom *et al.*, 1992). While anoxic conditions are not as severe as ischaemic, it is clear that variation exists in ionic events in grey matter and white matter. Traditionally this is thought to have been due to a lack of ischaemia-induced glutamate release in white matter, which was believed to be reserved for nerve endings in grey matter (Walz, 2012). Recent evidence suggests that white matter tracts contain glutamate which is released in a vesicular manner in response to electrical activity (Kukley, Capetillo-Zarate & Dietrich, 2007). Indeed, it has been shown that ischaemic conditions initiate the vesicular release of glutamate that acts at NMDA receptors on the myelin sheath and causes disruption and damage (Doyle *et al.*, 2018). Therefore, it is imperative to determine whether glutamatergic signalling is involved with the potassium response in white matter ischaemia.

3.1.3. Potassium channels in the brain

A wide variety of passive potassium channels exist in the membranes of neural cells which may be activated by specific conditions in order to carry a potassium current (fig. 3.2). The most common of these channels are the voltage dependent channels, subdivided into inwardly rectifying (K_{ir}) and outwardly rectifying (K_V) (Hubbard & Binder, 2016). Furthermore, two-pore domain potassium channels contribute to the resting leak current but show no voltage dependence (Braun, 2012).

Inwardly rectifying potassium channels are found extensively throughout the body and play a large role for setting the resting potential of the plasma membrane (Hibino *et al.*, 2010). These channels allow an inward current of potassium (fig. 3.2). Whilst subtypes of K_{ir} channels can be modulated by a variety of factors, such as G-proteins or ATP levels, they are united in that they are deactivated by a change in membrane potential more positive than the potassium equilibrium potential. Therefore, their constitutively active current is ceased by depolarisation of the membrane which occurs during ischaemia. K_{ir} channels are reversibly blocked by micromolar concentrations of Ba^{2+}.

Conversely, outwardly rectifying potassium channels are constitutively closed at the resting potential but opened by depolarisation of the membrane (Hubbard & Binder, 2016). K_V channels conduct an outward current of potassium leading to an increase in extracellular potassium (fig. 3.2). During an action potential, these channels cause a delayed hyperpolarisation of the membrane following depolarisation resulting from opening of voltage-gated sodium channels. This current can be blocked by tetraethylammonium ions.

A further mechanism of increased extracellular potassium concentration is the shrinkage of the extracellular space, instigated by swelling of neural cells due ion

gradient breakdown (Kumura *et al.*, 2003). The degree of shrinkage differs in grey and white matter, being more pronounced in the grey matter as it contains a high proportion of neuronal cell bodies. This may offer an additional explanation for the disparity in peak ischaemia-induced potassium elevation found in grey and white matter.

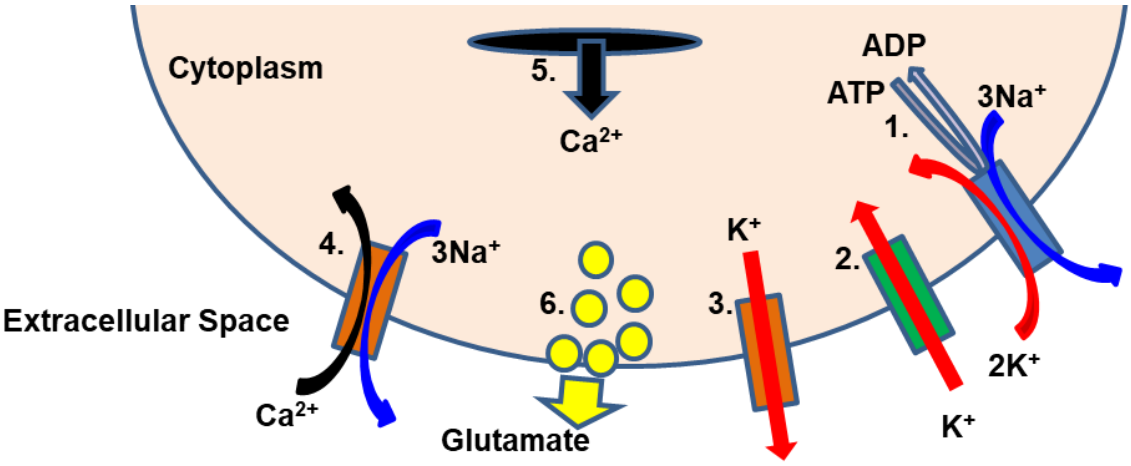

Figure 3. 2. Channels involved in ionic breakdown soon after onset of ischemia.

1. The Na^+/K^+-ATPase is a major driver of the negative resting potential by producing a net extrusion of cations. Potassium ions are taken up into the cell in exchange for sodium ions and the dephosphorylation of ATP. Lack of ATP during ischaemia results in lack of potassium uptake. **2.** K_{ir} allow potassium ions into the cell when the membrane is at resting potential or hyperpolarised. These channels are blocked upon depolarisation **3.** K_V produce an outward current of potassium when the membrane depolarises, which occurs early in ischaemia, but are blocked at the resting potential. **4.** The NCX, under pathological conditions of high intracellular sodium resulting from dysfunction of Na^+/K^+-ATPase, will reverse its usual function and cause accumulation of intracellular calcium. **5.** Elevated intracellular potassium initiates release of calcium from intracellular stores, via activation of receptors such as the ryanodine receptor. **6.** Increased intracellular calcium causes vesicular release of neurotransmitters, most notably glutamate. Glutamate can act at a variety of receptors to further exacerbate calcium entry into cells and initiate a cascade of events leading to cell death.

3.1.4. Potassium buffering

Increased extracellular potassium is a physiological occurrence resulting from membrane depolarisation during signalling and rapid redistribution is required to prevent neuronal impairment and damage during normal CNS function. The extracellular space is restrictive in space and tortuosity. Tortuosity is the obstruction of diffusion through a medium caused by environmental obstacles (Hrabe, Hrabetova & Segeth, 2004). As a result potassium must be cleared through the astrocyte syncytium (Chen & Nicholson, 2000). As the astrocyte membrane remains polarised, potassium is able to enter the cells through inwardly rectifying potassium channels, K_{ir} (Ransom & Sontheimer, 1995). The Na^+/K^+-ATPase is also crucial for the uptake of potassium into astrocytes during periods of high stimulation (D'Ambrosio, Gordon & Winn, 2002). ATP supply for the pump is limited but astrocytes are more capable to maintain function than neurons due to both lower energy expenditure and greater capacity for ATP production in ischaemic conditions (Leis, Bekar & Walz, 2005). As membrane depolarisation does not cause an influx of sodium ions in astrocytes, excessive activity of the sodium-potassium pump is not required to extrude Na^+ from the cells, which reduces ATP consumption (Takahashi *et al.*, 2000). Astrocytes also produce a large proportion of their energy through glycolysis independent of oxygen supply, which is limited in ischaemia (Kasischke *et al.*, 2004). This process can be maintained due to glycogen stores and ATP production can even be enhanced in response to ischaemia by increase in glycolytic enzymes (Brown, Baltan Tekkok & Ransom, 2004; Marrif & Juurlink, 1999). Overall, these specialisations allow astrocytes to continue buffering extracellular potassium for a time in ischaemic conditions.

3.1.5. Potassium clearance in white matter

Astrocytes are crucial for potassium buffering in grey matter but have limited access to myelinated axons. Astrocytes are still involved in potassium clearance in white matter structures with $K_{ir}4.1$ expressed on fine processes that contact at the nodes of Ranvier (Kalsi *et al.*, 2004). However, oligodendrocytes play a pivotal as potassium is most highly released in the internodal region where only oligodendrocytes have access (Bay & Butt, 2012; Larson *et al.*, 2018). Indeed, oligodendrocyte $K_{ir}4.1$ expression has been found within the myelin at juxta-axonal sites such as the inner wrap of myelin, as well as at perinodal sites on the cell body, providing the ideal location for removal of axonal released potassium (Schirmer *et al.*, 2018). Selective deletion of inwardly rectifying potassium channel, $K_{ir}4.1$, from oligodendrocytes in mice causes accumulation of extracellular potassium in white matter (Larson *et al.*, 2018). Furthermore, both astrocytes and oligodendrocytes in the optic nerve have been found to express $K_{ir}2.1$, which associate with $K_{ir}4.1$ to form a more strongly rectifying heteromeric channel (Brasko & Butt, 2018) However, contribution to potassium clearance under ischaemic conditions is yet to be investigated; it is unknown whether oligodendrocyte potassium buffering shows similar resilience to ischaemia compared to astrocytes.

3.1.6. Oxygen Glucose Deprivation

3.1.6.1. Advantages of oxygen glucose deprivation

Oxygen glucose deprivation provides the benefit of allowing detailed observation of mechanistic pathways that would not be possible using an *in vivo* model of ischaemia. For example, continuous monitoring of ion concentrations can be performed using microelectrodes or fluorescent markers which would be unfeasible in a live animal.

OGD is a highly reproducible condition that allows for tight control of variables such as media ion and substrate content as well as temperature. As such, variability of results is minimalised compared to *in vivo* models. This allows reduction in repeats required and, combined with the relative speed of the process, gives a high throughput of data collection.

3.1.6.2. Disadvantages of oxygen glucose deprivation

Removal of tissue or cells from the animal can result in alterations to physiological and pathological processes. For example, oedema is a prevalent pathological event during a stroke that can exacerbate neurological deficits (Dostovic *et al.*, 2016). When contained in the limited space of the skull, this swelling leads to increased intracranial pressure, which can in turn further occlude small blood vessels (Stokum, Gerzanich & Simard, 2016). However, tissues or cells subjected to OGD likely do not have such a volumetric limit and, therefore, will not experience such increased tissue pressure.

One of the major limitations of the isolated tissue OGD model is the lack of circulatory system. As such, there can be no residual perfusion from collateral blood vessels which is seen in focal ischaemia (Cuccione *et al.*, 2016). Additionally, impairment of the blood brain barrier will not result in infiltration of blood borne immune cells, particularly during reperfusion (Feng *et al.*, 2017).

Isolated tissues have a finite duration of viability once removed from the live animal. Usually a brain slice can be maintained for 6 to 12 hours (Buskila *et al.*, 2014). Consequently, OGD can only be used to observe characteristics and test therapeutics in the acute phase of ischaemic injury. Therefore, while OGD is ideal for investigation of early events like ionic dysregulation or glutamate excitotoxicity, it is less useful for observation of chronic occurrences like gliosis.

OGD is a model of global ischaemia, meaning the entire preparation undergoes the same condition. This is at odds with ischaemic stroke, where, generally, a local occlusion leads to focal ischaemia of brain tissue. Focal ischaemia results in a core where ischaemia is near complete, surrounded by partially perfused tissue; this is known as the penumbra and is at risk of cell death. Global OGD models cannot mimic the penumbra, which is where most salvageable tissue is located. Recently a focal OGD model, using microfluidic application of oxygen and glucose deficient media, has been developed (Richard *et al.*, 2010). However, this approach may not be compatible with investigation into white matter, as a rigorous OGD is required for white matter damage (Fern, 2014). Therefore, diffusion of oxygen in the microfluidic system may result in incomplete OGD and lack of white matter damage.

3.1.7. Ion Sensitive Microelectrodes

The two most common methods of observing alterations in ion concentrations are ion-sensitive microelectrodes (ISM) and ion-sensitive fluorescent indicator dyes (Voipio, Pasternack & MacLeod, 1994). Either technique can be used for measurement of intracellular or extracellular ion concentration but have contrasting advantages and disadvantages. While fluorescent indicator dyes are capable of high spatiotemporal resolution, they often suffer greatly in ion electivity with potassium dyes showing similar selectivity for sodium (Minta & Tsien, 1989). Furthermore, until recently, ratiometric potassium indicators had not been developed and so dyes could not be used to determine absolute values of potassium concentration (Shen *et al.*, 2019). Fluorescent indicators can also suffer from photo-bleaching after sustained observation. Ion-selective ionophores used in ISMs ensure high ion specificity and they can easily be used to calculate absolute concentrations (Voipio, Pasternack & MacLeod, 1994). In this

study, ion-sensitive microelectrodes were chosen to measure extracellular potassium concentration due to relative ease of setup and desire to compare absolute extracellular concentrations. Furthermore, measurements would be taken for a long duration which could lead to indicator bleaching or washout from the tissue.

Electrodes consist of a glass capillary pulled to a fine tip. ISM tips are filled with a liquid membrane with selective ion permeability in order to generate a potential difference between the electrode solution and the locus of measurement (Lee, Boron & Parker, 2013). The components of the solution contained in the electrode are carefully calculated and are stable throughout recording. Thus, with calibration, the activity of an ion can be calculated. The tip diameter can be varied depending on whether the ion activity is to be measured in the extracellular space or the cytoplasm. Larger tip diameters will not impale cells and thus record from the extracellular space. The high resistance caused by narrow tip entry point and the liquid membrane result in a relatively slow response time in the magnitude of seconds (Voipio, Pasternack & MacLeod, 1994). However, this degree of resolution is acceptable for measurement of ion dynamics in ischaemia. Accurate measurement of ion activity in a tissue also requires a reference electrode. This is a glass capillary drawn to the same tip and filled with the same solution but contains no ion selective liquid membrane. The reference electrode allows subtraction of interference by changes in field potential which may otherwise confound ion activity measurements.

The relationship between ion activity within and without the electrode can be explained using the Nernst equation. The ion-selective membrane produces a barrier, through which a net flow of electrically charged particles may flow and generate a potential

difference. The equilibrium potential is the electrical drive required to oppose net flow of ions and is given by the Nerst equation:

$$E = \frac{RT}{zF} Ln \frac{a_s}{a_f}$$

R is the gas constant and T is the temperature. The valency of the ion, in the case of potassium is 1, is given by z. F is the Faraday constant, a_f is the ion activity within the electrode and a_s is the activity in the sample. Therefore, at constant temperature, each ten-fold change in ion activity will result in a constant change in potential.

3.2. Aims and Objectives:

This chapter aims to determine whether potassium dynamics differ in grey and white matter during ischaemia. The study aspires to establish mechanisms which may contribute to these variations with the hope that therapeutic targets may be identified to improve outcome of white matter ischaemia.

- Potassium selective ion-sensitive microelectrodes will be used to measure extracellular potassium in grey and white matter regions of a mouse brain slice during oxygen-glucose deprivation.
- The vesicular nature of ischaemia-induced potassium release will be investigated by measuring extracellular potassium in the absence of calcium.
- Involvement of glutamate transmission will be established by employing a combination of AMPA/kainate and NMDA receptor antagonists.
- Voltage dependent potassium channel blockers will be used to investigate the route of potassium release in ischaemia.
- Brain slices will be stained with triphenyl tetrazolium chloride (TTC) to determine whether any of these conditions affects neural cell death.

3.3. Results

3.3.1. Ischaemia causes an increase in extracellular potassium concentration in grey matter

In order to confirm that OGD produces a potassium rise in the preparation, extracellular potassium concentration was measured in layer 5 of the secondary motor cortex (grey matter) during 1 hour oxygen/glucose deprivation and for a further 10 minutes after reperfusion. Following onset of OGD, potassium concentration began to rise after an average of 9.6±4.2 seconds (fig. 3.3). After an initial period of gradual increase, the rate of concentration increase accelerated until a maximal rate of 31.8± 7.0mM/minute was achieved (fig. 3.5b). After a further brief period of gradual potassium release, a peak concentration of 27.1± 2.2mM (fig. 3.5a) was reached 4.33±0.63 minutes into OGD. A slow decline to baseline followed. After restoration of oxygen and glucose, the concentration briefly dropped below the baseline of 3mM.

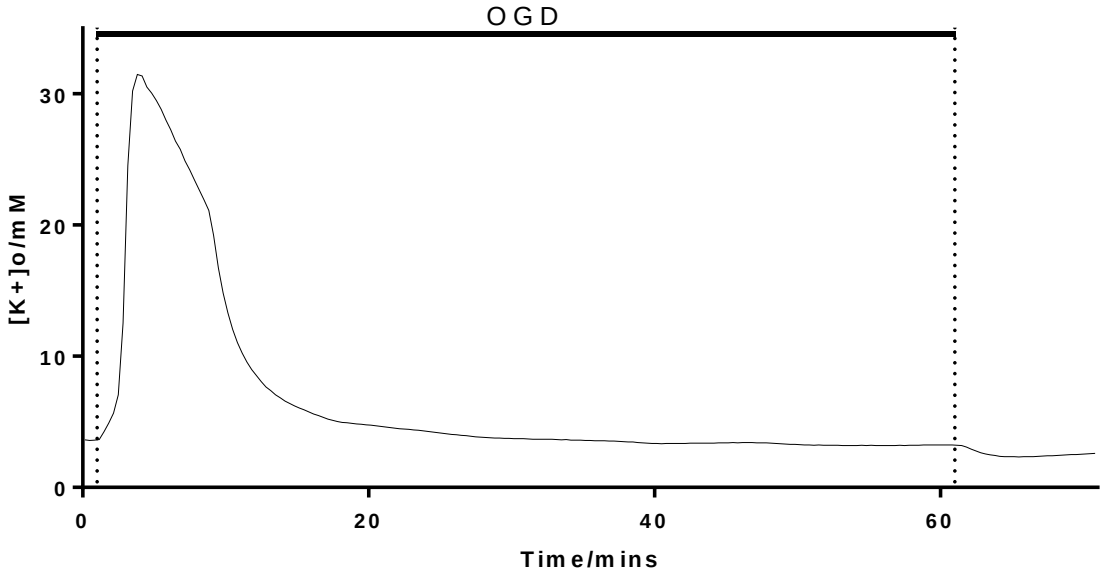

Figure 3. 3. Representative trace of extracellular potassium concentration in grey matter during OGD.

Following onset of OGD, extracellular potassium concentration initially rises slowly before an abrupt uncontrolled release of potassium. A peak is reached after a gradual curtailing of rapid release. Potassium concentration then steadily returns to baseline by the end of OGD. Reperfusion initiates a transient reduction in potassium concentration.

3.3.2. Ischaemia-induced potassium accumulation is more extreme in grey matter than white matter

Previous *ex vivo* investigations (Ransom *et al.*, 1992) have measured a lower anoxia-induced potassium accumulation in white matter compared to that of grey matter in this study. To determine if this characteristic was shared in the current study, potassium concentration was measured in the corpus callosum (white matter) during 1 hour OGD and 10 minutes reperfusion and compared to the profile in grey matter (fig. 3.4c). The baseline of extracellular potassium, prior to initiation of OGD was similar in grey and white matter (3.4±0.4mM, n=5 *vs* 3.1±0.1mM, n=5 respectively. P=0.4, fig. 3.5d). Following OGD initiation, the delay before commencement of potassium accumulation was significantly longer in white matter than grey matter (24.6±1.1 seconds (n=5) vs

9.6±4.2 seconds (n=6) respectively, P<0.0001). This reflects the lower metabolic demand of white matter compared to grey matter and resultant delay in reduction of ATP availability (Harris & Attwell, 2012). As in grey matter, an initial period of gradual extracellular potassium concentration increase was observed before the rate accelerated. However, the maximal rate achieved was much less in white matter compared to grey matter (6.7±1.9mM/minute (n=5) *vs* 31.8±7.0mM/minute (n=5) respectively, P=0.009, fig. 3.5b) suggesting a smaller outward current of K^+ in white matter. Extracellular potassium concentration came to a peak 5.16±1.01 (n=5) minutes after OGD was initiated, similar to grey matter (4.33±0.63 (n=6) minutes, P=0.488). The resulting peak was reduced in white matter compared to grey matter (16.0± 0.9mM (n=5) *vs* 27.1± 2.2mM (n=5) respectively, P=0.0015, fig. 3.5a). In both areas, the concentration began to fall shortly after a maximum was reached. While the rate of decline was greater initially in grey matter, this value was dependent on $[K^+]o$. Therefore, the period of potassium decline was fitted to an exponential decay curve revealing a similar half-life for both grey and white matter (6.1±1.2 minutes (n=5) *vs* 9.9±1.6 minutes (n=5) respectively, P=0.095, fig. 3.5c). This could suggest similar mechanics for extrusion of potassium from the extracellular space in grey and white matter.

After 10 minutes of reperfusion, the extracellular concentration of potassium had recovered to a similar level in both grey and white matter (3.2±0.6mM, n=5 *vs* 2.8±0.3mM, n=5 respectively. P=0.614, fig. 3.5e). The initial baseline concentration of potassium was not dissimilar to the final recovery concentration in either grey or white matter (P=0.892, P=0.919 respectively, fig. 3.5f).

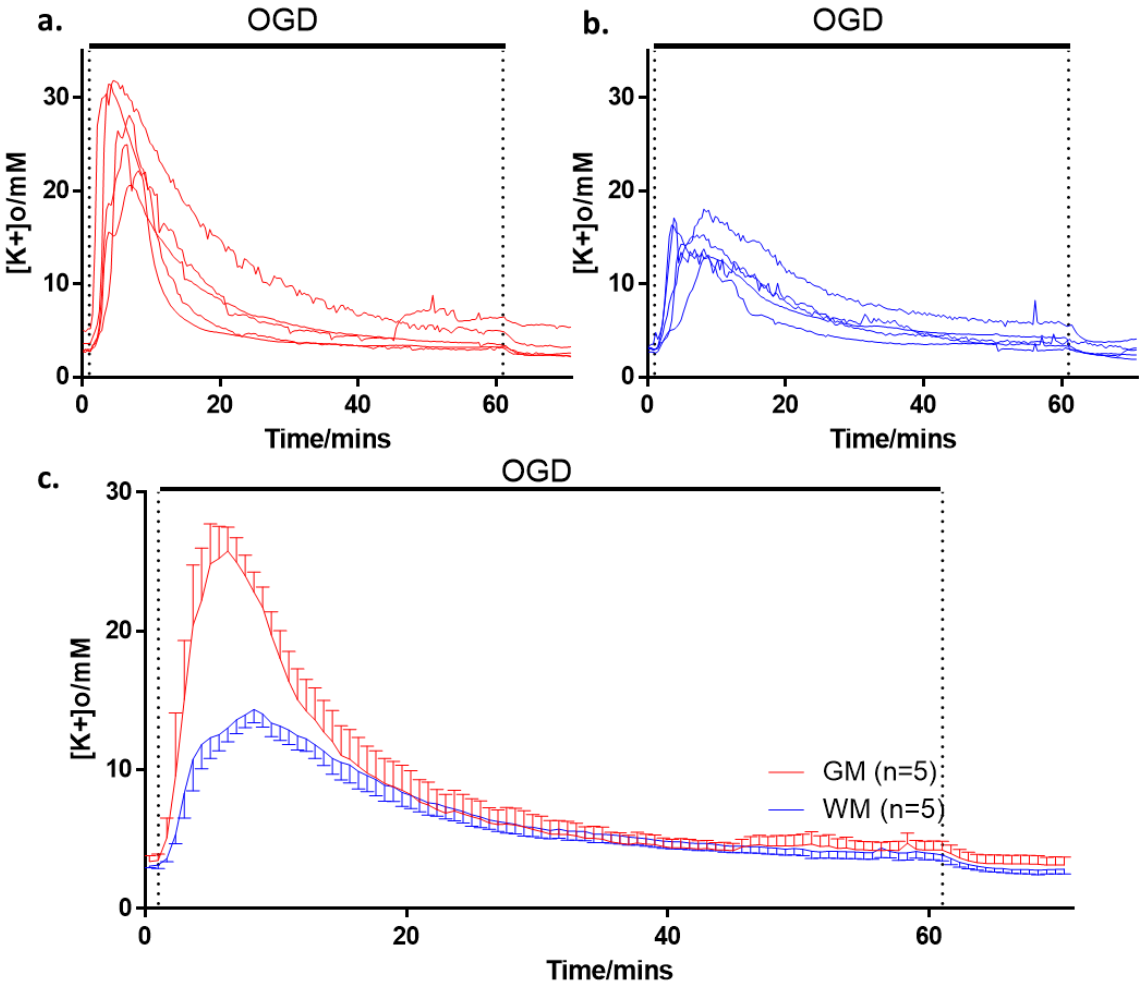

Figure 3. 4. Ischaemia induced potassium release exhibits a different time-course in grey and white matter.

a. Individual time-courses revealing extracellular potassium concentrations in grey matter over the course of 60 minutes OGD and 10 minutes reperfusion. **b.** Extracellular potassium concentration in white matter from brain slices subjected to 60 minutes of OGD and 10 minutes reperfusion. **c.** Average time-courses reveal ischaemia induced potassium release to be of greater magnitude in grey matter than white matter.

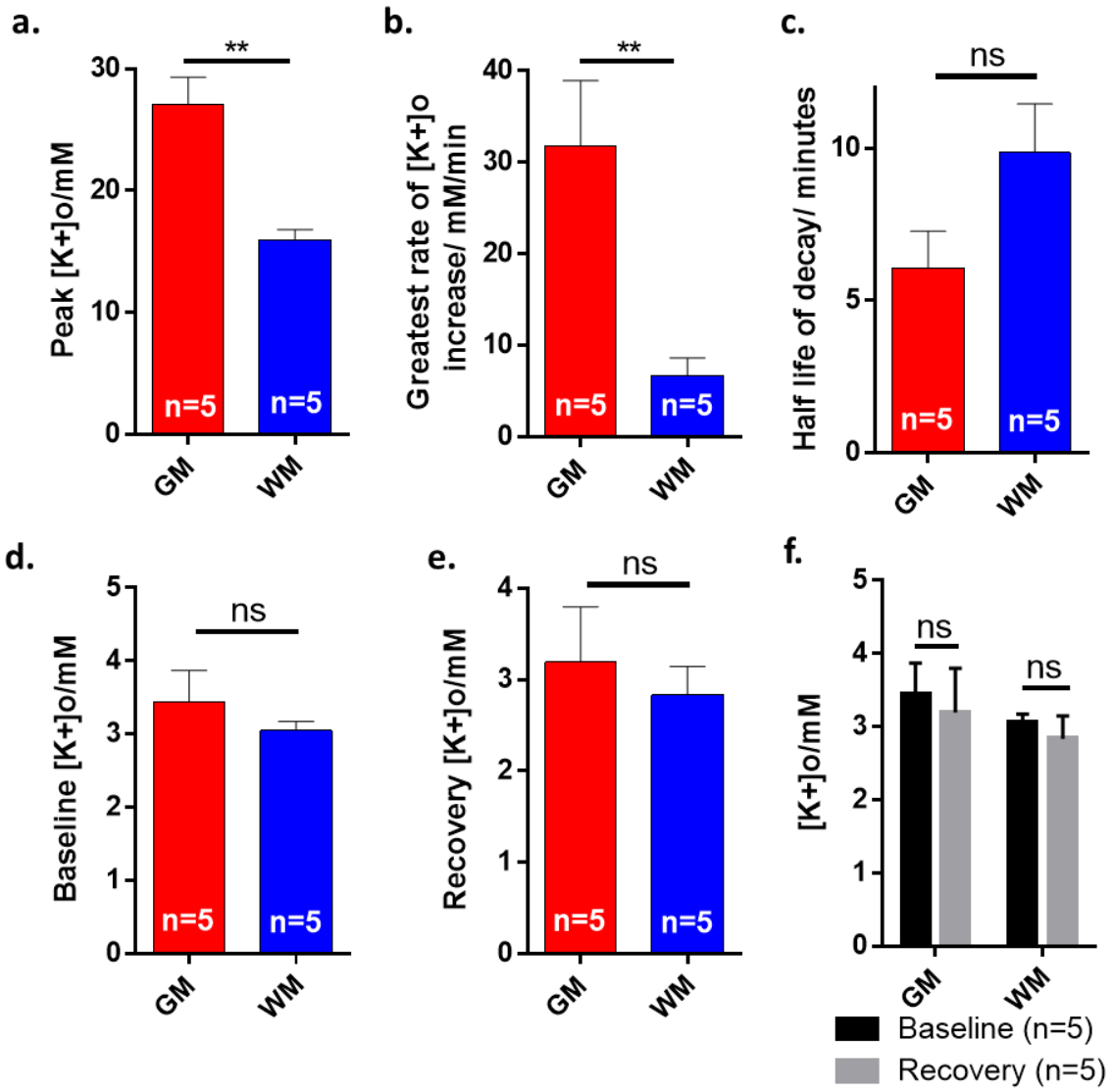

Figure 3. 5. Extracellular potassium concentration rises faster and to a greater level in grey matter compared to white matter.

a. The maximum extracellular concentration of potassium is significantly higher in grey matter than white matter (P=0.0015). **b.** The highest rate of potassium release was also far greater in grey matter compared with white matter (P=0.009). **c.** The half life of potassium concentration decay was similar in both regions with a less than significant trend for a faster decline in white matter (P=0.095). **d.** The extracellular concentration of potassium prior to OGD was not significantly different in grey and white matter (P=0.4). **e.** At the end of reperfusion, there is no significant difference in potassium concentration between grey and white matter (P=0.614). **f.** In grey and white matter, extracellular potassium concentration is similar before and after subjection to OGD (P=0.892, P=0.919 respectively)**.** (**a-e.** Unpaired T-test. **f.** Two-way ANOVA with Sidak's post-hoc).

3.3.3. Calcium removal and chelation reduces potassium release in grey matter

Intracellular calcium elevation is a vital step in vesicular release, essential for synaptic release of glutamate. To investigate the contribution of vesicular glutamate release to ischaemia-induced extracellular potassium elevation, $CaCl_2$ was excluded from the aCSF preparation and 50µM EGTA added to chelate any residual calcium (Fern, 1998). Slices were incubated in the solution for 2 hours prior to recording, in order to ensure maximal washout of endogenous calcium.

Again, the extracellular concentration of potassium was measured in the secondary motor cortex and corpus callosum during one hour of oxygen/glucose deprivation and for 10 minutes after. In grey matter, calcium free media caused a marked alteration in the time-course of ischaemia induced potassium release (fig. 3.6b). This alteration was characterised by a reduction in the peak concentration of extracellular potassium compared to control OGD (16.7±1.8mM, n=4 *vs* 27.1±2.2mM, n=5 respectively. P=0.0079, fig. 3.8b). However, in white matter the time-course was relatively unchanged (fig. 3.7b). The peak potassium concentration was unaffected compared to control (12.9±2.9mM, n=4 *vs* 16.0±0.9mM, n=5 respectively. P=0.734, fig. 3.8b). The maximal rate of potassium release was unaltered by calcium free media with a rate of 31.5±13.9mM/min (n=4, P=0.999) in grey matter and 11.3±6.0mM/min (n=4, P=0.99) in white matter (fig. 3.8c).

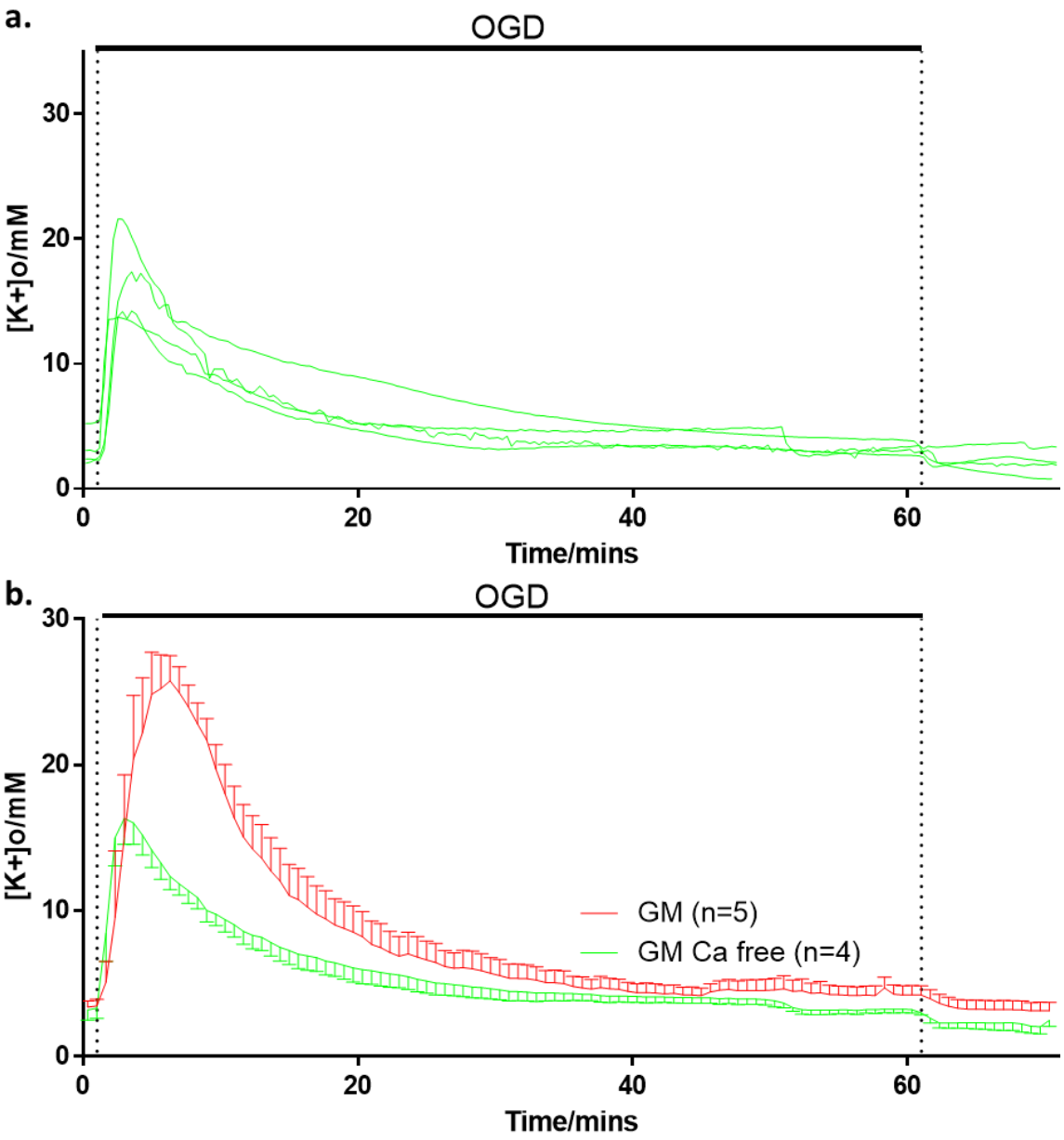

Figure 3. 6. The profile of ischaemia induced potassium release in grey matter is calcium dependent.

a. Time-courses of extracellular potassium during and after OGD in grey matter perfused with calcium free media. **b.** Excluding calcium from perfusate caused a large reduction in the release of potassium in grey matter.

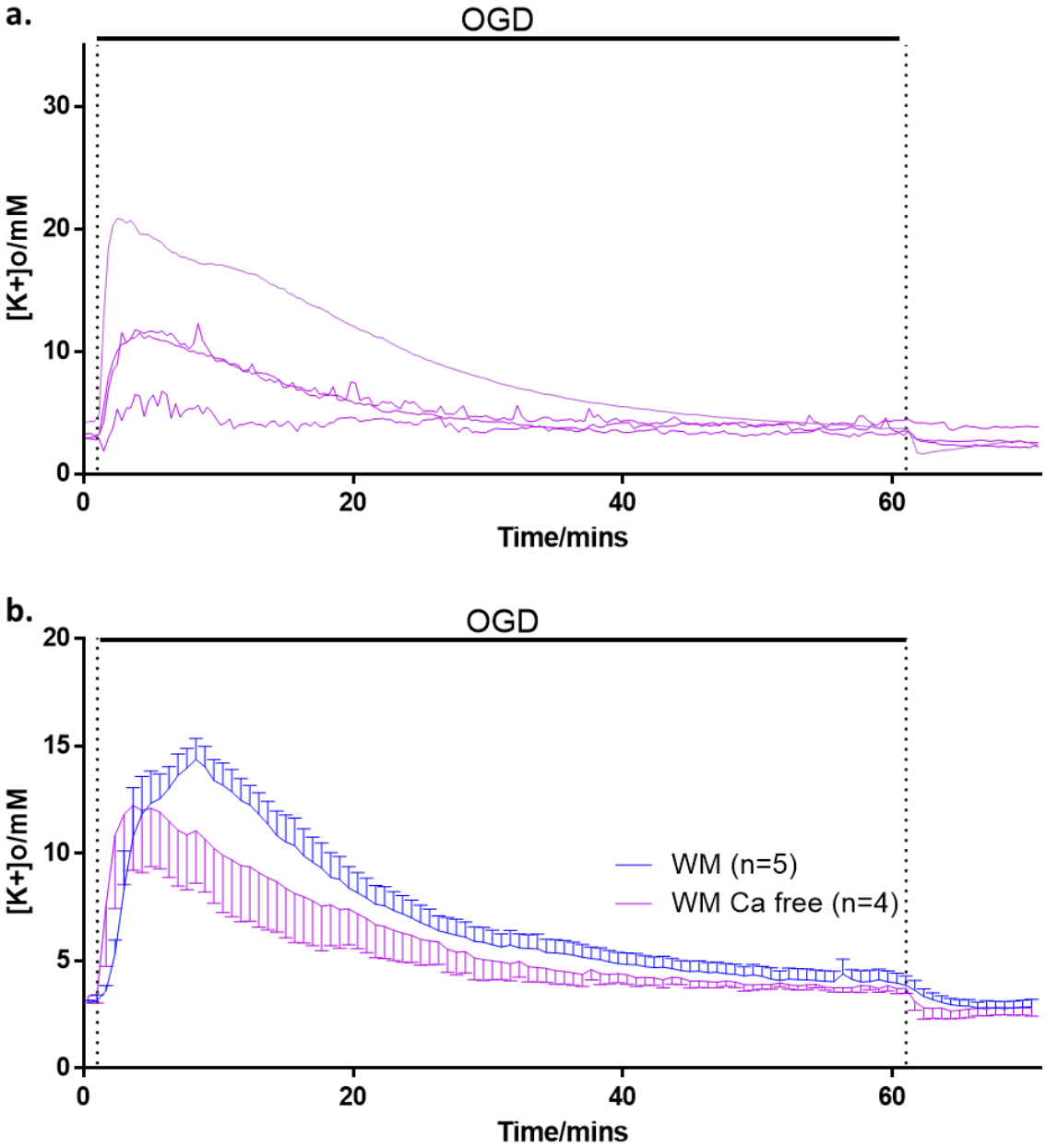

Figure 3. 7. The profile of ischaemia induced potassium release in white matter is calcium independent.

a. Time-courses of extracellular potassium during and after OGD in white matter perfused with calcium free media. **b.** Excluding calcium from perfusate caused relatively little change in extracellular potassium concentration during OGD.

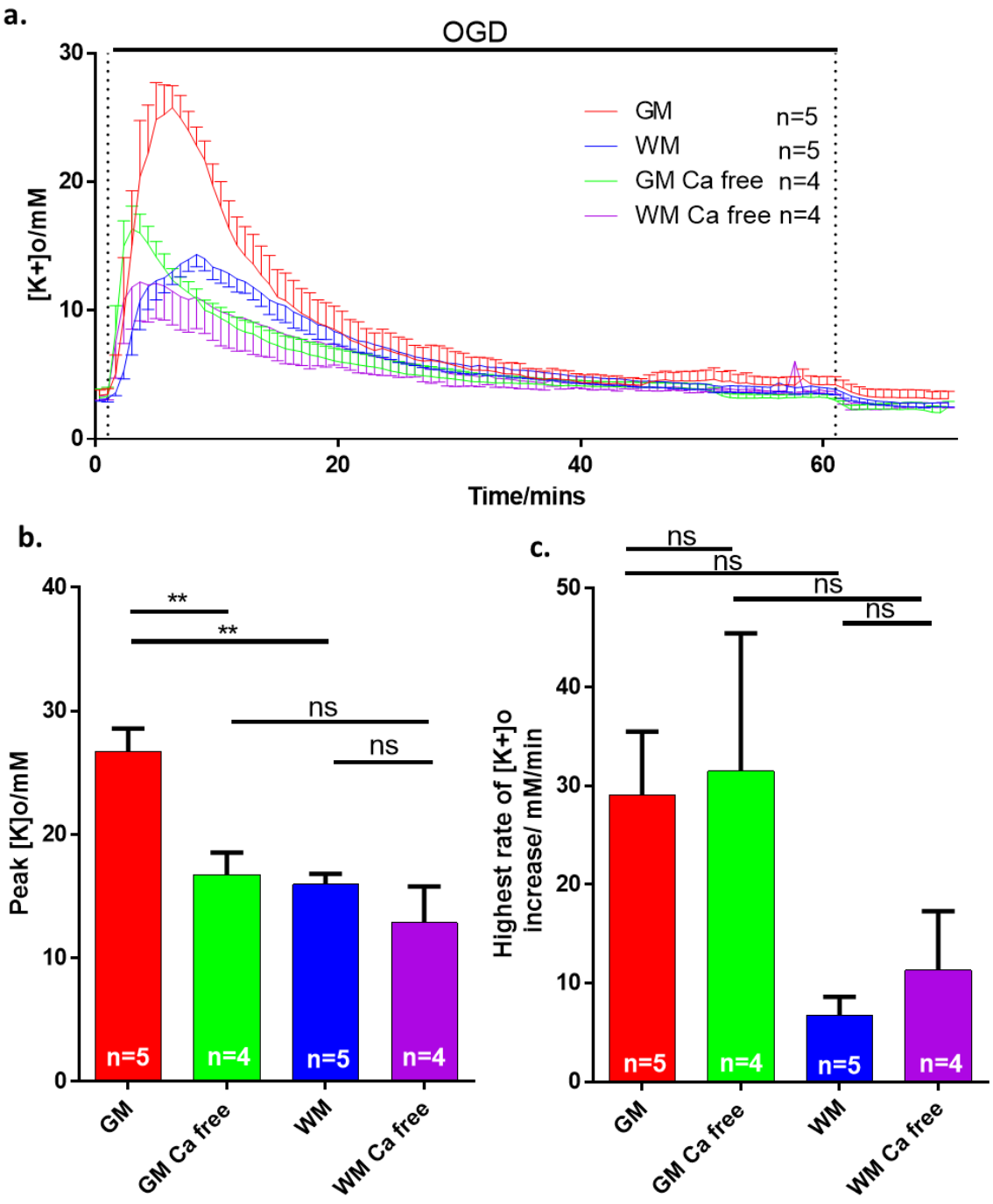

Figure 3. 8. Calcium free media differently affects grey and white matter.

a. Removal of calcium has a profound influence on the time-course of extracellular potassium concentration in grey matter but relatively little effect on white matter compared to their control counterparts. **b.** Calcium free media significantly reduces the peak extracellular concentration of potassium in grey matter (P=0.0079) but has no effect of the peak in white matter (P=0.734). **c.** Removal of calcium from the preparation has no effect on the rate of potassium release in grey or white matter. (One-way ANOVA with Sidak's post-hoc).

3.3.4. Glutamate receptor antagonists reduce potassium elevation in grey matter

In order to confirm the mode of action for calcium removal was prevention of glutamate neurotransmission, potassium accumulation was measured while brains were perfused with glutamate receptor antagonists. The NMDA receptor antagonist MK801 (50µM) and the AMPA/kainate receptor antagonist NBQX (20µM) were combined to achieve maximal reduction in glutamate induced EPSPs. Slices were incubated with the drugs for two hours in order to ensure maximal penetration into hydrophobic myelin.

Recording during one hour OGD and 10 minutes demonstrated a similar profile of potassium release as in control conditions but with a diminished maximal concentration (fig. 3.9b). Similar to calcium removal, glutamate receptor antagonism resulted in a significantly lowered peak concentration of extracellular potassium in grey matter compared to control conditions (17.4±1.4mM, n=4 *vs* 27.1±2.2mM, n=5 respectively. P=0.0036, fig. 3.11b). As in the calcium removal experiments, white matter potassium release was unaffected by the treatment (15.5±2.0mM, n=4 *vs* 16.0±0.9mM, n=5 respectively. P=0.994, fig. 3.11b).

Furthermore, addition of 50µM MK801 and 20µM NBQX caused a large reduction in the maximum rate of potassium release elicited by OGD compared to control (5.4±1.7mM/min, n=4 *vs* 31.8±7.0mM/minute, n=5 respectively. P=0.0074, fig. 3.11c). However, in white matter, there was no change in release rate with glutamate antagonists compared to control (7.6±2.6mM/min, n=4 *vs* 6.7±1.9mM/minute, n=5 respectively. P=0.999, fig. 3.11c). This suggests that glutamate neurotransmission is required for the rapid release phase two seen in Hansen's work (Hansen, 1978) and this study's grey matter control OGD.

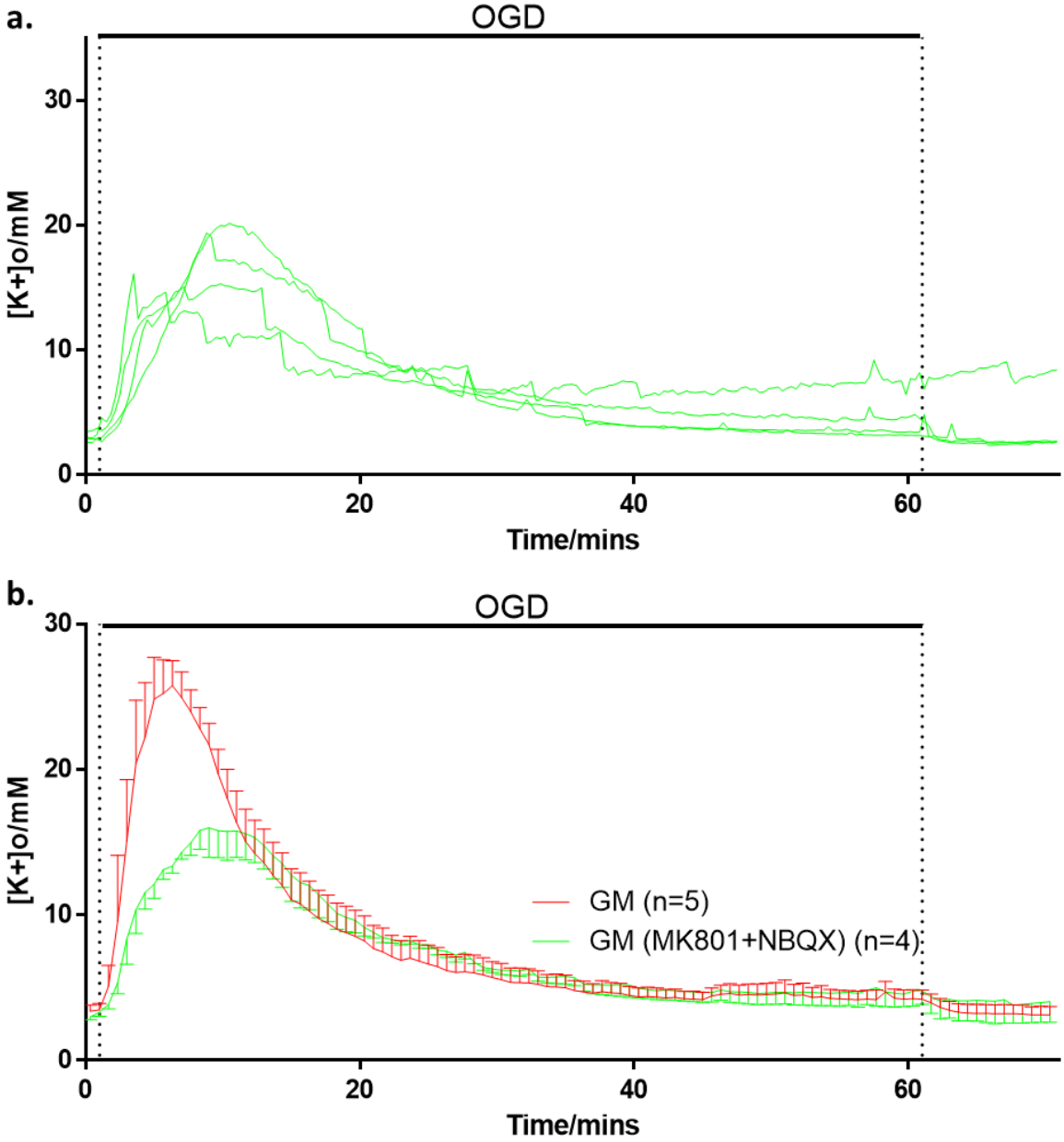

Figure 3. 9. The profile of ischaemia induced potassium release in grey matter is dependent on glutamate transmission.

a. Time-courses of extracellular potassium during and after OGD in grey matter perfused with media containing MK-801 (50µM) and NBQX (20µM). **b.** Antagonism of glutamate receptors caused a large reduction in the release of potassium from OGD in grey matter.

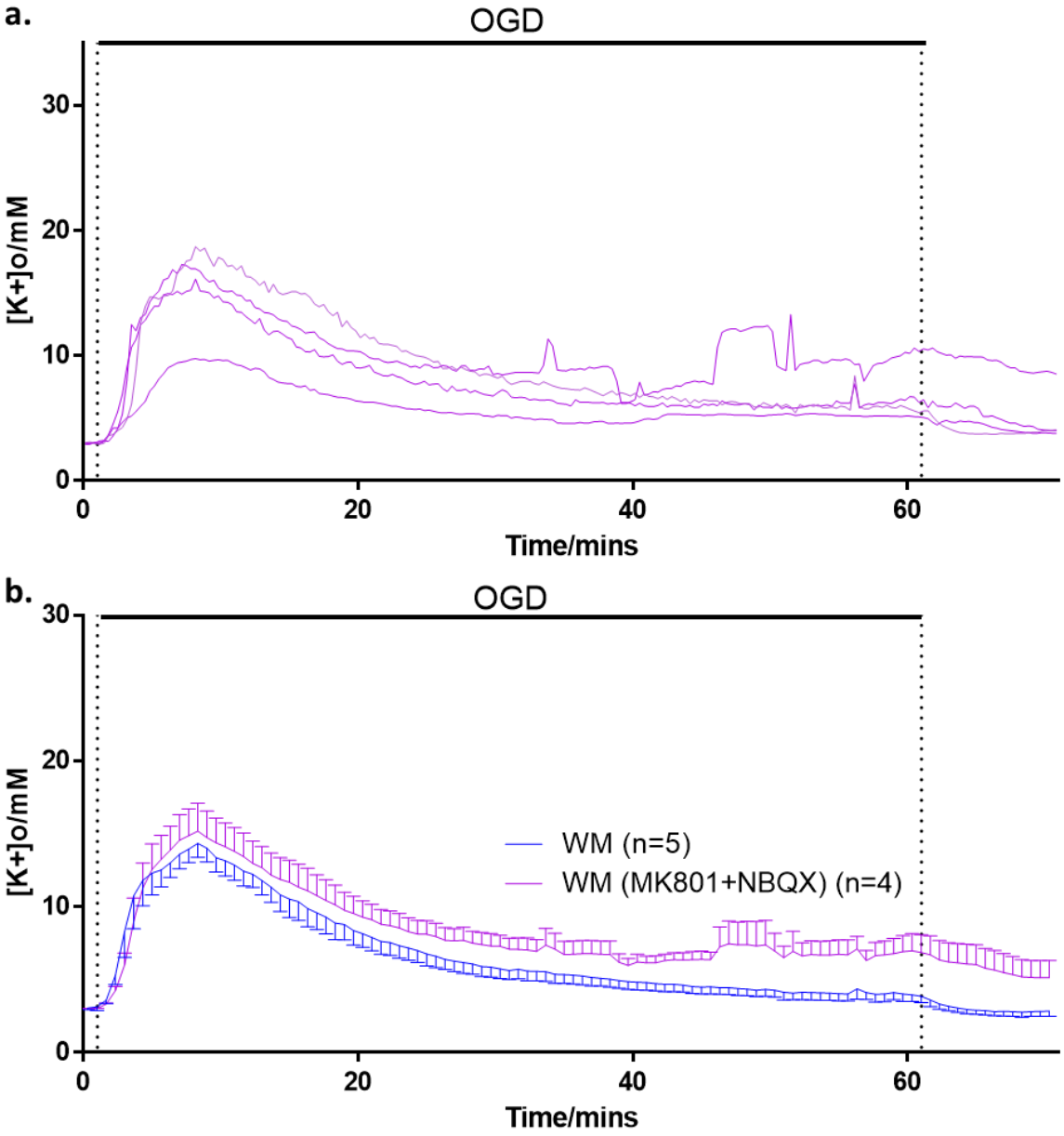

Figure 3. 10. The profile of ischaemia induced potassium release in white matter is not dependent on glutamate transmission.

a. Time-courses of extracellular potassium during and after OGD in white matter perfused with media containing MK-801 (50µM) and NBQX (20µM). **b.** Antagonism of glutamate receptors caused relatively little change in extracellular potassium concentration during OGD.

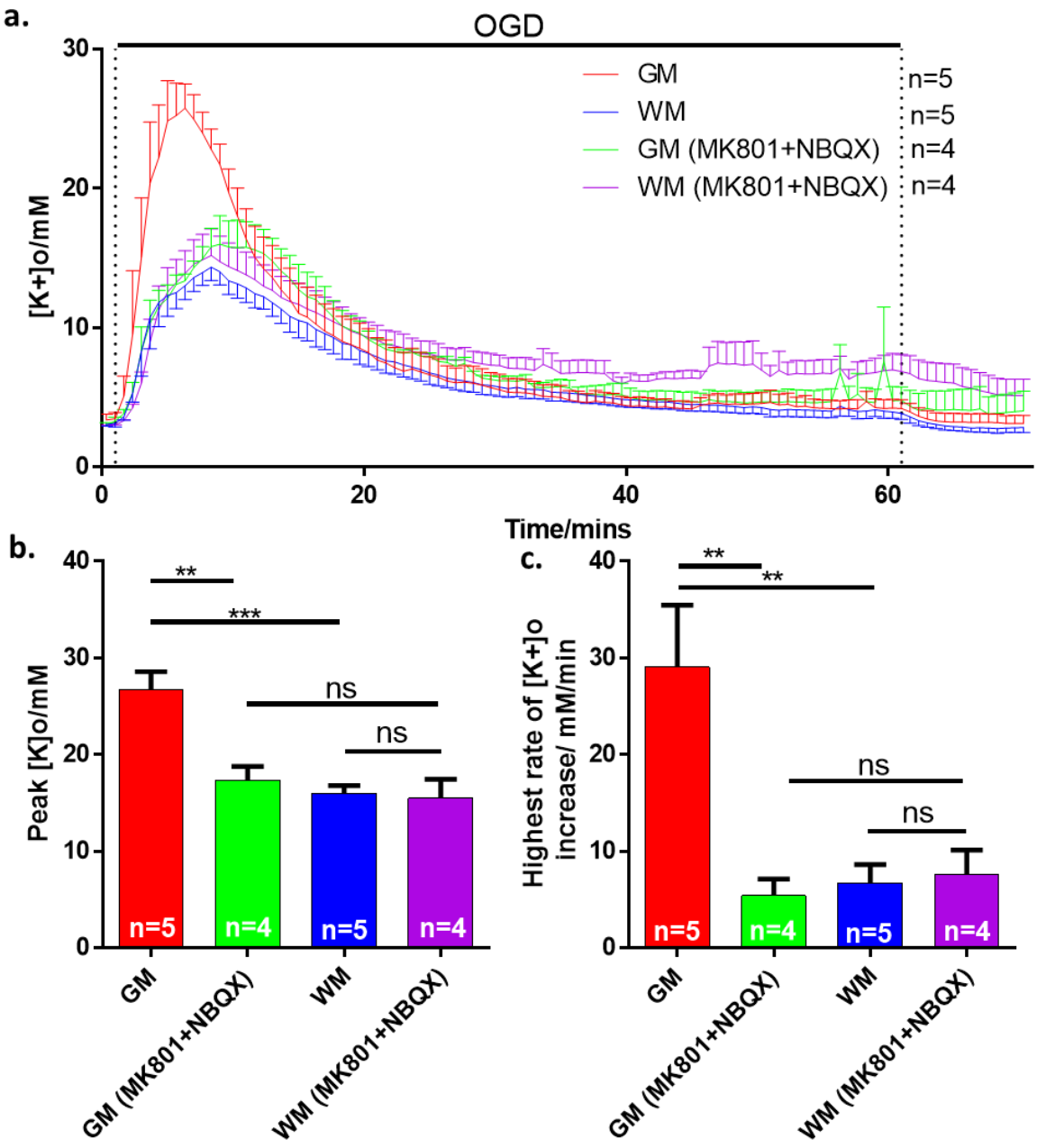

Figure 3. 11. Glutamate receptor antagonism reduces the peak and rate of ischemia induced potassium release.

a. Glutamate receptor antagonism with MK801 (50µM) and NBQX (20µM) causes a stark contrast in ischemic extracellular potassium concentration profile in grey matter while not affecting white matter. Potassium elevation in grey matter appears to occur much slower and to a lesser extent in grey matter in the presence of glutamate receptor antagonists. **b.** The peak concentration of potassium during OGD is significantly reduced by glutamate receptor antagonism in grey matter (P=0.0036) but not white matter (P=0.994). **c.** Addition of MK801 and NBQX significantly reduced the maximum rate of potassium release caused by OGD in grey matter (P=0.0074) but did not affect white matter (P=0.999). (One-way ANOVA with Sidak's post-hoc).

3.3.5. Broad-spectrum voltage dependent potassium channel blockers do not eradicate extracellular potassium concentration increase caused by ischaemia

In order to investigate the mechanism by which extracellular potassium concentration increases during OGD, slices were incubated with TEA (10mM) and $BaCl_2$ (300µM) (fig. 3.12 and fig. 3.13). These conditions block outwardly rectifying voltage gated potassium channels, K_V, and inwardly rectifying potassium channels, K_{ir}, respectively (Lenaeus *et al.*, 2005; Wang, Chiamvimonvat & Duff, 1993). The peak concentration of potassium measured in the extracellular space during OGD was significantly reduced by potassium channel blockers in grey matter compared to control OGD conditions (10.9±1.5mM, n=5 *vs* 27.1±2.2mM, n=5 respectively. P<0.0001, fig. 3.14b). The same was true of white matter, with TEA and $BaCl_2$ treated slices yielding a significantly lower peak concentration of extracellular potassium compared to control OGD (5.5±0.6mM, n=5 *vs* 16.0±0.9mM, n=5 respectively. P<0.001, fig. 3.14b). When taking into account the baseline potassium concentration of 3mM, potassium channel blockers reduced elevation in grey matter to 33% of control while this value was 19% of control on white matter. This suggests that mechanisms of potassium release, alternative to voltage dependent potassium channels, contribute more in grey matter than in white matter.

By contrast, no significant difference was found between the rate of potassium release in grey matter with and without TEA and $BaCl_2$ (27.1±13.2mM/min, n=5 *vs* 31.8±7.1mM/min, n=5 respectively. P=0.998, fig. 3.14c). The same was true comparing treated slices with untreated slices when measuring from white matter (1.3±0.1mM/min, n=5 *vs* 6.7±1.9mM/min, n=5 respectively. P=0.976, fig. 3.14c).

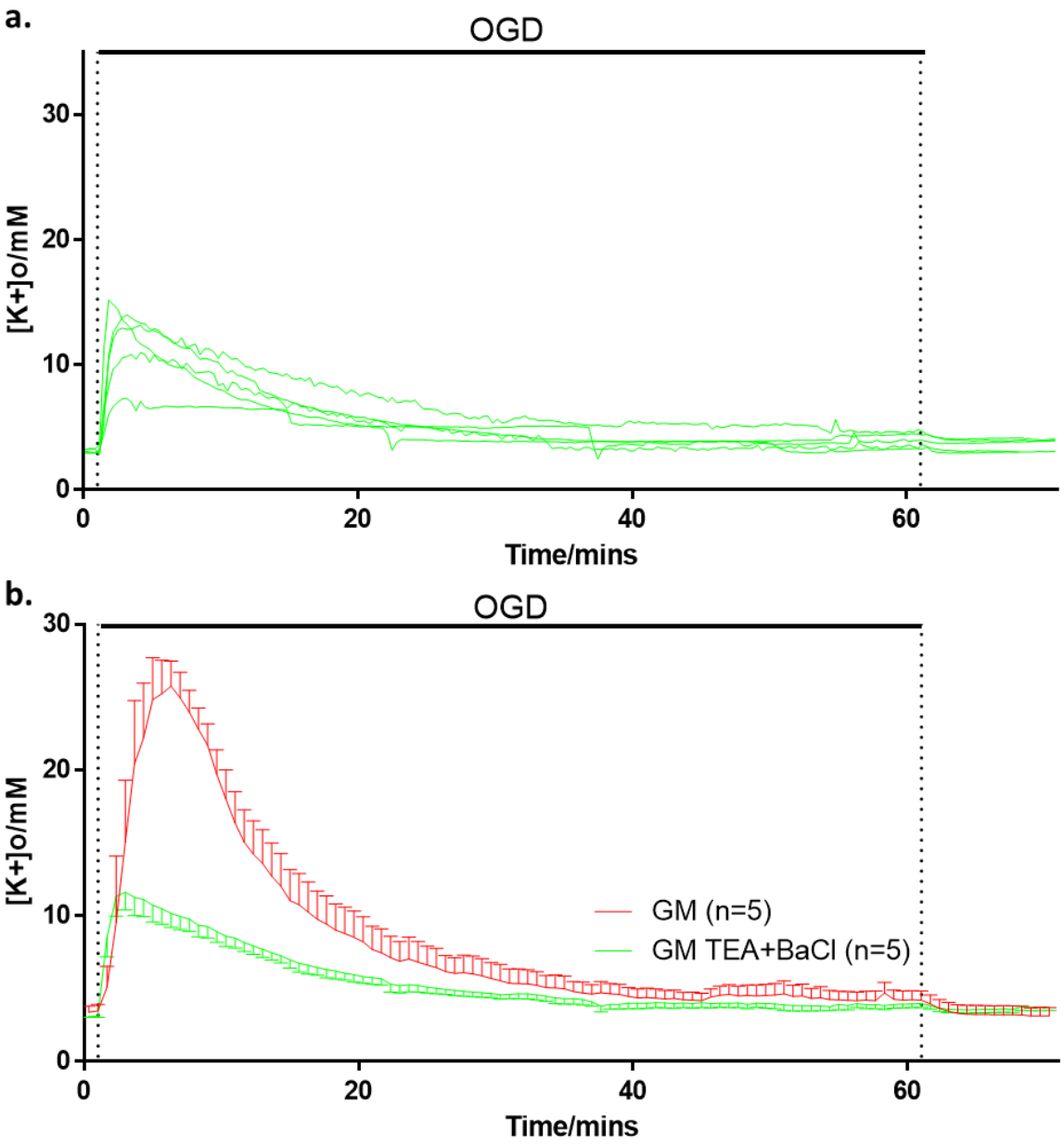

Figure 3. 12. Ischaemia induced potassium release in grey matter is dependent on open voltage gated potassium channels.

a. Time-courses of extracellular potassium during and after OGD in grey matter perfused with media containing TEA (10mM) and $BaCl_2$ (300µM). **b.** Blockage of potassium channels caused a large reduction in the release of potassium from OGD in grey matter.

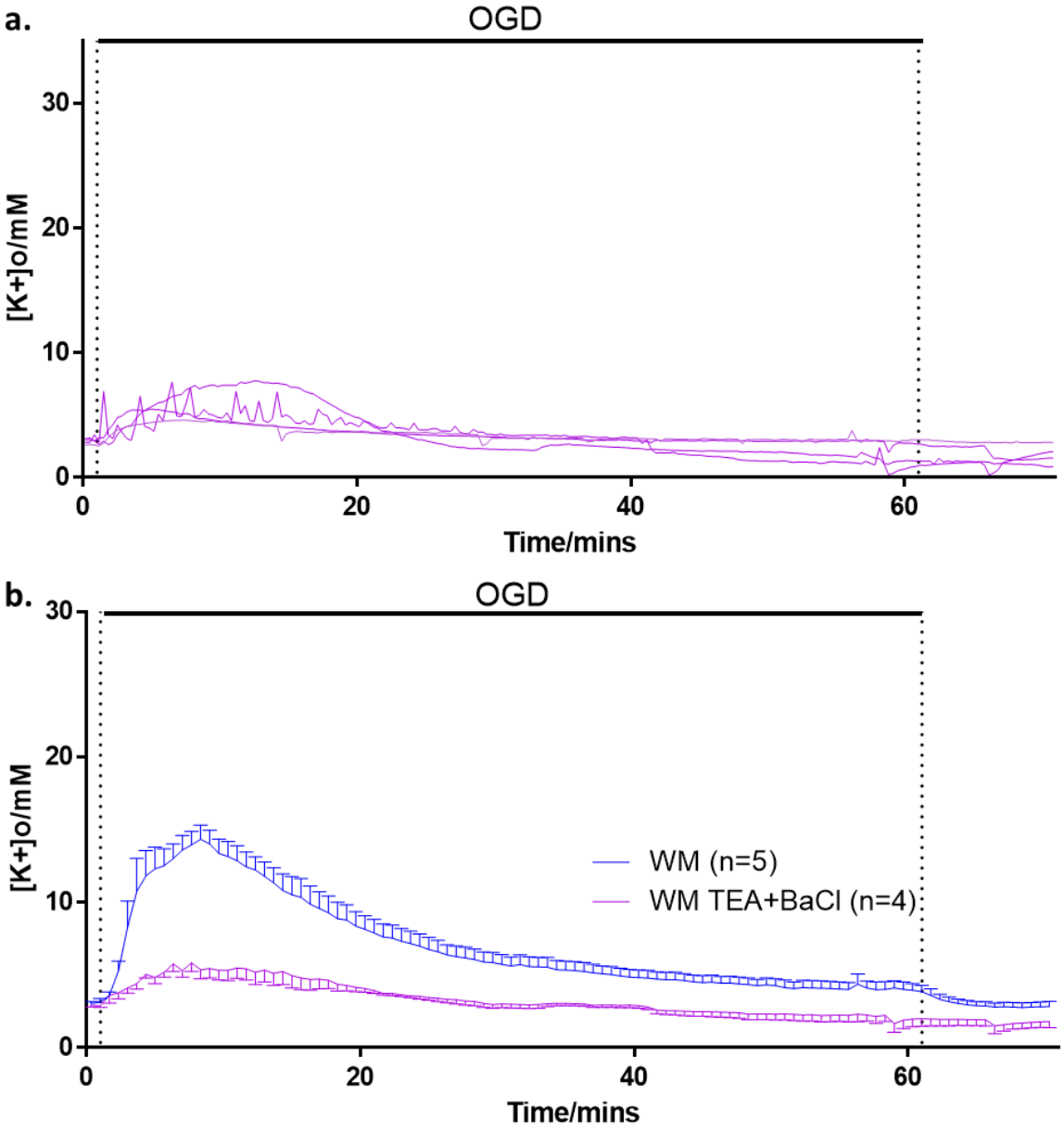

Figure 3. 13. Ischaemia induced potassium release in white matter is dependent on open voltage gated potassium channels.

a. Time-courses of extracellular potassium during and after OGD in white matter perfused with media containing TEA (10mM) and $BaCl_2$ (300µM). **b.** Blockage of potassium channels caused a large reduction in the release of potassium from OGD in white matter.

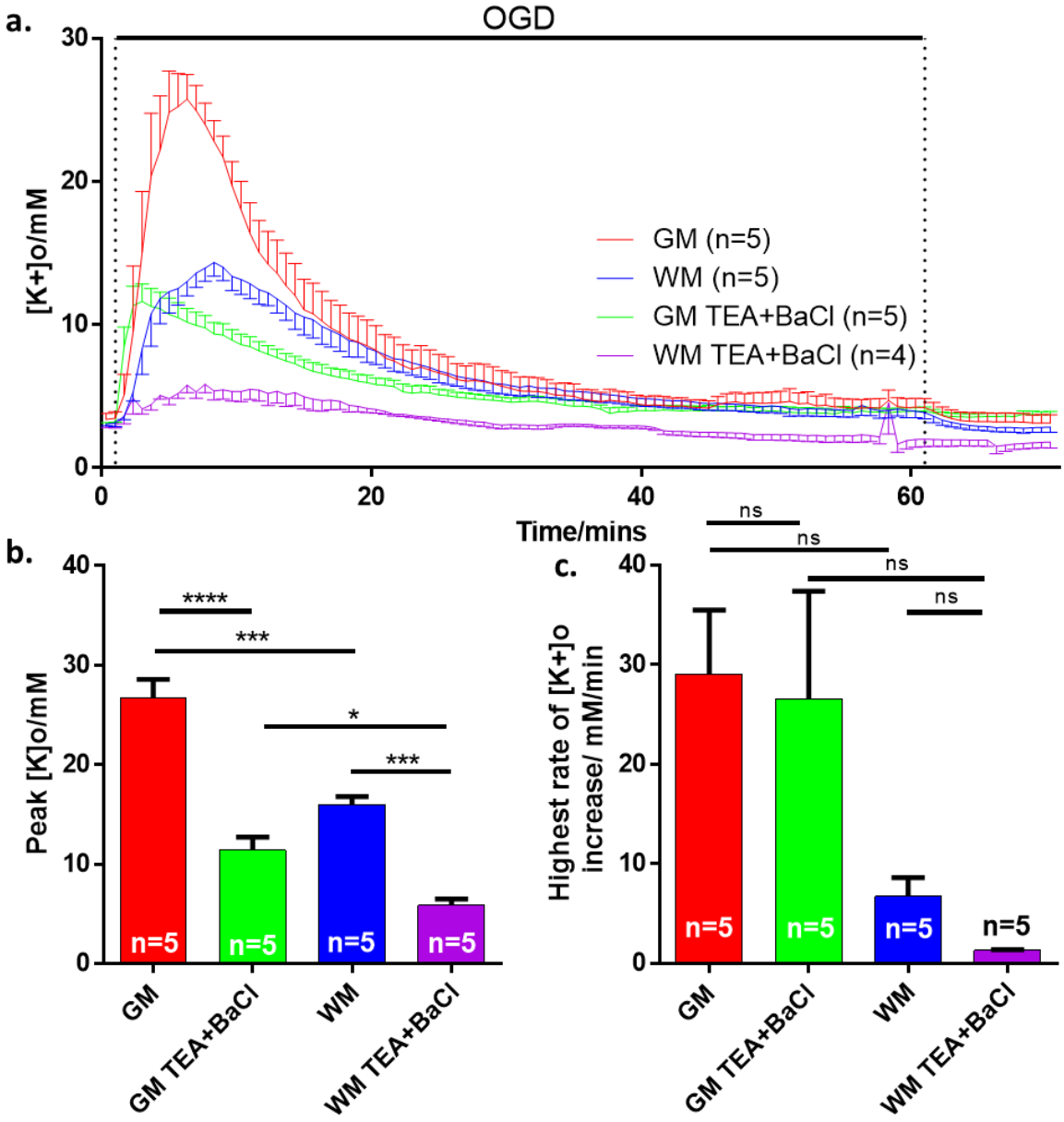

Figure 3. 14. Broad potassium channel blockage reduces but does not abolish ischemia-induced potassium release.

a. The profile of potassium release from both grey matter and white matter is drastically changed by addition of TEA (10mM) and $BaCl_2$ (300µM). **b.** Peak concentration of potassium elicited by OGD is significantly reduced by potassium channel blockers in grey and white matter ($P<0.0001$, $P=0.001$ respectively). However, OGD still results in the increase in extracellular potassium. **c.** The maximum rate of potassium release during OGD is unaffected by potassium channel blockers in grey or white matter. (One-way ANOVA with Sidak's post-hoc).

3.3.6. Tissue survival is unaffected by treatment conditions

In order to investigate the neuroprotection provided by the treatments, which had reduced extracellular potassium accumulation, TTC staining was employed to visualise live tissue and tissue damage. Tissue which had remained viable was stained red while dead tissue was not (fig. 3.15a).

Under control conditions, one hour of OGD and one hour of reperfusion resulted in 22.7±4.9% (n=6) of the tissue remaining alive (fig. 3.15a). This was significantly less than in slices which had not undergone OGD (86.1±9.9%, n=2, P=0.001). When supplied with calcium free aCSF and 50µM EGTA, 35.6±6.8% (n=7) of the slice remained viable. Addition of 50µM MK801 and 20µM NBQX, to inhibit glutamate neurotransmission, to the aCSF resulted in live tissue making up 28.6±10.5% (n=4) of the slice. When supplied with 10mM TEA and 300µM $BaCl_2$, to block potassium channels, 29.3±10.3% (n=4) of the tissue remained living. None of the treatment conditions were significantly different to control OGD conditions indicating lack of neuroprotection (P=0.43, P=0.915, P=0.888 respectively. Fig. 3.15a).

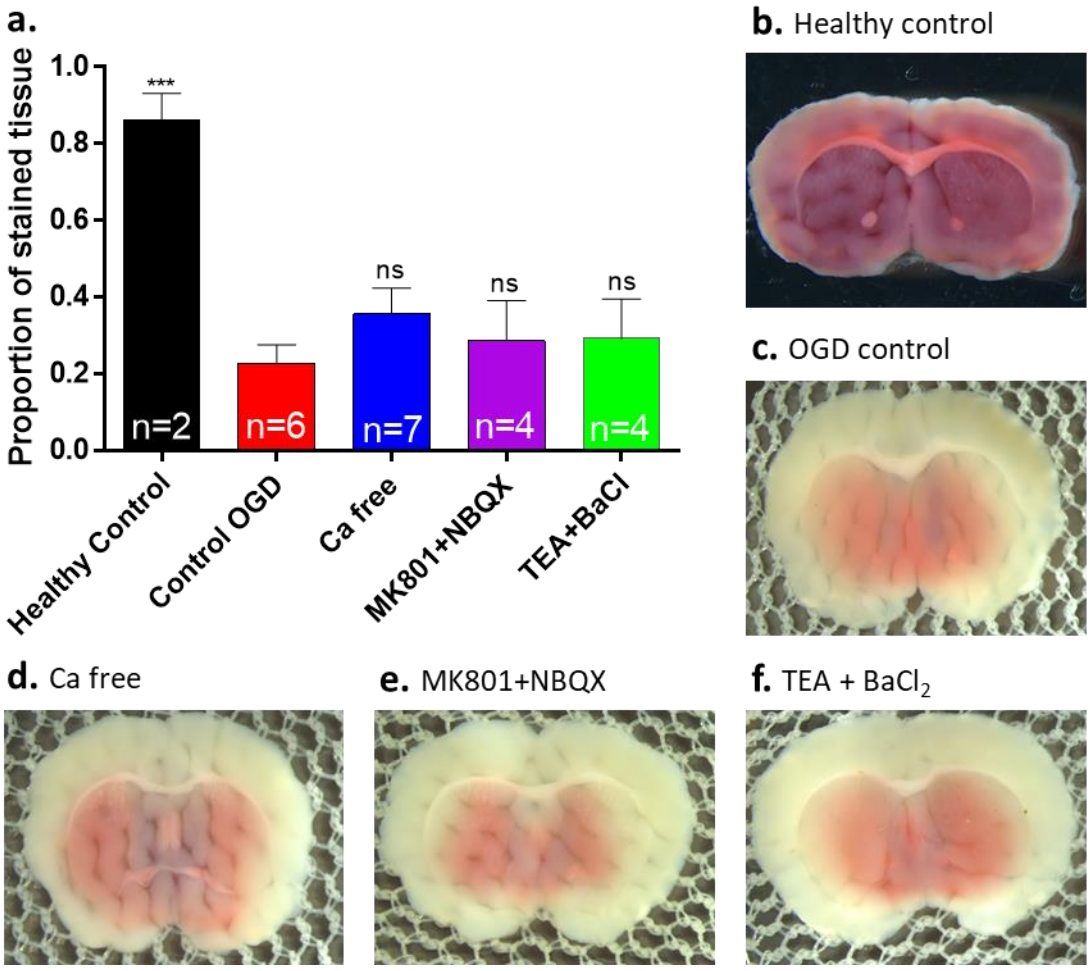

Figure 3. 15. Treatments did not increase tissue survival from 1h OGD.

a. One hour OGD significantly reduced the proportion of TTC staining relative to normal conditions (P=0.001). There was no significant difference between the proportion of red tissue to total tissue in slices treated with calcium free media, glutamate receptor antagonists and potassium channel blockers compared with OGD control conditions. **b-f.** Representative brain slices stained with TTC for each experimental condition. (One-way ANOVA with Dunnett's post-hoc).

3.3.7. Repeat OGD results in diminished potassium release

Considering the novel, gradual decline in $[K^+]o$ observed throughout 60 minutes of OGD, it was imperative to determine whether extracellular potassium was being taken up into glial cells and redistributed to neurons or whether it was lost from the tissue in the perfusate. In order to investigate this, brain slices were subjected to a truncated period

of OGD followed a short reperfusion step and another brief period of OGD. Extracellular potassium was measured throughout.

During the initial 20 minutes of OGD, the time-course of extracellular potassium concentration was similar to that seen in the previous experiments (fig. 3.16a). The duration was not sufficient for the concentration to fall to baseline. Upon reperfusion, potassium concentration rapidly fell back to baseline and remained at this level for the duration of reperfusion. Secondary OGD resulted in a rise in extracellular potassium, though the peak was significantly diminished relative to primary OGD (7.2±0.5mM, n=6 *vs* 31.2±5.0mM, n=6, respectively. P=0.0039, fig. 3.16b). The peak potassium concentration during the secondary OGD period was in fact similar to that measured at the end of the primary 20 minute OGD (7.9±0.8, n=6. P=0.346, fig. 3.16c).

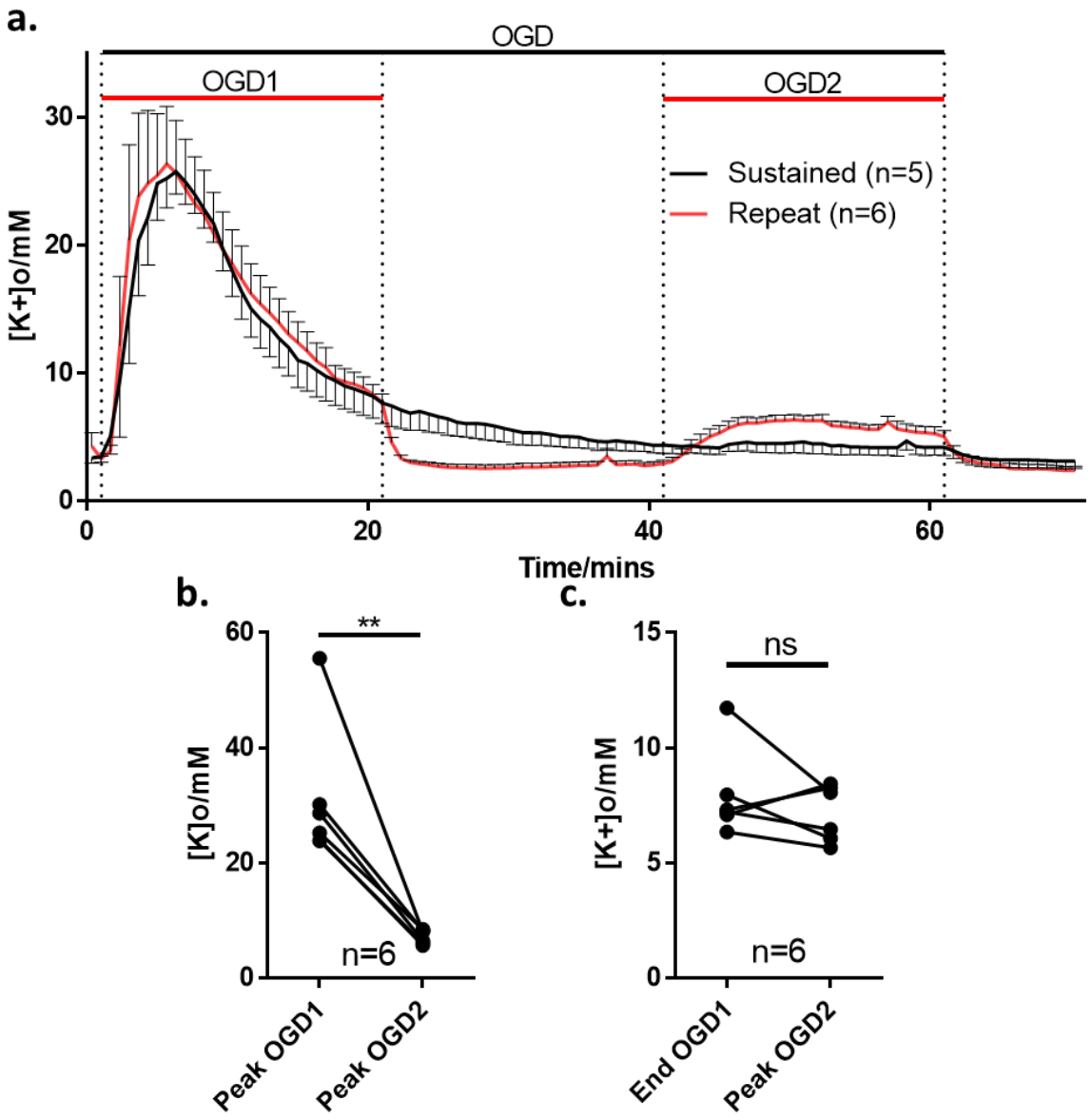

Figure 3. 16. Potassium stores are not replenished by brief reperfusion.

a. Time-course of repetitive OGD application reveals far diminished potassium release in subsequent OGD. The trend in extracellular potassium during secondary OGD is greater than the same period of sustained OGD. **b.** The peak of OGD-induced potassium release was significantly less during secondary OGD compared to the initial OGD (P=0.0039, n=6). **c.** There was no difference in extracellular potassium concentration at the end of the initial OGD and at the peak of secondary OGD (p=0.346, n=6). (Paired T-test).

3.4. Discussion

Ischaemia-induced potassium release is a well-established phenomenon. It has long been assumed that lack of synaptic input in the white matter would result in a diminished increase in extracellular potassium. However, recent advances demonstrating synapse-like communication between axons and myelin may challenge this assumption. The present study used potassium sensitive microelectrodes to measure extracellular potassium in grey and white matter of the mouse brain slice, during OGD. This technique confirmed that ischaemia-induced potassium rise is greater in grey matter than white matter. Furthermore, by inhibiting synaptic transmission, using calcium free media or glutamate receptor antagonists, it was shown that potassium release in grey matter is dependent on vesicular glutamate while this is not the case in white matter. Therefore, glutamate released at the axo-myelinic synapse in white matter is not responsible for rise in extracellular potassium during ischaemia.

3.4.1. Ischaemia-induced potassium fluctuations can be measured with ISMs

The goal of the present study was to determine differences in potassium release mechanics in grey and white matter, with particular interest in glutamate mediated release. However, in order to realise these goals, the ability to measure changes in extracellular potassium first had to be established.

The temporal profile of extracellular potassium concentration in the ischaemic rat cortex has been well characterised (Hansen, 1978). Therefore, by comparing the profile in the *ex vivo* mouse brain slice preparation, the validity of the use of ISMs in this preparation could be proven. Indeed, a similar release profile to that found by Hansen was observed in the secondary motor cortex of the mouse brain slice. There was a very brief period of

gradual increase in potassium concentration followed by a sharp acceleration in release rate. This was succeeded by a third phase of more gradual increase until a peak was reached after around 5 minutes of oxygen glucose deprivation. However, while the profile of extracellular potassium was similar, the values were far lesser in the mouse brain slice compared to the live rat brain. Peak extracellular potassium concentrations in the present study were similar those measured in the cortex of rat brain slices subject to OGD, where a maximum of 32mM was recorded (Perez-Pinzon, Tao & Nicholson, 1995).

There are several possible reasons for the variation in maximal potassium concentration between the models. There are great differences in susceptibility of animals to ischaemic insult, indeed, even between strains of mice. This is evidenced by the high variability in infarct volume created by middle cerebral artery occlusion in different rodent strains (Carmichael, 2005). Consequently, the animals may have different susceptibilities to ischaemia-induced potassium release. Probably of greater consequence is the shrinkage of the extracellular space caused by oedema during ischaemia. In the cat cortex, global cerebral ischaemia *in vivo* results in significant shrinkage of the extracellular space within 10 minutes (Kumura *et al.*, 2003). This reduction in volume will result in increased concentration of any contents of the extracellular space, including potassium. However, shrinkage will be less apparent in the current *ex vivo* brain slice model due to the lack of the restrictive volume of the skull. Consequently, the exacerbation of extracellular potassium concentration will be less pronounced than in the rat study by Hansen. Additionally, the study of global ischaemia in cats revealed that extracellular space shrinkage resulted in increased tortuosity. This means that K^+ released into the interstitial fluid will not be readily redistributed to areas

of lower concentration or the blood in the *in vivo* rat model. Added to this, the cessation of blood flow by injection of $MgCl_2$ in Hansen's study would prevent clearance of potassium from the brain. However, in the current *ex vivo* model, tortuosity will be less effected due to lack of shrinkage and so the excess potassium will be readily redistributed into the perfusate. This will result in a less exacerbated peak in extracellular potassium concentration. The variation of peak extracellular potassium measurement in different models of ischaemia is explored in Table 2.

Table 2: Ischaemic extracellular potassium dynamics

Reference	Brain region	Paradigm	Peak $[K^+]o$	Notes
		In vivo		
(Hansen, 1977)	Cortex	Nitrogen inhalation (10 mins)	90mM	Sustained plateau
(Hansen, 1978)	Cortex	Cardiac arrest (240s)	85mM	
(Hansen, Gjedde & Siemkowicz, 1980)	Cortex	Neck pressure cuff (10 mins)	75mM	Sustained plateau
	Basal ganglia	Neck pressure cuff (10 mins)	78mM	Sustained plateau
(Astrup, Rehncrona & Siesjo, 1980)	Cortex	Cardiac arrest (10 mins)	56mM	
(Gido, Kristian & Siesjo, 1997)	Cortex	MCAo (2h)	60mM	Sustained plateau
(Sick, Feng & Rosenthal, 1998)	Cortex	MCAo (3h)	58mM	Sustained plateau in the core, transient in penumbra
(Mori *et al.*, 2002)	Cortex	Cardiac arrest (15 mins)	65mM	ECS[1] shrunk 15%
(Stiefel & Marmarou, 2002)	Cortex	CCAo + hypotension (60 mins)	67mM	Continuous rise throughout
(Graf *et al.*, 2001)	Cortex	CCAo (120 mins)	~110mM	Sustained plateau
	Corona radiata	CCAo (120 mins)	~110mM	Rise until 60 mins
		Ex vivo		
(Perez-Pinzon, Tao & Nicholson, 1995)	Cortex	OGD until AD	32mM	ECS[2] shrunk 50%
	CA1	OGD until AD	45mM	ECS[2] shrunk 64%
	CA3	OGD until AD	12mM	ECS[2] shrunk 15%
(Ransom *et al.*, 1992)	Optic nerve	Anoxia (15 mins)	14mM	Slight decline after peak. ECS[2] reduced 18%

MCAO, middle cerebral artery occlusion; ECS, extracellular space; CCAo, common carotid artery occlusion; OGD, oxygen-glucose deprivation; AD, anoxic depolarisation.

[1] Calculated using cortical impedance

[2] Calculated from concentration of TMA^+

The current study established that potassium selective ISMs are able to measure fluctuations in extracellular concentration during oxygen glucose deprivation of a mouse brain slice. However, it must be noted that absolute values determined by this technique will not reflect values attained in human cerebral ischaemia. Thus, the technique can be used to determine proportional differences elicited in different brain regions and by different conditions.

3.4.2. Ischaemia-induced potassium release is greater in grey matter than white matter

The extracellular concentration of potassium during OGD was compared in layer 5 of the secondary motor cortex and in the corpus callosum. This process revealed that the profile of potassium rise was similar in both CNS components but differed in peak concentration where grey matter was significantly higher than in white matter. As the peak occurred at a similar time in both areas, the rate of increase in potassium concentration was greater in grey matter than in white matter.

This is the first time ischaemia-induced potassium release mechanisms have been investigated in grey and white matter in equal preparations and so these data provide novel insight into the differences between the two regions. Previous studies have investigated anoxia-induced potassium release in an isolated rat optic nerve (Ransom *et al.*, 1992). It was found that extracellular potassium rises to approximately 14mM in the anoxic rat optic nerve. This is only marginally lower than the 16mM found in the mouse corpus callosum in the present study. This minor discrepancy may be as a result of anoxic injury being less extreme than ischaemia. Furthermore, there may be differences between white matter regions, such as the presence of non-myelinated axons in the corpus callosum (Swadlow, Waxman & Geschwind, 1980). Additionally, the optic nerve

has no surrounding grey matter that may interact, or cause spread of a higher concentration of potassium, such as may occur in the corpus callosum.

There are several factors which may contribute to the difference in peak potassium concentration in grey and white matter. Again, the shrinkage of the extracellular space may play a role. Oedema disproportionately affects grey matter, resulting in an exacerbated reduction in extracellular volume compared to grey matter (Kumura *et al.*, 2003). This would cause a less pronounced increase in concentration of interstitial contents in white matter. However, shrinkage is also slower in white matter than grey matter, but there was no delay of peak potassium concentration seen.

Another possible reason for the lower potassium concentration during white matter ischaemia is the location of voltage gated potassium channels on axons. In myelinated axons, type 1 potassium channels are located in the juxtaparanodal region on the axon cylinder beneath the myelin sheath (Calvo *et al.*, 2016). As the majority of potassium release during white matter ischaemia is from axons, much of this will be contained within the periaxonal space, away from the measuring capability of the ISM. It would be very useful to determine the concentration of potassium reached in the periaxonal space during white matter ischaemia as this disturbance could act on the axon cylinder or the myelin to induce injury. However, due to the miniscule size of the space, a fluorescent potassium indicator would likely be required.

Both grey and white matter possess mechanisms for clearance of extracellular potassium, but these are overwhelmed in ischaemia. In grey matter, this process is primarily performed by astrocytes (Kofuji & Newman, 2004), whereas, in the white matter, oligodendrocytes play a pivotal role (Larson *et al.*, 2018). It is feasible that the potassium buffering capability of these cell types may be differently affected by

ischaemia. However, oligodendrocytes are known to be highly susceptible to ischaemic damage compared to astrocytes (Petito *et al.*, 1998). Therefore, this variation is unlikely to explain why ischaemia-induced potassium elevation is lesser in white matter. Indeed, the current study found no difference in the rate of decline in extracellular potassium following the initial peak.

3.4.3. Glutamate dependency of ischaemia-induced potassium release in grey matter

Likely the greatest contribution to difference between potassium release in grey and white matter is the activation of glutamate receptors. Ionotropic glutamate receptor currents are depolarising and will therefore contribute to opening of voltage gated potassium channels. Additionally, as non-selective cation channels, activated glutamate receptors will carry an outward potassium current and contribute to elevated extracellular potassium (Jonas, 1993; Scatton, 1993). This was investigated in more detail in this study. Firstly, the extent to which ischaemia-induced potassium release was calcium dependent in grey and white matter. It was found that the maximum extracellular concentration of potassium was significantly reduced by calcium free media in grey matter but unchanged in white matter. Removal of calcium from the media prevents fusion of vesicles with the plasma membrane and consequently precludes release of neurotransmitters (Hay, 2007). Similar results were seen when brain slices were incubated with a combination of NMDA receptor and AMPA/kainate receptor antagonists, MK-801 and NBQX. Together, these data indicate that potassium release in grey matter is partially dependent on vesicular release of glutamate that subsequently acts at ionotropic receptors. However, this is not the case in white matter. This is not surprising as layer 5 of the secondary motor cortex is abundant with pyramidal neuronal cell bodies (Kawaguchi, 2017). These cells receive glutamatergic synaptic input

that will cause membrane depolarisation and subsequent release of potassium through voltage gated potassium channels. Loss of ion homeostasis during ischaemia results in increased vesicular release of glutamate and so will cause excessive activation of VGKCs.

The lack of neuronal cell bodies in white matter precludes the involvement of classical synaptic activity. However, recent evidence has demonstrated the existence of the axo-myelinic synapse (Micu *et al.*, 2016). This involves vesicular release of glutamate from the axonal cylinder into the periaxonal space. Elevated glutamate levels then activate NMDA receptors on the myelin sheath allowing influx of cations into the myelinic compartment. Indeed, ischaemia has been shown to have similar effects at the axo-myelinic synapse as it does at the classical synapse. Oxygen glucose deprivation causes calcium dependent, vesicular release of glutamate from the axonal cytoplasm into the periaxonal space (Doyle *et al.*, 2018). As a result of the existence of this glutamatergic synapse and ischaemia-induced glutamate release, it may be expected for potassium rise in white matter to be partially glutamate mediated. However, glutamate is acting at receptors on the myelin membrane. While oligodendrocyte precursors express an array of voltage gated potassium channels, mature oligodendrocytes and their myelin display only a slight voltage dependency to their outward K^+ current (Sontheimer *et al.*, 1989). As a result, myelin depolarisation by elevated glutamate in ischaemia will not result in potassium release.

Myelinated axons express calcium permeable AMPA receptors at the nodes of Ranvier (Ouardouz *et al.*, 2009b). These channels are activated during ischaemia to produce an overload of intra-axonal calcium by calcium-induced calcium release (Ouardouz *et al.*, 2006). This is likely to cause depolarisation of the axon and subsequent release of potassium through voltage gated potassium channels. Therefore, it is unknown why

antagonism of AMPA receptors with NBQX did not reduce ischaemia-induced potassium release in the corpus callosum. It may be that potassium released from the axon in this manner may be into the periaxonal space, due to juxtaparanodal localisation of K_v channels (Poliak *et al.*, 2003). Potassium in the periaxonal space would not be measured by extracellular ISM recordings.

3.4.4. Ischaemia-induced potassium release is mostly dependent on voltage dependent potassium channels

The route of release of potassium was investigated by incubating the brain slices with broad voltage dependent potassium channel blockers, barium chloride and TEA, before and throughout OGD. This technique caused a large reduction in the peak of extracellular potassium on both components and almost eradicated it in white matter. These data clearly support the primary route of ischaemia-induced potassium release being dependent on voltage dependent potassium channels. While voltage dependent channels are expressed on cells throughout white matter, glial potassium channels tend to be inwardly rectifying, meaning little potassium would be released through these channels (Butt & Kalsi, 2006). Therefore, the near complete eradication of ischaemia-induced potassium release in these conditions supports the idea that the source of extracellular potassium in white matter is axonal depolarisation. Depolarisation causes extracellular potassium accumulation, both through direct release through voltage gated potassium channels as well as activation of glutamate receptors, which are non-selective cation channels (Jonas, 1993; Scatton, 1993).

Potassium channel block affected peak potassium concentration disproportionately in grey and white matter with white matter having a larger reduction. This may be due to differential shrinkage of the extracellular space between the two components (Kumura

et al., 2003). Reduced extracellular potassium will somewhat attenuate cell swelling as elevated extracellular potassium drives sodium and chloride influx into astrocytes through the NKCC1 channel (Chen & Sun, 2005). The consequent overload in intracellular ions causes astrocyte swelling by osmotic drive. However, astrocytic swelling will not be abolished by preventing potassium release as other mechanisms contribute. Ischaemia causes the opening of Cx43 hemichannels and allows astrocytic accumulation of Na^+, Ca^{2+} and H_2O (Wu *et al.*, 2013). Furthermore, glutamate may act on metabotropic glutamate receptors to upregulate aquaporin 4 channels and allow further influx of water to the cells (Shi *et al.*, 2017). Therefore, the failure of voltage dependent potassium channel blockers to completely eradicate increase in extracellular potassium concentration from OGD may be due to reduced extracellular volume.

An alternative mechanism by which potassium release may continue is through two pore domain potassium channels. These channels are widely expressed throughout the nervous system and contribute to potassium leak currents (Ryoo & Park, 2016). These channels are only weakly inhibited by TEA and so would likely still be active in the present study. These diverse channels are gated by an array of physical properties and so some may have increased activity during ischaemia. Indeed, TREK1 expression in astrocytes is increased in response to ischaemia and its activation by linoleic acid improves survival rate of mice challenged with cerebral ischaemia (Heurteaux *et al.*, 2004; Wang *et al.*, 2012). This demonstrates the dichotomy of potassium release in cerebral damage and protection. Potassium efflux currents can hyperpolarise a membrane to convey protection against depolarisation induced ionic dysregulation. However, elevated extracellular potassium can induce membrane depolarisation as well as cause cell swelling.

3.4.5. Extracellular potassium decay is likely mostly due to washout

Most studies investigating changes in extracellular potassium during ischaemia only observe only a short period before re-establishing energy supply (Hansen, 1978; Ransom *et al.*, 1992). Those that have observed longer durations used *in vivo* models, such as MCAo, and found ischaemic potassium rise to either be stable or gradually increase (Gido, Kristian & Siesjo, 1997; Stiefel & Marmarou, 2002). This is the first time extracellular potassium has been measured in an *ex vivo* preparation throughout an hour of OGD. Therefore, the discovery of a gradual decline in extracellular potassium, after the initial peak, observed in the current study was surprising. This decay in extracellular potassium could have profound effects on pathology in ischaemia if it is due to inherent potassium clearance mechanisms. As discussed, astrocytes and oligodendrocytes both possess inwardly rectifying potassium channels that can cause the uptake of elevated extracellular potassium. If these cells were capable of removing excess potassium from the extracellular space over one hour, this may protect neurons and axons from damage caused by ionic breakdown. Therefore, it was decided to attempt to understand the mechanism by which potassium was removed from the extracellular space of the isolated brain tissue. This involved an intermittent approach to OGD with initial OGD truncated at 20 minutes. This was followed by 20 minutes of reperfusion before another 20 minutes of OGD. If the removed potassium were still in the brain tissue, it could be redistributed so that subsequent OGD would result in a high release of potassium again. However, the secondary OGD resulted in a far lesser peak in potassium that was similar in magnitude to the concentration at the end of the primary OGD. After cessation of the initial OGD, the remaining elevation in extracellular potassium rapidly dropped to baseline. However, failure of the peak during secondary

OGD to exceed this level suggests that only this remaining extracellular potassium was redistributed to the neuronal compartment.

It is possible that neuronal potassium content was not replenished due to the short duration of reperfusion; however, it has been found that glial levels of potassium return to baseline within 2 minutes of repetitive olfactory tract stimulation (Ballanyi, Grafe & ten Bruggencate, 1987). While quantities of potassium will be far greater in OGD than repetitive stimulation, this gives an indication of the rapid redistribution of potassium following glial buffering. Therefore, it is likely that decay in extracellular potassium is due to washout in the perfusate. This is also corroborated by an unaltered half-life of decay in grey and white matter as well as unchanged dynamics when inwardly rectifying potassium channels are blocked with TEA. One would expect blockage to prevent uptake of potassium into the glial cells and result in maintained extracellular potassium concentration.

Washout of potassium will not occur *in vivo* as perfusion of the tissue is lost by cessation of blood flow. Therefore, it is likely that extracellular potassium concentration in stroke remains high for significantly longer than in this *ex vivo* isolated brain slice model. This may be a major disadvantage of the OGD perfusion model as the tissue is constantly perfused with media only perturbed by the lack of oxygen and glucose. Any toxic products of ischaemia may be lost resulting in missing mechanisms of disease progression. Incubation in a stationary media may in part reduce these issues as toxins and ions would not be washed away. However, a large degree of dilution would still occur as the volume of media required to maintain the slice would be far greater than the extracellular space.

3.4.6. TTC staining was unaffected by reduction in potassium release

Triphenyl tetrazolium chloride (TTC) staining was used on brain slices after reperfusion to investigate cell death under different conditions. Under normal oxygenated aCSF conditions, staining of the brain slice was complete. However, exposure to OGD caused widespread loss of staining, with no significant difference caused by any drug treatments. This lack of histological protection was unexpected as calcium free media is known to improve integrity of evoked field excitatory post synaptic potentials in the hippocampus and compound action potentials in the optic nerve following OGD (Jalini *et al.*, 2016; Stys & Jiang, 2002). Furthermore, antagonism of glutamate receptors is also known to prevent cellular damage from ischaemia (Kochhar, Zivin & Mazzarella, 1991; Nakamichi, 1998). Additionally, blockade of voltage gated potassium channels with TEA has been found to reduce neuronal apoptosis *in vitro* and reduce infarct volume *in vivo* (Wei *et al.*, 2003). Therefore, it should be expected that each of these treatments would increase staining with TTC compared to control OGD conditions. It is possible the degree of injury caused by 60 minutes of OGD in the mouse brain slice is too severe to allow effective protection by interference with ionic dysregulation. As demonstrated later in this thesis, this duration is sufficient to cause near complete irreversible loss of compound action propagation in the mouse optic nerve (fig. 6.1).

It is likely that the technique used was not sensitive enough to neural cell damage as variability within all groups was high. TTC staining is usually performed on slices of a freshly removed brain; however, it has been used on tissue subject to OGD *ex vivo* (Zhao *et al.*, 2018). This study did not use area of staining but instead, extracted pigment from stained tissue and quantified it using spectrophotometry. This technique may have yielded more reliable results than the present study.

Variability in the present study may have been a result traumatic insult. Removal of the brain slice from the chamber was often difficult with the brain slice stuck to the mesh. Any stretching of the mesh during movement would cause distortion of the tissue which may result in cell loss. Any handling during dissection and placement of the slice in the chamber could have yielded minor trauma leading to increased susceptibility to ischaemic insult. Furthermore, it was not possible to maintain oxygenation of the TTC solution and so the slices may have experienced mild hypoxia during the 10-minute staining, leading to further loss of cell viability. This was not seen in the healthy control slices, but vulnerability may have been increased by prior OGD conditions.

Interestingly, TTC staining was consistently lost from an external to internal manner. Staining of the cerebral cortex was always completely lost while some or all of the striatum was spared. The septal area nearly always maintained staining. This may be due to region specific vulnerability to ischaemic insult which is known to be greater in higher brain structures (Wahul *et al.*, 2018). Alternatively, the perfusion method of OGD may result in greater exposure of the exterior regions to insult. The flow rate must be kept so that the slice is not fully submerged as this would prevent access of humidified gas and cause mild hypoxia throughout incubation. The flooding also interfered with ISM measurements. Therefore, with only small amounts of perfusate flowing over the brain slice, diffusion of the OGD solution to the centre of the slice may be delayed compared to the exterior.

The staining of white matter with TTC was not effective. Combined with the limited proportion of white matter in the rodent brain, this staining was not used for investigating white matter damage.

3.5. Conclusion

Oxygen-glucose deprivation in isolated mouse brain slices results in rapid increase in extracellular potassium concentration followed by a gradual decline to return to baseline. The elevation is greater in grey matter than white matter but does not reach levels seen in the intact rat brain. The higher peak concentration seen in grey matter is dependent on vesicular release of glutamate to act on ionotropic glutamate receptors. This dependency is not seen in white matter. In both grey and white matter, nearly all potassium release is via voltage dependant potassium channels. Prevention of ischaemia-induced potassium release was not sufficient to improve cell survival depicted by TTC staining.

Chapter 4:

Ischaemia-Induced pH Dynamics in Grey and White Matter

Abstract:

The extracellular pH of the brain is tightly regulated as minor disturbances can alter membrane excitability and activate deleterious enzyme cascades. Homeostasis relies on a diverse array of proton channels and pumps that depend on maintained ionic gradients. Lack of oxygen supply and impaired metabolite clearance during ischaemia results in an accumulation of lactic acid and consequent drop in extracellular pH. Furthermore, breakdown of ionic gradients early in ischaemia impairs cellular ability to regulate pH. The pH dynamics induced by ischaemia are yet to be directly compared in grey and white matter structures but may differ due to varying metabolic demands.

Proton sensitive microelectrodes were used to measure extracellular pH in 400µm coronal mouse brain slices during one hour of OGD. Measurements were taken from the secondary motor cortex for grey matter and the corpus callosum for white matter. The baseline pH was found to be similar in each tissue at 7.23 in grey matter and 7.14 in white matter. Upon initiation of OGD the extracellular space rapidly acidified to a similar level of 6.93 in grey matter and 7.04 in white matter. After the initial acidification of the extracellular space, pH began to gradually rise throughout the duration of OGD.

The results from this chapter indicate that, despite contrasting metabolic demand, pH dynamics in grey and white matter during ischaemia are similar. The gradual rise in extracellular pH after a peak acidification may suggest an enduring buffering system or loss of protons into the perfusion media.

4.1. Introduction

Regulation of intracellular and extracellular pH, pH_i and pH_o respectively, is of vital importance in all tissues due to its modulation of enzymes and interactions with many molecular systems. This is particularly key in the brain due to the pH sensitivity of many ion channels, including NMDA channels, leading to alterations in neuronal excitability and signal conduction if left unchecked (Tang, Dichter & Morad, 1990). Many mechanisms of pH regulation throughout cells in the body are conserved within the brain. However, the sensitivity of brain activity to pH and the highly diverse cell types and brain regions have resulted in more specific methods of regulation. Regulation of pH within the CNS is a highly complex process and this chapter will give a broad overview.

The major ions contributing to pH_i and pH_o regulation are H^+ and HCO_3^-, neither of which may cross the membrane freely. These ions are transported across the membrane through ion channels or receptors in order to maintain physiological pH_i. These transporters can be classified as acid-loaders, if they result in net acidification of the cytoplasm, or acid extruders if they cause loss of intracellular acidification.

4.1.1. Neuronal pH_i regulation

There is much evidence regarding the transporters involved in neuronal pH_i regulation including brain region specific variations (Chesler, 2003). Broadly, the main acid-loading transporter in neurons is the Cl^--HCO_3^- exchanger, AE3 (anion exchanger 3) (Ruffin *et al.*, 2014). Under physiological ion concentrations, the AE3 acts to extrude HCO_3^- and import Cl^- to the neuron. Loss of function of AE3, either through mutation or deletion, causes susceptibility to epilepsy and greater mortality rate from seizures (Hentschke *et al.*,

2006; Sander *et al.*, 2002). This is due to increased neuronal excitability at higher pH_i values and demonstrates the importance of tight pH_i regulation.

There are two key types of acid-extruding transporters involved in the pH homeostasis of neurons (Ruffin *et al.*, 2014). Sodium-Hydrogen exchangers, NHE, are driven by high extracellular Na^+ under resting conditions to cause exportation of hydrogen ions leading to a net loss of acidity. Sodium-coupled bicarbonate transporters (NCBTs) also take advantage of the high extracellular Na^+ gradient in order to drive transport of HCO_3^- into neurons, again leading to a net loss of intracellular acidity. There are multiple forms of neuronal NCBTs, some of which are electroneutral as they carry equal Na^+ and HCO_3^- into the cell, while others are electrogenic as these ions are carried in different quantities. Furthermore, some NCBTs exchange Na^+ and HCO_3^- for Cl^- in an electroneutral manner. This means that driving forces on the transporter can be chloride dependent and also gives rise to further modulation of neuronal excitability.

4.1.2. Astrocyte pH_i regulation

Similar to neurons, the NHE plays a major role in the setting of resting astrocyte pH (Kimelberg & Ricard, 1982). However, in astrocytes, this channel is inhibited by pathologically low extracellular pH (6.9), which would likely accompany acid accumulation in an ischaemic insult (Mellergard & Siesjo, 1991). Therefore, under these conditions, the NHE would not be able to contribute to the extrusion of H^+ from astrocytes to restore correct pH_i. Electrogenic Na^+-HCO_3^- cotransport has been demonstrated in astrocytes as a method of acid extrusion. This transporter is potentiated by membrane depolarisation, which leads to astrocyte alkalisation upon cortical stimulation (Chesler & Kraig, 1987). Furthermore, this alkalisation is prevented

if astrocyte depolarisation is attenuated by addition of potassium channel blocker, Ba^{2+} (Chesler & Kraig, 1989).

Cl^-/HCO_3^- exchangers have also been demonstrated in astrocytes. Rat cortical astrocytes were shown to increase in pH upon the removal of extracellular chloride, consistent with a chemical gradient driving extrusion of HCO_3^- from the cells under physiological conditions (Shrode & Putnam, 1994). This effect was independent of Na^+ concentration, therefore, eliminating Na^+-coupled Cl^-/HCO_3^- exchanger activity from involvement.

Recent evidence has demonstrated the high dependence on V-ATPase for intracellular pH regulation in optic nerve astrocytes (Hansen *et al.*, 2015). This is opposed to the relatively menial contribution of the V-ATPase to intracellular buffering in cultured astrocytes. V-ATPase is a proton pump requiring phosphorylation by ATP in order to remove H^+ from the cytoplasm into either membrane bound compartments, like vacuoles, or into the extracellular space (Pamarthy *et al.*, 2018). V-ATPase has been found to be present on the plasma membrane of astrocyte processes and soma, suggesting it regulates intracellular pH by exporting protons to the extracellular space (Hansen *et al.*, 2015). However, the reliance of the pump on ATP supply may result in its inhibition during ischaemia.

4.1.3. Oligodendrocyte pH_i regulation

Cultured cerebellar oligodendrocyte pH is unaffected by removal of Cl^- ions or application of stilbenes which indicates a lack of Cl^-/HCO_3^- exchanger (Boussouf & Gaillard, 2000). This may explain the relatively high resting pH_i of these oligodendrocytes at 7.04. Both NHE and NCBT were found to be active in these cells. The particular NCBT present in oligodendrocytes appears to be electrogenic and transport Na^+ and HCO_3^- in a ratio of 1:3 with a reversal potential of around -60mV (Boussouf, Lambert & Gaillard,

1997). Therefore, this transporter would be in approximate equilibrium at oligodendrocyte resting potential.

4.1.4. Activity dependent shifts in neuronal pH_i

Application of excitatory amino acids to cultured mammalian neurons results in a calcium dependent intracellular acidification (Irwin et al., 1994). The calcium dependence of these pH_i shifts may be an accumulation of different mechanisms. Entry of Ca^{2+} into the neuron results in increased metabolic demand and production of carbonic and lactic acid (Wang, Randall & Thayer, 1994). However, other activity driven processes such as fuelling the Na^+/K^+-ATPase to restore membrane polarisation will also drive metabolic acidosis. Furthermore, mitochondria act to buffer increased intracellular calcium by accumulation through the H^+/Ca^{2+} exchanger, resulting in increased intracellular acidity (Werth & Thayer, 1994). H^+/Ca^{2+} exchangers play a further role in activity dependent acidification, in the form of the plasmalemmal Ca^{2+}-ATPase (Trapp *et al.*, 1996). This enzyme facilitates the uptake of H^+ ions in order to export calcium into the extracellular space, to combat pathological concentrations of intracellular Ca^{2+} occurring.

4.1.5. Activity dependent shifts in glial pH_i

As previously mentioned, depolarisation of astrocytes by increased extracellular K^+, from neuronal activity, results in astrocytic alkalisation. This is due to the activation of electrogenic Na^+-HCO_3^- cotransporters (Chesler & Kraig, 1987). This alkalisation serves a multitude of physiological purposes. Intracellular alkalisation increases glycolytic rate, therefore increasing production of metabolic substrates in order to support neurons during periods of intense activity (Trivedi & Danforth, 1966). Gap junctions have increased conductance in a more alkaline environment, which allows astrocytes to more

quickly dissipate elevated potassium, released by firing neurons, throughout the syncytium (Spray, Harris & Bennett, 1981). Furthermore, glutamate uptake into astrocytes is reliant on export of HCO_3^- from the cell (Bouvier *et al.*, 1992). Therefore, astrocytic alkalisation will drive glutamate uptake from synapses and act to prevent excitotoxic concentrations of extracellular glutamate.

4.1.6. Regulation of interstitial pH

Brain interstitial fluid is maintained at approximately pH 7.3 (Cragg, Patterson & Purves, 1977). However, in brain slices and other *ex vivo* CNS preparations, the extracellular fluid is much more acidic than this due to loss of the necessary blood flow to remove CO_2 (Voipio & Kaila, 1993).

The buffering of extracellular brain pH is primarily by conversion between CO_2 and HCO_3^- which can occur slowly or can be enzymatically enhanced by carbonic anhydrase, which catalyses both the hydration and dehydration directions (Maren, 1967). This enzyme will act to oppose pH_o transients caused by neuronal activity (Kraig, Ferreira-Filho & Nicholson, 1983). In the brain, carbonic anhydrase is located in astrocytes, oligodendrocytes and in the extracellular fluid. Inhibition of extracellular carbonic anhydrase leads to far greater fluxes in pH initiated by neuronal activity (Chen & Chesler, 1992).

Following neuronal activity, the extracellular space first becomes alkaline before a subsequent acidic shift. This alkaline shift is independent of glial input as these cells also become alkaline and therefore, should act as a proton donator. Interstitial alkalosis is neuronal in nature and has HCO_3^- independent and dependent mechanisms. The HCO_3^- independent component has yet to be clarified but may involve a combination of H^+ cotransport with glutamate uptake as well as exchange with elevated intracellular Ca^{2+}.

Activation of GABA receptors by interneuron stimulation allows flow of HCO_3^- out of the cell to contribute to extracellular alkalosis. Delayed interstitial acidosis appears due to increased production of CO_2 and acidic substrates from elevated metabolism. These are then extruded into the interstitium.

4.1.7. Effect of pH shifts on neuronal activity

Extracellular alkalisation resulting from neuronal activity leads to increased excitability of neuronal membranes (Tang, Dichter & Morad, 1990). NMDA receptor pores are blocked by extracellular protons and therefore, increase in extracellular pH will result in greater NMDA currents. Additionally, GABAergic currents are suppressed by increased extracellular pH, resulting in further increased neuronal excitability by reduction of inhibitory input (Krishek *et al.*, 1996). Conversely, extracellular acidosis reduces neuronal excitability by blockage of NMDA receptors and increased activity of $GABA_A$ receptors.

4.1.8. Effect of ischaemia on intracellular and extracellular pH

During cerebral ischaemia, production of lactic acid and deficiency in its clearance results in extracellular acidosis (Mutch & Hansen, 1984). Although maintenance of intracellular pH is largely an active process, there remains a dichotomy in pH between the intracellular and extracellular compartments for at least an hour following initiation of focal ischemia (Nedergaard *et al.*, 1991). One hour after occlusion of the middle cerebral artery and common carotid artery (MCA-CCAO), extracellular pH had fallen from 7.24 to 6.43, whereas intracellular pH fell from 7.01 to 6.86. However, after 4 hours, extracellular and intracellular pH were at 6.61 and 6.62 respectively, indicating a failure of membranes to maintain proton gradients. Interestingly, the extent of extracellular acidification is dependent on glycogen stores prior to ischaemic onset.

Treatment with glucose prior to ischaemia exacerbates decline in extracellular pH to 5.88 but did not affect intracellular pH decline. On the other hand, hypoglycaemia prevented decline in both intracellular and extracellular acidosis. Exacerbated brain acidosis in hyperglycaemic animals leads to increased oedema and greater infarction and necrosis despite delaying depletion of ATP and anoxic depolarisation (Smith & Siesjö, 1988).

There is conflicting evidence as to the consequences of extracellular acidification on cell survival (Lipton, 1999). The levels of acidosis reached during cerebral ischaemia are not sufficient to cause cellular damage on their own (Cohen *et al.*, 1990). As previously discussed, decline in extracellular pH causes reduces NMDA mediated calcium entry and subsequent protection from glutamate excitotoxicity (Takadera, Shimada & Mohri, 1992). However, AMPA/kainate receptors are potentiated by extracellular proton accumulation and their component in ischaemia-mediated cell death is exacerbated by acidosis (McDonald *et al.*, 1998). Furthermore, lowered extracellular pH appears to prevent extrusion of Ca^{2+} from cells following ischaemic insult, which would exacerbate cell death mechanisms. Elevated concentration of extracellular H^+ may lead to reversal of the sodium-proton exchanger leading to increased detrimental accumulation of intracellular Na^+ (Piper *et al.*, 1996). It is also possible acidosis leads to accentuation of free radical production during and following ischaemia by iron delocalisation (Wei, Huang & Quast, 1997). Together, these studies suggest the detrimental effects of cerebral acidification overcome any potential benefits and, therefore, amelioration of lactic acid accumulation may provide an effective therapeutic approach.

4.1.9. Ischaemia-induced acidification of astrocytes

Astrocytes are known to rapidly acidify upon ischaemic onset to a greater extent than other brain compartments (Kraig & Chesler, 1990). This is likely due to high levels of glycogen stores which are mobilised during metabolic deprivation to undergo glycolysis, thereby resulting in lactic acid production (Rossi, Brady & Mohr, 2007). Furthermore, depletion of ATP will result in failure of the V-ATPase to extrude protons from the cytoplasm. As this is believed to the one of the primary mechanisms of astrocytic pH regulation, failure would lead to excessive acid build up (Hansen *et al.*, 2015).

Rapid astrocytic acidification caused by ischaemia has a profound contribution towards glutamate excitotoxicity in neurons (Beppu *et al.*, 2014). Triggering acidosis of Bergmann glia by optogenetic manipulation causes an inward current in surrounding neurons, representative of glutamate excitation. During oxygen glucose deprivation, this characteristic current could be prevented by optogenetic alkalisation of the Bergmann glia. This alkalisation was sufficient to reduce infarct size in an *in vivo* model of focal ischaemia. Together, this clearly demonstrates the detrimental nature of ischaemia-induced astrocyte acidification. However, mechanisms leading to the exacerbated acidosis experienced by astrocytes are yet to be elucidated.

4.1.10. Ischaemia-induced pH shifts in white matter

Relatively little is known about the pH dynamics in white matter and their effects on cells and their processes. Oligodendrocytes are known to be particularly susceptible to oxidative stress due to low levels of glutathione (Thorburne & Juurlink, 1996). Therefore, the mobilisation of protein-bound iron by lactic acidosis is able to cause enhanced levels of free radical production by the Fenton reaction (Oubidar *et al.*, 1994). Furthermore, axons are known to be susceptible to damage from acidosis by activation of acid sensing

ion channel-1 (ASIC1) (Friese *et al.*, 2007). This channel enables influx of Na^+ and Ca^{2+} into the axons in response to elevated extracellular protons, as experienced during ischaemia, thus contributing to membrane depolarisation and activation of calcium dependent cell death mechanics.

No study has directly investigated any differences in pH dynamics that may occur between grey and white matter or mechanisms that may cause these to occur. This knowledge may prove vital for understanding susceptibility of white matter to damage from ischaemic insult as well as provide guidance for possible therapeutic interventions.

4.2. Aims and Objectives:

This study aims to determine whether pH dynamics differ in grey and white matter following onset of stroke. If differences are found, mechanistic variations resulting in the discrepancy will be investigated.

- Proton selective ion-sensitive microelectrodes will be used to measure extracellular pH in grey and white matter of mouse brain slices throughout one hour of oxygen glucose deprivation.
- The process will be repeated with ion channel and receptor antagonists if a difference is found.

4.3. Results

4.3.1. OGD causes biphasic changes in extracellular pH

Extracellular pH from layer 5 of the secondary motor cortex of the isolated mouse brain slice was measured using proton-selective ion sensitive microelectrodes. Upon subjection to oxygen glucose deprivation, concentration of protons in the extracellular space began to rapidly increase causing a decrease in pH (fig. 4.1). This acidification occurred over 2 to 3 minutes before reaching a peak. Subsequently, the extracellular pH began to steadily increase until it surpassed the initial baseline level. This continued, though at a decelerating rate, until the slice was reperfused with regular aCSF and oxygen. Reperfusion caused a slight decrease in pH.

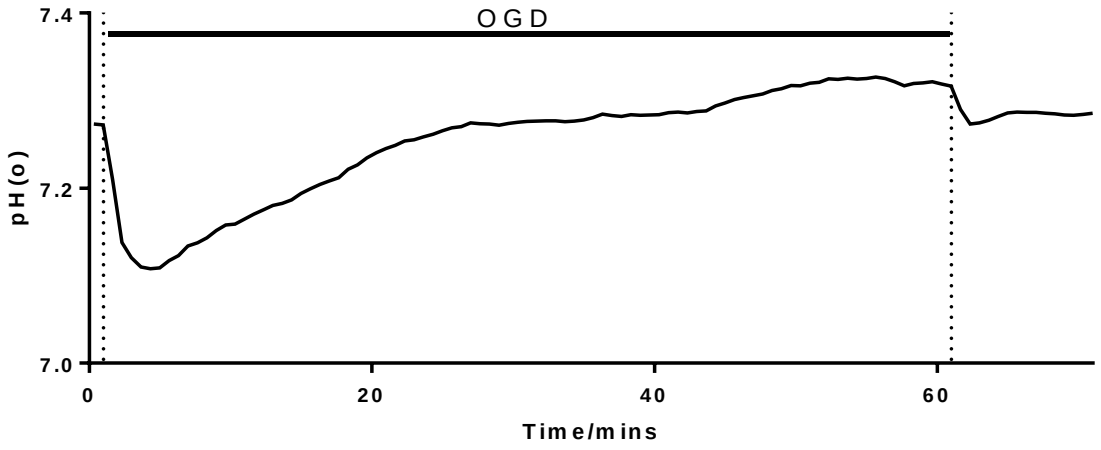

Figure 4. 1. OGD causes rapid acidification followed by gradual alkalisation.

Representative trace of extracellular pH from the mouse brain slice cortex during oxygen glucose deprivation.

4.3.2. OGD induced extracellular pH changes are the same in grey and white matter

Extracellular pH was measured in the corpus callosum during OGD and a similar profile of pH dynamics was found (fig. 4.2a). The baseline $pH_{(o)}$ was no different with a mean of 7.23±0.03 (n=5) and 7.14±0.06 (n=5) in grey and white matter respectively (P=0.213, fig. 4.2b). Similarly, the peak acidification was found not to be significantly different between grey and white matter (6.93±0.05, n=5 and 7.02±0.05, n=5, respectively. P=0.248, fig. 4.2c). The area under the curve, during OGD, for each time-course was calculated and the mean values for grey and white matter did not significantly differ (7.06±1.16mins, n=5 and 7.35±1.65mins, n=5, respectively. P=0.889, fig. 4.2d). Finally, the extracellular pH after 10 minutes of reperfusion was not significantly different in grey and white matter (7.35±0.05, n=5 and 7.25±0.06, n=5, respectively. P=0.355, fig. 4.2e).

As the pH dynamics were not affected by brain matter type, it was deemed unnecessary to explore mechanisms that may differ between grey and white matter.

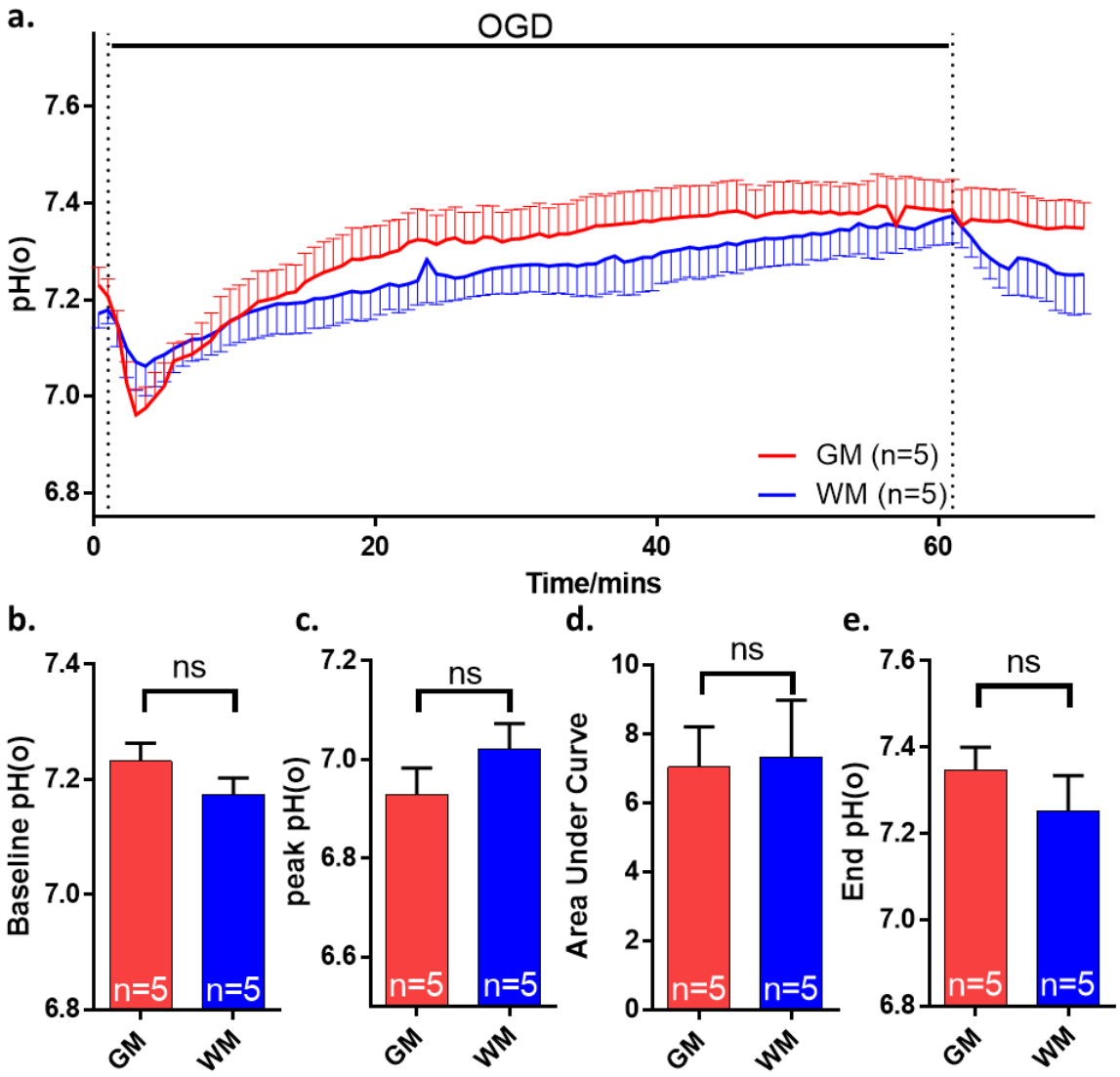

Figure 4. 2. pH dynamics during OGD do not vary between grey and white matter.

a. In both grey and white matter OGD initially causes rapid acidification of tissue before a gradual increase in pH slowing down until reperfusion. **b.** Baseline pH recordings were not significantly different in grey and white matter (P=0.213, n=5). **c.** The peak acidification of tissue was not significantly different between grey and white matter (P=0.248, n=5). **d.** The area under the curve during OGD was unaffected by tissue type (P=0.889, n=5). **e.** The pH(o) following 10 minutes of reperfusion was not significantly different in grey and white matter (P=0.355, n=5). (Unpaired T-test).

4.4. Discussion

Ischaemia results in acidification of the extracellular space due to excess production of lactic acid. As grey matter has a greater metabolic demand than white matter, it may be expected that extracellular pH would fall more in grey matter than white matter, but this has not previously been directly studied. The present study used proton sensitive microelectrodes to measure extracellular pH in the grey and white matter of a mouse brain slice during OGD. It was found that OGD induced a similar acidification of the extracellular space in grey matter as in white matter. Therefore, pH dynamics in the two tissues may not differ during a stroke.

4.4.1. Extracellular pH of different models

This study aimed to determine differences in pH dynamics in grey and white matter during ischaemic insult. Proton selective ion-sensitive microelectrodes were used to record the extracellular pH. Using this method, the baseline pH for grey matter was established at 7.23 while white matter was found to be 7.17, though this difference was not significant. Interestingly, these values are lower than have been established in previous studies with a baseline of between 7.34 and 7.39 found *in vivo* in the parietal cortex of Wistar rats (Katsura *et al.*, 1991; Mutch & Hansen, 1984). Of course, isolated tissue preparations often have lower extracellular pH due to lack of circulatory clearance of CO_2 leading to increased concentration of carbonic acid (Voipio & Kaila, 1993). On the other hand, baseline $pH_{(o)}$ recordings from the isolated rat optic nerve were found to be approximately 7.3 (Ransom *et al.*, 1992). This was again, more alkaline than found in the present study despite being an isolated tissue preparation with reduced CO_2 clearance. It is possible that a slower rate of perfusion was used in the present study that may further reduce the rate of CO_2 clearance under control conditions.

4.4.2. Diminished ischaemic acidification in the mouse brain slice

Following onset of oxygen glucose deprivation, the extracellular pH rapidly fell in both grey and white matter. This is likely due to production of lactic acid through glycolysis by astrocytes in response to cessation of oxidative phosphorylation (Rossi, Brady & Mohr, 2007). Again, there was no significant difference in the extent of this extracellular acidification between grey and white matter. The degree of acidification was far lesser in the present study than in previous studies. During complete cerebral ischaemia of the rat, extracellular pH of the parietal cortex falls to approximately 6.75 compared to just 6.93 in the present study (Mutch & Hansen, 1984). Similar to the diminished peak in ischaemia-induced potassium release found in the present study, this may be due to volume changes in the different model. Oedema will cause greater shrinkage of the extracellular space in the *in vivo* model, where the skull limits the volume the brain may occupy, compared to the isolated brain slice (Kumura *et al.*, 2003). As a result, extracellular protons generated by glycolytic production of lactate will be confined to a smaller space *in vivo*, resulting in a higher concentration and lower pH. However, the shift in pH of the isolated rat optic nerve during anoxia has been measured at -0.31 compared to just -0.15 in the present study (Ransom *et al.*, 1992). This variation cannot be explained by limitation of skull volume as both preparations are isolated in nature. One possible explanation for the difference in pH shift seen in these white matter preparations is the variation between anoxia and ischaemia. Hyperglycaemia results in an exacerbated fall in pH during focal ischaemia as the increased stores of glucose allow for prolonged glycolysis and increased lactate production (Marsh, Anderson & Sundt, 1986). Therefore, anoxia will result in a greater acidic shift in extracellular pH than OGD as the continued supply of glucose to the tissue will allow far greater rates of glycolysis.

A further contribution to the reduced peak in acidity in the present *ex vivo* study, relative to some *in vivo* studies, may be explained by other findings from the measurement of extracellular potassium in this preparation. It was found likely that potassium released from cells into the extracellular space was washed away in the perfusate. Similarly, this is likely to occur with released lactic acid, meaning that, as the lactic acid is released, it is also lost from the preparation. This would result in a lesser maximal acidic shift in pH. The washout of lactate may also help explain the gradual rise in pH after the initial spike in acidity. This phenomenon has not been seen in studies performed *in vivo*, where acidification of the extracellular space continues for at least 25 minutes after initiation of complete ischaemia (Katsura *et al.*, 1991). In complete cerebral ischaemia, lack of circulation would result in continued accumulation of lactic acid for as long as glycolysis occurred. In the isolated rat optic nerve preparation, anoxia was only employed for a brief period and so it is not known whether the pH would have risen after the endpoint (Ransom *et al.*, 1992). This washout of lactic acid is another potential disadvantage of using OGD in an isolated preparation. Prolonged acidification of the extracellular space may lead to interference with enzyme systems and dysregulation of ionic gradients (Rehncrona & Kagstrom, 1983). Thus, these mechanisms may be lacking during OGD in perfusion chambers.

4.4.3. Buffering of the extracellular pH

Although the washout of lactic acid may explain the loss of acid shift throughout OGD, it does not account for the slight alkalisation of the tissue, relative to baseline, towards the end of OGD. The increase in pH recorded by the electrodes may be accounted to potential drift, possibly as a result of interference by CO_2 (Lee, Boron & Parker, 2013). Potential drift can occur when recording for long periods and may confound results.

However, this explanation is not in conjunction with the shift towards baseline seen, following reperfusion. It would be expected that, if recorded pH had passed above baseline by potential drift, it would remain at this new baseline after reperfusion. As this is not the case, there may be a buffering mechanism at play that has resulted in alkalisation of the extracellular space, though this does not occur during *in vivo* studies.

As prolonged experience of tissue acidosis is likely to be deleterious in ischaemia, it was decided to determine whether the area under the curve for pH varied between grey and white matter. Similar to baseline and peak pH, no significant difference was found in the area under the curve between the two CNS components. If the reduction of acidity seen after the initial peak is purely due to washout of lactic acid, this similarity may be because washout is at the same rate in both areas. On the other hand, if buffering mechanisms are responsible for the slight alkalisation observed in late OGD, this may indicate that buffering mechanisms are similar in both grey and white matter.

Finally, the extracellular pH after 10 minutes of reperfusion was found not to be significantly different in grey and white matter. Furthermore, when this value was compared to the initial baseline in a paired manner, there was no significant difference found between the two. Although the extracellular pH had returned to baseline by the end of recording, it is possible that prolonged recording may have elucidated continued pH dynamics. It was found that, following anoxia of the rat optic nerve, extracellular pH underwent some complex changes over a sustained duration (Ransom *et al.*, 1992). Initial, return to baseline was followed by a secondary acidification before returning to a steady state at baseline.

4.5. Conclusion

Ischaemia causes acidification due to excessive production of lactate through glycolysis. In this chapter, it has been demonstrated that oxygen-glucose deprivation in the isolated mouse brain slice causes a rapid reduction in pH of the extracellular space. This is followed by a gradual alkalisation until baseline is re-established upon return of oxygen and glucose supply. This latter increase in pH is at odds with established profiles of the in-tact ischaemic brain. No difference was found in the ischaemia-induced pH dynamics between grey and white matter suggesting similar mechanisms of acid buffering in the two regions.

Chapter 5:

Glutamate Receptors in Cuprizone Excitotoxicity

Abstract:

Demyelinating diseases such as multiple sclerosis can have devastating effects on patient quality of life. One proposed mechanism of demyelination is pathological activity of glutamate receptors leading to excitotoxicity in oligodendrocytes. Glutamate receptor subtypes are differentially expressed throughout the oligodendrocyte with AMPA receptors mainly found on the cell soma and NMDA receptors localised to the processes and myelin. Damage to oligodendrocytes and myelin can cause irreversible loss of CAP propagation. Glutamate receptor antagonists have failed in the clinic due to adverse effects at therapeutic concentrations. We investigated whether AMPAR and NMDAR antagonists could act in synergy at a lower concentration to prevent demyelination with hope that a more acceptable therapeutic approach could be developed.

A novel *ex vivo* model of demyelination, involving application of 1mM cuprizone to mouse optic nerves, was used to determine efficacy of combined glutamate receptor antagonists. Cuprizone application for 100 minutes caused a reduction in compound action potential (CAP) amplitude to 45.3% of baseline. Injury to CAP amplitude by cuprizone application was prevented by incubation of nerves with, the NMDA receptor antagonists, 10µM memantine or 50µM QNZ46. However, when in combination with AMPA receptor antagonists, perampanel or CP 465022, the protective concentration was reduced to 1µM. AMPA receptor antagonists alone were unable to protect from cuprizone mediated CAP loss.

The results from this chapter support the possibility of using a synergistic combination of glutamate receptor antagonists to treat demyelinating disease while avoiding unacceptable adverse effects. Furthermore, it has been demonstrated that glutamate dependent cuprizone-induced injury is primarily mediated through NMDA receptor currents.

5.1. Introduction

Multiple Sclerosis (MS) is a devastating debilitating illness that progressively infiltrates aspects of a sufferer's abilities resulting in a large reduction in quality of life. MS is currently the most common non-traumatic cause of disability in young people in the western world, with incidence ever increasing. Disability can range hugely between patients as well as different stages of disease progression, depending on which CNS area the disease presents. For example, often, an early sign of MS will be optic neuritis, involving pain and loss of vision in one eye (Dobson & Giovannoni, 2019).

MS is a disease of the CNS causing oligodendrocyte death, demyelination and loss of axons. Classically, this has been understood to compose of both autoimmune and neurodegenerative components. Early stage MS usually presents as rapid loss of function that gradually recovers followed by a period of remittance before another relapse of disability. This stage has been believed to be immune in mechanism. Though recovery may be near complete, the sufferer will not regain full function. However, as the disease progresses, a trend of increasing progressive functional impairment will prevail. This aspect is thought to be neurodegenerative in nature. However, this view is likely to be too simplistic. Furthermore, in around 15% of MS cases, the progressive stage of degeneration is seen from disease onset.

5.1.1. Models of MS

Several mouse models of demyelination have been developed to allow investigation of disease mechanics. Each possesses advantages and disadvantages (Torkildsen *et al.*, 2008). The experimental autoimmune encephalitis (EAE) model involves inducing inflammatory demyelination by application of myelin antigens or myelin-specific T-

lymphocytes. This autoimmune phenotype followed by resolution of immune response and subsequent recovery closely mimic the disease mechanisms of MS and make the model ideal for studying relapses and remission (Constantinescu *et al.*, 2011).

The cuprizone model involves incorporating bis-cyclohexanone oxaldihydrazone (cuprizone), a copper chelator, into the mouse diet (Torkildsen *et al.*, 2008). Cuprizone ingestion results in progressive toxic demyelination and loss of axons while feeding is ongoing. While proliferation of OPCs and development of new oligodendrocytes occur during cuprizone feeding, significant remyelination is usually seen after cessation of cuprizone administration (Vega-Riquer *et al.*, 2019). Cuprizone ingestion appears to specifically injure oligodendrocytes, the myelinating cells in the brain, which causes myelin loss from axons. One possible explanation for this is due to impairment of mitochondrial enzyme reactions involving cytochrome oxidase and monoamine oxidase, dependent on presence of copper. Thus, chelation of copper causes oligodendrocytes to die due to weakened metabolism (Zendedel, Beyer & Kipp, 2013). This process is discussed further in section 5.4.3.

A novel potential mechanism of cuprizone induced demyelination being investigated is non-desensitising activation of NMDA receptors and consequent glutamate excitotoxicity (Stys, You & Zamponi, 2012). The copper binding site of prion protein (PrP^C) interacts with NMDA receptors, only when bound to copper, to reduce affinity with co-modulator, glycine. Therefore, copper chelation with cuprizone may reduce PrP^C competition with glycine. As glycine acts to reduce desensitisation of NMDA receptors, this copper dependent interaction would prevent excessive NMDA calcium currents required for excitotoxicity. Chelation of copper by cuprizone results in a non-desensitising element to NMDA receptor currents, similar to those found in PrP^C null

mouse neurons (You *et al.*, 2012). Myelin is known to be susceptible to injury from NMDA receptor activation as glutamate is released in a vesicular manner from axons into the periaxonal space (Doyle *et al.*, 2018). Therefore, it may be the case that cuprizone causes primary myelin damage by calcium accumulation through non-desensitising NMDA receptors. This mechanism is discussed further in section 5.4.3.

Recently, the cuprizone model has been further developed in an attempt to incorporate the autoimmune component, known to play a key role in MS pathology, into the model (Caprariello *et al.*, 2018). This was achieved by administrating oral cuprizone, as normal, but truncated at two weeks. Mice are then treated with an immune boosting combination of Freund's adjunct and pertussis toxin, similar to the EAE model, except excluding exogenous myelin fragments. The mice are then left for a further two weeks to allow dissipation of cuprizone and formation of an autoimmune response. The model was named Cuprizone Autoimmune Encephalitis (CAE). The two-week period of cuprizone treatment is sufficiently short to cause alteration to myelin structure but not demyelination, as evidenced by electron micrographs. However, in combination with the immune boost and incubation, significant demyelination and elevated inflammation are induced.

The CAE model has been used to show that the autoimmune response is elicited by presence of altered myelin (Caprariello *et al.*, 2018); One week of cuprizone treatment was not sufficient to cause alterations and therefore, no inflammation was induced. However, three weeks of treatment caused a severe degree of demyelination and clearance of myelin debris, thereby also causing no inflammatory response. Furthermore, the component of altered myelin responsible for autoimmune initiation has been demonstrated to be citrullination of myelin basic protein (MBP). Inhibition of

peptidyl arginine deiminases (PADs), which cause citrullination of MBP, during the cuprizone phase, prevented inflammation and demyelination. This was not the case if PADs were inhibited during the immune boost phase as myelin had already been altered. Moreover, splenocytes harvested from CAE mice proliferated intensely in response to myelin fragments from CAE mice but not those treated with PAD inhibitor during the cuprizone phase. There was even a response to myelin taken from naïve mice but again, prevented by treatment of the naïve mice with PAD inhibitor. This demonstrates that even physiological levels of citrullination are sufficient to induce an autoimmune response once the splenocytes have been primed. This study has revealed a possible link between the demyelinating and autoimmune components of MS as well as a conceivable mechanism underlying progressive demyelination in MS. Peptidyl arginine deiminases are dependent on elevated calcium levels to enact citrullination (Witalison, Thompson & Hofseth, 2015). Taken together with the knowledge that cuprizone has indirect interactions with NMDA receptors, it is feasible that cuprizone treatment causes citrullination of MBP by enhancing calcium currents through the NMDA receptor.

5.1.2. Myelin Basic Protein citrullination in Multiple Sclerosis

Lending credence to the idea that MBP citrullination is a key pathological step in MS disease progression is the evidence that 45% of MBP in MS patients is citrullinated compared to just 18% in healthy population (Wood *et al.*, 1996). Myelin basic protein binds by noncovalent action to negative lipid residues on two opposing lipid bilayers in order to stabilise the compact lamination of the myelin structure (Hu *et al.*, 2004). There are several ways in which citrullination may affect MBP function and, in turn, detriment myelin physiology. The generation of an autoimmune response can take place via complimentary mechanisms. Firstly, the citrullinated residues themselves act as a neo-

epitope against which the immune system may respond (Schellekens *et al.*, 1998). Furthermore, MBP citrullination results in conformational changes to the protein structure as α-helices unravel and the protein extends (Bates & Harauz, 2003). This unravelling leads to further presentation of immunogenic epitopes, as well as allowing proteolysis of the protein and consequent production of further epitopes and loss of function (Musse & Harauz, 2007). Contributing to loss of lipid adhesive function is the loss of positive charge resulting from conversion of arginine residues to citrulline (Wood & Moscarello, 1989). Impaired adhesion leads to loss of myelin compaction and even demyelination. Therefore, citrullination of MBP could significantly contribute to loss of signal conduction through white matter in MS and subsequent behavioural deficits.

5.1.3. Excitotoxicity in MS

The involvement of glutamate toxicity as a mechanism in MS disease progression is becoming increasingly evident (Macrez *et al.*, 2016). This increased level of glutamate can come from a whole host of sources. Immune cells, primarily monocytes, macrophages, microglia, and dendritic cells release glutamate through the cysteine/glutamate antiporter (Xc^-) which has been found to be upregulated in multiple sclerosis as well as mouse models of the disease. Glutamate released by these immune cells acts to facilitate further infiltration into the CNS by acting on epithelial cells as well as possibly acting directly on myelin to cause excitotoxicity. Furthermore, increased expression of voltage gated sodium channels (VGSC) in axons as compensation for loss of conduction from demyelination may lead to axonal depolarisation and vesicular release of glutamate. VGSCs may also be upregulated by the inflammatory cytokine TNFα. This is supported by the increased levels of sodium channel $Na_V1.6$ in plaques containing T-Cells and activated microglia, from MS tissue samples. Expression of

glutamate transporters, EAAT1 and EAAT2, have been found to be reduced in oligodendrocytes within MS plaques in the progressive stage of the disease (Werner, Pitt & Raine, 2001). This alteration would reduce the uptake of glutamate from the extracellular space and allow accumulation. Reduced transporter expression may be as a result of inflammatory mediators released by activated microglia or due to a positive feedback mechanism of AMPA receptor activation (Loria *et al.*, 2010; Pitt *et al.*, 2003). It is also possible that increased production of glutamate due to overexpression of glutaminase contributes to increased extracellular concentration. Glutaminase expression is thought to be increased in presence of proinflammatory mediators. In combination, these mechanisms lead to an increase in extracellular glutamate in active white matter lesions, reaching pathological levels.

Pathological concentrations of glutamate have been found to affect a variety of cells within the CNS in MS and animal models. Axons appear to become damaged due to excessive activation of AMPA receptors but not NMDA receptors as shown by the protective nature of AMPAR antagonists (Pitt, Werner & Raine, 2000). AMPAR activation may lead to axonal damage by induction of calcium induced calcium release from intracellular stores, leading to influx of calcium ions into mitochondria and consequent mitochondrial stress (Joshi *et al.*, 2015).

AMPAR overactivation also appears to mediate oligodendrocyte cell death in *ex vivo* and *in vitro* animal studies (Matute, 2011). Calcium influx through AMPAR could cause mobilisation of zinc stores and consequent activation of the pro-apoptotic MAPK pathway. However, NMDAR dependent Ca^{2+} influx has been linked to myelinic and oligodendrocyte process destruction (Micu *et al.*, 2006). In particular, NMDAR lacking the GluN2 subunit, which are activated by glycine alone and experience reduced

blockage by Mg^{2+}, cause myelin damage and could therefore be a therapeutic target to prevent broad blockage side effects (Pina-Crespo *et al.*, 2010). The protection afforded by opposition of glutamate receptor overactivation in the EAE model is explored in Table 3.

Table 3: Glutamate receptor antagonists protect white matter structures in the EAE model of demyelination

Reference	Animal	Receptor	Treatment	Findings
(Pitt, Werner & Raine, 2000)	Mice (4-6 weeks)	AMPA/kainate	NBQX	Reduced oligodendrocyte cell death and axonal degeneration
(Smith *et al.*, 2000)	Rats	AMPA/kainate	NBQX	Reduced clinical score and neuronal cell death
(Evonuk *et al.*, 2020)	Mice (8-10 weeks	AMPA (GluA4)	Inducible deletion from oligodendrocytes	Reduced clinical scores, myelin degradation and protected myelinated axons
(Suhs *et al.*, 2014)	Rat (8-10 weeks)	NMDA	Memantine or MK801	Protected retinal ganglion cells and axons and reduced demyelination
(Farjam *et al.*, 2014)	Mice (9-12 weeks)	NMDA (GluN2B)	RO25-6981	Reduced neurological score, inflammation, demyelination and axonal degeneration

5.1.4. Glutamate antagonist adverse effects

Glutamate excitotoxicity plays a key damaging role in many acute and neurodegenerative conditions including stroke (Lai, Zhang and Wang, 2014), Huntington's disease (Estrada Sanchez, Mejia-Toiber & Massieu, 2008) and Alzheimer's disease (Hynd, Scott & Dodd, 2004). Therefore, antagonists of the NMDA receptor should be valuable therapeutic interventions. Furthermore, a vast cohort of these drugs exist that enact different mechanisms of antagonism at the NMDA receptor and for different subtypes. However, despite this abundance, very few NMDA receptor antagonists have been approved for human use, with treatment of Alzheimer's with memantine being one of the few examples.

The largest barricade to use of NMDA receptor antagonists is the narrow margin of activity between physiology and pathology (Lipton, 2004). Therefore, while many NMDAR antagonists have tested well in preclinical trials, they are generally accompanied by adverse side effects intolerable to patients in the clinic. The diverse roles of the glutamatergic system give rise to many different side effects including memory deficits, hallucinations and coma (Kohr, 2007; Newcomer, Farber & Olney, 2000).

Memantine, shows particular promise as a therapeutic agent as it binds the NMDA receptor in a non-comeptitive, open pore manner (Lipton, 2004). As a result, receptor activity is reduced to a greater extent at higher concentrations of agonist, meaning that pathological levels of glutamate are opposed.

5.1.5. Combined glutamate receptor antagonists

The different compositions of NMDA and AMPA receptors mean that highly selective drugs have been developed that act at each receptor. Furthermore, diversity within each receptor type has resulted in development of antagonists with high affinity for specific subtypes. By using a combination of these drugs, it is possible to inhibit both NMDA and AMPA overactivation with very little off-target effects.

Combination therapy has been shown to be highly effective in models of epilepsy. In the amygdala-kindled model of partial epilepsy, the anticonvulsant effects of AMPA receptor antagonist, NBQX, were significantly potentiated by pre-treatment with, NMDA receptor antagonist, MK-801 (Loscher, Rundfeldt & Honack, 1993). Importantly, this potentiation of anticonvulsive effect was not accompanied by worsening of adverse effects such as motor impairment and hyperlocomotion. Combination of NBQX and ifenprodil, an NMDA receptor antagonist, has recently been trialled in the kainate model of epilepsy (Schidlitzki et al., 2017). However, in this investigation, treatment with NBQX with ifenprodil at non-toxic individual concentrations resulted in higher mortality when in combination. When concentrations were lowered, mice treated with the combination exhibited fewer seizures 2 weeks after kainate exposure. This suggests that, while antagonising AMPA and NMDA receptor activation has a synergistic therapeutic effect, care must be taken with dosage so as not to potentiate adverse effects.

Dyskinesia in Parkinson's patients treated with levodopa are believed to be related to changes in AMPA and NMDA receptor activity due to alteration of phosphorylation patterns (Bibbiani et al., 2005). Treatment of primates with a high dose of levodopa produced dyskinesia in primates that was significantly attenuated by a combination of GYKI-47261, an AMPAR antagonist, and amantadine, an NMDAR antagonist. However,

at the same dose individually, no significant reduction in severity occurred. The duration of antiparkinsonian effect of levodopa reduces with prolonged treatment. Hemiparkinsonian rats, treated with levodopa twice daily for 21 days, had their response duration to levodopa completely restored by administration of subthreshold concentrations of AMPA and NMDA receptor antagonists combined. These data support the hypothesis that both AMPA and NMDA receptors have altered activity in response to prolonged levodopa treatment.

As either activity of NMDAR or AMPAR has proven to be detrimental in models of MS, there is reason to believe that antagonists of these receptors may act synergistically to counter damage. Therefore, this study will determine the efficacy of two different sets of AMPA and NMDA receptor antagonists to oppose demyelination in a new mouse model of MS.

5.1.6. Cuprizone treatment *ex vivo*

This study will expose the isolated *ex vivo* mouse optic nerve directly to cuprizone in solution in order to elicit rapid, reproducible demyelination of the nerve. Typically, cuprizone is used as a demyelinating tool *in vivo* by ingestion. It is also sometimes used to study affects on oligodendrocytes and their precursors *in vitro*. Application of cuprizone to glial cultures has been found to prevent differentiation of OPCs into oligodendrocytes, possibly be altering mitochondria (Cammer, 1999). Furthermore, cultured oligodendrocyte cell line, MO3.13, is found to have reduced viability in the presence of 1mM cuprizone whereas astrocyte cultures are unaffected (Taraboletti *et al.*, 2017). *In vitro* studies have demonstrated that cuprizone can be applied directly to cells to impart toxicity but cuprizone is yet to be used to study myelin toxicity in an

isolated white matter tract. This may be due to poor solubility in water meaning difficulty of application (Fries *et al.*, 2019).

5.2. Aims and Objectives

This study aims to establish a new *ex vivo* cuprizone model of demyelination with the isolated mouse optic nerve. The new model will be used to establish the efficacy of combined glutamate receptor antagonists to prevent demyelination in the hope of finding an effective treatment for multiple sclerosis.

- As cuprizone is not water soluble, an appropriate solvent will be found by exposing the MON to solvents and measuring the effect on compound action potential amplitude.
- CAP amplitude will be measured whilst the MON is exposed to dissolved 1mM cuprizone for 100 minutes in order to establish potential for demyelination.
- CAP amplitude from cuprizone exposed nerves will be compared in the presence of NMDAR and AMPAR antagonists separately and in combination to determine protection.

5.3. Results

5.3.1. Establishing the ex vivo cuprizone model of demyelination

As cuprizone has not been used as a method of demyelination in an *ex vivo* mouse optic nerve preparation previously, it was first necessary to determine the most suitable vehicle to allow compound action potential recordings. To achieve a concentration of 1mM cuprizone in aCSF, either 3% v/v ethanol or DMSO was required. Therefore, it was important to confirm that the chosen vehicle did not have any negative effects on CAP amplitude. Control experiments were performed involving perfusion of nerves with regular oxygenated aCSF for 10 minutes to establish a baseline followed by continued aCSF for 130 minutes. In vehicle experiments, vehicle was applied for 100 minutes after 10 minutes baseline and then regular aCSF for 30 minutes. CAP amplitude was plotted over the duration of the experiments as well as a comparison between the last 5 minutes of recording and the baseline.

A gradual decline in compound action potential amplitude over the duration was observed in the control aCSF experiments (fig. 5.1a). Following 130 minutes of perfusion, CAP amplitude had reduced in proportion to baseline to 0.806±0.046 (n=4) (fig. 5.1b). Exposure to 3% v/v ethanol caused an immediate, stark reduction in CAP amplitude which continued to slowly decline throughout the rest of ethanol exposure (fig. 5.1a). Following removal of ethanol from the perfusion, CAP amplitude rose but did not meet the level of control experiments. Ethanol application for 100 minutes and 30 minutes of recovery in regular aCSF caused a significant reduction of CAP amplitude (0.567±0.086, n=4) compared to aCSF alone (P=0.04, fig. 5.1b). On the other hand, application of 3% v/v DMSO in aCSF appeared to cause an initial potentiation of CAP amplitude relative to baseline which was significant at 30 minutes of treatment (P=0.0079, fig. 5.1a).

However, upon washout with regular aCSF, the elevated CAP reduced to levels comparable with control experiments. At the end of the duration, CAP amplitude relative to baseline in DMSO treated nerves had reduced to 0.898±0.047 (n=6) which was not significantly different to nerves treated with aCSF alone (P=0.46, fig. 5.1b).

It was decided that DMSO was the most suitable vehicle for cuprizone application as, although CAP amplitude was slightly increased during application, there was no effect at the end of the experiment. Consequently, nerves were treated with 1mM cuprizone in aCSF with 3% v/v DMSO for 100 minutes followed by recovery in regular aCSF for 30 minutes. During the cuprizone treatment, there was a steady decline in CAP amplitude over time (fig. 5.2a). This was followed by a continued decline during the washout phase that was comparable to that seen in DMSO treatment alone. At the end of the recovery phase, CAP amplitude as a proportion of baseline had fallen to 0.453±0.058 (n=9) which was significantly lower than nerves treated with DMSO for 100 minutes (p=0.0001, fig. 5.2b). Therefore, it was established that the mouse optic nerve exposed to 100 minutes of 1mM cuprizone, dissolved in aCSF with 3% DMSO was an appropriate model to investigate demyelination. The reduction in amplitude by cuprizone is seen across the whole CAP rather than individual peaks (fig. 5.2c).

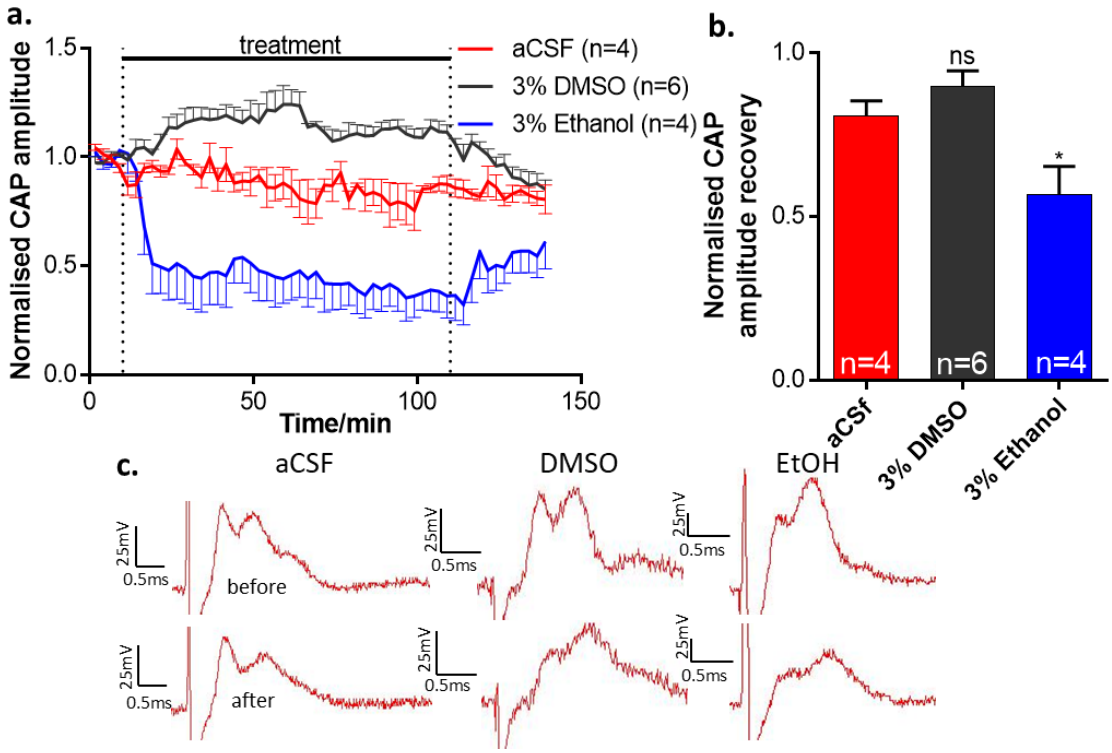

Figure 5. 1. 3% DMSO v/v is a suitable vehicle for cuprizone

a. Maintaining perfusion with aCSF over 140 minutes causes a very gradual decline in CAP amplitude. Addition of 3% DMSO causes mild potentiation of CAP amplitude which reverses upon return to normal aCSF. Addition of 3% ethanol causes a rapid, marked reduction in CAP amplitude which is maintained throughout the 100 minutes of exposure and is only partially reversed upon reperfusion with aCSF. **b.** Following 30 minutes recovery in regular aCSF, exposure to 3% DMSO for 100 minutes had caused no significant difference to CAP amplitude. However, 100 minutes of 3% ethanol exposure had caused a significant reduction in CAP amplitude (P=0.0404). **c.** Representative CAP from prior to treatment and after 100 minutes of treatment and 30 minutes of recovery time. (One-way ANOVA with Dunnett's post-hoc).

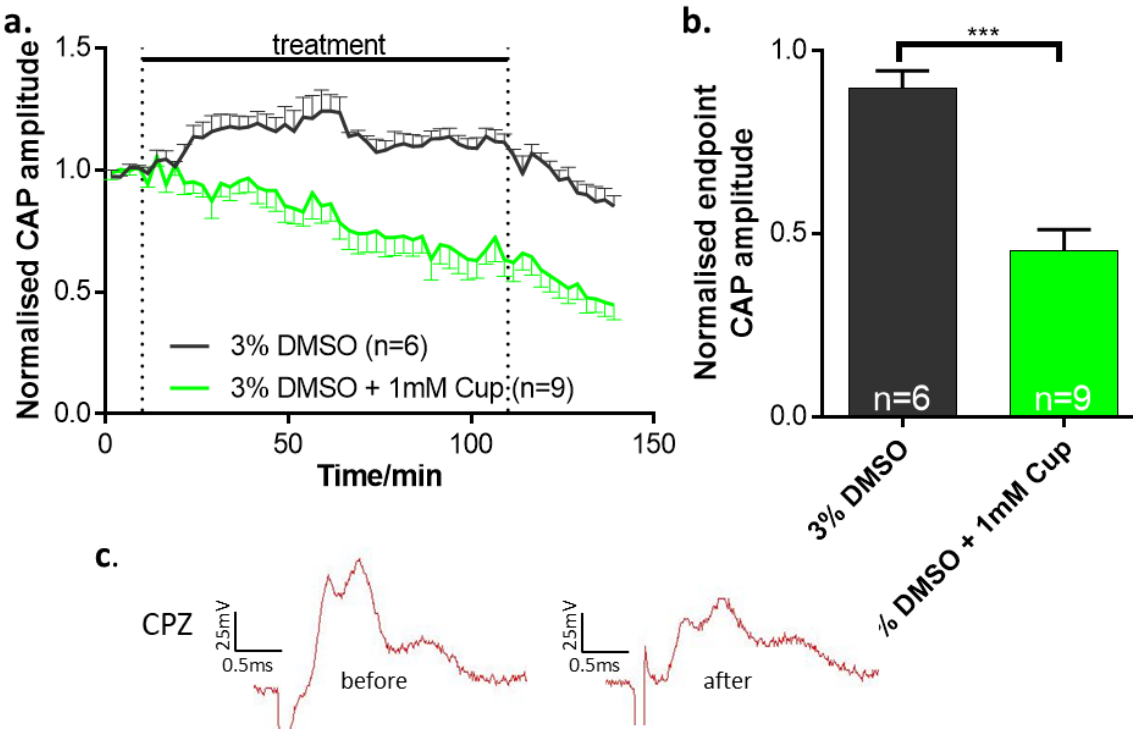

Figure 5. 2. 1mm Cuprizone in 3% v/v DMSO causes robust functional loss in the MON

a. Exposure to 1mM cuprizone dissolved in 3% DMSO in aCSF caused an accelerated rate of reduction in CAP over time. **b.** At the end of 100 minutes exposure to 1mM cuprizone in 3% DMSO in aCSF and 30 minutes of recovery in aCSF, CAP amplitude had been significantly reduced (p=0.0001) compared to 3% DMSO alone. **c.** Representative compound action potential traces. (Unpaired T-test).

5.3.2. Memantine and Perampanel act in a synergistic manner to prevent cuprizone induced CAP decline

The newly established model was employed to investigate the possibility of using a combination of memantine, an NMDA receptor antagonist, and perampanel, an AMPA receptor antagonist, to treat demyelinating disease. Glutamate antagonists were applied throughout 2 hours of incubation as well as 100 minutes of cuprizone treatment and 30 minutes washout. The drugs were applied at different concentrations both in combination and separately.

Compared to vehicle controls, a combination of 1µM memantine and 1µM perampanel (fig. 5.3b) resulted in no significant reduction of CAP amplitude from cuprizone treatment, with a final value of 0.648±0.07 (n=5, P=0.06, fig. 5.4d). However, at a concentration of 0.2µM (fig. 5.3a), the combination of memantine and perampanel was not sufficient to prevent cuprizone induced reduction in CAP amplitude (0.469±0.064, n=4. P=0.001, fig. 5.4d). When separated, neither memantine (fig. 5.3c) nor perampanel (fig. 5.4a) were capable of preventing cuprizone induced damage at a concentration of 1µM with proportional CAP amplitude reduced to 0.493±0.061 (n=5, p=0.0009) and 0.372±0.048 (n=5, p<0.0001) respectively. At a concentration of 10µM, memantine (fig. 5.4d) prevented significant cuprizone induced CAP reduction (0.78±0.085, n=5, p=0.7) but damage was still present in perampanel (fig. 5.4b) treated MONs (0.481±0.079, n=5, p=0.0003).

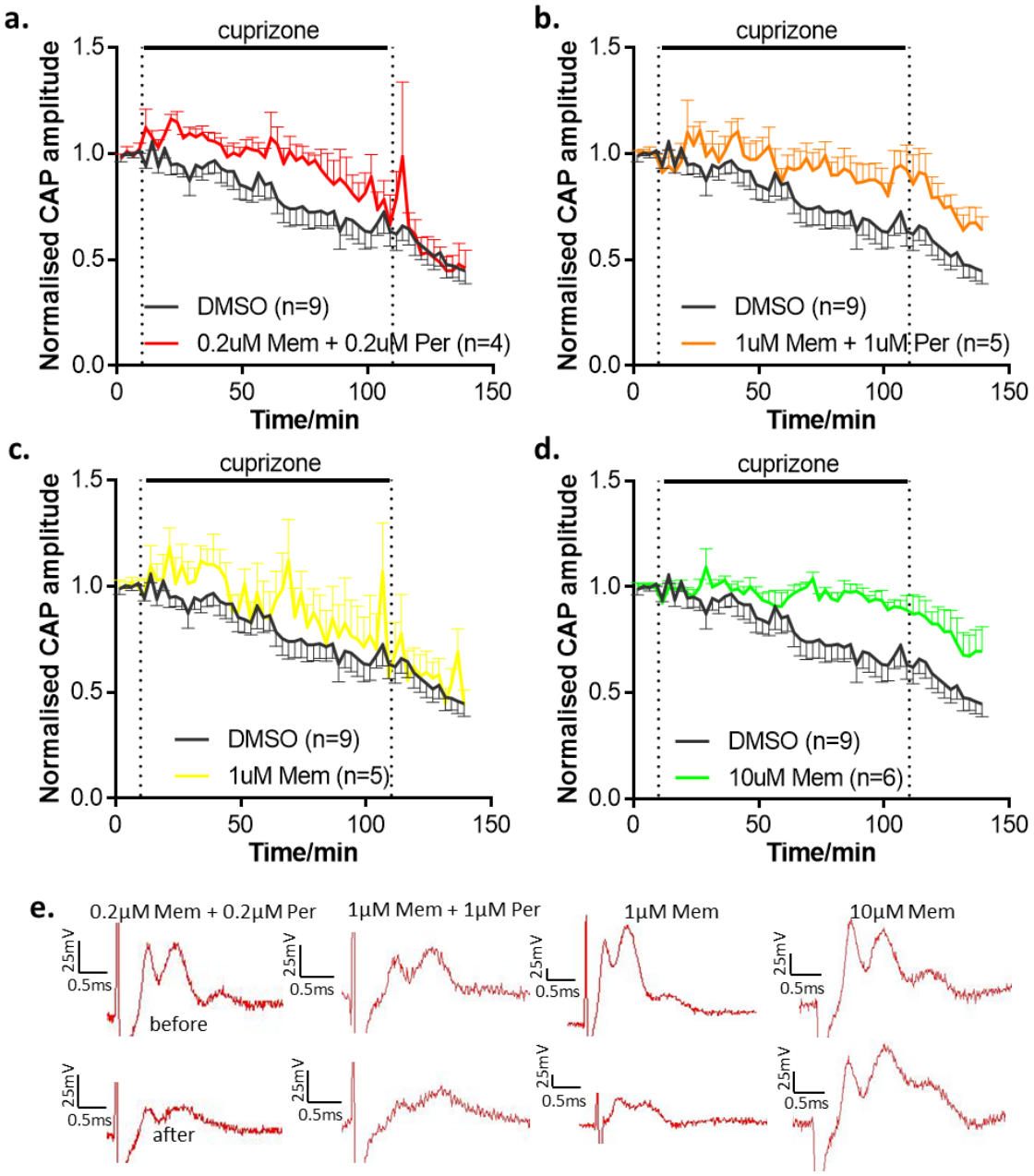

Figure 5. 3. FDA approved GluR antagonists alter timeline of cuprizone demyelination

a. At a low concentration of 0.2µM, combined memantine and perampanel have little effect on the loss of CAP amplitude from 1mM cuprizone. **b**. The combination at 1mM reduce the rate of CAP decline. **c.** Alone, 1mM memantine does not alter CAP amplitude loss. **d.** At a higher concentration of 10µM, memantine reduces the rate of CAP amplitude decline. **e.** representative CAP traces for each treatment before and after cuprizone application.

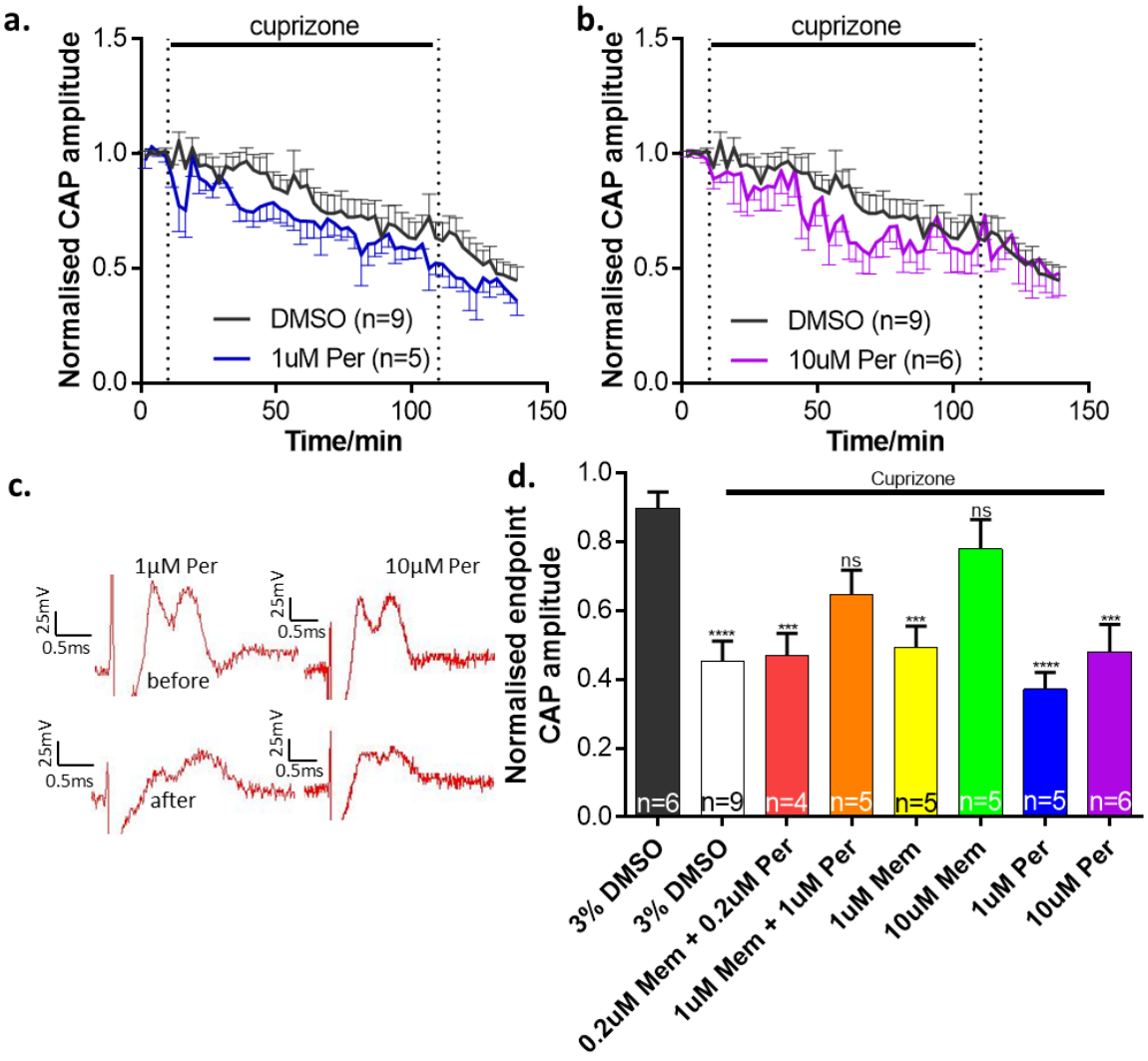

Figure 5. 4. Synergistic effect of memantine and peramanel on cuprizone induced CAP loss.

a-b. Treatment with perampanel alone at 1µM or 10µM was insufficient to alter cuprizone induced CAP amplitude decline. **c.** Representative CAP traces for perampanel treated nerves. **d.** A combination of 1µM memantine and 1µM perampanel, as well as individual treatment with 10µM memantine, was able to prevent the significant loss of CAP amplitude caused by 100 minutes cuprizone exposure seen in all other treatments. (One-way ANOVA with Dunnett's post-hoc).

5.3.3. QNZ46 and CP465022 in combination prevent cuprizone induced CAP reduction

Subsequently, derivatives of the quinazolin-4-one backbone were then tested in combination and separately to determine efficacy for protection against cuprizone induced myelin damage. QNZ46 is a noncompetitive NMDA receptor antagonist with high affinity for GluN2C/D containing channels. These channels are highly expressed at the axo-myelinic synapse and could therefore play a large role in myelin damage resulting from cuprizone insult. CP465022 is a noncompetitive AMPA receptor antagonist with high binding affinity.

Similar to memantine and perampanel, a combination of QNZ46 and CP465022 at 1µM each (fig. 5.5b) prevented significant damage by 100 minutes of 1mM cuprizone exposure compared to aCSF controls (p=0.98, fig. 5.6d). Over the 100 minutes of cuprizone treatment and 30 minutes of aCSF recovery, proportional CAP amplitude reduced to 0.805±0.065 (n=5) relative to baseline. At 0.2µM (fig. 5.5a), the combination of QNZ46 and CP465022 was unable to prevent cuprizone induced CAP inhibition, with a final amplitude of 0.583±0.042 (n=5, p=0.027, fig. 5.6d). However, when separated, neither QNZ46 (fig. 5.5c) nor CP465022 (fig. 5.6b) at 1µM were capable of preventing damage by cuprizone (0.565±0.114, n=5, p=0.017 and 0.566±0.054, n=5, p=0.017 respectively. Fig. 5.6d). This result corresponds with the combination of memantine and perampanel. Furthermore, treatment with 50µM QNZ46 (fig. 5.5d) also prevented cuprizone induced acceleration of CAP amplitude decline with a final value of 0.683±0.033 (n=4, p=0.31, fig. 5.6d). Interestingly, at a concentration of 50µM (fig. 5.6b), CP465022 greatly accelerated the reduction in CAP amplitude when 1mM cuprizone was applied, resulting in a proportional amplitude of 0.043±0.036 (n=4, p<0.0001, fig. 5.6d).

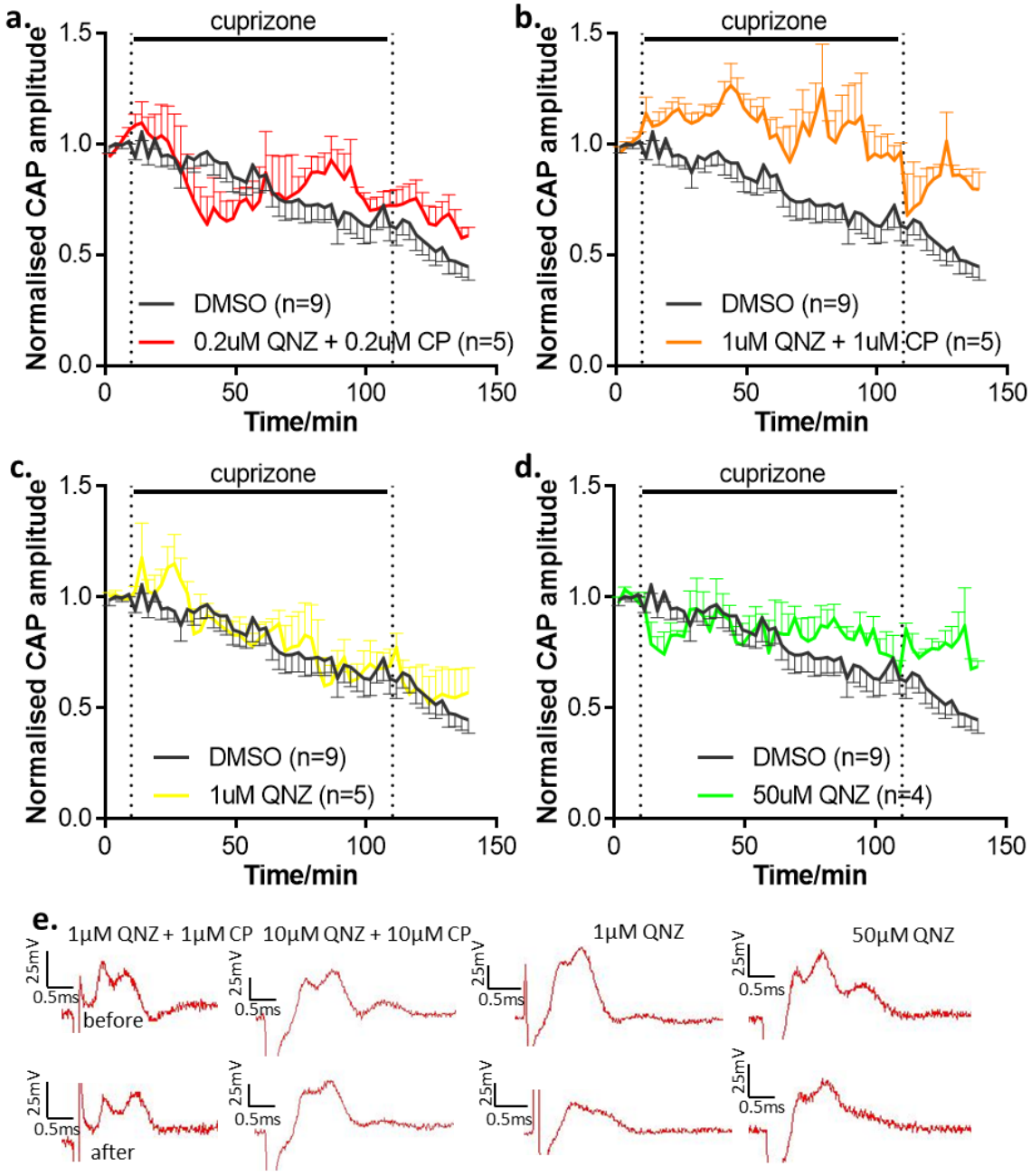

Figure 5. 5. Experimental GluR antagonists alter timeline of cuprizone demyelination

a. A combination of QNZ46 and CP 465022 at 0.2µM does not affect the rate of CAP loss from 1mM cuprizone treatment. **b.** At 1µM, the combination of QNZ46 and CP 465022 diminishes CAP amplitude decline. **c.** Alone, 1µM QNZ46 is insufficient to slow CAP decline. **d.** A higher concentration of 50µM QNZ46 prevents progression of cuprizone induced CAP amplitude loss. **e** Representative CAP traces for each treatment before and after cuprizone exposure.

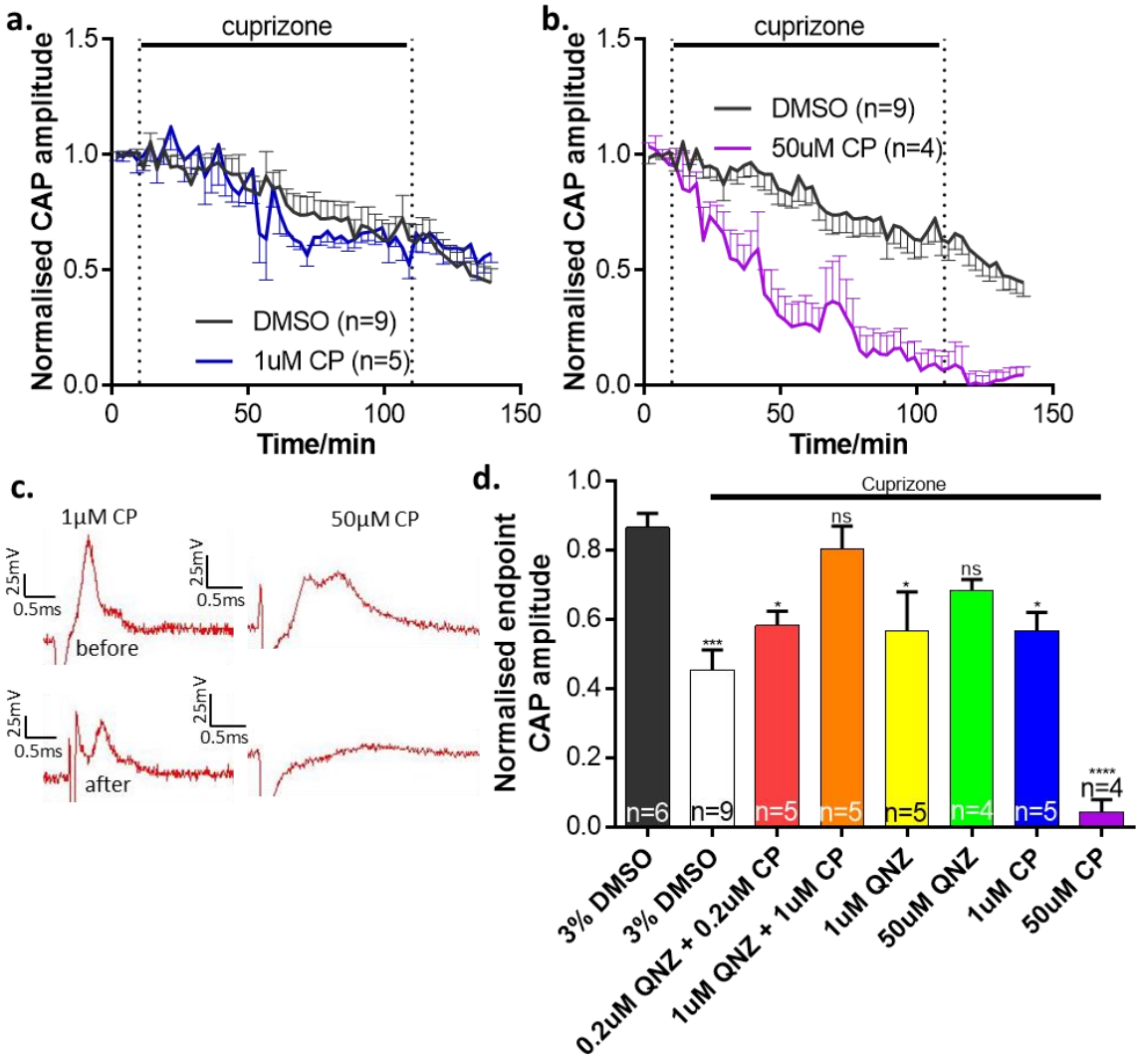

Figure 5. 6. QNZ 46 and CP 465022 provide protection against cuprizone induced CAP impairment in a synergistic manner.

a. Alone, 1µM CP 465022 does not alter the time-course of cuprizone induced CAP decline. **b**. At a higher concentration of 50µM, CP 465022 caused massive decline in CAP amplitude. **c.** Representative traces of CAPs before and after cuprizone exposure. **d.** A combination of 1µM QNZ 46 and 1µM CP 465022 as well as treatment with 50µM QNZ 46 alone prevented the significant reduction in CAP amplitude caused by application of 1mM cuprizone for 100 minutes. Perfusion with 50µM CP 465022 caused a dramatic reduction on CAP amplitude following cuprizone treatment. (One-way ANOVA with Dunnett's post-hoc).

5.4. Discussion

Glutamate excitotoxicity is believed to be a key mechanism of demyelination in multiple sclerosis. However, glutamate receptor antagonists are not used to treat MS in the clinic due to adverse effects at required doses. This study used a novel *ex vivo* mouse optic nerve cuprizone model of demyelination to determine whether a combination of AMPAR and NMDAR antagonists could protect CAP amplitude at a lower concentration than separately. It was found that NMDA receptor antagonists were able to protect CAP amplitude from cuprizone induced impairment. When in combination with AMPA receptor antagonists, a lower concentration was required. This supports the possibility of using a combined regimen of glutamate receptor antagonists to treat MS. The results also suggest that cuprizone mediated demyelination is primarily dependent on NMDA receptor currents.

5.4.1. Model of demyelination

Here, a new *ex vivo* model of demyelination has been established. Cuprizone, a copper chelator, dissolved in artificial cerebrospinal fluid is perfused over a fresh mouse optic nerve to cause functional impairment of action potential propagation. This model has many advantages over the traditional *in vivo* cuprizone model, where cuprizone is administered to live mice through dietary intake over the course of weeks to produce a demyelinated phenotype. The time-course of the new model occurs in just 100 minutes where previously, weeks would have been required. This reduces, both, time the animal must be cared for, as well as suffering the animal must endure. This also means that results can be gathered much quicker. The *ex vivo* nature of this model allows ease of treatment application by addition to the perfusion media rather than a further procedure for the animal. Furthermore, the direct access to the central white matter

tract provided by the optic nerve allows more detailed investigation of demyelinating processes. For example, compound action potentials can be measured prior to and following cuprizone treatment, permitting direct comparison to determine the exact impact of cuprizone. If optic nerves were collected in the *in vivo* model, only compound action potentials in the demyelinated state would be measurable.

The new *ex vivo* model does exhibit some disadvantages, relative to the *in vivo* model. As the nerves can only be kept alive outside of the live mouse for several hours, no remyelination will occur. Therefore, the model is only useful for investigation of the acute mechanisms of demyelination and not recovery there from. The new model is ideal for testing treatments that reduce initial demyelination but cannot be used to test treatments to encourage remyelination. A further drawback of sacrificing the mouse is that behavioural impairments cannot be investigated directly and must be inferred from functional deficits. Additionally, as the injury occurs on such a rapid timescale compared to the *in vivo* model, and indeed multiple sclerosis, it is possible that different or altered mechanisms are at play.

The biotoxicity conveyed by ingestion of cuprizone is not yet fully understood. Indeed, cuprizone's access to the brain has been questioned due to its inability to cross the intestinal epithelium (Benetti *et al.*, 2010). Consequently, it has been assumed that chronic copper chelation of the whole body must be the mode of action for cuprizone demyelination. Thus, the direct application of cuprizone to optic nerves in the new *ex vivo* model may contain complications with the possibility of cuprizone interacting with cells itself. However, cuprizone was also found not to cross the neuronal membrane and was well tolerated by cultured neurons, suggesting its direct interactions may be limited. In accordance with this, cultured astrocytes remained viable when treated with 1mM

cuprizone for 24h (Taraboletti *et al.*, 2017). However, cultured oligodendrocytes showed impaired metabolism and loss of viability under the same parameters. The study by Taraboletti also found cuprizone was capable of crossing the oligodendrocyte cell membrane which could enable a more direct action than chelation of copper. Intracellular cuprizone was only detected at 30nM, 48 hours after application of 10µM cuprizone. Therefore, it is unlikely that intracellular actions of cuprizone will come into effect within the 100-minute application of the current study.

On the other hand, recent studies have found that, while blood levels of copper are reduced, there is no difference in copper concentration in the brain after 6 weeks of cuprizone treatment (Moldovan *et al.*, 2015). In accordance, *in vitro* analysis of cultured oligodendrocytes treated with cuprizone has found perturbation to metabolic processes, independent of copper chelation (Taraboletti *et al.*, 2017). This study found that internalised cuprizone was able to directly bind with pyroxidol-5'-phosphate to interfere with aminotransferace activity. Cuprizone was found to interfere with amino acid metabolism and reducing NAD^+ generation. NAD^+ is required for aerobic glycolysis, performed in oligodendrocytes, as well as consumed by enzymes involved in myelination (Funfschilling *et al.*, 2012; Li *et al.*, 2007). Consequently, mitochondria are put under stress and reactive oxygen species production is increased.

5.4.2. Vehicle for cuprizone

Previous experiments in the lab performed in a reduced preparation on mouse brain slices had used cuprizone dissolved in ethanol mixed with aCSF at 3% v/v. This method of solubilising was attempted in the perfusion chamber for optic nerves. However, when measuring compound action potentials from the optic nerves, it was noticed that CAP amplitude rapidly reduced upon application of the cuprizone and ethanol mix. As

cuprizone had not been previously applied directly to optic nerves, it was not known if this conduction block was due to cuprizone or the ethanol vehicle. Therefore, experiments were performed using 3% ethanol without cuprizone to determine its effect on CAP amplitude. Again, a rapid impairment of CAP propagation was seen after addition of ethanol which recovered, but not fully, following reperfusion with regular aCSF. Thus, it was decided that ethanol was not a suitable vehicle for cuprizone as it would not allow for visualisation of the effects of cuprizone throughout treatment and it would contribute to irreversible damage. Therefore, if any treatments were found to effectively reduce damage, it would not be known if they combat impairment from cuprizone or ethanol.

In the toad sciatic nerve, ethanol delivers biphasic modulation of compound action potential amplitude (Quevedo, Baldeig & Concha, 1976). At low concentrations of 85mM, ethanol causes minor enhancement of CAP amplitude. However, at 342mM and 513mM, ethanol causes a rapid reduction in CAP amplitude within 5 minutes with upwards of 50% reduction after 30 minutes. As 513mM is 3%v/v, this is in accordance of our finding that ethanol as a vehicle causes significant conduction block. This inhibition of CAP amplitude at high concentrations of ethanol was related to a reduction in membrane permeability of Na^+ and K^+. However, it is unknown what drove the irreversible functional deficit caused by 3% ethanol treatment. Morton's digital neuroma is a condition causing chronic neuropathic foot pain and is often successfully treated by injection of diluted ethanol to cause sclerosis of the nerve (Hughes *et al.*, 2007). However, when evaluating the validity of the treatment, no histological changes were found following injection of 4%, 20% or 30% ethanol to the rat sciatic nerve

(Mazoch *et al.*, 2014). Thus, it is inconclusive whether 3% ethanol should cause irreversible nerve damage.

Cuprizone is similarly soluble in DMSO and so experiments were performed to determine effect of 3% v/v DMSO on CAP amplitude. A small enhancement of CAP amplitude was seen shortly after addition of DMSO, compared to aCSF treatment alone. However, this was reversed upon return to regular aCSF conditions and final CAP amplitude was not significantly different to aCSF treatment for the duration. Therefore, although using DMSO as a vehicle would partially obscure effects of cuprizone during treatment, it would not provide any protection or damage to the nerve overall, making it a superior vehicle to ethanol.

Interestingly, treatment with DMSO has also been found to have profound effects on membrane excitability (Tamagnini *et al.*, 2014). DMSO at concentrations as low as 0.05% v/v have been found to reduce input resistance and intrinsic excitability of pyramidal neurons. However, it was also found there was a small but insignificant increase in action potential peak. This is likely to be exacerbated at higher concentrations of DMSO and could be represented in the current study with the increased CAP amplitude in the presence of 3% DMSO.

The addition of 1mM cuprizone in 3% DMSO caused a very gradual decline in CAP amplitude compared to 3% DMSO alone. The final CAP amplitude in cuprizone treated nerves was around half that of vehicle control treated nerves. This functional deficit suggests large levels of demyelination or axonopathy have occurred. *In vivo* cuprizone treatment is known to primarily cause insult to myelin and oligodendrocytes with secondary axonal degeneration and so, this is likely the case in this *ex vivo* model (Slowik *et al.*, 2015). However, the direct application and rapid nature of the model could result

in different pathological mechanisms such as the impairment of amino acid metabolism seen in cultured oligodendrocytes treated with cuprizone (Taraboletti *et al.*, 2017).

Fluoromyelin staining in the corpus callosum of cuprizone treated mouse brain slices, by other laboratory members, has revealed reduced staining compared to vehicle controls. Furthermore, scanning electron microscopy of cuprizone treated optic nerves has demonstrated loss of myelin integrity and reduced density compared to vehicle controls. Together, this implicates myelin disruption as the cause of functional impairment of CAP propagation by cuprizone treatment.

5.4.3. Cuprizone induced demyelination is glutamate receptor dependent

Though there is disagreement about the method of action of cuprizone, copper chelation is still the most commonly accepted. This would mean its addition to a preparation will see residual copper stores from the tissue removed. Previously, it has been believed that removal of copper causes impairment of copper dependent cytochrome c oxidase activity in the oligodendrocyte respiratory chain. Reduced mitochondrial output causes reactive oxygen species production, macrophage recruitment and promotion of proinflammatory cytokines. The oligodendrocytes are believed to die as a result (Patergnani *et al.*, 2017). Oligodendrocytes are particularly susceptible to oxidative stress due to their low intrinsic levels of glutathione peroxidase activity, at less than 15% those seen in astrocytes, and high levels of iron (Juurlink, Thorburne & Hertz, 1998). Consequently, oligodendrocyte capacity for peroxide scavenging is severely limited. Furthermore, due to production and maintenance of vast sheathes of lipid bilayers, oligodendrocytes can have the highest metabolic demands of any brain cell (Connor & Menzies, 1996). Additionally, iron homeostasis is perturbed by cuprizone treatment due to the copper dependency of ferroxidases and ferratin (Jhelum

et al., 2020). As a result, ferrous iron concentration increases and cannot be stored by ferratin causing in an increase in iron-mediated free radicals. Thus, a fine balance between metabolic output and overwhelming ROS scavenging systems is put out of equilibrium by cuprizone treatment. This could explain why cuprizone toxicity is limited to oligodendrocytes and their precursors. Indeed, Schwann cells have a high basal expression of antioxidant enzymes, which may justify the limitation of demyelination to the CNS (Vincent *et al.*, 2009). Copper chelation will likely result in employment of these damaging mechanisms to oligodendrocytes in the new *ex vivo* cuprizone model employed in the present study. However, gradual CAP impairment begins minutes after introduction of cuprizone, suggesting a more rapid mechanism of action is at play. It is possible that the high concentration of cuprizone causes sufficient copper chelation to perturb axonal metabolism through the mitochondrial impairment previously discussed. This could result in CAP conduction block due to failure of membrane repolarisation resulting from lack of ATP supply to the sodium-potassium pump, as is seen in ischaemic conditions (Bakiri *et al.*, 2008; Baltan, 2012; Baltan *et al.*, 2008; Doyle *et al.*, 2018). However, when axonal metabolic output is perturbed in these studies, CAP conduction is abolished relatively rapidly and recovers following reperfusion, which was not seen in the *ex vivo* cuprizone model.

In this new *ex vivo* cuprizone model, demyelination can be prevented by antagonism of glutamate receptors, especially that of NMDA receptors. This implicates glutamate receptor activation and, likely, excitotoxicity in cuprizone-induced demyelination. However, cuprizone is not known to have any direct effects on the glutamate receptors. One potential link between cuprizone and glutamate receptor overactivation is the high copper affinity of, PrP^C, an NMDA modulator (Black *et al.*, 2014; Hijazi *et al.*, 2003). PrP^C

is well known for its conversion to the misfolded form PrP^{SC} which causes neurodegenerative diseases by triggering further misfolding of other PrP^{C} proteins to form damaging aggregates. However, relatively little is known about the physiological function of PrP^{C} itself. The protein is anchored to the extracellular leaflet by its C-terminus while its N-terminus contains 4 to 5 octapeptide repeats which mediate its high copper affinity. Copper causes significant conformational change to the protein, supporting a key role in the function of PrP^{C}.

Further clues to the function of PrP^{C} are given by the detrimental effects of its deletion in mice. Under normal conditions, the phenotype of this knockout is relatively mild with minor impairment of spatial memory (Criado *et al.*, 2005), likely caused by changes to long term potentiation (Curtis *et al.*, 2003). They also suffer from peripheral demyelination as age progresses due to inability of communication for myelin maintenance between neurons and Schwann cells (Bremer *et al.*, 2010). This phenomenon was not detected in central white matter, but it is possible this mechanism plays a role in the cuprizone induced demyelination. Perhaps more interestingly, PrP^{C} appears to be vital in mitigation of several forms of insult. Seizure severity from injection of pilocarpine or pentylenetetrazole progresses at a far greater rate in knockout mice and likelihood of resulting death is significantly increased (Walz *et al.*, 1999). Additionally, PrP^{C} knockout mice experience lower nociceptive thresholds to both inflammatory and neuropathic pain which can be recovered by application of, NMDA receptor antagonist, MK-801 (Gadotti & Zamponi, 2011). Altogether, these studies paint a convincing picture that PrP^{C} has a modulatory effect on glutamate neurotransmission.

Investigations by Khosravani et al. have aimed to determine how PrP^{C} may modulate NMDA receptor activation. PrP^{C} null mice exhibit a greater number of population spikes

in hippocampal slices which are blocked by amino-5-phosphonovaleric acid, an NMDA receptor antagonist (Khosravani *et al.*, 2008). Furthermore, NMDA specific currents were enhanced in both amplitude and duration due to increased deactivation time. Interestingly, when neurons treated with copper chelator, BCS or cuprizone, are applied with physiological levels of glycine and NMDA, the resulting current does not desensitise (You *et al.*, 2012). Furthermore, the same study found identical results in PrP^C null neurons without addition of copper chelators and these effects are not additive. Additionally, immunoprecipitation of PrP^C with the GluN1 subunit is reduced with copper chelation. This suggests copper modulates NMDA receptor activity via binding to PrP^C. The NMDA receptor activity appears to be enhanced when PrP^C is not bound due to a greater affinity for glycine binding.

In the experimental autoimmune encephalitis model of MS, deletion of PrP^C has been found to exacerbate disease progression (Ingram *et al.*, 2009). This effect has been attributed to a regulatory role for the protein in T lymphocyte reactivity to the CNS. This phenomenon would not occur in the current *ex vivo* cuprizone model due to lack of T-cell infiltration in the isolated preparation. However, further studies have found that mice lacking PrP^C in the CNS but sufficient in the immune system experience greater disease progression in EAE than mice deficient in the immune system but sufficient in the CNS (Gourdain *et al.*, 2012). This would suggest a CNS origin to the increased susceptibility in agreement with the hypothesis of glutamate receptor interactions.

If copper chelation perturbs axonal metabolism in the present study, in a similar way to ischaemic conditions, this may result in release of glutamate from the axon cylinder. Vesicular glutamate release is known to occur under ischaemic conditions in rat white matter (Doyle *et al.*, 2018). Elevated glutamate concentration in the periaxonal space

may cause myelinic NMDA receptor activation and subsequent myelin damage. This demonstrates another pathway by which cuprizone treatment may elicit glutamate receptor dependent CAP impairment. A combination of increased glutamate release from metabolic impairment and loss of NMDA receptor desensitisation from PrP^C interactions may have devastating consequences for myelinic calcium accumulation and subsequent damage.

In the current *ex vivo* cuprizone study, both memantine and QNZ-46, NMDA receptor antagonists, are capable of preventing cuprizone induced loss of compound action potential. This supports the hypothesis that NMDA currents in myelin are enhanced by cuprizone treatment, possibly due to loss of affinity of PrP^C to the GluN1 subunit and subsequent binding of glycine. This enhanced NMDA current would consequently drive destruction of myelin and therefore loss of action potential propagation. However, factors which convey oligodendrocyte specificity to cuprizone toxicity are yet to be elucidated.

5.4.4. Synergism of antagonism of NMDA and AMPA receptors

The present study revealed that, in combination, NMDA and AMPA receptor antagonists were effective at preventing cuprizone induced CAP loss at a lower concentration than NMDA receptor antagonisms alone. However, AMPA receptor antagonism alone, did not result in CAP protection from cuprizone. At resting membrane potential, NMDA receptors are blocked by a high affinity of Mg^{2+} to the transmembrane pore. However, upon membrane depolarisation the pore is unblocked, and NMDA currents can occur. AMPA receptor activation will contribute to membrane depolarisation and, therefore, antagonism of AMPARs alongside NMDARs will further reduce destructive influx of Ca^{2+}.

This would lead to a synergistic effect of antagonism of the two receptor types on myelin protection in the cuprizone model.

AMPA receptor desensitisation is only mildly affected by PrP^C overexpression, unlike NMDA receptors, and cation influx is unaffected (Huang *et al.*, 2018). However, there is evidence of modulation of AMPA receptors by copper ions (Weiser & Wienrich, 1996). Application of copper inhibits AMPA receptors in cultured neurons with an IC50 of just 4.3µM. Chelation of copper by BCS significantly increased AMPA receptor currents indicating an alternative mechanism of regulation by copper ions (Huang *et al.*, 2018). Therefore, in the current *ex vivo* cuprizone model, AMPA receptor currents will be enhanced by the chelation of copper by cuprizone, leading to a depolarisation of the membrane potential and greater unblocking of NMDA receptors by Mg^{2+}. This gives further reasoning to the success of combined AMPA and NMDA receptor antagonism in the cuprizone model.

It is unknown why AMPA receptor antagonism alone, by use of perampanel or CP 465022, was insufficient to preserve optic never function. Some studies have suggested that AMPA receptor mediated currents are the primary cause of glutamate excitotoxicity in oligodendrocytes (Leuchtmann *et al.*, 2003). Oligodendrocytes express AMPA receptors lacking in the GluA2 subunit which are highly permeable to calcium and, therefore, able to contribute to calcium induced cell death (Christensen *et al.*, 2016). Consistent with this, conditional knockout of GluA4 subunits from mature oligodendrocytes reduces symptom severity in EAE mice (Evonuk *et al.*, 2020). The knockout mice exhibited a reduction in myelin damage and increased viability of myelinated axons but not unmyelinated axons. This indicates that behavioural protection conveyed by the lack of GluA4 subunits is by prevention of demyelination

and secondary axonal loss. Overall, the data is compelling for a role of oligodendrocyte AMPA receptors in glutamate mediated cell death in MS. However, AMPA receptor activation did not appear to be the primary cause of functional loss in the new *ex vivo* cuprizone model.

The inhibition of NMDA receptors by memantine is highly voltage dependent (Frankiewicz *et al.*, 1996). At -35mV, NMDA currents in CA1 hippocampal slices are reduced to just 11% of control. However, at +40mV, this suppression is only to 95% of control. Therefore, membrane depolarisation by activity of AMPA receptors would drastically reduce the ability of memantine treatment to prevent calcium entry to myelin and oligodendrocytes through NMDA channels. This is likely to contribute to the synergistic effect of combined treatment with perampanel as the inhibition of AMPA receptors will prevent membrane depolarisation and allow sustained blockage of NMDA receptors with memantine.

5.5. Conclusion

This study has found that cuprizone induced demyelination can be reproduced in an *ex vivo* optic nerve preparation in just 100 minutes in order to produce significant functional loss of white matter. This procedure could prove invaluable in early preclinical drug studies for determination of potential therapeutic agents.

The current study has demonstrated that injury mechanisms in the new cuprizone model are glutamate mediated. This is important as glutamate excitotoxicity has been implicated as a deleterious phenomenon in progressive MS. Therefore, agents that protect white matter function in the *ex vivo* model may hold promise for treatment of the human disease.

Loss of white matter function in the new model could be attenuated by a combination of NMDA and AMPA receptor antagonists. These drugs provided protection at a lower concentration when in combination compared to use alone. This would indicate a synergistic effect between the drugs. A combination of clinically approved drugs, memantine and perampanel, afforded protection of compound action potential amplitude which gives promise to a swift route to the clinic for use in progressive MS. Furthermore, a combination of experimental drugs, QNZ46 and CP 465022, also proved efficacious at preventing CAP reduction by cuprizone. As QNZ46 is specific to NMDA receptors containing GluN2C/D, which are expressed in myelin, adverse effects caused by antagonism of neuronal NMDA receptors may be avoided.

Chapter 6:

Glutamate Receptors in Ischaemic Excitotoxicity

Abstract:

White matter is extremely susceptible to insult from ischaemic stroke and glutamate excitotoxicity is thought to play a key role in this injury. Extracellular glutamate rises in white matter during ischaemia from a variety of sources such as reverse transport from astrocytes. Glutamate is also released from axons in a vesicular manner into the periaxonal space to act on myelin NMDA receptors during ischaemia. Therefore, there may be a synergistic protection of white matter by inhibiting AMPA receptors, located mainly on the oligodendrocyte soma, and NMDA receptors, found mainly on cell processes and myelin.

The ability of glutamate receptor antagonists to protect optic nerves from ischaemic damage caused by OGD conditions was assessed. Following 50 minutes of OGD and 60 minutes of recovery, CAP amplitude had reduced to 11.2% of baseline, in the absence of glutamate receptor antagonists. Incubation with a combination of 10µM memantine and 10µM perampanel did not alter OGD-induced CAP destruction. However, incubation with 10µM QNZ46 and 10µM CP 465022 improved CAP amplitude recovery to 24.5% of baseline. Furthermore, the AMPA receptor antagonist, CP 465022, alone at 10µM was sufficient to protect CAP amplitude to 34.7% of baseline, while the NMDA receptor antagonist, QNZ46, did not afford protection at 10µM.

These results do not support a synergistic action of AMPAR and NMDAR antagonists in the protection of white matter from ischaemic insult. The protection of CAP amplitude afforded by CP 465022 may indicate that glutamate-mediated ischaemic white matter injury is primarily dependent on AMPA receptor currents.

6.1. Introduction

Ischaemic stroke is a devastating condition that can cause destruction of all components of white matter. The events that follow the cessation of delivery of metabolic substrates lead to a dramatic rise in extracellular glutamate to pathological levels (Benveniste *et al.*, 1984). While ischaemia induced glutamate release has traditionally been thought of as a grey matter phenomenon, recent evidence supports its involvement in white matter pathology (Doyle *et al.*, 2018). Vesicular release of glutamate from axons causes extracellular concentrations to rise by around 25μM and act on GluN2C/D glutamate receptors to cause myelin injury. Activation of myelinic glutamate receptors is a proposed mechanism by which cuprizone enacts white matter damage. I will therefore determine whether combined NMDA and AMPA receptor antagonists protect WM in a model of ischaemic stroke in a similar fashion to my findings in cuprizone toxicity. Additional support for the prospect of combined glutamate receptor antagonists in WM ischaemia is the recent demonstration of GluA4 receptors in myelin (Christensen *et al.*, 2016). As membrane depolarisation by AMPA receptors can lead to unblocking of NMDA receptors, their activation under ischaemic conditions could contribute to excitotoxic WM damage.

6.1.1. Glutamate receptor expression in human white matter

Though WM glutamate receptor expression in rodents is well characterised, the situation in humans has only recently become more understood (Christensen *et al.*, 2016). NMDA receptors are made up of multiple subunits but must possess the GluN1 subunit for function. In humans, GluN1 is found to be expressed in the myelin sheath and particularly highly in oligodendrocyte processes adjacent to the myelin. The GluN1 subunit is also expressed in the cytoplasm of oligodendrocyte soma. However, GluN1

antibodies do not colocalise with the axon cylinder, demonstrating lack of NMDA receptor expression in this component. This is in agreement with expression studies in rodent white matter.

The GluA4 subunit conveys a particularly high permeability of calcium to AMPA receptors (Santos *et al.*, 2006). Cells expressing this subunit are particularly susceptible to glutamate mediated damage due to excessive calcium influx initiating cell death pathways. Strong expression of GluA4 subunits has been demonstrated in human white matter (Christensen *et al.*, 2016). The subunit is found throughout the oligodendrocyte, on the soma, the processes and dispersed amidst the myelin sheath. This may underlie the high susceptibility of oligodendrocytes to damage from ischaemic insult. Furthermore, GluA4 antibodies have been found to colocalise with the axon cylinder on or near the axolemma in areas where the myelin sheath is separated.

6.1.2. Glutamate mediated oligodendrocyte and myelin damage

Oligodendrocytes are the most abundant cell in white matter and are profoundly affected by ischaemic injury (Fern & Matute, 2019). This vulnerability is exacerbated by age as glutamate transport proteins become increasingly expressed (Baltan *et al.*, 2008). Consequently, reverse glutamate transport, occurring in stroke due to breakdown of ionic gradients, paired with vesicular glutamate release from axons, results in pathological extracellular glutamate. In the oligodendrocyte soma, glutamate excitotoxicity is believed to be primarily mediated through AMPA/kainate receptors which are abundantly expressed (Matute *et al.*, 2007; Salter & Fern, 2005). Interestingly, antagonism of NMDA receptors has been found to cause a gradual decline in compound action potential area during the reperfusion phase of OGD and does not provide protection from ischaemia in young or old animals. However, these findings conflict with

more recent data that suggest GluN2C/D antagonism protects myelin from ischaemic injury and reduces functional loss in rat optic nerves (Doyle *et al.*, 2018). The protection conveyed in this later study may be due to specific antagonism of NMDA receptors expressed in myelin without confounding effects from other components.

Ischaemia induces a membrane current in oligodendrocytes (Bakiri *et al.*, 2008). This current can be partially blocked by antagonism of NMDA receptors using D-AP5. This would suggest NMDA receptor activation in ischaemia contributes towards cation influx into oligodendrocytes. Interestingly, this study found no beneficial effect of AMPA/kainate receptor antagonism on ischaemia induced CAP decline. However, NMDA receptor antagonists were able to partially prevent ischaemic injury. This directly conflicts with other studies prioritising AMPA receptor mediated excitotoxicity in white matter.

Calcium accumulation in oligodendrocytes and myelin is mediated by distinct glutamate receptors (Micu *et al.*, 2006; Salter & Fern, 2005). In the oligodendrocyte soma antagonism of AMPA receptors completely inhibited the ischaemic rise in intracellular Ca^{2+}. Calcium levels in myelin also rise during ischaemia and cause myelin damage. Antagonism of NMDA receptors greatly opposed this phenomenon in myelin while AMPA receptor antagonists had a minimal effect. Furthermore, antagonists specifically targeting GluN2A and GluN2B containing receptors did not significantly affect calcium accumulation in myelin. This underlines the importance of GluN2C/D receptor subunits in ischaemic myelin disruption.

6.1.3. Glutamate mediated axonal injury

Expression of AMPA and kainate receptors has been demonstrated in myelinated large spinal cord axons (Ouardouz *et al.*, 2009a). Potentially, this could lead to excitotoxic

damage when exposed to high concentrations of glutamate. Indeed, injection of AMPA into the rat external capsule, a white matter tract of the basal ganglia, leads to significant axonal damage characterised by axonal swelling and bulbs (Fowler *et al.*, 2003). This effect is attenuated by antagonism of AMPA receptors using SDP 502, as well as reducing concomitant myelin and neuronal damage. This would implicate axons as a site of glutamate mediated injury. However, it is unknown whether axonal damage occurs as a secondary complication of demyelination. Axonal integrity is tightly correlated with myelin support. Loss of expression of proteolipid protein-1 from myelin results in axonal degeneration even without loss of myelin itself (Garbern *et al.*, 2002). Therefore, disruption of myelin by ischaemia induced glutamate toxicity may contribute to axonal damage. Furthermore, although AMPA/kainate receptor expression has been demonstrated in large axons, in smaller diameter axons, it is much harder to illustrate due to reduced dimensions between the axon cylinder and myelin sheath (Fern & Matute, 2019).

Investigation of glutamate mediated injury in unmyelinated axons remains elusive due to their small diameter. However, phenotypically, unmyelinated axons and premyelinated axons are similar and the optic nerve of neonatal rats provides a representative premyelinated tract. In these tracts, expression of NMDA receptors has been demonstrated on axons (Huria *et al.*, 2015). Furthermore, agonism of NMDA receptors exacerbates ischaemic injury to premyelinated axons while their antagonism greatly improves functional outcome and axon viability. Therefore, axonal injury in premyelinated white matter tracts appears to be NMDA receptor mediated and it is possible this translates to unmyelinated axons in mature white matter tracts.

6.1.4. Source of glutamate in white matter ischaemia

The fibrous astrocytes of white matter are significantly more susceptible to ischaemic damage than protoplasmic astrocytes of the grey matter though this does not appear to be due to glutamate receptor expression (Shannon, Salter & Fern, 2007). While glutamate excitotoxicity does not play a major role in astrocyte cell death, the cells have been considered the principle source of extracellular glutamate in white matter ischaemia. However, investigation into the early spike in extracellular glutamate concentration reveals this is not alleviated by inhibition of astrocytic glutamate release pathways (Doyle *et al.*, 2018). Conversely, astrocytes are responsible for a delayed increase in extracellular glutamate due to cell damage disrupting the membrane and allowing extrusion of intracellular glutamate (Fern, 2001). This is particularly the case in white matter due to the susceptibility of fibrous astrocytes to ischaemic insult. Ischaemia induced astrocyte disruption is highly linked to the activity of the NKCC1 transporter leading to excessive swelling of the cells (Chen & Sun, 2005). This transporter is essential for potassium clearance and sodium homeostasis in normal physiology but, in the high extracellular potassium climate of ischaemia, causes overwhelming ionic and osmotic influx into astrocytes.

In Bergmann glia, a type of grey matter astrocyte, acidification induced by optogenetic stimulation results in the release of glutamate (Beppu *et al.*, 2014). Grey matter astrocyte acidosis is well characterised in ischaemia and so this would lead to ischaemia induced glutamate release. However, some evidence suggests that white matter astrocytes regulate pH via different mechanisms to grey matter astrocytes (Hansen *et al.*, 2015). This could contribute towards the lack of astrocytic glutamate release early in white matter ischaemia pathology.

The principle source of extracellular glutamate soon after onset of ischaemia is vesicular release of glutamate from the axon cylinder (Doyle *et al.*, 2018). The release of glutamate is uniform along the cylinder. Consequently, while some glutamate is released at the nodes of Ranvier to gain access to the extracellular space, most will be released into the isolated periaxonal space. This would implicate glutamate activity at myelinic NMDA receptors playing a key role in the ischaemic white matter damage. Importantly, if this is the case, therapeutics aiming to oppose NMDAR mediated myelin destruction must be capable of penetrating myelin to the periaxonal space. It is possible that studies reporting no benefit of NMDA receptor antagonism in white matter ischaemia are not allowing sufficient time for diffusion of the drugs to their target.

6.1.5. Combined glutamate receptor antagonists

Overall, there is evidence to support the possibility that combining antagonists of AMPA/kainate and NMDA receptors would prove beneficial for injury prevention in white matter ischaemia. The predominance of AMPA receptor mediated calcium influx in the oligodendrocyte soma and NMDA receptor mediated calcium influx in myelin would indicate a combination could prevent calcium overload throughout all components (Micu *et al.*, 2006). Indeed, studies have already demonstrated the efficacy of combining memantine, an NMDA receptor antagonist, with NBQX, an AMPA/kainate receptor antagonist, at reducing OGD induced CAP decline (Bakiri *et al.*, 2008). This study also found the NMDA receptor antagonist MK801 to protect CAP area from OGD. The evidence supporting white matter protection provided by antagonism of glutamate receptors in ischaemia is summarised in Table 4.

Table 4: Glutamate receptor antagonists in models of white matter ischaemia

Reference	Preparation	Ischaemia	Receptors blocked	Findings
	Cerebellum slices			
(Karadottir *et al.*, 2005)	Rat (p7-11)	OGD + metabolic[1]	AMPA/k + NMDA	OL and OPC ischaemic current mediated by NMDA more than AMPA/k
	Optic Nerve			
(Salter & Fern, 2005)	Mice (p7-13 or p25)	OGD	AMPA/k	Prevented loss of OL soma but not processes
			AMPA/k + NMDA	Prevented loss of OL soma and processes
(Alix & Fern, 2009)	Rat (p10)	OGD	AMPA/k + NMDA	Preferential protection of small premyelinated axons
(Micu *et al.*, 2006)	Rat adult	NaN_3 + 0mM glucose	AMPA/k	Blocked calcium rise in OL soma but not processes
			NMDA	Complete block of calcium rise in OL processes but partial in soma
			NMDA (GluN2A/B)	No significant effect on calcium rise
(Doyle *et al.*, 2018)	Rat (p90-120)	OGD	NMDA (GluN2C/D)	Increased CAP recovery, prevented structural changes to myelin
(Baltan *et al.*, 2008)	Mice (12 or 24 month)	OGD	AMPA/k	Prevented complete loss of CAP during OGD and improved CAP recovery
			NMDA	No effect on CAP during OGD, reduced CAP recovery
	In vivo			
(Follett *et al.*, 2004)	Rat (p7)	H/I[2]	AMPA/k	Reduced loss of myelin
(Manning *et al.*, 2008)	Rat (p6)	H/I	NMDA	Reduced loss of developing and mature OL
(McCracken *et al.*, 2002)	Rat adult	MCAo	AMPA	Reduced damage to axons and OLs in the cortex but not subcortex
(Schabitz, Li & Fisher, 2000)	Rat adult	MCAo	NMDA	Increased optical density of axons and myelin
(Kanellopoulos *et al.*, 2000)	Rat adult	Spinal cord ischaemia	AMPA/k	Reduced locomotor deficit corresponding with increased axonal counts, not GM protection

OGD, oxygen-glucose deprivation; AMPA/k, AMPA and kainate receptors; OL, oligodendrocyte; OPC, oligodendrocyte precursor; CAP, compound action potential; H/I, hypoxia/ischaemia; MCAo, middle cerebral artery occlusion; GM, grey matter.

[1] 2mM Iodoacetate and 100µM Rotenone or 25µM Antimycin

[2] Hypoxia/Ischaemia – Carotid artery ligation and 1h hypoxia at 6% O_2

Further to oligodendrocyte and myelin protection, the possibility of widespread AMPA/kainate receptors on myelinated axon cylinders raises the potential of AMPA receptor antagonists for prevention of ischaemia induced axonal degeneration (Ouardouz *et al.*, 2009a). However, while it is known that exogenous AMPA elicits axonal injury, there is currently no evidence that this is directly mediated by axonal AMPA receptors (Fowler *et al.*, 2003). Additionally, the majority of axonal damage in ischaemia is believed to me mediated by calcium overload by reversal of the Na^{+}/Ca^{2+} exchanger and activation of voltage gated calcium channels (Stys, 2005). Therefore, axonal AMPA receptor antagonism is unlikely to contribute significantly to protection of white matter function in combined AMPA and NMDA antagonist therapy.

Again, the present study will focus on the efficacies of combining clinically approved drugs memantine and perampanel for reduction in optic nerve CAP decline. If successful, the approved use in other neurological conditions would ensure a faster route to clinical use in stroke. This would mean sooner benefits for quality of life in victims of stroke and reduced burden on the healthcare system if disability could be prevented. In support of this treatment option, memantine has proven beneficial for CAP integrity in optic nerves when pre-applied for 2 hours, in combination with NBQX (Bakiri *et al.*, 2008). This is promising for efficacy in combination with the, AMPA receptor antagonist, perampanel. The present study will also investigate the potential of experimental drugs QNZ46 and CP 465022. The composition of myelinic NMDA receptors, containing GluN2C/D subunits, gives promise to the use of QNZ46 as it is specific to these subunits. QNZ46 has successfully reduced OGD induced CAP decline in rat optic nerves (Doyle *et al.*, 2018). Conversely, GluN2C containing NMDA receptors in neurons are neuroprotective in ischaemia (Chung *et al.*, 2016). This is evidenced by their presence in neurons

conveying an increase in resistance to NMDA toxicity and their deletion causing increased cell death in hippocampal neurons. While this contraindication will not cause deleterious effects of QNZ46 in the MON model due to lack of neuronal cell bodies, this could conflict with clinical use. The principle mode of action of CP465022 is AMPA receptor antagonism which should promote oligodendrocyte survival. However, it also has a potent blocking effect of the persistent activity of sodium channel, $Na_V1.6$. This channel colocalises with the sodium-calcium exchanger at the nodes of Ranvier on the axon cylinder (Craner *et al.*, 2004a). Depolarisation will cause activity of the channel resulting in influx of sodium and reversal of the exchanger and consequent calcium overload (Alrashdi *et al.*, 2019). Therefore, opposition of this channel using CP 465022 could potentiate beneficial effects.

6.2. Aims and Objectives

This study aims to investigate whether combined glutamate receptor antagonists can prevent functional loss of white matter in the MON OGD model of ischaemia. This will help determine the potential of combining AMPA/kainate and NMDA receptor antagonists as a therapeutic intervention for stroke.

- The optimal duration of OGD will be determined by finding a time which causes near but incomplete reduction in CAP amplitude.
- The minimum concentration of combined antagonists required to reduce OGD induced CAP amplitude decline in the MON will be elucidated.
- The efficacy of individual drug treatments to reduce CAP amplitude decline will be compared to the combined efficacy to reveal any synergy in mechanism.

6.3. Results

6.3.1. Establishment of mouse optic nerve OGD protocol

Before combined glutamate receptor antagonist therapy could be tested for efficacy in white matter ischemia, an appropriate model had to be optimised. Previous work from the group regarding CAP impairment from OGD had been performed on rat optic nerves (RON). However, in order to be consistent with combined therapy findings from the cuprizone study, the mouse optic nerve (MON) was chosen.

Previous RON studies have employed OGD for a duration of 60 minutes and so this technique was investigated in the MON. The amplitude of CAP began to fall within 2 minutes and this decline rapidly accelerated (fig. 6.1a). Following a brief period of sharp decline in CAP amplitude, this began to level off before reaching zero and remaining as such for the duration of OGD. Upon reperfusion with regular aCSF and restoration of O_2, the CAP amplitude remained at zero for several minutes before raising ever so slightly and reaching a plateau of 4.7±2% (n=8, fig. 6.1b), relative to baseline recordings.

The recovery of CAP amplitude following 60 minutes OGD was very limited and some repeats did not show any increase at all after reperfusion; as a result, a shorter duration of OGD at 50 minutes was investigated. Following 50 minutes OGD, CAP amplitude began to increase earlier into reperfusion than after 60 minutes and to a greater extent, reaching a plateau of 11.2±2.9% (n=8, fig. 6.1b), relative to baseline. The difference between these two means was not significant (P=0.101); however, it was desirable for control conditions to have a greater recovery when testing protection from drugs and so further experiments used 50 minutes of OGD. Furthermore, the peaked shape of the

compound action potential was better retained after 50 minutes of OGD compared to 60 minutes, making this condition more appropriate (fig. 6.1c).

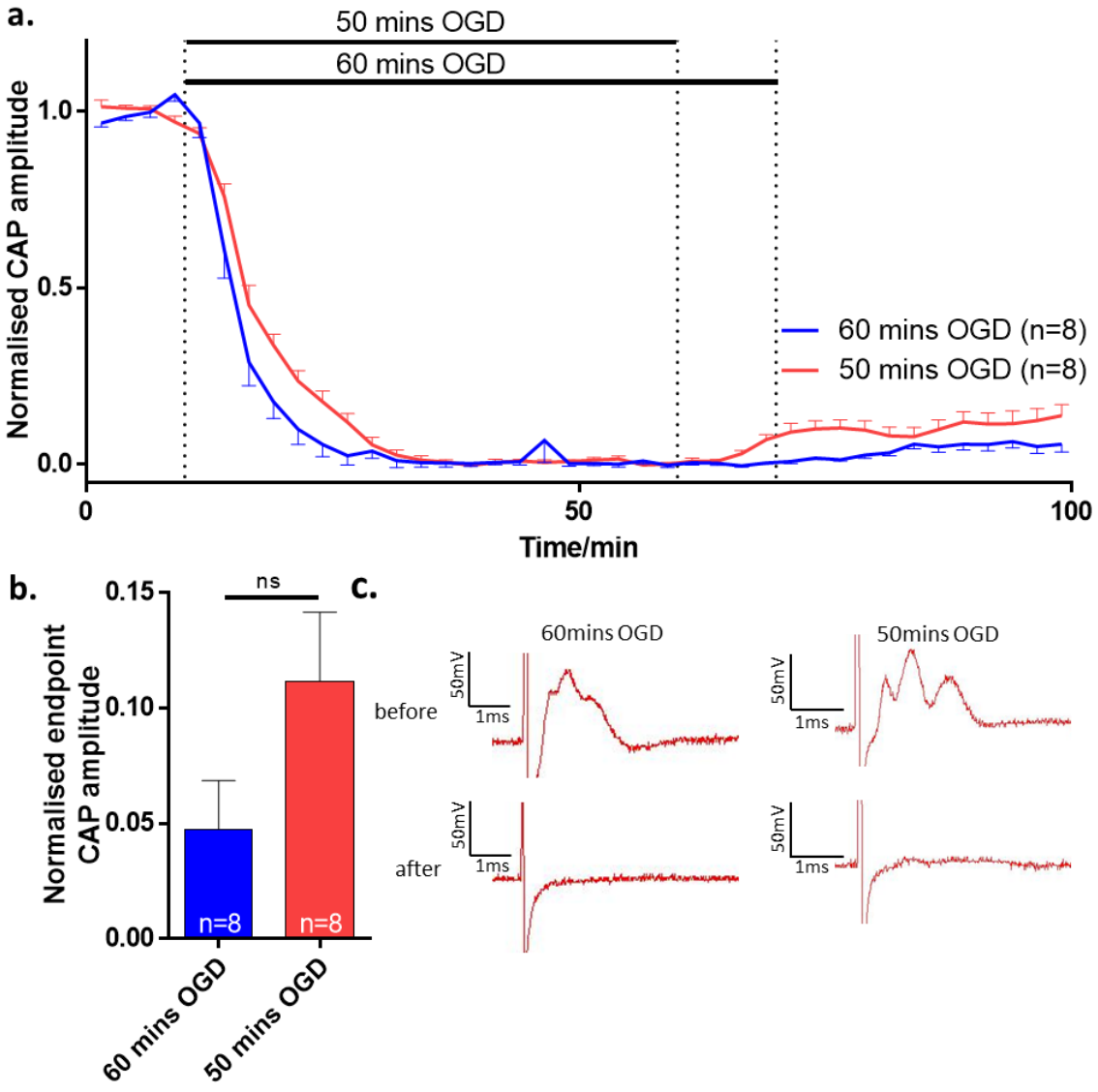

Figure 6. 1. Shorter duration OGD more appropriate for testing protection of drugs.

a. CAP amplitude is blocked by subjection to OGD but recovers a small amount upon restoration of oxygen and glucose. **b.** Following OGD, CAP amplitude recovery trends towards a greater extent if duration is shortened from 60 mins to 50 mins (P=0.1). **c.** Representative CAP traces demonstrate slightly less irreversible functional impairment caused by 50 minutes of OGD compared to 60 minutes. (Unpaired T-test).

6.3.2. Memantine and Perampanel are not protective against ischaemia induced CAP disruption

Following the successful protection of white matter function from cuprizone induced insult, it was decided to investigate the efficacy of memantine and perampanel in OGD. Although a combination of 1µM memantine and 1µM perampanel has proven efficacious in the cuprizone model, 50 minutes OGD induced a far more substantial reduction in CAP amplitude. Consequently, a greater concentration of 10µM memantine and 10µM perampanel combined was chosen to be investigated in the MON OGD model. The optic nerves were maintained in the perfusion chamber with aCSF containing the drugs for 2 hours prior to OGD induction. The OGD and reperfusion solutions continued to supply the drugs.

Perfusion with memantine and perampanel resulted in a similar rate of decline in CAP amplitude on induction of OGD (fig. 6.2a). Action potential propagation was completely blocked by OGD, similar to control conditions. Following reperfusion after 50 minutes of OGD, CAP amplitude began to recover similar to control conditions, to a final level of 0.114±0.044 proportional to baseline (n=5, fig. 6.2b). This degree of CAP amplitude loss was not significantly different to that of control conditions (P=0.968).

As no functional protection was conferred by a combination of 10µM memantine and 10µM perampanel, it was decided that investigation of lower concentrations or separating the drugs was unnecessary.

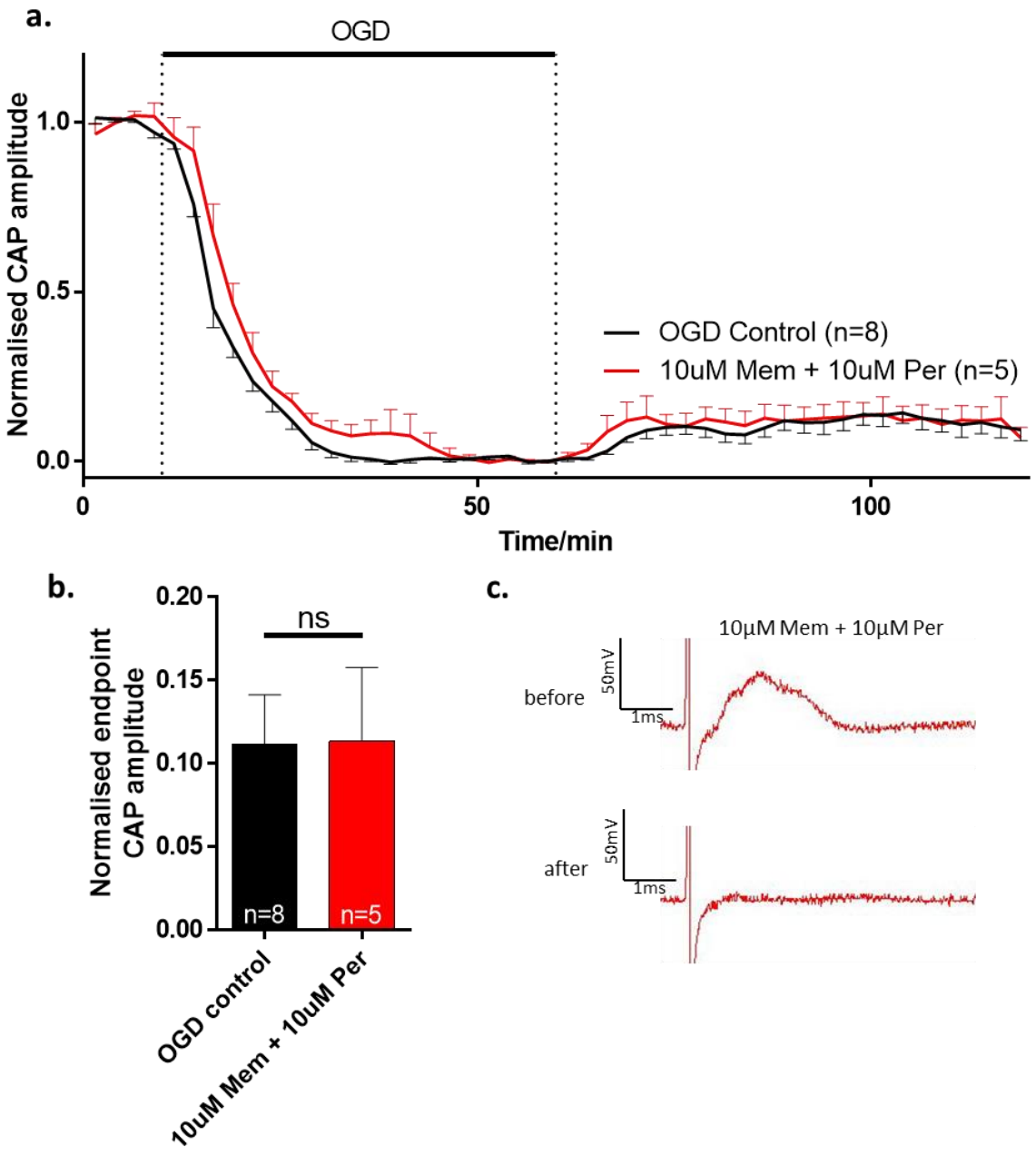

Figure 6. 2. Combined memantine and perampanel treatment is not protective against white matter ischaemia.

a. Perfusion with media containing 10µM memantine and 10µM does not alter the time-course of CAP impairment from 50 minutes OGD. **b.** Following OGD and 1h recovery, CAP amplitude is not significantly enhanced by treatment with memantine and perampanel relative to control conditions (P=0.968). **c.** Representative CAPs before and after 50 minutes OGD and 1h reperfusion demonstrate treatment with memantine and perampanel did not protect CAP shape. (Unpaired T-test).

6.3.3. CP 465022 provides functional protection in white matter from ischaemia

Although the success of combined memantine and perampanel in cuprizone WM damage had not translated to protection from OGD WM damage, the possibility of protection using QNZ46 and CP 465022 was explored. QNZ46 is readily absorbed by myelin, giving it greater access to NMDA receptors expressed on myelin (Doyle *et al.*, 2018). CP 465022 shares a backbone structure with QNZ46 and will likely have similar myelin-penetrating properties (Mosley *et al.*, 2010). Therefore, it was hoped that this combination of glutamate receptor antagonists may show more efficacy in WM protection than memantine and perampanel.

Again, the profile of CAP inhibition by OGD was unaffected by combined QNZ46 and CP 465022 at either 1µM or 10µM each (fig. 6.3a,b). After 50 minutes of OGD and commencement of reperfusion, CAP amplitude began to recover. In optic nerves perfused with 1µM QNZ46 and CP 465022, this recovery was similar to control conditions and a final amplitude of 0.109±0.024 (n=5, fig. 6.4d) relative to baseline. This value was not significantly different to control conditions (P>0.999). However, at a higher concentration of 10µM QNZ46 and CP 465022, CAP amplitude recovered at a more rapid rate and reached a higher level of 0.245±0.033 (n=6, fig. 6.4d) relative to baseline. This was significantly higher than under control conditions (P=0.0226).

In order to determine whether QNZ46 and CP 465022 were working synergistically in order to protect CAP propagation from ischaemic injury, the two drugs were tested separately. Protection conferred by CP 465022 was investigated at 1µM and 10µM (fig. 6.3c,d respectively). At 1µM CP 465022 did not convey any protection to final CAP amplitude, remaining at 0.176±0.054 (n=4, fig. 6.4d) which was not significantly higher than in control conditions (P=0.616). However, when treated with 10µM CP465022, CAP

amplitude began to rapidly recover during reperfusion to reach a final value of 0.347±0.032 (n=5, fig. 6.4d) relative to baseline. This recovery was significantly higher in treated nerves compared to control conditions (P=0.0001).

The efficacy of QNZ46 at preventing OGD-induced CAP deterioration was subsequently tested. At 10µM, QNZ46 did not alter the profile of CAP decline and recovery during OGD and reperfusion compared to control condition (fig. 6.4a). At the end of the experiment, the mean CAP amplitude for treated optic nerves reached a level of 0.098±0.57 (n=4, fig. 6.4d) relative to baseline. This value was not significantly different to that of control conditions (P>0.999). Subsequently, a higher concentration of 50µM QNZ46 was employed; however, in order to prevent precipitation at this concentration, phosphate was removed from the aCSF and 200µM cyclodextrin was added. Using this technique, 50µM QNZ46 appeared to cause CAP amplitude to decline much more rapidly upon OGD onset compared to regular aCSF and OGD solutions (fig. 6.4b). Furthermore, during reperfusion, CAP amplitude recovered at a slower rate and reached a lesser level of 0.025±0.008 (n=4, fig. 6.4d) relative to baseline. However, this value was not significantly lower than under control conditions (P=0.332).

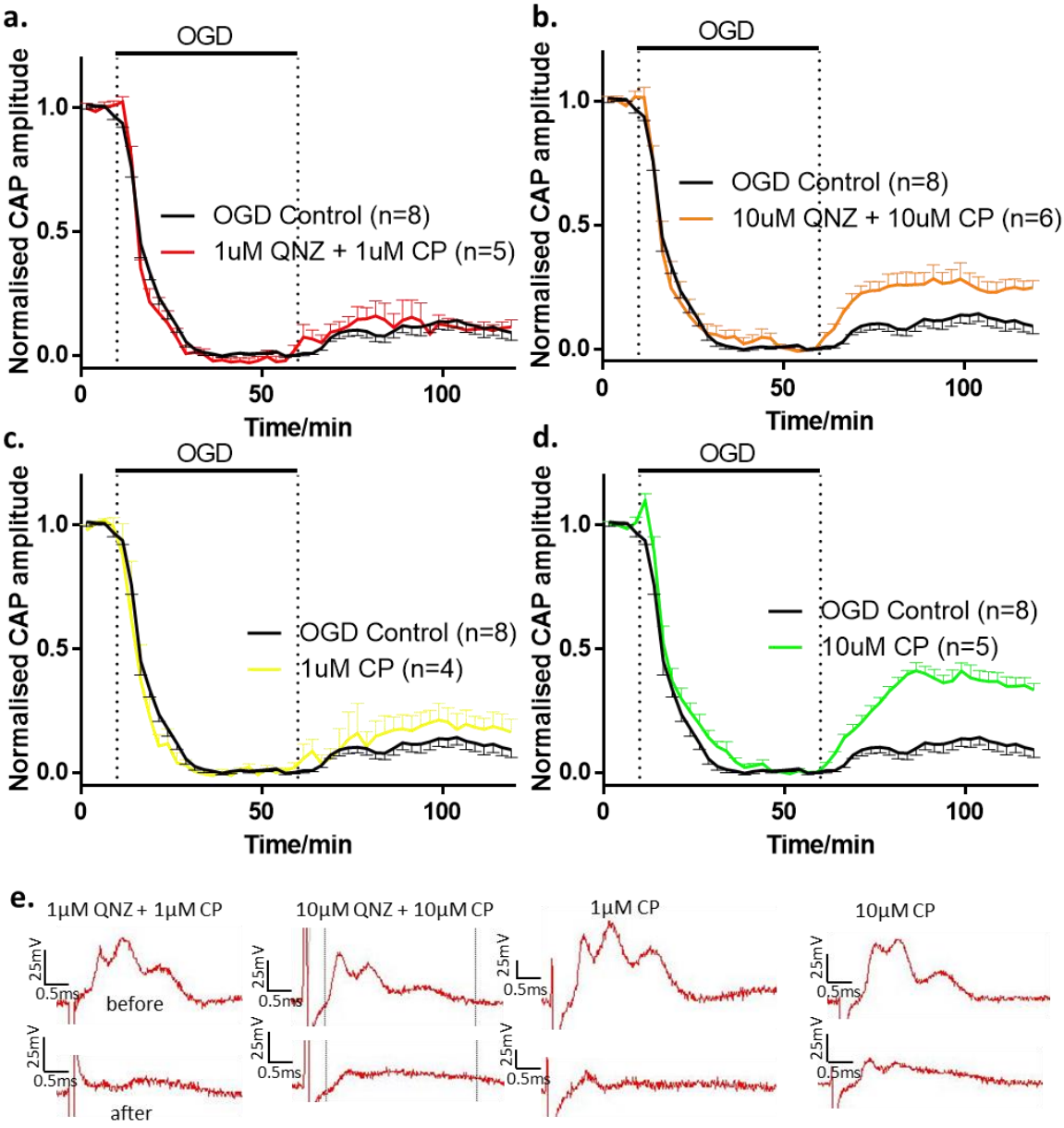

Figure 6. 3. Treatment with CP 465022 improves functional outcome following 50 minutes OGD.

a. Combined treatment with QNZ46 and CP 465022, each at 1µM, does not alter CAP amplitude impairment from OGD. **b.** At 10µM, combined treatment appears to reduce irreversible damage caused by OGD. **c.** Treatment with 1µM CP 465022 alone has a slightly protective effect on CAP amplitude. **d.** CP 465022 at 10µM is sufficient to enhance CAP amplitude recovery following OGD. **e.** Representative CAPs before and after 50 minutes OGD and 1h reperfusion demonstrate the improved resilience of CAP shape when treated with 10µM CP 465022.

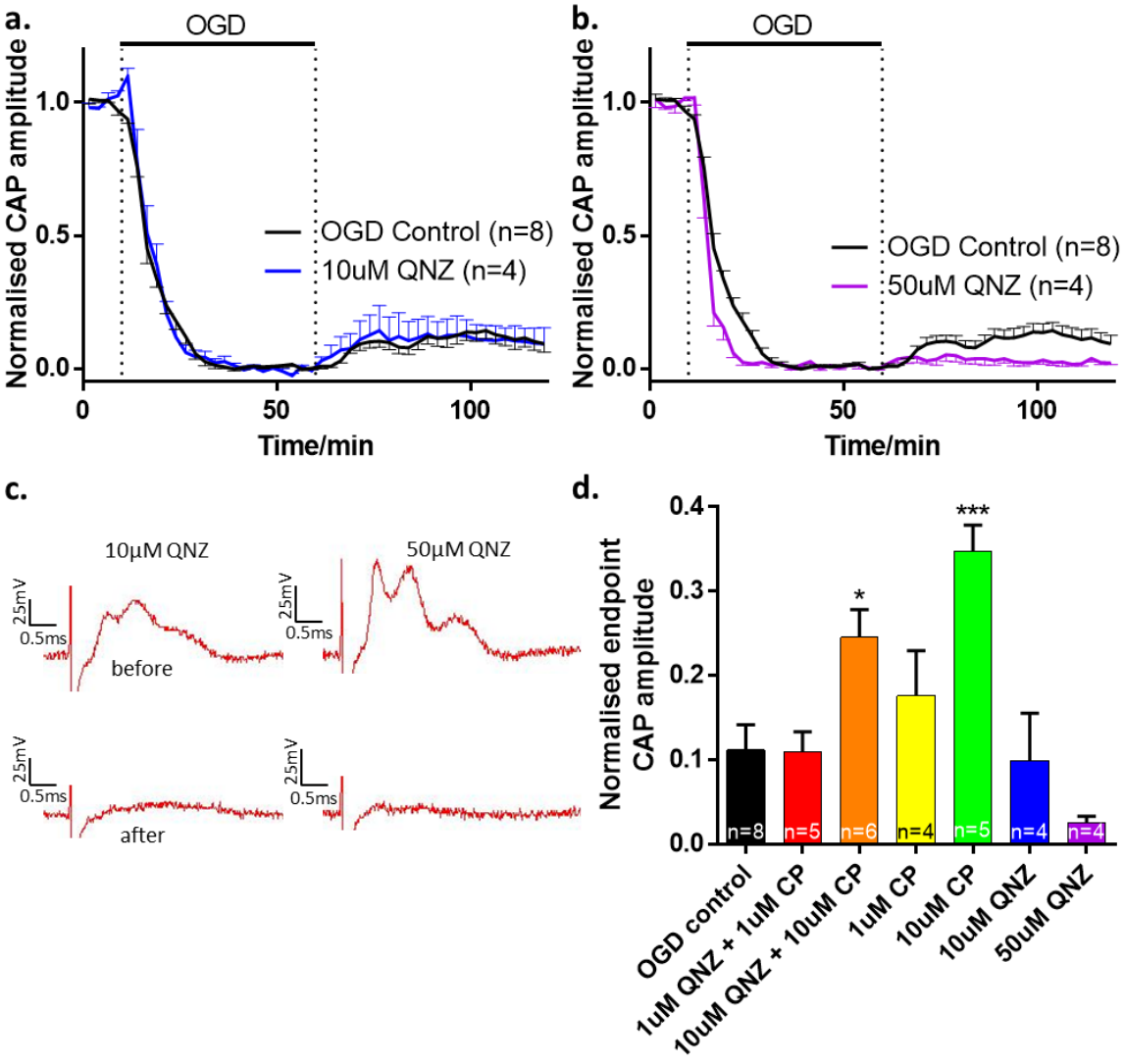

Figure 6. 4. QNZ46 is not beneficial for functional optic nerve functional outcome following OGD.

a. Treatment with 10µM QNZ46 did not alter the time-course of CAP amplitude disruption by 50 minutes OGD. **b.** QNZ46 at 50µM slightly worsened CAP amplitude recovery following OGD. **c.** Representative CAP traces demonstrate the ineffectiveness of QNZ46 to prevent CAP impairment resulting from OGD. **d.** CAP amplitude following 50 minutes OGD and 1h reperfusion was significantly enhanced by treatment either with combined QNZ46 and CP 465022, each at 10µM, or CP 465022 alone at 10µM (P=0.0226, P=0.0001 respectively). (One-way ANOVA with Dunnett's post-hoc).

6.4. Discussion

Similar to MS, glutamate excitotoxicity is thought to play a destructive role in ischaemic stroke in white matter. Glutamate receptor antagonists have not been successful in the clinic due to unacceptable adverse effects at high concentrations. Therefore, if lower concentrations of a combined regimen of glutamate receptor antagonists could were protective, side effects may be avoided. In the present study, a combination of AMPAR and NMDAR antagonists were applied to the mouse optic nerve during 1 hour of OGD and CAP amplitude was measured for the duration and 30 minutes recovery. While a combination of AMPAR and NMDAR antagonists improved CAP amplitude recovery, this effect was mimicked using AMPAR antagonist alone. This suggests that glutamate mediated ischaemic injury in white matter is primarily dependent on AMPA receptor currents. The results do not support the use of a regimen of combined glutamate receptor antagonists for treatment of white matter stroke.

6.4.1. The oxygen glucose deprivation model of ischaemia

Subjection of *ex vivo* neural tissue to oxygen glucose deprivation is a commonly employed model of ischaemic stroke (Tasca, Dal-Cim & Cimarosti, 2015). In order to maintain continuity of methodology with previous studies from the lab, it was hoped a duration of 60 minutes OGD could be employed in the mouse optic nerve. However, after 60 minutes of OGD, reperfusion did not result in a noticeable recovery in CAP amplitude. This is consistent with other studies which have performed 1 hour of OGD on mouse optic nerves. One study found no recovery of CAP area in Swiss Wester mice and a 6.3% recovery in Thy-1 mito CFP (+) mice (Baltan, 2012). This demonstrates a small window of variability between mouse strains in susceptibility to OGD. However, these mice were 12 months of age which is far older than the mice used in the present study.

As white matter susceptibility to damage by ischaemic insult is known to increase with age, it is possible a greater recovery in CAP after 60 minutes OGD should have been recorded in the present study (Baltan *et al.*, 2008). The blockade of CAP propagation was also more rapid in the present study compared to the study by Baltan. In the present study, blockage was complete around 20 minutes after onset whereas, in the study by Baltan, this took over 30 minutes. It is possible that oxygen deprivation was more complete in the present study with minimal interference from atmospheric oxygen, resulting in faster metabolic collapse. Indeed, in another study employing 20 minutes OGD in the mouse optic nerve, the CAP area was reduced to just below 20% after 20 minutes suggesting a less severe injury to the present study (Bakiri *et al.*, 2008). However, in the Bakiri study, no recovery was demonstrated in control nerves during reperfusion, after 20 minutes, which is in contrast with an established view of relatively little irreversible functional damage at that timepoint. For example, 30 minutes of OGD followed by reperfusion resulted in almost 70% recovery, in another study (Yin *et al.*, 2016).

While it would have been beneficial to establish recovery of CAP amplitude at further shorter OGD durations, it was decided the degree of functional loss experienced at 50 minutes was acceptable and time was better spent investigating therapeutic efficacy. When considering the evidence that only 30% of the CAP is lost after 30 minutes, much irreversible damage must occur between 30 minute and 50 minutes of OGD. After 50 minutes of OGD, 89% of the CAP amplitude was lost. Of course, CAP area and CAP amplitude are not directly comparable but should fall in a similar manner from OGD.

6.4.2. Ischaemic white matter damage is AMPA receptor mediated

This study investigated the potential of four different glutamate receptor antagonists and two combinations for treatment of white matter ischaemia. In the *ex vivo* cuprizone model, either combination of AMPA and NMDA receptor antagonist had effectively preserved ability of white matter to propagate action potentials. Both models are believed to involve a degree of glutamate excitotoxicity in their pathogenesis (Bakiri *et al.*, 2008; Namekata *et al.*, 2014). Furthermore, both models involve injury to myelin and oligodendrocytes (Doyle *et al.*, 2018; Hawkins & Butt, 2013; Vega-Riquer *et al.*, 2019). Therefore, it was hypothesised that a similar mode of action may benefit in OGD as in cuprizone.

A combination of 10μM memantine and 10μM perampanel did not reduce CAP decline from OGD. This is a much higher concentration than was necessary to protect from cuprizone induced injury. However, 50 minutes of OGD causes a substantially greater injury than 100 minutes of cuprizone treatment, so it is possible the regimen was not sufficient to overcome this insult. However, higher concentrations caused precipitation in the perfusate resulting in unknown dissolved concentration and problems with flow rate of the perfusate as well as deposition of precipitate on the nerve. As no protection was conveyed by a combination of memantine and perampanel, it was decided against investigating efficacy of each individually. Interestingly, as low as 1μM memantine has been found protective from 20 minutes of ischaemia, when in combination with 25μM NBQX (Bakiri *et al.*, 2008). Of course, the injury conveyed by 20 minutes of OGD is significantly less than that of 50 minutes. It is possible that very early pathological mechanisms occurring in ischaemic insult are glutamate mediated, whereas other modes of damage may take hold before 50 minutes. Curiously, memantine has previously been found to attenuate white matter damage in a rat model of

periventricular leukomalacia (Manning *et al.*, 2008). This is a form of white matter ischemia experienced in neonates and could signify benefits of the drug in OGD. However, the profile of NMDA receptor expression throughout development changes dramatically with relocalising from the oligodendrocyte cell body to the myelin sheath (Baltan, 2016). Thus, oligodendrocyte protection seen in neonates through use of NMDA receptors would not translate to the adult white matter.

A combination of 10µM QNZ46 and 10µM CP 465022 was sufficient to significantly reduce CAP amplitude decline induced by 50 minutes OGD. Again, this concentration was more than that necessary to prevent functional white matter injury from 100 minutes of cuprizone. However, in this instance, 10µM CP 465022 alone was found to be more protective of impulse propagation than in combination. Furthermore, 10µM QNZ46 offered no protection from ischaemic insult. This suggests that any protection seen from the combined treatment was likely solely due to presence of CP 465022. This is in contrast to previous studies which have found QNZ46 to significantly increase CAP area recovery in the rat optic nerve following 1 hour OGD (Doyle *et al.*, 2018). The efficacy of CP 465022 would indicate that glutamate mediated CAP amplitude loss in white matter ischaemia is predominantly facilitated by AMPA receptors. This is in agreement with other studies that have found only AMPA receptor antagonism to be protective during OGD of the mouse optic nerve (Baltan *et al.*, 2008). These receptors are primarily located on the oligodendrocyte cell body and due to their composition containing GluA4 subunits, allow calcium influx to the cytoplasm (Evonuk *et al.*, 2020). Thus, their inhibition by use of CP 465022 would be expected to protect oligodendrocytes from glutamate excitotoxicity. It is possible that antagonism of NMDA receptors, mainly located on processes and myelin, did not convey any protection to the

CAP integrity because sustained injury to oligodendrocytes resulted in unpreventable secondary degeneration of myelin (Salter & Fern, 2005).

Of course, it cannot be ruled out that CP 465022 improved CAP recovery by inhibition of $Na_V1.6$ channels. This would prevent sodium accumulation in axons and consequent reversal of the sodium/calcium exchanger and overload of intracellular calcium. This could in fact explain the difference in protection conveyed by perampanel and CP 465022, both of which are AMPA receptor antagonists.

Interestingly, perampanel and CP 465022 both share the same non-competitive binding site on the AMPA receptor (Hanada *et al.*, 2011). This was demonstrated by the displacement of perampanel by CP 465022. CP 465022 has a lower IC_{50} of 25nM compared to 93nM for perampanel in rat primary cortical neurons. This may underlie the greater efficacy of CP 465022 in the current study. However, the IC_{50} of perampanel is far superseded by the concentration used in this study and so it is likely that perampanel is not protective.

While this study found CP 465022 to be functionally protective of white matter, previous studies have found the drug not to be neuroprotective *in vivo* (Menniti *et al.*, 2003). Therefore, it is possible the protection seen in the current study would not translate to animal models. However, the study by Menniti focused on protection of hippocampal neurons and infarct size following middle cerebral artery occlusion. This method results in minimal white matter damage due to the low proportion of white matter in the rodent brain compared to humans. Therefore, if CP 465022 primarily acted on oligodendrocytes to promote functional survival, this may not be seen in gross infarct size. However, this does not mean that the treatment would not be beneficial to human patients as loss of white matter functionality contributes greatly to disability (Wang *et al.*, 2016).

Consequently, when investigating the benefits of CP 465022 treatment *in vivo*, it would be crucial to determine white matter integrity, possibly through use of diffusion tensor imaging MRI.

6.5. Conclusion

This study has found that combined treatment with NMDA and AMPA receptor antagonists is far less efficacious in the treatment of ischaemic insult compared to cuprizone. This may be due to the exacerbated white matter damage caused by the oxygen glucose deprivation model. While a high concentration of QNZ46 and CP 465022 combined was able to prevent some irreversible damage from OGD, this was no more than CP 465022 treatment alone. This indicates that AMPA receptors located on oligodendrocyte cell bodies are key to loss of white matter function in ischaemia. This is also in agreement with previous studies which have found no benefits of NMDA receptor antagonism in stroke models.

Chapter 7:

Discussion

7.1. Overview

The experiments in this study have been performed to gain understanding of disturbance of ionic activity in white matter diseases. These alterations have also been related to functional impairments in the disease models. In Chapter Three, potassium release was investigated in the oxygen-glucose deprivation model of cerebral ischaemia. It was demonstrated that, in both grey and white matter, ischaemia-induced potassium release occurs mostly through voltage dependent potassium channels. However, while route of exit was similar in both regions, release in grey matter showed a high degree of glutamate dependency which was not seen in white matter. This is the first-time potassium release profiles and mechanisms have been compared in grey and white matter. This novel finding reveals that the ischaemia-induced glutamate transmission demonstrated in previous studies at the axo-myelinic synapse does not result in release of potassium into the extracellular space (Doyle *et al.*, 2018). Glutamate released at the axo-myelinic synapse acts on receptors on the myelin sheath. The membrane of the sheath is not excitable and so cation influx through activated NMDA receptors will not result in opening of voltage gated potassium channels and subsequent efflux into the extracellular space.

The study also revealed a major disadvantage of the use of perfusion chambers for incubation of isolated preparations. Over the duration of OGD, elevated extracellular potassium gradually declined to return to baseline. It was found that this reduction was largely due to washout of the released potassium into the perfusate and consequent removal from the preparation. This process is not consistent with the human disease of stroke where cessation of blood supply results in sustained accumulation of released products. Consequently, it may be beneficial for the methodology of OGD in a perfusion

chamber to be adapted such that OGD solution more closely mimics the cerebral environment during ischaemia. This could have wide ranging consequences for preclinical investigation of stroke and may contribute to poor translation of results into clinical trials. This approach has been taken for investigation of injury mechanisms in cultured astrocytes with the use of hypoxic, acidic, ion-shifted Ringer (HAIR) solution (Bondarenko & Chesler, 2001a; Bondarenko & Chesler, 2001b; Bondarenko, Svichar & Chesler, 2005). Cultured astrocytes are highly resistant to hypoxic insult alone, taking between 12 and 24 hours to show signs of injury. Meanwhile, astrocytic cell death can be seen as early as 30 minutes into animal ischaemic models (Garcia *et al.*, 1993). This timescale is much more closely replicated in cultured astrocytes when using HAIR solution, indicating the cerebral environment is involved in astrocytic injury. It may be possible to use a similar technique in the isolated optic nerve. However, addition of ions at the onset of OGD may result in an exacerbated peak and greater injury. It was out of the scope of this study to investigate such measures.

One of the major ions that become dysregulated during ischaemia is the proton due to rapid production through glycolysis and impairment of membrane channels. Therefore, in Chapter Four, the profile of pH dynamics during OGD was investigated in both grey and white matter. Astrocytes are largely responsible for the homeostasis of pH in brain matter and astrocyte subtype differs between grey and white matter; grey matter contains protoplasmic astrocytes while white matter contains fibrous astrocytes. Additionally, grey matter contains an abundance of neuronal cell bodies, which are energy intensive, compared to white matter. Therefore, it may be expected that ischaemic pH dynamics would differ between the two CNS components. However, proton selective ISMs revealed similar profiles of pH dynamics during OGD for both grey

and white matter. This involved an initial acidification followed by a gradual shift towards more alkaline than baseline. This alkalisation was lost upon reperfusion with a return to baseline pH. Again, this profile is not consistent with that seen during *in vivo* cerebral ischaemia. Acid accumulation is far greater and more sustained in the intact brain and so cellular damage may be exacerbated compared to the perfusion chamber model. These data lend credence to the idea of an OGD solution that contains toxins produced during ischaemia.

As glutamate activity has been shown to be highly detrimental in many white matter diseases, Chapter Five concerned the antagonism of combinations of glutamate receptors in multiple sclerosis. In this study, MS was modelled by application of a demyelinating agent, cuprizone, to the isolated mouse optic nerve. This resulted in a robust and reproducible loss of compound action potential amplitude over 100 minutes of exposure. The *ex vivo* cuprizone model is novel to this study and could provide a high throughput method of testing MS therapeutics in a preclinical setting. Two combinations of AMPA and NMDA receptor antagonists were found to effectively preserve CAP amplitude from cuprizone insult. These combinations worked in synergism with a far lower concentration required compared to treatment independently. Thus, it is possible that adverse side effects often seen with glutamate receptor antagonists may be avoided. Of particular interest to the therapeutic treatment of MS, a combination of memantine and perampanel was sufficient to prevent cuprizone induced functional impairment of the mouse optic nerve. These drugs are already approved by the FDA for clinical treatment of Alzheimer's and epilepsy, respectively. As a result, their progression through clinical trials to the practise would be greatly accelerated and potentially improve quality of life for many people with MS far sooner. Furthermore, a combination

of experimental glutamate receptor antagonists, QNZ46 and CP 465022, was capable of preventing cuprizone induced demyelination. As QNZ46 is highly selective for NMDA receptors containing GluN2C/D subunits, largely localised on myelin, it may be possible to avoid side effects associated with inhibition of neuronal NMDA receptors.

Interestingly, higher concentrations of both NMDA receptor antagonists, memantine and QNZ46, were protective of CAP amplitude. This was not the case for AMPA receptor antagonists, perampanel and CP 465022. Glutamate receptor subtypes are highly localised in the adult white matter with AMPA receptors concentrated on the oligodendrocyte cell body and NMDA receptors largely on non-compact myelin. Therefore, it may be interpreted from protection conferred by NMDA receptor antagonists that cuprizone demyelination occurs by direct action on myelin. This is opposed to the possibility that demyelination is secondary to oligodendrocyte perturbation. Classically it has been thought that cuprizone causes demyelination by impairment of oligodendrocyte metabolism. This may be the case with prolonged exposure to a lower concentration *in vivo* but does not seem to be the case in the present model.

In Chapter Six, the same principle of synergistic action of glutamate receptor antagonists was investigated for stroke by use of the OGD model in mouse optic nerves. Glutamate levels are known to become pathologically high in white matter during OGD due to vesicular release from axons. Combined with the knowledge that NMDA and AMPA receptors are expressed differentially throughout the oligodendrocyte-myelin complex, it was thought that combined antagonism would show some promise. However, the clinically approved drugs that had proven successful in the cuprizone model of MS failed to show any protection of CAP amplitude in the OGD model of stroke. This is a curious

finding as low concentrations of memantine have been found to impart protection when in combination with another AMPA receptor antagonist, NBQX. It may be that perampanel is not so effective at combatting ischaemia induced glutamate excitotoxicity as NBQX. Alternatively, the increased duration of OGD in the present study may have allowed initiation of further disease mechanics that cannot be opposed by memantine.

More success was shown when optic nerves were treated with a combination of experimental drugs, QNZ46 and CP 465022. This combination showed greater recovery of CAP amplitude than control OGD alone but at a far higher concentration than was necessary in the cuprizone model. Furthermore, CP 465022 alone was sufficient to improve CAP amplitude recovery at the same concentration as in combination. This suggests that protection conferred by the combination can be attributed to CP 465022. As CP 465022 is an AMPA receptor antagonist, it is likely that glutamate excitotoxicity in white matter OGD is mediated primarily by activation of AMPA receptors which are largely located on the oligodendrocyte cell body. This is in agreement with other studies which have found only AMPA receptor antagonism to be protective of ischaemic white matter insult. On the other hand, it is possible that CP 465022 acts to protect CAP amplitude by inhibition of $Na_v1.6$ channels at the nodes of Ranvier. This would prevent axonal overload of calcium and may explain the lack of efficacy of perampanel which does not have this same capability.

7.2. Glutamate in white matter damage

The outcomes from experiments explored in Chapters Five and Six clearly demonstrate the destructive contribution of glutamate receptor activation in different white matter injuries. In this thesis, only white matter injury in multiple sclerosis and ischaemic stroke are explored. However, glutamate excitotoxicity has been implicated as a deleterious

mechanism in numerous neurological diseases, such as traumatic brain injury and Alzheimer's disease.

Interestingly, the difference in successful treatments between the models of MS and stroke suggest that glutamate exerts toxicity through different mechanisms in each disease. In the cuprizone model of MS, QNZ46 showed greater efficacy at preventing CAP loss than CP 465022. This would implicate NMDA receptor currents in the toxicity of cuprizone. On the other hand, CP 465022 successfully reduced ischaemia-induced CAP loss, supporting the hypothesis that AMPA receptor currents play a key role in pathogenesis of white matter stroke.

Of course, it is possible that the *ex vivo* cuprizone model does not closely mimic the pathological mechanisms of MS, and as such, the human disease progression is not reliant on NMDA receptor activation. This may well be the case as one of the proposed mechanisms of cuprizone toxicity is through prevention of copper bound PrP^C interactions with the NMDA receptor. However, regardless of the direct mechanism involved in the human disease, the study has demonstrated that NMDA receptor currents are capable of causing irreversible myelin damage.

The contribution of a particular subtype of glutamate receptors to white matter damage may be dependent on the source of glutamate. For instance, while AMPA receptor antagonists had little effect on cuprizone induced demyelination, they have been found to effectively reduce demyelination and axonal loss in the EAE model (Evonuk *et al.*, 2020). This may be due to the excessive release of glutamate from activated microglia in the EAE model (Shijie *et al.*, 2009). As this will result in increased concentration of glutamate in the extracellular space, AMPA receptors on the oligodendrocyte cell body will be activated resulting in cell death and secondary degeneration of the myelin.

However, glutamate released from the axon tubule will cause increased concentration in the periaxonal space and consequent activation of NMDA receptors on the myelin, causing primary myelin damage.

7.3. Glutamate antagonists as treatment

The primary focus of this research should be to identify methods of improving patients' quality of life. This thesis has demonstrated the efficacy of combined AMPA and NMDA receptor antagonism for preventing white matter damage in the cuprizone model of demyelination. This is potentially hugely beneficial as a treatment option for multiple sclerosis, particularly primary progressive MS. Overactivation of NMDA receptors results in excessive accumulation of intracellular calcium and results in alteration of mitochondrial activity and subsequent cellular damage (Rosenstock *et al.*, 2010). Mitochondrial function is drastically impaired in progressive MS and therefore memantine has been theorised to be beneficial in MS treatment (Kalman, Laitinen & Komoly, 2007). However, when trialled in humans, patients with MS suffered reversible neurological impairment in response to 30mg/day of memantine (Villoslada *et al.*, 2009). NMDA receptor currents exert contrasting roles in MS, producing excitotoxicity but also compensatory synaptic plasticity (Rossi *et al.*, 2013). Therefore, treatment of MS with memantine alone is not possible due to the severity of adverse effects. However, the new data demonstrates that it may be possible to treat patients with MS with a lower dose of memantine if combined with a low dose of perampanel. The use of perampanel for treatment of MS has also previously been trialled unsuccessfully, though due to lack of efficacy rather than adverse effects (Krauss, 2013). The results of these trials are echoed in the findings of this thesis. Memantine requires a high concentration to exert protection from cuprizone insult while perampanel alone does not provide

protection. Therefore, it is promising that the efficacy of a combination of low concentrations may provide protection of white matter in patients with MS.

This treatment regimen is ideal for use in chronic white matter illnesses such as MS as the drugs have long half-lives allowing for infrequent dosage and minimal peaks in tissue concentration. The slow infiltration of drugs into the white matter is not problematic if treatment is to be sustained. However, this may cause complications when treating acute illnesses such as stroke. In this study, a combination of memantine and perampanel did not provide protection from ischaemic insult. However, a combination of a higher concentration of experimental NMDA and AMPA receptor antagonists as well as AMPA receptor antagonist alone did reduce functional loss. Optic nerves were incubated with the drugs for two hours prior to ischaemic onset in order to allow the drugs access to the myelin. Of course, it is not possible to know when a stroke will occur and, as such, acute treatment two hours prior will not be possible. As such, one possible method to incorporate this as a treatment would be long-term application in people highly at risk of stroke. This may include patients who have recently suffered a transient ischaemic attack (TIA) as this greatly increases chances of having a subsequent, more damaging ischaemic stroke (Hill & Coutts, 2011). However, in the oxygen glucose deprivation model, a higher concentration of antagonist was required than in the cuprizone model. This may result in increased adverse effects which could prohibit chronic use in patients at risk. Therefore, if this treatment were to be considered, the duration after TIA would have to be balanced as there is 3% chance of stroke within 2 days of TIA, 5% at 7 days and as much as 17% within 90 days (Gupta, Farrell & Mittal, 2014). A further issue in treatment of stroke is that neither of the clinically approved drugs successfully reduced white matter damage in the OGD model. While CP 465022

did reduce loss of CAP amplitude, it has not yet been clinically approved for any disease and was found not to be protective in an *in vivo* model of stroke (Menniti *et al.*, 2003). CP 465022 was administered 90 minutes after onset of focal ischaemia in the *in vivo* study and so, it may be beneficial to determine whether pre-treatment produces a more efficacious reduction in behavioural abnormality.

7.4. Concluding remarks

The goal of this thesis was to establish the role that breakdown of ion homeostasis plays in white matter damage from neurological disease. The work presented focused on ionotropic glutamate receptor activation. It was found that ischaemia induced release of potassium, in white matter, was not dependent on glutamate receptor activation, unlike in grey matter. However, potassium elevation still persisted in white matter. No mechanisms of pH breakdown unique to white matter were elucidated in this study. Evidence was put forth that demonstrated a greater contribution of NMDA receptor currents to cuprizone induced white matter damage while AMPA currents played a greater role in ischaemic damage. A potential novel treatment for multiple sclerosis in the form of synergistic antagonism of AMPA and NMDA receptors was identified. Overall, the work in this thesis has contributed to the knowledge of mechanisms of white matter injury and identified possible therapeutic targets.

Bibliography

Aboul-Enein, F., Rauschka, H., Kornek, B., Stadelmann, C., Stefferl, A., Bruck, W., Lucchinetti, C., Schmidbauer, M., Jellinger, K. & Lassmann, H. (2003) 'Preferential loss of myelin-associated glycoprotein reflects hypoxia-like white matter damage in stroke and inflammatory brain diseases'. *J Neuropathol Exp Neurol*, 62 (1), pp. 25-33.

Abrams, C. K. & Scherer, S. S. (2012) 'Gap junctions in inherited human disorders of the central nervous system'. *Biochim Biophys Acta*, 1818 (8), pp. 2030-2047.

Alam, S., Lingenfelter, K. S., Bender, A. M. & Lindsley, C. W. (2017) 'Classics in Chemical Neuroscience: Memantine'. *ACS Chem Neurosci*, 8 (9), pp. 1823-1829.

Alix, J. J. & Fern, R. (2009) 'Glutamate receptor-mediated ischemic injury of premyelinated central axons'. *Ann Neurol*, 66 (5), pp. 682-693.

Almeida, R. G., Czopka, T., Ffrench-Constant, C. & Lyons, D. A. (2011) 'Individual axons regulate the myelinating potential of single oligodendrocytes in vivo'. *Development*, 138 (20), pp. 4443-4450.

Alrashdi, B., Dawod, B., Schampel, A., Tacke, S., Kuerten, S., Marshall, J. S. & Cote, P. D. (2019) 'Nav1.6 promotes inflammation and neuronal degeneration in a mouse model of multiple sclerosis'. *J Neuroinflammation*, 16 (1), pp. 215.

Andrews, H., White, K., Thomson, C., Edgar, J., Bates, D., Griffiths, I., Turnbull, D. & Nichols, P. (2006) 'Increased axonal mitochondrial activity as an adaptation to myelin deficiency in the Shiverer mouse'. *J Neurosci Res*, 83 (8), pp. 1533-1539.

Arancibia-Carcamo, I. L. & Attwell, D. (2014) 'The node of Ranvier in CNS pathology'. *Acta Neuropathol*, 128 (2), pp. 161-175.

Arumugam, T. V., Okun, E. & Mattson, M. P. (2009) 'Basis of Ionic Dysregulation in Cerebral Ischemia', *New Strategies in Stroke Intervention: Ionic Transporters, Pumps,and New Channels.* pp. 1-13.

Astrup, J., Rehncrona, S. & Siesjo, B. K. (1980) 'The increase in extracellular potassium concentration in the ischemic brain in relation to the preischemic functional activity and cerebral metabolic rate'. *Brain Res*, 199 (1), pp. 161-174.

Bakiri, Y., Hamilton, N. B., Karadottir, R. & Attwell, D. (2008) 'Testing NMDA receptor block as a therapeutic strategy for reducing ischaemic damage to CNS white matter'. *Glia*, 56 (2), pp. 233-240.

Ballanyi, K., Grafe, P. & ten Bruggencate, G. (1987) 'Ion activities and potassium uptake mechanisms of glial cells in guinea-pig olfactory cortex slices'. *J Physiol*, 382 pp. 159-174.

Baltan, S. (2012) 'Histone deacetylase inhibitors preserve function in aging axons'. *J Neurochem*, 123 Suppl 2 pp. 108-115.

Baltan, S. (2016) 'Age-specific localization of NMDA receptors on oligodendrocytes dictates axon function recovery after ischemia'. *Neuropharmacology*, 110 (Pt B), pp. 626-632.

Baltan, S., Besancon, E. F., Mbow, B., Ye, Z., Hamner, M. A. & Ransom, B. R. (2008) 'White matter vulnerability to ischemic injury increases with age because of enhanced excitotoxicity'. *J Neurosci*, 28 (6), pp. 1479-1489.

Bates, I. R. & Harauz, G. (2003) 'Molecular dynamics exposes alpha-helices in myelin basic protein'. *J Mol Model*, 9 (5), pp. 290-297.

Bauer, N. G., Richter-Landsberg, C. & Ffrench-Constant, C. (2009) 'Role of the oligodendroglial cytoskeleton in differentiation and myelination'. *Glia*, 57 (16), pp. 1691-1705.

Bay, V. & Butt, A. M. (2012) 'Relationship between glial potassium regulation and axon excitability: a role for glial Kir4.1 channels'. *Glia*, 60 (4), pp. 651-660.

Benetti, F., Ventura, M., Salmini, B., Ceola, S., Carbonera, D., Mammi, S., Zitolo, A., D'Angelo, P., Urso, E., Maffia, M., Salvato, B. & Spisni, E. (2010) 'Cuprizone neurotoxicity, copper deficiency and neurodegeneration'. *Neurotoxicology*, 31 (5), pp. 509-517.

Benveniste, H., Drejer, J., Schousboe, A. & Diemer, N. H. (1984) 'Elevation of the extracellular concentrations of glutamate and aspartate in rat hippocampus during transient cerebral ischemia monitored by intracerebral microdialysis'. *J Neurochem*, 43 (5), pp. 1369-1374.

Beppu, K., Sasaki, T., Tanaka, K. F., Yamanaka, A., Fukazawa, Y., Shigemoto, R. & Matsui, K. (2014) 'Optogenetic countering of glial acidosis suppresses glial glutamate release and ischemic brain damage'. *Neuron*, 81 (2), pp. 314-320.

Bezzi, P., Carmignoto, G., Pasti, L., Vesce, S., Rossi, D., Rizzini, B. L., Pozzan, T. & Volterra, A. (1998) 'Prostaglandins stimulate calcium-dependent glutamate release in astrocytes'. *Nature*, 391 (6664), pp. 281-285.

Bezzi, P., Domercq, M., Brambilla, L., Galli, R., Schols, D., De Clercq, E., Vescovi, A., Bagetta, G., Kollias, G., Meldolesi, J. & Volterra, A. (2001) 'CXCR4-activated astrocyte glutamate release via TNFalpha: amplification by microglia triggers neurotoxicity'. *Nat Neurosci*, 4 (7), pp. 702-710.

Black, S. A., Stys, P. K., Zamponi, G. W. & Tsutsui, S. (2014) 'Cellular prion protein and NMDA receptor modulation: protecting against excitotoxicity'. *Front Cell Dev Biol*, 2 pp. 45.

Blackstone, C., O'Kane, C. J. & Reid, E. (2011) 'Hereditary spastic paraplegias: membrane traffic and the motor pathway'. *Nat Rev Neurosci*, 12 (1), pp. 31-42.

Blakemore, W. F. & Patterson, R. C. (1978) 'Suppression of remyelination in the CNS by X-irradiation'. *Acta Neuropathol*, 42 (2), pp. 105-113.

Bolton, C. & Paul, C. (1997) 'MK-801 limits neurovascular dysfunction during experimental allergic encephalomyelitis'. *J Pharmacol Exp Ther*, 282 (1), pp. 397-402.

Bolton, S. & Butt, A. M. (2005) 'The optic nerve: a model for axon-glial interactions'. *J Pharmacol Toxicol Methods*, 51 (3), pp. 221-233.

Bondarenko, A. & Chesler, M. (2001a) 'Calcium dependence of rapid astrocyte death induced by transient hypoxia, acidosis, and extracellular ion shifts'. *Glia*, 34 (2), pp. 143-149.

Bondarenko, A. & Chesler, M. (2001b) 'Rapid astrocyte death induced by transient hypoxia, acidosis, and extracellular ion shifts'. *Glia*, 34 (2), pp. 134-142.

Bondarenko, A., Svichar, N. & Chesler, M. (2005) 'Role of Na+-H+ and Na+-Ca2+ exchange in hypoxia-related acute astrocyte death'. *Glia*, 49 (1), pp. 143-152.

Boussouf, A. & Gaillard, S. (2000) 'Intracellular pH changes during oligodendrocyte differentiation in primary culture'. *J Neurosci Res*, 59 (6), pp. 731-739.

Boussouf, A., Lambert, R. C. & Gaillard, S. (1997) 'Voltage-dependent Na(+)-HCO3- cotransporter and Na+/H+ exchanger are involved in intracellular pH regulation of cultured mature rat cerebellar oligodendrocytes'. *Glia*, 19 (1), pp. 74-84.

Bouvier, M., Szatkowski, M., Amato, A. & Attwell, D. (1992) 'The glial cell glutamate uptake carrier countertransports pH-changing anions'. *Nature*, 360 (6403), pp. 471-474.

Brand-Schieber, E. & Werner, P. (2003) 'AMPA/kainate receptors in mouse spinal cord cell-specific display of receptor subunits by oligodendrocytes and astrocytes and at the nodes of Ranvier'. *Glia*, 42 (1), pp. 12-24.

Brasko, C. & Butt, A. M. (2018) 'Expression of Kir2.1 Inward Rectifying Potassium Channels in Optic Nerve Glia: Evidence for Heteromeric Association with Kir4.1 and Kir5.1.'. *Neuroglia*, 1 pp. 176-187.

Braun, A. P. (2012) 'Two-pore domain potassium channels: variation on a structural theme'. *Channels (Austin)*, 6 (3), pp. 139-140.

Bremer, J., Baumann, F., Tiberi, C., Wessig, C., Fischer, H., Schwarz, P., Steele, A. D., Toyka, K. V., Nave, K. A., Weis, J. & Aguzzi, A. (2010) 'Axonal prion protein is required for peripheral myelin maintenance'. *Nat Neurosci*, 13 (3), pp. 310-318.

Brown, A. M., Baltan Tekkok, S. & Ransom, B. R. (2004) 'Energy transfer from astrocytes to axons: the role of CNS glycogen'. *Neurochem Int*, 45 (4), pp. 529-536.

Bueno, A., De Olmos, S., Heimer, L. & De Olmos, J. (2003) 'NMDA-antagonist MK-801-induced neuronal degeneration in Wistar rat brain detected by the Amino-Cupric-Silver method'. *Exp Toxicol Pathol*, 54 (4), pp. 319-334.

Buskila, Y., Breen, P. P., Tapson, J., van Schaik, A., Barton, M. & Morley, J. W. (2014) 'Extending the viability of acute brain slices'. *Sci Rep*, 4 pp. 5309.

Butt, A. M., Duncan, A. & Berry, M. (1994) 'Astrocyte associations with nodes of Ranvier: ultrastructural analysis of HRP-filled astrocytes in the mouse optic nerve'. *J Neurocytol*, 23 (8), pp. 486-499.

Butt, A. M., Duncan, A., Hornby, M. F., Kirvell, S. L., Hunter, A., Levine, J. M. & Berry, M. (1999) 'Cells expressing the NG2 antigen contact nodes of Ranvier in adult CNS white matter'. *Glia*, 26 (1), pp. 84-91.

Butt, A. M., Ibrahim, M. & Berry, M. (1997) 'The relationship between developing oligodendrocyte units and maturing axons during myelinogenesis in the anterior medullary velum of neonatal rats'. *J Neurocytol*, 26 (5), pp. 327-338.

Butt, A. M. & Kalsi, A. (2006) 'Inwardly rectifying potassium channels (Kir) in central nervous system glia: a special role for Kir4.1 in glial functions'. *J Cell Mol Med*, 10 (1), pp. 33-44.

Butt, A. M., Papanikolaou, M. & Rivera, A. (2019) 'Physiology of Oligodendroglia'. *Adv Exp Med Biol*, 1175 pp. 117-128.

Butt, A. M., Pugh, M., Hubbard, P. & James, G. (2004) 'Functions of optic nerve glia: axoglial signalling in physiology and pathology'. *Eye (Lond)*, 18 (11), pp. 1110-1121.

Butt, A. M. & Ransom, B. R. (1989) 'Visualization of oligodendrocytes and astrocytes in the intact rat optic nerve by intracellular injection of lucifer yellow and horseradish peroxidase'. *Glia*, 2 (6), pp. 470-475.

Byravan, S., Foster, L. M., Phan, T., Verity, A. N. & Campagnoni, A. T. (1994) 'Murine oligodendroglial cells express nerve growth factor'. *Proc Natl Acad Sci U S A*, 91 (19), pp. 8812-8816.

Caldwell, J. H., Schaller, K. L., Lasher, R. S., Peles, E. & Levinson, S. R. (2000) 'Sodium channel Na(v)1.6 is localized at nodes of ranvier, dendrites, and synapses'. *Proc Natl Acad Sci U S A*, 97 (10), pp. 5616-5620.

Calvo, M., Richards, N., Schmid, A. B., Barroso, A., Zhu, L., Ivulic, D., Zhu, N., Anwandter, P., Bhat, M. A., Court, F. A., McMahon, S. B. & Bennett, D. L. (2016) 'Altered potassium channel distribution and composition in myelinated axons suppresses hyperexcitability following injury'. *Elife*, 5 pp. e12661.

Cammer, W. (1999) 'The neurotoxicant, cuprizone, retards the differentiation of oligodendrocytes in vitro'. *J Neurol Sci*, 168 (2), pp. 116-120.

Caprariello, A. V., Rogers, J. A., Morgan, M. L., Hoghooghi, V., Plemel, J. R., Koebel, A., Tsutsui, S., Dunn, J. F., Kotra, L. P., Ousman, S. S., Wee Yong, V. & Stys, P. K. (2018) 'Biochemically altered myelin triggers autoimmune demyelination'. *Proc Natl Acad Sci U S A*, 115 (21), pp. 5528-5533.

Carmichael, S. T. (2005) 'Rodent models of focal stroke: size, mechanism, and purpose'. *NeuroRx*, 2 (3), pp. 396-409.

Chan, S. L. & Mattson, M. P. (1999) 'Caspase and calpain substrates: roles in synaptic plasticity and cell death'. *J Neurosci Res*, 58 (1), pp. 167-190.

Chari, D. M. (2007) 'Remyelination in multiple sclerosis'. *Int Rev Neurobiol*, 79 pp. 589-620.

Chen, H. & Sun, D. (2005) 'The role of Na-K-Cl co-transporter in cerebral ischemia'. *Neurol Res*, 27 (3), pp. 280-286.

Chen, J. C. & Chesler, M. (1992) 'pH transients evoked by excitatory synaptic transmission are increased by inhibition of extracellular carbonic anhydrase'. *Proc Natl Acad Sci U S A*, 89 (16), pp. 7786-7790.

Chen, K. C. & Nicholson, C. (2000) 'Changes in brain cell shape create residual extracellular space volume and explain tortuosity behavior during osmotic challenge'. *Proc Natl Acad Sci U S A*, 97 (15), pp. 8306-8311.

Chesler, M. (2003) 'Regulation and modulation of pH in the brain'. *Physiol Rev*, 83 (4), pp. 1183-1221.

Chesler, M. & Kraig, R. P. (1987) 'Intracellular pH of astrocytes increases rapidly with cortical stimulation'. *Am J Physiol*, 253 (4 Pt 2), pp. R666-670.

Chesler, M. & Kraig, R. P. (1989) 'Intracellular pH transients of mammalian astrocytes'. *J Neurosci*, 9 (6), pp. 2011-2019.

Choi, D. W. (1987) 'Ionic dependence of glutamate neurotoxicity'. *J Neurosci*, 7 (2), pp. 369-379.

Chong, S. Y., Rosenberg, S. S., Fancy, S. P., Zhao, C., Shen, Y. A., Hahn, A. T., McGee, A. W., Xu, X., Zheng, B., Zhang, L. I., Rowitch, D. H., Franklin, R. J., Lu, Q. R. & Chan, J. R. (2012) 'Neurite outgrowth inhibitor Nogo-A establishes spatial segregation and extent of oligodendrocyte myelination'. *Proc Natl Acad Sci U S A*, 109 (4), pp. 1299-1304.

Christensen, P. C., Samadi-Bahrami, Z., Pavlov, V., Stys, P. K. & Moore, G. R. W. (2016) 'Ionotropic glutamate receptor expression in human white matter'. *Neurosci Lett*, 630 pp. 1-8.

Chung, C., Marson, J. D., Zhang, Q. G., Kim, J., Wu, W. H., Brann, D. W. & Chen, B. S. (2016) 'Neuroprotection Mediated through GluN2C-Containing N-methyl-D-aspartate (NMDA) Receptors Following Ischemia'. *Sci Rep*, 6 pp. 37033.

Coetzee, T., Fujita, N., Dupree, J., Shi, R., Blight, A., Suzuki, K., Suzuki, K. & Popko, B. (1996) 'Myelination in the absence of galactocerebroside and sulfatide: normal structure with abnormal function and regional instability'. *Cell*, 86 (2), pp. 209-219.

Cohen, Y., Chang, L. H., Litt, L., Kim, F., Severinghaus, J. W., Weinstein, P. R., Davis, R. L., Germano, I. & James, T. L. (1990) 'Stability of brain intracellular lactate and 31P-metabolite levels at reduced intracellular pH during prolonged hypercapnia in rats'. *J Cereb Blood Flow Metab*, 10 (2), pp. 277-284.

Connor, J. R. & Menzies, S. L. (1996) 'Relationship of iron to oligodendrocytes and myelination'. *Glia*, 17 (2), pp. 83-93.

Constantinescu, C. S., Farooqi, N., O'Brien, K. & Gran, B. (2011) 'Experimental autoimmune encephalomyelitis (EAE) as a model for multiple sclerosis (MS)'. *Br J Pharmacol*, 164 (4), pp. 1079-1106.

Cragg, P., Patterson, L. & Purves, M. J. (1977) 'The pH of brain extracellular fluid in the cat'. *J Physiol*, 272 (1), pp. 137-166.

Craner, M. J., Hains, B. C., Lo, A. C., Black, J. A. & Waxman, S. G. (2004a) 'Co-localization of sodium channel Nav1.6 and the sodium-calcium exchanger at sites of axonal injury in the spinal cord in EAE'. *Brain*, 127 (Pt 2), pp. 294-303.

Craner, M. J., Newcombe, J., Black, J. A., Hartle, C., Cuzner, M. L. & Waxman, S. G. (2004b) 'Molecular changes in neurons in multiple sclerosis: altered axonal expression of Nav1.2 and Nav1.6 sodium channels and Na+/Ca2+ exchanger'. *Proc Natl Acad Sci U S A*, 101 (21), pp. 8168-8173.

Criado, J. R., Sanchez-Alavez, M., Conti, B., Giacchino, J. L., Wills, D. N., Henriksen, S. J., Race, R., Manson, J. C., Chesebro, B. & Oldstone, M. B. (2005) 'Mice devoid of prion protein have cognitive deficits that are rescued by reconstitution of PrP in neurons'. *Neurobiol Dis*, 19 (1-2), pp. 255-265.

Cuccione, E., Padovano, G., Versace, A., Ferrarese, C. & Beretta, S. (2016) 'Cerebral collateral circulation in experimental ischemic stroke'. *Exp Transl Stroke Med*, 8 pp. 2.

Curtis, J., Errington, M., Bliss, T., Voss, K. & MacLeod, N. (2003) 'Age-dependent loss of PTP and LTP in the hippocampus of PrP-null mice'. *Neurobiol Dis*, 13 (1), pp. 55-62.

D'Ambrosio, R., Gordon, D. S. & Winn, H. R. (2002) 'Differential role of KIR channel and Na(+)/K(+)-pump in the regulation of extracellular K(+) in rat hippocampus'. *J Neurophysiol*, 87 (1), pp. 87-102.

Dale, J. M. & Garcia, M. L. (2012) 'Neurofilament Phosphorylation during Development and Disease: Which Came First, the Phosphorylation or the Accumulation?'. *J Amino Acids*, 2012 pp. 382107.

Dawson, M. R., Polito, A., Levine, J. M. & Reynolds, R. (2003) 'NG2-expressing glial progenitor cells: an abundant and widespread population of cycling cells in the adult rat CNS'. *Mol Cell Neurosci*, 24 (2), pp. 476-488.

De Moraes, C. G. (2013) 'Anatomy of the visual pathways'. *J Glaucoma*, 22 Suppl 5 pp. S2-7.

Disanto, G., Berlanga, A. J., Handel, A. E., Para, A. E., Burrell, A. M., Fries, A., Handunnetthi, L., De Luca, G. C. & Morahan, J. M. (2010) 'Heterogeneity in multiple sclerosis: scratching the surface of a complex disease'. *Autoimmune Dis*, 2011 pp. 932351.

Dobson, R. & Giovannoni, G. (2019) 'Multiple sclerosis - a review'. *Eur J Neurol*, 26 (1), pp. 27-40.

Domercq, M., Sanchez-Gomez, M. V., Areso, P. & Matute, C. (1999) 'Expression of glutamate transporters in rat optic nerve oligodendrocytes'. *Eur J Neurosci*, 11 (7), pp. 2226-2236.

Domercq, M., Sanchez-Gomez, M. V., Sherwin, C., Etxebarria, E., Fern, R. & Matute, C. (2007) 'System xc- and glutamate transporter inhibition mediates microglial toxicity to oligodendrocytes'. *J Immunol*, 178 (10), pp. 6549-6556.

Dostovic, Z., Dostovic, E., Smajlovic, D., Ibrahimagic, O. C. & Avdic, L. (2016) 'Brain Edema After Ischaemic Stroke'. *Med Arch*, 70 (5), pp. 339-341.

Doyle, S., Hansen, D. B., Vella, J., Bond, P., Harper, G., Zammit, C., Valentino, M. & Fern, R. (2018) 'Vesicular glutamate release from central axons contributes to myelin damage'. *Nature Communications*, 9 (1), pp. 1032.

Duncan, I. D., Hammang, J. P. & Trapp, B. D. (1987) 'Abnormal compact myelin in the myelin-deficient rat: absence of proteolipid protein correlates with a defect in the intraperiod line'. *Proc Natl Acad Sci U S A*, 84 (17), pp. 6287-6291.

Dyer, C. A. & Benjamins, J. A. (1989a) 'Organization of oligodendroglial membrane sheets. I: Association of myelin basic protein and 2',3'-cyclic nucleotide 3'-phosphohydrolase with cytoskeleton'. *J Neurosci Res*, 24 (2), pp. 201-211.

Dyer, C. A. & Benjamins, J. A. (1989b) 'Organization of oligodendroglial membrane sheets: II. Galactocerebroside:antibody interactions signal changes in cytoskeleton and myelin basic protein'. *J Neurosci Res*, 24 (2), pp. 212-221.

Edgar, J. & Griffiths, I. (2014) 'White Matter Structure: A Microscopist's View', *Diffusion MRI.* Academic Press, pp. 74-103.

Edgar, J. M., McCulloch, M. C., Thomson, C. E. & Griffiths, I. R. (2008) 'Distribution of mitochondria along small-diameter myelinated central nervous system axons'. *J Neurosci Res*, 86 (10), pp. 2250-2257.

Elmslie, K. S. (2019) ' Action Potential: Ionic Mechanisms', *eLS.* John Wiley & Sons, Ltd (Ed.), pp. 1-10.

Engl, E. & Attwell, D. (2015) 'Non-signalling energy use in the brain'. *J Physiol*, 593 (16), pp. 3417-3429.

Erecinska, M. & Silver, I. A. (1994) 'Ions and energy in mammalian brain'. *Prog Neurobiol*, 43 (1), pp. 37-71.

Esiri, M. M. (2009) 'MS: is it one disease?'. *Int MS J*, 16 (2), pp. 39-41.

Estrada Sanchez, A. M., Mejia-Toiber, J. & Massieu, L. (2008) 'Excitotoxic neuronal death and the pathogenesis of Huntington's disease'. *Arch Med Res*, 39 (3), pp. 265-276.

Evonuk, K. S., Doyle, R. E., Moseley, C. E., Thornell, I. M., Adler, K., Bingaman, A. M., Bevensee, M. O., Weaver, C. T., Min, B. & DeSilva, T. M. (2020) 'Reduction of AMPA receptor activity on mature oligodendrocytes attenuates loss of myelinated axons in autoimmune neuroinflammation'. *Sci Adv*, 6 (2), pp. eaax5936.

Farjam, M., Beigi Zarandi, F. B., Farjadian, S., Geramizadeh, B., Nikseresht, A. R. & Panjehshahin, M. R. (2014) 'Inhibition of NR2B-Containing N-methyl-D-Aspartate Receptors (NMDARs) in Experimental Autoimmune Encephalomyelitis, a Model of Multiple Sclerosis'. *Iran J Pharm Res*, 13 (2), pp. 695-705.

Feher, J. (2017) 'The Origin of the Resting Membrane Potential', *Quantitative Human Physiology (Second Edition).* Academic Press, pp. 255-264.

Feng, Y., Liao, S., Wei, C., Jia, D., Wood, K., Liu, Q., Wang, X., Shi, F. D. & Jin, W. N. (2017) 'Infiltration and persistence of lymphocytes during late-stage cerebral ischemia in middle cerebral artery occlusion and photothrombotic stroke models'. *J Neuroinflammation*, 14 (1), pp. 248.

Ferguson, B., Matyszak, M. K., Esiri, M. M. & Perry, V. H. (1997) 'Axonal damage in acute multiple sclerosis lesions'. *Brain*, 120 (Pt 3) pp. 393-399.

Fern, R. (1998) 'Intracellular calcium and cell death during ischemia in neonatal rat white matter astrocytes in situ'. *J Neurosci*, 18 (18), pp. 7232-7243.

Fern, R. (2001) 'Ischemia: astrocytes show their sensitive side'. *Prog Brain Res*, 132 pp. 405-411.

Fern, R. (2014) 'Focal Ischemic White Matter Injury in Experimental Models.', *White Matter Injury in Stroke and CNS Disease. Springer Series in Translational Stroke Research, vol 4.*: Springer, pp. 169-179.

Fern, R. & Matute, C. (2019) 'Glutamate receptors and white matter stroke'. *Neurosci Lett*, 694 pp. 86-92.

Fitsiori, A., Nguyen, D., Karentzos, A., Delavelle, J. & Vargas, M. I. (2011) 'The corpus callosum: white matter or terra incognita'. *Br J Radiol*, 84 (997), pp. 5-18.

Follett, P. L., Deng, W., Dai, W., Talos, D. M., Massillon, L. J., Rosenberg, P. A., Volpe, J. J. & Jensen, F. E. (2004) 'Glutamate receptor-mediated oligodendrocyte toxicity in periventricular leukomalacia: a protective role for topiramate'. *J Neurosci*, 24 (18), pp. 4412-4420.

Fowler, J. H., McCracken, E., Dewar, D. & McCulloch, J. (2003) 'Intracerebral injection of AMPA causes axonal damage in vivo'. *Brain Res*, 991 (1-2), pp. 104-112.

Fox, M. A., Afshari, F. S., Alexander, J. K., Colello, R. J. & Fuss, B. (2006) 'Growth conelike sensorimotor structures are characteristic features of postmigratory, premyelinating oligodendrocytes'. *Glia*, 53 (5), pp. 563-566.

Frankiewicz, T., Potier, B., Bashir, Z. I., Collingridge, G. L. & Parsons, C. G. (1996) 'Effects of memantine and MK-801 on NMDA-induced currents in cultured neurones and on synaptic transmission and LTP in area CA1 of rat hippocampal slices'. *Br J Pharmacol*, 117 (4), pp. 689-697.

Franklin, R. J. & Hinks, G. L. (1999) 'Understanding CNS remyelination: clues from developmental and regeneration biology'. *J Neurosci Res*, 58 (2), pp. 207-213.

Friede, R. L. & Samorajski, T. (1970) 'Axon caliber related to neurofilaments and microtubules in sciatic nerve fibers of rats and mice'. *Anat Rec*, 167 (4), pp. 379-387.

Fries, M., Mertens, M., Teske, N., Kipp, M., Beyer, C., Willms, T., Valkonen, A., Rissanen, K., Albrecht, M. & Clarner, T. (2019) 'Water-Soluble Cuprizone Derivative: Synthesis, Characterization, and in Vitro Studies'. *ACS Omega*, 4 (1), pp. 1685-1689.

Friese, M. A., Craner, M. J., Etzensperger, R., Vergo, S., Wemmie, J. A., Welsh, M. J., Vincent, A. & Fugger, L. (2007) 'Acid-sensing ion channel-1 contributes to axonal degeneration in autoimmune inflammation of the central nervous system'. *Nat Med*, 13 (12), pp. 1483-1489.

Frohman, E. M., Racke, M. K. & Raine, C. S. (2006) 'Multiple sclerosis--the plaque and its pathogenesis'. *N Engl J Med*, 354 (9), pp. 942-955.

Fruttiger, M., Montag, D., Schachner, M. & Martini, R. (1995) 'Crucial role for the myelin-associated glycoprotein in the maintenance of axon-myelin integrity'. *Eur J Neurosci*, 7 (3), pp. 511-515.

Fu, Y., Sun, W., Shi, Y., Shi, R. & Cheng, J. X. (2009) 'Glutamate excitotoxicity inflicts paranodal myelin splitting and retraction'. *PLoS One*, 4 (8), pp. e6705.

Funfschilling, U., Supplie, L. M., Mahad, D., Boretius, S., Saab, A. S., Edgar, J., Brinkmann, B. G., Kassmann, C. M., Tzvetanova, I. D., Mobius, W., Diaz, F., Meijer, D., Suter, U., Hamprecht, B., Sereda, M. W., Moraes, C. T., Frahm, J., Goebbels, S. & Nave, K. A. (2012) 'Glycolytic oligodendrocytes maintain myelin and long-term axonal integrity'. *Nature*, 485 (7399), pp. 517-521.

Gadotti, V. M. & Zamponi, G. W. (2011) 'Cellular prion protein protects from inflammatory and neuropathic pain'. *Mol Pain*, 7 pp. 59.

Gajardo-Gomez, R., Labra, V. C. & Orellana, J. A. (2016) 'Connexins and Pannexins: New Insights into Microglial Functions and Dysfunctions'. *Front Mol Neurosci*, 9 pp. 86.

Garbern, J. Y., Yool, D. A., Moore, G. J., Wilds, I. B., Faulk, M. W., Klugmann, M., Nave, K. A., Sistermans, E. A., van der Knaap, M. S., Bird, T. D., Shy, M. E., Kamholz, J. A. & Griffiths, I. R. (2002) 'Patients lacking the major CNS myelin protein, proteolipid protein 1, develop length-dependent axonal degeneration in the absence of demyelination and inflammation'. *Brain*, 125 (Pt 3), pp. 551-561.

Garcia, J. H., Yoshida, Y., Chen, H., Li, Y., Zhang, Z. G., Lian, J., Chen, S. & Chopp, M. (1993) 'Progression from ischemic injury to infarct following middle cerebral artery occlusion in the rat'. *Am J Pathol*, 142 (2), pp. 623-635.

Garden, G. A. & Moller, T. (2006) 'Microglia biology in health and disease'. *J Neuroimmune Pharmacol*, 1 (2), pp. 127-137.

Gibson, E. M., Purger, D., Mount, C. W., Goldstein, A. K., Lin, G. L., Wood, L. S., Inema, I., Miller, S. E., Bieri, G., Zuchero, J. B., Barres, B. A., Woo, P. J., Vogel, H. & Monje, M. (2014) 'Neuronal activity promotes oligodendrogenesis and adaptive myelination in the mammalian brain'. *Science*, 344 (6183), pp. 1252304.

Gido, G., Kristian, T. & Siesjo, B. K. (1997) 'Extracellular potassium in a neocortical core area after transient focal ischemia'. *Stroke*, 28 (1), pp. 206-210.

Ginhoux, F., Greter, M., Leboeuf, M., Nandi, S., See, P., Gokhan, S., Mehler, M. F., Conway, S. J., Ng, L. G., Stanley, E. R., Samokhvalov, I. M. & Merad, M. (2010) 'Fate mapping analysis reveals that adult microglia derive from primitive macrophages'. *Science*, 330 (6005), pp. 841-845.

Gleichmann, M. & Mattson, M. P. (2011) 'Neuronal calcium homeostasis and dysregulation'. *Antioxid Redox Signal*, 14 (7), pp. 1261-1273.

Goldberg, M. P. & Ransom, B. R. (2003) 'New light on white matter'. *Stroke*, 34 (2), pp. 330-332.

Gourdain, P., Ballerini, C., Nicot, A. B. & Carnaud, C. (2012) 'Exacerbation of experimental autoimmune encephalomyelitis in prion protein (PrPc)-null mice: evidence for a critical role of the central nervous system'. *J Neuroinflammation*, 9 pp. 25.

Graf, R., Kumura, E., Dohmen, C., Rosner, G. & Heiss, W.-D. (2001) 'Pathophysiological Consequences of White Matter Compared to Gray Matter Ischemia'. Tokyo Springer Japan, pp. 195-201.

Gupta, H. V., Farrell, A. M. & Mittal, M. K. (2014) 'Transient ischemic attacks: predictability of future ischemic stroke or transient ischemic attack events'. *Ther Clin Risk Manag*, 10 pp. 27-35.

Gwag, B. J., Koh, J. Y., DeMaro, J. A., Ying, H. S., Jacquin, M. & Choi, D. W. (1997) 'Slowly triggered excitotoxicity occurs by necrosis in cortical cultures'. *Neuroscience*, 77 (2), pp. 393-401.

Gyllensten, L. & Malmfors, T. (1963) 'Myelinization of the optic nerve and its dependence on visual function--a quantitative investigation in mice'. *J Embryol Exp Morphol*, 11 pp. 255-266.

Hanada, T. (2014) 'The discovery and development of perampanel for the treatment of epilepsy'. *Expert Opin Drug Discov*, 9 (4), pp. 449-458.

Hanada, T., Hashizume, Y., Tokuhara, N., Takenaka, O., Kohmura, N., Ogasawara, A., Hatakeyama, S., Ohgoh, M., Ueno, M. & Nishizawa, Y. (2011) 'Perampanel: a novel, orally active, noncompetitive AMPA-receptor antagonist that reduces seizure activity in rodent models of epilepsy'. *Epilepsia*, 52 (7), pp. 1331-1340.

Hanisch, U. K. & Kettenmann, H. (2007) 'Microglia: active sensor and versatile effector cells in the normal and pathologic brain'. *Nat Neurosci*, 10 (11), pp. 1387-1394.

Hansen, A. J. (1977) 'Extracellular potassium concentration in juvenile and adult rat brain cortex during anoxia'. *Acta Physiol Scand*, 99 (4), pp. 412-420.

Hansen, A. J. (1978) 'The extracellular potassium concentration in brain cortex following ischemia in hypo- and hyperglycemic rats'. *Acta Physiol Scand*, 102 (3), pp. 324-329.

Hansen, A. J., Gjedde, A. & Siemkowicz, E. (1980) 'Extracellular potassium and blood flow in the post-ischemic rat brain'. *Pflugers Arch*, 389 (1), pp. 1-7.

Hansen, D. B., Garrido-Comas, N., Salter, M. & Fern, R. (2015) 'HCO3(-)-independent pH regulation in astrocytes in situ is dominated by V-ATPase'. *J Biol Chem*, 290 (13), pp. 8039-8047.

Hansen, K. B. & Traynelis, S. F. (2011) 'Structural and mechanistic determinants of a novel site for noncompetitive inhibition of GluN2D-containing NMDA receptors'. *J Neurosci*, 31 (10), pp. 3650-3661.

Harris, J. J. & Attwell, D. (2012) 'The energetics of CNS white matter'. *J Neurosci*, 32 (1), pp. 356-371.

Hartmann, J. & Konnerth, A. (2005) 'Determinants of postsynaptic Ca2+ signaling in Purkinje neurons'. *Cell Calcium*, 37 (5), pp. 459-466.

Hawkins, V. & Butt, A. (2013) 'TASK-1 channels in oligodendrocytes: a role in ischemia mediated disruption'. *Neurobiol Dis*, 55 pp. 87-94.

Hay, J. C. (2007) 'Calcium: a fundamental regulator of intracellular membrane fusion?'. *EMBO Rep*, 8 (3), pp. 236-240.

Hentschke, M., Wiemann, M., Hentschke, S., Kurth, I., Hermans-Borgmeyer, I., Seidenbecher, T., Jentsch, T. J., Gal, A. & Hubner, C. A. (2006) 'Mice with a targeted disruption of the Cl-/HCO3- exchanger AE3 display a reduced seizure threshold'. *Mol Cell Biol*, 26 (1), pp. 182-191.

Heurteaux, C., Guy, N., Laigle, C., Blondeau, N., Duprat, F., Mazzuca, M., Lang-Lazdunski, L., Widmann, C., Zanzouri, M., Romey, G. & Lazdunski, M. (2004) 'TREK-1, a K+ channel involved in neuroprotection and general anesthesia'. *EMBO J*, 23 (13), pp. 2684-2695.

Hibino, H., Inanobe, A., Furutani, K., Murakami, S., Findlay, I. & Kurachi, Y. (2010) 'Inwardly rectifying potassium channels: their structure, function, and physiological roles'. *Physiol Rev*, 90 (1), pp. 291-366.

Hijazi, N., Shaked, Y., Rosenmann, H., Ben-Hur, T. & Gabizon, R. (2003) 'Copper binding to PrPC may inhibit prion disease propagation'. *Brain Res*, 993 (1-2), pp. 192-200.

Hill, M. D. & Coutts, S. B. (2011) 'Preventing stroke after transient ischemic attack'. *CMAJ*, 183 (10), pp. 1127-1128.

Hirano, A. & Llena, J. F. (1995) 'Morphology of central nervous system axons', *The Axon: Structure, Function and Pathophysiology.* Oxford University Press.

Ho, P. W., Reutens, D. C., Phan, T. G., Wright, P. M., Markus, R., Indra, I., Young, D. & Donnan, G. A. (2005) 'Is white matter involved in patients entered into typical trials of neuroprotection?'. *Stroke*, 36 (12), pp. 2742-2744.

Hollenbeck, P. J. & Saxton, W. M. (2005) 'The axonal transport of mitochondria'. *J Cell Sci*, 118 (Pt 23), pp. 5411-5419.

Hollmann, M., Hartley, M. & Heinemann, S. (1991) 'Ca2+ permeability of KA-AMPA--gated glutamate receptor channels depends on subunit composition'. *Science*, 252 (5007), pp. 851-853.

Hrabe, J., Hrabetova, S. & Segeth, K. (2004) 'A model of effective diffusion and tortuosity in the extracellular space of the brain'. *Biophys J*, 87 (3), pp. 1606-1617.

Hu, H. J. & Song, M. (2017) 'Disrupted Ionic Homeostasis in Ischemic Stroke and New Therapeutic Targets'. *J Stroke Cerebrovasc Dis*, 26 (12), pp. 2706-2719.

Hu, Y., Doudevski, I., Wood, D., Moscarello, M., Husted, C., Genain, C., Zasadzinski, J. A. & Israelachvili, J. (2004) 'Synergistic interactions of lipids and myelin basic protein'. *Proc Natl Acad Sci U S A*, 101 (37), pp. 13466-13471.

Huang, S., Chen, L., Bladen, C., Stys, P. K. & Zamponi, G. W. (2018) 'Differential modulation of NMDA and AMPA receptors by cellular prion protein and copper ions'. *Mol Brain*, 11 (1), pp. 62.

Hubbard, J. A. & Binder, D. K. (2016) 'Potassium Channels', *Astrocytes and Epilepsy.* pp. 147–169.

Huettner, J. E. (2015) 'Glutamate receptor pores'. *J Physiol*, 593 (1), pp. 49-59.

Hughes, R. J., Ali, K., Jones, H., Kendall, S. & Connell, D. A. (2007) 'Treatment of Morton's neuroma with alcohol injection under sonographic guidance: follow-up of 101 cases'. *AJR Am J Roentgenol*, 188 (6), pp. 1535-1539.

Huria, T., Beeraka, N. M., Al-Ghamdi, B. & Fern, R. (2015) 'Premyelinated central axons express neurotoxic NMDA receptors: relevance to early developing white-matter injury'. *J Cereb Blood Flow Metab*, 35 (4), pp. 543-553.

Hynd, M. R., Scott, H. L. & Dodd, P. R. (2004) 'Glutamate-mediated excitotoxicity and neurodegeneration in Alzheimer's disease'. *Neurochem Int*, 45 (5), pp. 583-595.

Ingram, R. J., Isaacs, J. D., Kaur, G., Lowther, D. E., Reynolds, C. J., Boyton, R. J., Collinge, J., Jackson, G. S. & Altmann, D. M. (2009) 'A role of cellular prion protein in programming T-cell cytokine responses in disease'. *FASEB J*, 23 (6), pp. 1672-1684.

Jalini, S., Ye, H., Tonkikh, A. A., Charlton, M. P. & Carlen, P. L. (2016) 'Raised Intracellular Calcium Contributes to Ischemia-Induced Depression of Evoked Synaptic Transmission'. *PLoS One*, 11 (3), pp. e0148110.

Jhelum, P., Santos-Nogueira, E., Teo, W., Haumont, A., Lenoel, I., Stys, P. K. & David, S. (2020) 'Ferroptosis Mediates Cuprizone-Induced Loss of Oligodendrocytes and Demyelination'. *J Neurosci*, 40 (48), pp. 9327-9341.

Jonas, P. (1993) 'AMPA-type glutamate receptors--nonselective cation channels mediating fast excitatory transmission in the CNS'. *EXS*, 66 pp. 61-76.

Joshi, D. C., Tewari, B. P., Singh, M., Joshi, P. G. & Joshi, N. B. (2015) 'AMPA receptor activation causes preferential mitochondrial Ca(2)(+) load and oxidative stress in motor neurons'. *Brain Res*, 1616 pp. 1-9.

Juurlink, B. H., Thorburne, S. K. & Hertz, L. (1998) 'Peroxide-scavenging deficit underlies oligodendrocyte susceptibility to oxidative stress'. *Glia*, 22 (4), pp. 371-378.

Kaller, M. S., Lazari, A., Blanco-Duque, C., Sampaio-Baptista, C. & Johansen-Berg, H. (2017) 'Myelin plasticity and behaviour-connecting the dots'. *Curr Opin Neurobiol*, 47 pp. 86-92.

Kalman, B., Laitinen, K. & Komoly, S. (2007) 'The involvement of mitochondria in the pathogenesis of multiple sclerosis'. *J Neuroimmunol*, 188 (1-2), pp. 1-12.

Kalsi, A. S., Greenwood, K., Wilkin, G. & Butt, A. M. (2004) 'Kir4.1 expression by astrocytes and oligodendrocytes in CNS white matter: a developmental study in the rat optic nerve'. *J Anat*, 204 (6), pp. 475-485.

Kanda, H., Ling, J., Tonomura, S., Noguchi, K., Matalon, S. & Gu, J. G. (2019) 'TREK-1 and TRAAK Are Principal K(+) Channels at the Nodes of Ranvier for Rapid Action Potential Conduction on Mammalian Myelinated Afferent Nerves'. *Neuron*, 104 (5), pp. 960-971 e967.

Kanellopoulos, G. K., Xu, X. M., Hsu, C. Y., Lu, X., Sundt, T. M. & Kouchoukos, N. T. (2000) 'White matter injury in spinal cord ischemia: protection by AMPA/kainate glutamate receptor antagonism'. *Stroke*, 31 (8), pp. 1945-1952.

Karadottir, R., Cavelier, P., Bergersen, L. H. & Attwell, D. (2005) 'NMDA receptors are expressed in oligodendrocytes and activated in ischaemia'. *Nature*, 438 (7071), pp. 1162-1166.

Karasek, M., Swiltoslawski, J. & Zieliniska, A. (2004) 'Ultrastructure of the central nervous system: the basics'. *Folia Neuropathol*, 42 Suppl B pp. 1-9.

Kasischke, K. A., Vishwasrao, H. D., Fisher, P. J., Zipfel, W. R. & Webb, W. W. (2004) 'Neural activity triggers neuronal oxidative metabolism followed by astrocytic glycolysis'. *Science*, 305 (5680), pp. 99-103.

Katchman, A. N. & Hershkowitz, N. (1993) 'Early anoxia-induced vesicular glutamate release results from mobilization of calcium from intracellular stores'. *J Neurophysiol*, 70 (1), pp. 1-7.

Katsura, K., Ekholm, A., Asplund, B. & Siesjo, B. K. (1991) 'Extracellular pH in the brain during ischemia: relationship to the severity of lactic acidosis'. *J Cereb Blood Flow Metab*, 11 (4), pp. 597-599.

Kawaguchi, Y. (2017) 'Pyramidal Cell Subtypes and Their Synaptic Connections in Layer 5 of Rat Frontal Cortex'. *Cereb Cortex*, 27 (12), pp. 5755-5771.

Keynes, R. D. & Elinder, F. (1999) 'The screw-helical voltage gating of ion channels'. *Proc Biol Sci*, 266 (1421), pp. 843-852.

Khosravani, H., Zhang, Y., Tsutsui, S., Hameed, S., Altier, C., Hamid, J., Chen, L., Villemaire, M., Ali, Z., Jirik, F. R. & Zamponi, G. W. (2008) 'Prion protein attenuates excitotoxicity by inhibiting NMDA receptors'. *J Cell Biol*, 181 (3), pp. 551-565.

Kimelberg, H. K. & Ricard, C. (1982) 'Control of intracellular pH in primary astrocyte cultures by external Na+'. *Trans. Am. Soc. Neurochem*, 13 pp. 112.

Kobelt, G., Thompson, A., Berg, J., Gannedahl, M., Eriksson, J., Group, M. S. & European Multiple Sclerosis, P. (2017) 'New insights into the burden and costs of multiple sclerosis in Europe'. *Mult Scler*, 23 (8), pp. 1123-1136.

Kochhar, A., Zivin, J. A. & Mazzarella, V. (1991) 'Pharmacologic Studies of the Neuroprotective Actions of a Glutamate Antagonist in Ischemia'. *Journal of Neurotrauma*, 8 (3), pp. 175-186.

Kofuji, P. & Newman, E. A. (2004) 'Potassium buffering in the central nervous system'. *Neuroscience*, 129 (4), pp. 1045-1056.

Kohr, G. (2007) 'NMDA receptor antagonists: tools in neuroscience with promise for treating CNS pathologies'. *J Physiol*, 581 (Pt 1), pp. 1-2.

Kornek, B., Storch, M. K., Bauer, J., Djamshidian, A., Weissert, R., Wallstroem, E., Stefferl, A., Zimprich, F., Olsson, T., Linington, C., Schmidbauer, M. & Lassmann, H. (2001) 'Distribution of a calcium channel subunit in dystrophic axons in multiple sclerosis and experimental autoimmune encephalomyelitis'. *Brain*, 124 (Pt 6), pp. 1114-1124.

Kraig, R. P. & Chesler, M. (1990) 'Astrocytic acidosis in hyperglycemic and complete ischemia'. *J Cereb Blood Flow Metab*, 10 (1), pp. 104-114.

Kraig, R. P., Ferreira-Filho, C. R. & Nicholson, C. (1983) 'Alkaline and acid transients in cerebellar microenvironment'. *J Neurophysiol*, 49 (3), pp. 831-850.

Krauss, G. L. (2013) 'Perampanel: a selective AMPA antagonist for treating seizures'. *Epilepsy Curr*, 13 (6), pp. 269-272.

Krishek, B. J., Amato, A., Connolly, C. N., Moss, S. J. & Smart, T. G. (1996) 'Proton sensitivity of the GABA(A) receptor is associated with the receptor subunit composition'. *J Physiol*, 492 (Pt 2) pp. 431-443.

Kristian, T. & Siesjo, B. K. (1998) 'Calcium in ischemic cell death'. *Stroke*, 29 (3), pp. 705-718.

Krnjevic, K. (2008) 'Electrophysiology of cerebral ischemia'. *Neuropharmacology*, 55 (3), pp. 319-333.

Kukley, M., Capetillo-Zarate, E. & Dietrich, D. (2007) 'Vesicular glutamate release from axons in white matter'. *Nat Neurosci*, 10 (3), pp. 311-320.

Kumura, E., Dohmen, C., Graf, R., Yoshimine, T. & Heiss, W. D. (2003) 'Significant shrinkage of extracellular space during global cerebral ischemia: differences in gray and white matter ischemia'. *Acta Neurochir Suppl*, 86 pp. 67-70.

Lappe-Siefke, C., Goebbels, S., Gravel, M., Nicksch, E., Lee, J., Braun, P. E., Griffiths, I. R. & Nave, K. A. (2003) 'Disruption of Cnp1 uncouples oligodendroglial functions in axonal support and myelination'. *Nat Genet*, 33 (3), pp. 366-374.

Larson, V. A., Mironova, Y., Vanderpool, K. G., Waisman, A., Rash, J. E., Agarwal, A. & Bergles, D. E. (2018) 'Oligodendrocytes control potassium accumulation in white matter and seizure susceptibility'. *Elife*, 7

Lau, A. & Tymianski, M. (2010) 'Glutamate receptors, neurotoxicity and neurodegeneration'. *Pflugers Arch*, 460 (2), pp. 525-542.

Laule, C., Vavasour, I. M., Kolind, S. H., Li, D. K., Traboulsee, T. L., Moore, G. R. & MacKay, A. L. (2007) 'Magnetic resonance imaging of myelin'. *Neurotherapeutics*, 4 (3), pp. 460-484.

Lazzaro, J. T., Paternain, A. V., Lerma, J., Chenard, B. L., Ewing, F. E., Huang, J., Welch, W. M., Ganong, A. H. & Menniti, F. S. (2002) 'Functional characterization of CP-465,022, a selective, noncompetitive AMPA receptor antagonist'. *Neuropharmacology*, 42 (2), pp. 143-153.

Lee, S. K., Boron, W. F. & Parker, M. D. (2013) 'Monitoring ion activities in and around cells using ion-selective liquid-membrane microelectrodes'. *Sensors (Basel)*, 13 (1), pp. 984-1003.

Lee, S. Y. & Kim, J. H. (2015) 'Mechanisms underlying presynaptic Ca2+ transient and vesicular glutamate release at a CNS nerve terminal during in vitro ischaemia'. *J Physiol*, 593 (13), pp. 2793-2806.

Lee, Y., Morrison, B. M., Li, Y., Lengacher, S., Farah, M. H., Hoffman, P. N., Liu, Y., Tsingalia, A., Jin, L., Zhang, P. W., Pellerin, L., Magistretti, P. J. & Rothstein, J. D. (2012) 'Oligodendroglia metabolically support axons and contribute to neurodegeneration'. *Nature*, 487 (7408), pp. 443-448.

Leis, J. A., Bekar, L. K. & Walz, W. (2005) 'Potassium homeostasis in the ischemic brain'. *Glia*, 50 (4), pp. 407-416.

Leist, M., Volbracht, C., Kuhnle, S., Fava, E., Ferrando-May, E. & Nicotera, P. (1997) 'Caspase-mediated apoptosis in neuronal excitotoxicity triggered by nitric oxide'. *Mol Med*, 3 (11), pp. 750-764.

Lenaeus, M. J., Vamvouka, M., Focia, P. J. & Gross, A. (2005) 'Structural basis of TEA blockade in a model potassium channel'. *Nat Struct Mol Biol*, 12 (5), pp. 454-459.

Letourneau, P. C. (2009) 'Actin in axons: stable scaffolds and dynamic filaments'. *Results Probl Cell Differ*, 48 pp. 65-90.

Leuchtmann, E. A., Ratner, A. E., Vijitruth, R., Qu, Y. & McDonald, J. W. (2003) 'AMPA receptors are the major mediators of excitotoxic death in mature oligodendrocytes'. *Neurobiol Dis*, 14 (3), pp. 336-348.

Lewerenz, J. & Maher, P. (2015) 'Chronic Glutamate Toxicity in Neurodegenerative Diseases-What is the Evidence?'. *Front Neurosci*, 9 pp. 469.

Li, S., Mealing, G. A., Morley, P. & Stys, P. K. (1999) 'Novel injury mechanism in anoxia and trauma of spinal cord white matter: glutamate release via reverse Na+-dependent glutamate transport'. *J Neurosci*, 19 (14), pp. RC16.

Li, S. & Stys, P. K. (2000) 'Mechanisms of ionotropic glutamate receptor-mediated excitotoxicity in isolated spinal cord white matter'. *J Neurosci*, 20 (3), pp. 1190-1198.

Li, W., Zhang, B., Tang, J., Cao, Q., Wu, Y., Wu, C., Guo, J., Ling, E. A. & Liang, F. (2007) 'Sirtuin 2, a mammalian homolog of yeast silent information regulator-2 longevity regulator, is an oligodendroglial protein that decelerates cell differentiation through deacetylating alpha-tubulin'. *J Neurosci*, 27 (10), pp. 2606-2616.

Liewald, D., Miller, R., Logothetis, N., Wagner, H. J. & Schuz, A. (2014) 'Distribution of axon diameters in cortical white matter: an electron-microscopic study on three human brains and a macaque'. *Biol Cybern*, 108 (5), pp. 541-557.

Lipton, P. (1999) 'Ischemic cell death in brain neurons'. *Physiol Rev*, 79 (4), pp. 1431-1568.

Lipton, S. A. (2004) 'Failures and successes of NMDA receptor antagonists: molecular basis for the use of open-channel blockers like memantine in the treatment of acute and chronic neurologic insults'. *NeuroRx*, 1 (1), pp. 101-110.

Liu, D., Slevin, J. R., Lu, C., Chan, S. L., Hansson, M., Elmer, E. & Mattson, M. P. (2003) 'Involvement of mitochondrial K+ release and cellular efflux in ischemic and apoptotic neuronal death'. *J Neurochem*, 86 (4), pp. 966-979.

Lodish, H. F. (2000) *Molecular cell biology.* 4th edn. New York: W.H. Freeman.

Loria, F., Petrosino, S., Hernangomez, M., Mestre, L., Spagnolo, A., Correa, F., Di Marzo, V., Docagne, F. & Guaza, C. (2010) 'An endocannabinoid tone limits excitotoxicity in vitro and in a model of multiple sclerosis'. *Neurobiol Dis*, 37 (1), pp. 166-176.

Loscher, W., Rundfeldt, C. & Honack, D. (1993) 'Low doses of NMDA receptor antagonists synergistically increase the anticonvulsant effect of the AMPA receptor antagonist NBQX in the kindling model of epilepsy'. *Eur J Neurosci*, 5 (11), pp. 1545-1550.

Lucchinetti, C., Bruck, W., Parisi, J., Scheithauer, B., Rodriguez, M. & Lassmann, H. (2000) 'Heterogeneity of multiple sclerosis lesions: implications for the pathogenesis of demyelination'. *Ann Neurol*, 47 (6), pp. 707-717.

Lundgaard, I., Osorio, M. J., Kress, B. T., Sanggaard, S. & Nedergaard, M. (2014) 'White matter astrocytes in health and disease'. *Neuroscience*, 276 pp. 161-173.

Macrez, R., Stys, P. K., Vivien, D., Lipton, S. A. & Docagne, F. (2016) 'Mechanisms of glutamate toxicity in multiple sclerosis: biomarker and therapeutic opportunities'. *Lancet Neurol*, 15 (10), pp. 1089-1102.

Mahmoud, S., Gharagozloo, M., Simard, C. & Gris, D. (2019) 'Astrocytes Maintain Glutamate Homeostasis in the CNS by Controlling the Balance between Glutamate Uptake and Release'. *Cells*, 8 (2),

Mancardi, G. & Saccardi, R. (2008) 'Autologous haematopoietic stem-cell transplantation in multiple sclerosis'. *Lancet Neurol*, 7 (7), pp. 626-636.

Manning, S. M., Talos, D. M., Zhou, C., Selip, D. B., Park, H. K., Park, C. J., Volpe, J. J. & Jensen, F. E. (2008) 'NMDA receptor blockade with memantine attenuates white matter injury in a rat model of periventricular leukomalacia'. *J Neurosci*, 28 (26), pp. 6670-6678.

Maren, T. H. (1967) 'Carbonic anhydrase: chemistry, physiology, and inhibition'. *Physiol Rev*, 47 (4), pp. 595-781.

Marrif, H. & Juurlink, B. H. (1999) 'Astrocytes respond to hypoxia by increasing glycolytic capacity'. *J Neurosci Res*, 57 (2), pp. 255-260.

Marsh, W. R., Anderson, R. E. & Sundt, T. M., Jr. (1986) 'Effect of hyperglycemia on brain pH levels in areas of focal incomplete cerebral ischemia in monkeys'. *J Neurosurg*, 65 (5), pp. 693-696.

Matute, C. (2011) 'Glutamate and ATP signalling in white matter pathology'. *J Anat*, 219 (1), pp. 53-64.

Matute, C., Alberdi, E., Domercq, M., Sanchez-Gomez, M. V., Perez-Samartin, A., Rodriguez-Antiguedad, A. & Perez-Cerda, F. (2007) 'Excitotoxic damage to white matter'. *J Anat*, 210 (6), pp. 693-702.

Mazoch, M. J., Cheema, G. A., Suva, L. J. & Thomas, R. L. (2014) 'Effects of alcohol injection in rat sciatic nerve as a model for Morton's neuroma treatment'. *Foot Ankle Int*, 35 (11), pp. 1187-1191.

McCracken, E., Fowler, J. H., Dewar, D., Morrison, S. & McCulloch, J. (2002) 'Grey matter and white matter ischemic damage is reduced by the competitive AMPA receptor antagonist, SPD 502'. *J Cereb Blood Flow Metab*, 22 (9), pp. 1090-1097.

McDonald, J. W., Bhattacharyya, T., Sensi, S. L., Lobner, D., Ying, H. S., Canzoniero, L. M. & Choi, D. W. (1998) 'Extracellular acidity potentiates AMPA receptor-mediated cortical neuronal death'. *J Neurosci*, 18 (16), pp. 6290-6299.

McKhann, G. M., 2nd, D'Ambrosio, R. & Janigro, D. (1997) 'Heterogeneity of astrocyte resting membrane potentials and intercellular coupling revealed by whole-cell and gramicidin-perforated patch recordings from cultured neocortical and hippocampal slice astrocytes'. *J Neurosci*, 17 (18), pp. 6850-6863.

Mellergard, P. E. & Siesjo, B. K. (1991) 'Astrocytes fail to regulate intracellular pH at moderately reduced extracellular pH'. *Neuroreport*, 2 (11), pp. 695-698.

Menniti, F. S., Buchan, A. M., Chenard, B. L., Critchett, D. J., Ganong, A. H., Guanowsky, V., Seymour, P. A. & Welch, W. M. (2003) 'CP-465,022, a selective noncompetitive AMPA receptor antagonist, blocks AMPA receptors but is not neuroprotective in vivo'. *Stroke*, 34 (1), pp. 171-176.

Micu, I., Jiang, Q., Coderre, E., Ridsdale, A., Zhang, L., Woulfe, J., Yin, X., Trapp, B. D., McRory, J. E., Rehak, R., Zamponi, G. W., Wang, W. & Stys, P. K. (2006) 'NMDA receptors mediate calcium accumulation in myelin during chemical ischaemia'. *Nature*, 439 (7079), pp. 988-992.

Micu, I., Plemel, J. R., Caprariello, A. V., Nave, K. A. & Stys, P. K. (2018) 'Axo-myelinic neurotransmission: a novel mode of cell signalling in the central nervous system'. *Nat Rev Neurosci*, 19 (1), pp. 49-58.

Micu, I., Plemel, J. R., Lachance, C., Proft, J., Jansen, A. J., Cummins, K., van Minnen, J. & Stys, P. K. (2016) 'The molecular physiology of the axo-myelinic synapse'. *Exp Neurol*, 276 pp. 41-50.

Minta, A. & Tsien, R. Y. (1989) 'Fluorescent indicators for cytosolic sodium'. *J Biol Chem*, 264 (32), pp. 19449-19457.

Mittelbronn, M., Dietz, K., Schluesener, H. J. & Meyermann, R. (2001) 'Local distribution of microglia in the normal adult human central nervous system differs by up to one order of magnitude'. *Acta Neuropathol*, 101 (3), pp. 249-255.

Mizuno, S., Tra, D. T., Mizobuchi, A., Iseki, H., Mizuno-Iijima, S., Kim, J. D., Ishida, J., Matsuda, Y., Kunita, S., Fukamizu, A., Sugiyama, F. & Yagami, K. (2014) 'Truncated Cables1 causes agenesis of the corpus callosum in mice'. *Lab Invest*, 94 (3), pp. 321-330.

Moldovan, N., Al-Ebraheem, A., Lobo, L., Park, R., Farquharson, M. J. & Bock, N. A. (2015) 'Altered transition metal homeostasis in the cuprizone model of demyelination'. *Neurotoxicology*, 48 pp. 1-8.

Molyneux, P. D., Kappos, L., Polman, C., Pozzilli, C., Barkhof, F., Filippi, M., Yousry, T., Hahn, D., Wagner, K., Ghazi, M., Beckmann, K., Dahlke, F., Losseff, N., Barker, G. J., Thompson, A. J. & Miller, D. H. (2000) 'The effect of interferon beta-1b treatment on MRI measures of cerebral atrophy in secondary progressive multiple sclerosis. European Study Group on Interferon beta-1b in secondary progressive multiple sclerosis'. *Brain*, 123 (Pt 11) pp. 2256-2263.

Mori, K., Miyazaki, M., Iwase, H. & Maeda, M. (2002) 'Temporal profile of changes in brain tissue extracellular space and extracellular ion (Na(+), K(+)) concentrations after cerebral ischemia and the effects of mild cerebral hypothermia'. *J Neurotrauma*, 19 (10), pp. 1261-1270.

Mori, S. & Leblond, C. P. (1969) 'Identification of microglia in light and electron microscopy'. *J Comp Neurol*, 135 (1), pp. 57-80.

Mosley, C. A., Acker, T. M., Hansen, K. B., Mullasseril, P., Andersen, K. T., Le, P., Vellano, K. M., Brauner-Osborne, H., Liotta, D. C. & Traynelis, S. F. (2010) 'Quinazolin-4-one derivatives: A novel class of noncompetitive NR2C/D subunit-selective N-methyl-D-aspartate receptor antagonists'. *J Med Chem*, 53 (15), pp. 5476-5490.

Musse, A. A. & Harauz, G. (2007) 'Molecular "negativity" may underlie multiple sclerosis: role of the myelin basic protein family in the pathogenesis of MS'. *Int Rev Neurobiol*, 79 pp. 149-172.

Mutch, W. A. & Hansen, A. J. (1984) 'Extracellular pH changes during spreading depression and cerebral ischemia: mechanisms of brain pH regulation'. *J Cereb Blood Flow Metab*, 4 (1), pp. 17-27.

Nakamichi, T. (1998) '[Glutamate neurotoxicity during spinal cord ischemia--the neuroprotective effects of adenosine]'. *Jpn J Thorac Cardiovasc Surg*, 46 (4), pp. 354-360.

Namekata, K., Kimura, A., Harada, C., Yoshida, H., Matsumoto, Y. & Harada, T. (2014) 'Dock3 protects myelin in the cuprizone model for demyelination'. *Cell Death Dis*, 5 pp. e1395.

Nedergaard, M., Kraig, R. P., Tanabe, J. & Pulsinelli, W. A. (1991) 'Dynamics of interstitial and intracellular pH in evolving brain infarct'. *Am J Physiol*, 260 (3 Pt 2), pp. R581-588.

Newcombe, J., Uddin, A., Dove, R., Patel, B., Turski, L., Nishizawa, Y. & Smith, T. (2008) 'Glutamate receptor expression in multiple sclerosis lesions'. *Brain Pathol*, 18 (1), pp. 52-61.

Newcomer, J. W., Farber, N. B. & Olney, J. W. (2000) 'NMDA receptor function, memory, and brain aging'. *Dialogues Clin Neurosci*, 2 (3), pp. 219-232.

Newland, C. F., Adelman, J. P., Tempel, B. L. & Almers, W. (1992) 'Repulsion between tetraethylammonium ions in cloned voltage-gated potassium channels'. *Neuron*, 8 (5), pp. 975-982.

Nimmerjahn, A., Kirchhoff, F. & Helmchen, F. (2005) 'Resting microglial cells are highly dynamic surveillants of brain parenchyma in vivo'. *Science*, 308 (5726), pp. 1314-1318.

Norton, W. T., Aquino, D. A., Hozumi, I., Chiu, F. C. & Brosnan, C. F. (1992) 'Quantitative aspects of reactive gliosis: a review'. *Neurochem Res*, 17 (9), pp. 877-885.

Ohno, N., Kidd, G. J., Mahad, D., Kiryu-Seo, S., Avishai, A., Komuro, H. & Trapp, B. D. (2011) 'Myelination and axonal electrical activity modulate the distribution and motility of mitochondria at CNS nodes of Ranvier'. *J Neurosci*, 31 (20), pp. 7249-7258.

Olney, J. W., Labruyere, J. & Price, M. T. (1989) 'Pathological changes induced in cerebrocortical neurons by phencyclidine and related drugs'. *Science*, 244 (4910), pp. 1360-1362.

Ouardouz, M., Coderre, E., Basak, A., Chen, A., Zamponi, G. W., Hameed, S., Rehak, R., Yin, X., Trapp, B. D. & Stys, P. K. (2009a) 'Glutamate receptors on myelinated spinal cord axons: I. GluR6 kainate receptors'. *Ann Neurol*, 65 (2), pp. 151-159.

Ouardouz, M., Coderre, E., Zamponi, G. W., Hameed, S., Yin, X., Trapp, B. D. & Stys, P. K. (2009b) 'Glutamate receptors on myelinated spinal cord axons: II. AMPA and GluR5 receptors'. *Ann Neurol*, 65 (2), pp. 160-166.

Ouardouz, M., Malek, S., Coderre, E. & Stys, P. K. (2006) 'Complex interplay between glutamate receptors and intracellular Ca2+ stores during ischaemia in rat spinal cord white matter'. *J Physiol*, 577 (Pt 1), pp. 191-204.

Oubidar, M., Boquillon, M., Marie, C., Schreiber, L. & Bralet, J. (1994) 'Ischemia-induced brain iron delocalization: effect of iron chelators'. *Free Radic Biol Med*, 16 (6), pp. 861-867.

Palmer, L. M. & Stuart, G. J. (2006) 'Site of action potential initiation in layer 5 pyramidal neurons'. *J Neurosci*, 26 (6), pp. 1854-1863.

Pamarthy, S., Kulshrestha, A., Katara, G. K. & Beaman, K. D. (2018) 'The curious case of vacuolar ATPase: regulation of signaling pathways'. *Mol Cancer*, 17 (1), pp. 41.

Pascual, O., Ben Achour, S., Rostaing, P., Triller, A. & Bessis, A. (2012) 'Microglia activation triggers astrocyte-mediated modulation of excitatory neurotransmission'. *Proc Natl Acad Sci U S A*, 109 (4), pp. E197-205.

Patergnani, S., Fossati, V., Bonora, M., Giorgi, C., Marchi, S., Missiroli, S., Rusielewicz, T., Wieckowski, M. R. & Pinton, P. (2017) 'Mitochondria in Multiple Sclerosis: Molecular Mechanisms of Pathogenesis'. *Int Rev Cell Mol Biol*, 328 pp. 49-103.

Pellerin, L. & Magistretti, P. J. (2012) 'Sweet sixteen for ANLS'. *J Cereb Blood Flow Metab*, 32 (7), pp. 1152-1166.

Perez-Pinzon, M. A., Tao, L. & Nicholson, C. (1995) 'Extracellular potassium, volume fraction, and tortuosity in rat hippocampal CA1, CA3, and cortical slices during ischemia'. *J Neurophysiol*, 74 (2), pp. 565-573.

Perge, J. A., Koch, K., Miller, R., Sterling, P. & Balasubramanian, V. (2009) 'How the optic nerve allocates space, energy capacity, and information'. *J Neurosci*, 29 (24), pp. 7917-7928.

Peters, A. (1966) 'The node of Ranvier in the central nervous system'. *Q J Exp Physiol Cogn Med Sci*, 51 (3), pp. 229-236.

Petito, C. K., Olarte, J. P., Roberts, B., Nowak, T. S., Jr. & Pulsinelli, W. A. (1998) 'Selective glial vulnerability following transient global ischemia in rat brain'. *J Neuropathol Exp Neurol*, 57 (3), pp. 231-238.

Piani, D., Spranger, M., Frei, K., Schaffner, A. & Fontana, A. (1992) 'Macrophage-induced cytotoxicity of N-methyl-D-aspartate receptor positive neurons involves excitatory amino acids rather than reactive oxygen intermediates and cytokines'. *Eur J Immunol*, 22 (9), pp. 2429-2436.

Pina-Crespo, J. C., Talantova, M., Micu, I., States, B., Chen, H. S., Tu, S., Nakanishi, N., Tong, G., Zhang, D., Heinemann, S. F., Zamponi, G. W., Stys, P. K. & Lipton, S. A. (2010) 'Excitatory glycine responses of CNS myelin mediated by NR1/NR3 "NMDA" receptor subunits'. *J Neurosci*, 30 (34), pp. 11501-11505.

Piper, H. M., Balser, C., Ladilov, Y. V., Schafer, M., Siegmund, B., Ruiz-Meana, M. & Garcia-Dorado, D. (1996) 'The role of Na+/H+ exchange in ischemia-reperfusion'. *Basic Res Cardiol*, 91 (3), pp. 191-202.

Pitt, D., Nagelmeier, I. E., Wilson, H. C. & Raine, C. S. (2003) 'Glutamate uptake by oligodendrocytes: Implications for excitotoxicity in multiple sclerosis'. *Neurology*, 61 (8), pp. 1113-1120.

Pitt, D., Werner, P. & Raine, C. S. (2000) 'Glutamate excitotoxicity in a model of multiple sclerosis'. *Nat Med*, 6 (1), pp. 67-70.

Pivovarov, A. S., Calahorro, F. & Walker, R. J. (2018) 'Na(+)/K(+)-pump and neurotransmitter membrane receptors'. *Invert Neurosci*, 19 (1), pp. 1.

Poliak, S., Salomon, D., Elhanany, H., Sabanay, H., Kiernan, B., Pevny, L., Stewart, C. L., Xu, X., Chiu, S. Y., Shrager, P., Furley, A. J. & Peles, E. (2003) 'Juxtaparanodal clustering of Shaker-like K+ channels in myelinated axons depends on Caspr2 and TAG-1'. *J Cell Biol*, 162 (6), pp. 1149-1160.

Quevedo, L., Baldeig, J. & Concha, J. (1976) 'Effects of ethanol on compound action potential and refractory periods of toad sciatic nerve'. *Pharmacology*, 14 (2), pp. 148-152.

Randle, J. C., Guet, T., Cordi, A. & Lepagnol, J. M. (1992) 'Competitive inhibition by NBQX of kainate/AMPA receptor currents and excitatory synaptic potentials: importance of 6-nitro substitution'. *Eur J Pharmacol*, 215 (2-3), pp. 237-244.

Ransom, B. R., Butt, A. M. & Black, J. A. (1991) 'Ultrastructural identification of HRP-injected oligodendrocytes in the intact rat optic nerve'. *Glia*, 4 (1), pp. 37-45.

Ransom, B. R., Walz, W., Davis, P. K. & Carlini, W. G. (1992) 'Anoxia-induced changes in extracellular K+ and pH in mammalian central white matter'. *J Cereb Blood Flow Metab*, 12 (4), pp. 593-602.

Ransom, C. B. & Sontheimer, H. (1995) 'Biophysical and pharmacological characterization of inwardly rectifying K+ currents in rat spinal cord astrocytes'. *J Neurophysiol*, 73 (1), pp. 333-346.

Rasband, M. N., Tayler, J., Kaga, Y., Yang, Y., Lappe-Siefke, C., Nave, K. A. & Bansal, R. (2005) 'CNP is required for maintenance of axon-glia interactions at nodes of Ranvier in the CNS'. *Glia*, 50 (1), pp. 86-90.

Rehncrona, S. & Kagstrom, E. (1983) 'Tissue lactic acidosis and ischemic brain damage'. *Am J Emerg Med*, 1 (2), pp. 168-174.

Richard, M. J., Saleh, T. M., El Bahh, B. & Zidichouski, J. A. (2010) 'A novel method for inducing focal ischemia in vitro'. *J Neurosci Methods*, 190 (1), pp. 20-27.

Rivers, L. E., Young, K. M., Rizzi, M., Jamen, F., Psachoulia, K., Wade, A., Kessaris, N. & Richardson, W. D. (2008) 'PDGFRA/NG2 glia generate myelinating oligodendrocytes and piriform projection neurons in adult mice'. *Nat Neurosci*, 11 (12), pp. 1392-1401.

Rodriguez, M. & Scheithauer, B. (1994) 'Ultrastructure of multiple sclerosis'. *Ultrastruct Pathol*, 18 (1-2), pp. 3-13.

Rogawski, M. A. & Hanada, T. (2013) 'Preclinical pharmacology of perampanel, a selective non-competitive AMPA receptor antagonist'. *Acta Neurol Scand Suppl*, (197), pp. 19-24.

Rogawski, M. A. & Wenk, G. L. (2003) 'The neuropharmacological basis for the use of memantine in the treatment of Alzheimer's disease'. *CNS Drug Rev*, 9 (3), pp. 275-308.

Rosenstock, T. R., Bertoncini, C. R., Teles, A. V., Hirata, H., Fernandes, M. J. & Smaili, S. S. (2010) 'Glutamate-induced alterations in Ca2+ signaling are modulated by mitochondrial Ca2+ handling capacity in brain slices of R6/1 transgenic mice'. *Eur J Neurosci*, 32 (1), pp. 60-70.

Rosenzweig, S. & Carmichael, S. T. (2013) 'Age-dependent exacerbation of white matter stroke outcomes: a role for oxidative damage and inflammatory mediators'. *Stroke*, 44 (9), pp. 2579-2586.

Rossi, D. J., Brady, J. D. & Mohr, C. (2007) 'Astrocyte metabolism and signaling during brain ischemia'. *Nat Neurosci*, 10 (11), pp. 1377-1386.

Rossi, S., Studer, V., Moscatelli, A., Motta, C., Coghe, G., Fenu, G., Caillier, S., Buttari, F., Mori, F., Barbieri, F., Castelli, M., De Chiara, V., Monteleone, F., Mancino, R., Bernardi, G., Baranzini, S. E., Marrosu, M. G., Oksenberg, J. R. & Centonze, D. (2013) 'Opposite roles of NMDA receptors in relapsing and primary progressive multiple sclerosis'. *PLoS One*, 8 (6), pp. e67357.

Rothhammer, V. & Quintana, F. J. (2015) 'Control of autoimmune CNS inflammation by astrocytes'. *Semin Immunopathol*, 37 (6), pp. 625-638.

Rothman, S. M., Thurston, J. H. & Hauhart, R. E. (1987) 'Delayed neurotoxicity of excitatory amino acids in vitro'. *Neuroscience*, 22 (2), pp. 471-480.

Ruffin, V. A., Salameh, A. I., Boron, W. F. & Parker, M. D. (2014) 'Intracellular pH regulation by acid-base transporters in mammalian neurons'. *Front Physiol*, 5 pp. 43.

Rumsby, M., Afsari, F., Stark, M. & Hughson, E. (2003) 'Microfilament and microtubule organization and dynamics in process extension by central glia-4 oligodendrocytes: evidence for a microtubule organizing center'. *Glia*, 42 (2), pp. 118-129.

Rungta, R. L., Choi, H. B., Tyson, J. R., Malik, A., Dissing-Olesen, L., Lin, P. J. C., Cain, S. M., Cullis, P. R., Snutch, T. P. & MacVicar, B. A. (2015) 'The cellular mechanisms of neuronal swelling underlying cytotoxic edema'. *Cell*, 161 (3), pp. 610-621.

Ryoo, K. & Park, J. Y. (2016) 'Two-pore Domain Potassium Channels in Astrocytes'. *Exp Neurobiol*, 25 (5), pp. 222-232.

Saab, A. S., Tzvetanova, I. D. & Nave, K. A. (2013) 'The role of myelin and oligodendrocytes in axonal energy metabolism'. *Curr Opin Neurobiol*, 23 (6), pp. 1065-1072.

Saab, A. S., Tzvetavona, I. D., Trevisiol, A., Baltan, S., Dibaj, P., Kusch, K., Mobius, W., Goetze, B., Jahn, H. M., Huang, W., Steffens, H., Schomburg, E. D., Perez-Samartin, A., Perez-Cerda, F., Bakhtiari, D., Matute, C., Lowel, S., Griesinger, C., Hirrlinger, J., Kirchhoff, F. & Nave, K. A. (2016) 'Oligodendroglial NMDA Receptors Regulate Glucose Import and Axonal Energy Metabolism'. *Neuron*, 91 (1), pp. 119-132.

Saher, G., Brugger, B., Lappe-Siefke, C., Mobius, W., Tozawa, R., Wehr, M. C., Wieland, F., Ishibashi, S. & Nave, K. A. (2005) 'High cholesterol level is essential for myelin membrane growth'. *Nat Neurosci*, 8 (4), pp. 468-475.

Salter, M. G. & Fern, R. (2005) 'NMDA receptors are expressed in developing oligodendrocyte processes and mediate injury'. *Nature*, 438 (7071), pp. 1167-1171.

Sander, T., Toliat, M. R., Heils, A., Leschik, G., Becker, C., Ruschendorf, F., Rohde, K., Mundlos, S. & Nurnberg, P. (2002) 'Association of the 867Asp variant of the human anion exchanger 3 gene with common subtypes of idiopathic generalized epilepsy'. *Epilepsy Res*, 51 (3), pp. 249-255.

Santos, A. E., Duarte, C. B., Iizuka, M., Barsoumian, E. L., Ham, J., Lopes, M. C., Carvalho, A. P. & Carvalho, A. L. (2006) 'Excitotoxicity mediated by Ca2+-permeable GluR4-containing AMPA receptors involves the AP-1 transcription factor'. *Cell Death Differ*, 13 (4), pp. 652-660.

Scatton, B. (1993) 'The NMDA receptor complex'. *Fundam Clin Pharmacol*, 7 (8), pp. 389-400.

Schabitz, W. R., Li, F. & Fisher, M. (2000) 'The N-methyl-D-aspartate antagonist CNS 1102 protects cerebral gray and white matter from ischemic injury following temporary focal ischemia in rats'. *Stroke*, 31 (7), pp. 1709-1714.

Schellekens, G. A., de Jong, B. A., van den Hoogen, F. H., van de Putte, L. B. & van Venrooij, W. J. (1998) 'Citrulline is an essential constituent of antigenic determinants recognized by rheumatoid arthritis-specific autoantibodies'. *J Clin Invest*, 101 (1), pp. 273-281.

Schirmer, L., Mobius, W., Zhao, C., Cruz-Herranz, A., Ben Haim, L., Cordano, C., Shiow, L. R., Kelley, K. W., Sadowski, B., Timmons, G., Probstel, A. K., Wright, J. N., Sin, J. H., Devereux, M., Morrison, D. E., Chang, S. M., Sabeur, K., Green, A. J., Nave, K. A., Franklin, R. J. & Rowitch, D. H. (2018) 'Oligodendrocyte-encoded Kir4.1 function is required for axonal integrity'. *Elife*, 7

Seewann, A., Vrenken, H., van der Valk, P., Blezer, E. L., Knol, D. L., Castelijns, J. A., Polman, C. H., Pouwels, P. J., Barkhof, F. & Geurts, J. J. (2009) 'Diffusely abnormal white matter in chronic multiple sclerosis: imaging and histopathologic analysis'. *Arch Neurol*, 66 (5), pp. 601-609.

Shannon, C., Salter, M. & Fern, R. (2007) 'GFP imaging of live astrocytes: regional differences in the effects of ischaemia upon astrocytes'. *J Anat*, 210 (6), pp. 684-692.

Shen, Y., Wu, S. Y., Rancic, V., Aggarwal, A., Qian, Y., Miyashita, S. I., Ballanyi, K., Campbell, R. E. & Dong, M. (2019) 'Genetically encoded fluorescent indicators for imaging intracellular potassium ion concentration'. *Commun Biol*, 2 (1), pp. 18.

Shenoda, B. (2015) 'The role of Na+/Ca2+ exchanger subtypes in neuronal ischemic injury'. *Transl Stroke Res*, 6 (3), pp. 181-190.

Shi, Z., Zhang, W., Lu, Y., Lu, Y., Xu, L., Fang, Q., Wu, M., Jia, M., Wang, Y., Dong, L., Yan, X., Yang, S. & Yuan, F. (2017) 'Aquaporin 4-Mediated Glutamate-Induced Astrocyte Swelling Is Partially Mediated through Metabotropic Glutamate Receptor 5 Activation'. *Front Cell Neurosci*, 11 pp. 116.

Shijie, J., Takeuchi, H., Yawata, I., Harada, Y., Sonobe, Y., Doi, Y., Liang, J., Hua, L., Yasuoka, S., Zhou, Y., Noda, M., Kawanokuchi, J., Mizuno, T. & Suzumura, A. (2009) 'Blockade of glutamate release from microglia attenuates experimental autoimmune encephalomyelitis in mice'. *Tohoku J Exp Med*, 217 (2), pp. 87-92.

Shrode, L. D. & Putnam, R. W. (1994) 'Intracellular pH regulation in primary rat astrocytes and C6 glioma cells'. *Glia*, 12 (3), pp. 196-210.

Sick, T. J., Feng, Z. C. & Rosenthal, M. (1998) 'Spatial stability of extracellular potassium ion and blood flow distribution in rat cerebral cortex after permanent middle cerebral artery occlusion'. *J Cereb Blood Flow Metab*, 18 (10), pp. 1114-1120.

Sierra, A., Abiega, O., Shahraz, A. & Neumann, H. (2013) 'Janus-faced microglia: beneficial and detrimental consequences of microglial phagocytosis'. *Front Cell Neurosci*, 7 pp. 6.

Simard, J. M., Kent, T. A., Chen, M., Tarasov, K. V. & Gerzanich, V. (2007) 'Brain oedema in focal ischaemia: molecular pathophysiology and theoretical implications'. *Lancet Neurol*, 6 (3), pp. 258-268.

Sisti, H. M., Geurts, M., Gooijers, J., Heitger, M. H., Caeyenberghs, K., Beets, I. A., Serbruyns, L., Leemans, A. & Swinnen, S. P. (2012) 'Microstructural organization of corpus callosum projections to prefrontal cortex predicts bimanual motor learning'. *Learn Mem*, 19 (8), pp. 351-357.

Slowik, A., Schmidt, T., Beyer, C., Amor, S., Clarner, T. & Kipp, M. (2015) 'The sphingosine 1-phosphate receptor agonist FTY720 is neuroprotective after cuprizone-induced CNS demyelination'. *Br J Pharmacol*, 172 (1), pp. 80-92.

Smith, K. J., Blakemore, W. F. & McDonald, W. I. (1979) 'Central remyelination restores secure conduction'. *Nature*, 280 (5721), pp. 395-396.

Smith, M. L. & Siesjö, B. K. (1988) 'Acidosis-Related Brain Damage: Immediate and Delayed Events.', *Mechanisms of Cerebral Hypoxia and Stroke. Advances in Behavioral Biology.* Springer, pp. 57-71.

Smith, T., Groom, A., Zhu, B. & Turski, L. (2000) 'Autoimmune encephalomyelitis ameliorated by AMPA antagonists'. *Nat Med*, 6 (1), pp. 62-66.

Solessio, E., Linn, D. M., Perlman, I. & Lasater, E. M. (2000) 'Characterization with barium of potassium currents in turtle retinal Muller cells'. *J Neurophysiol*, 83 (1), pp. 418-430.

Somjen, G. G. (1979) 'Extracellular potassium in the mammalian central nervous system'. *Annu Rev Physiol*, 41 pp. 159-177.

Song, X., Jensen, M. O., Jogini, V., Stein, R. A., Lee, C. H., McHaourab, H. S., Shaw, D. E. & Gouaux, E. (2018) 'Mechanism of NMDA receptor channel block by MK-801 and memantine'. *Nature*, 556 (7702), pp. 515-519.

Sontheimer, H., Trotter, J., Schachner, M. & Kettenmann, H. (1989) 'Channel expression correlates with differentiation stage during the development of oligodendrocytes from their precursor cells in culture'. *Neuron*, 2 (2), pp. 1135-1145.

Spray, D. C., Harris, A. L. & Bennett, M. V. (1981) 'Gap junctional conductance is a simple and sensitive function of intracellular pH'. *Science*, 211 (4483), pp. 712-715.

Srinivasan, R., Sailasuta, N., Hurd, R., Nelson, S. & Pelletier, D. (2005) 'Evidence of elevated glutamate in multiple sclerosis using magnetic resonance spectroscopy at 3 T'. *Brain*, 128 (Pt 5), pp. 1016-1025.

Stiefel, K. M., Torben-Nielsen, B. & Coggan, J. S. (2013) 'Proposed evolutionary changes in the role of myelin'. *Front Neurosci*, 7 pp. 202.

Stiefel, M. F. & Marmarou, A. (2002) 'Cation dysfunction associated with cerebral ischemia followed by reperfusion: a comparison of microdialysis and ion-selective electrode methods'. *J Neurosurg*, 97 (1), pp. 97-103.

Stokum, J. A., Gerzanich, V. & Simard, J. M. (2016) 'Molecular pathophysiology of cerebral edema'. *J Cereb Blood Flow Metab*, 36 (3), pp. 513-538.

Sturrock, R. R. (1980) 'Myelination of the mouse corpus callosum'. *Neuropathol Appl Neurobiol*, 6 (6), pp. 415-420.

Stys, P. K. (2005) 'General mechanisms of axonal damage and its prevention'. *J Neurol Sci*, 233 (1-2), pp. 3-13.

Stys, P. K. (2011) 'The axo-myelinic synapse'. *Trends Neurosci*, 34 (8), pp. 393-400.

Stys, P. K. & Jiang, Q. (2002) 'Calpain-dependent neurofilament breakdown in anoxic and ischemic rat central axons'. *Neurosci Lett*, 328 (2), pp. 150-154.

Stys, P. K., Waxman, S. G. & Ransom, B. R. (1992) 'Ionic mechanisms of anoxic injury in mammalian CNS white matter: role of Na+ channels and Na(+)-Ca2+ exchanger'. *J Neurosci*, 12 (2), pp. 430-439.

Stys, P. K., You, H. & Zamponi, G. W. (2012) 'Copper-dependent regulation of NMDA receptors by cellular prion protein: implications for neurodegenerative disorders'. *J Physiol*, 590 (6), pp. 1357-1368.

Stys, P. K., Zamponi, G. W., van Minnen, J. & Geurts, J. J. (2012) 'Will the real multiple sclerosis please stand up?'. *Nat Rev Neurosci*, 13 (7), pp. 507-514.

Suda, S. & Kimura, K. (2019) 'Therapeutic potential of AMPA receptor antagonist perampanel against cerebral ischemia: beyond epileptic disorder'. *Neural Regen Res*, 14 (9), pp. 1525-1526.

Suhs, K. W., Fairless, R., Williams, S. K., Heine, K., Cavalie, A. & Diem, R. (2014) 'N-methyl-D-aspartate receptor blockade is neuroprotective in experimental autoimmune optic neuritis'. *J Neuropathol Exp Neurol*, 73 (6), pp. 507-518.

Sun, D., Lye-Barthel, M., Masland, R. H. & Jakobs, T. C. (2009) 'The morphology and spatial arrangement of astrocytes in the optic nerve head of the mouse'. *J Comp Neurol*, 516 (1), pp. 1-19.

Sun, H. S. & Feng, Z. P. (2013) 'Neuroprotective role of ATP-sensitive potassium channels in cerebral ischemia'. *Acta Pharmacol Sin*, 34 (1), pp. 24-32.

Sun, H. S., Feng, Z. P., Miki, T., Seino, S. & French, R. J. (2006) 'Enhanced neuronal damage after ischemic insults in mice lacking Kir6.2-containing ATP-sensitive K+ channels'. *J Neurophysiol*, 95 (4), pp. 2590-2601.

Swadlow, H. A., Waxman, S. G. & Geschwind, N. (1980) 'Small-diameter nonmyelinated axons in the primate corpus callosum'. *Arch Neurol*, 37 (2), pp. 114-115.

Szeto, V., Chen, N. H., Sun, H. S. & Feng, Z. P. (2018) 'The role of KATP channels in cerebral ischemic stroke and diabetes'. *Acta Pharmacol Sin*, 39 (5), pp. 683-694.

Takadera, T., Shimada, Y. & Mohri, T. (1992) 'Extracellular pH modulates N-methyl-D-aspartate receptor-mediated neurotoxicity and calcium accumulation in rat cortical cultures'. *Brain Res*, 572 (1-2), pp. 126-131.

Takahashi, S., Shibata, M., Gotoh, J. & Fukuuchi, Y. (2000) 'Astroglial cell death induced by excessive influx of sodium ions'. *Eur J Pharmacol*, 408 (2), pp. 127-135.

Tamagnini, F., Scullion, S., Brown, J. T. & Randall, A. D. (2014) 'Low concentrations of the solvent dimethyl sulphoxide alter intrinsic excitability properties of cortical and hippocampal pyramidal cells'. *PLoS One*, 9 (3), pp. e92557.

Tang, C. M., Dichter, M. & Morad, M. (1990) 'Modulation of the N-methyl-D-aspartate channel by extracellular H+'. *Proc Natl Acad Sci U S A*, 87 (16), pp. 6445-6449.

Taraboletti, A., Walker, T., Avila, R., Huang, H., Caporoso, J., Manandhar, E., Leeper, T. C., Modarelli, D. A., Medicetty, S. & Shriver, L. P. (2017) 'Cuprizone Intoxication Induces Cell Intrinsic Alterations in Oligodendrocyte Metabolism Independent of Copper Chelation'. *Biochemistry*, 56 (10), pp. 1518-1528.

Tasca, C. I., Dal-Cim, T. & Cimarosti, H. (2015) 'In vitro oxygen-glucose deprivation to study ischemic cell death'. *Methods Mol Biol*, 1254 pp. 197-210.

Tekkok, S. B. & Goldberg, M. P. (2001) 'Ampa/kainate receptor activation mediates hypoxic oligodendrocyte death and axonal injury in cerebral white matter'. *J Neurosci*, 21 (12), pp. 4237-4248.

Thorburne, S. K. & Juurlink, B. H. (1996) 'Low glutathione and high iron govern the susceptibility of oligodendroglial precursors to oxidative stress'. *J Neurochem*, 67 (3), pp. 1014-1022.

Ting, J. T., Daigle, T. L., Chen, Q. & Feng, G. (2014) 'Acute brain slice methods for adult and aging animals: application of targeted patch clamp analysis and optogenetics'. *Methods Mol Biol*, 1183 pp. 221-242.

Tomasch, J. (1954) 'Size, distribution, and number of fibres in the human corpus callosum'. *Anat Rec*, 119 (1), pp. 119-135.

Torkildsen, O., Brunborg, L. A., Myhr, K. M. & Bo, L. (2008) 'The cuprizone model for demyelination'. *Acta Neurol Scand Suppl*, 188 pp. 72-76.

Trapp, B. D. & Kidd, G. J. (2004) 'Structure of the myelinated axon', *Myelin biology and disorders.* Academic Press, pp. 3-27.

Trapp, S., Luckermann, M., Kaila, K. & Ballanyi, K. (1996) 'Acidosis of hippocampal neurones mediated by a plasmalemmal Ca2+/H+ pump'. *Neuroreport*, 7 (12), pp. 2000-2004.

Traynelis, S. F., Wollmuth, L. P., McBain, C. J., Menniti, F. S., Vance, K. M., Ogden, K. K., Hansen, K. B., Yuan, H., Myers, S. J. & Dingledine, R. (2010) 'Glutamate receptor ion channels: structure, regulation, and function'. *Pharmacol Rev*, 62 (3), pp. 405-496.

Trivedi, B. & Danforth, W. H. (1966) 'Effect of pH on the kinetics of frog muscle phosphofructokinase'. *J Biol Chem*, 241 (17), pp. 4110-4112.

Turski, L., Huth, A., Sheardown, M., McDonald, F., Neuhaus, R., Schneider, H. H., Dirnagl, U., Wiegand, F., Jacobsen, P. & Ottow, E. (1998) 'ZK200775: a phosphonate quinoxalinedione AMPA antagonist for neuroprotection in stroke and trauma'. *Proc Natl Acad Sci U S A*, 95 (18), pp. 10960-10965.

Vassilev, P. M., Scheuer, T. & Catterall, W. A. (1988) 'Identification of an intracellular peptide segment involved in sodium channel inactivation'. *Science*, 241 (4873), pp. 1658-1661.

Vaughn, J. E. & Peters, A. (1967) 'Electron microscopy of the early postnatal development of fibrous astrocytes'. *Am J Anat*, 121 (1), pp. 131-152.

Vega-Riquer, J. M., Mendez-Victoriano, G., Morales-Luckie, R. A. & Gonzalez-Perez, O. (2019) 'Five Decades of Cuprizone, an Updated Model to Replicate Demyelinating Diseases'. *Curr Neuropharmacol*, 17 (2), pp. 129-141.

Verkhratsky, A. & Butt, A. (2013) 'Astroglia', *Glial Physiology and Pathophysiology.* pp. 105-244.

Villoslada, P., Arrondo, G., Sepulcre, J., Alegre, M. & Artieda, J. (2009) 'Memantine induces reversible neurologic impairment in patients with MS'. *Neurology*, 72 (19), pp. 1630-1633.

Vincent, A. M., Kato, K., McLean, L. L., Soules, M. E. & Feldman, E. L. (2009) 'Sensory neurons and schwann cells respond to oxidative stress by increasing antioxidant defense mechanisms'. *Antioxid Redox Signal*, 11 (3), pp. 425-438.

Voipio, J. & Kaila, K. (1993) 'Interstitial PCO2 and pH in rat hippocampal slices measured by means of a novel fast CO2/H(+)-sensitive microelectrode based on a PVC-gelled membrane'. *Pflugers Arch*, 423 (3-4), pp. 193-201.

Voipio, J., Pasternack, M. & MacLeod, K. (1994) 'Ion-sensitive microelectrodes', *Microelectrode techniques. The Plymouth Workshop Handbook.* The Company of Biologists Ltd, pp. 275-316.

Wahul, A. B., Joshi, P. C., Kumar, A. & Chakravarty, S. (2018) 'Transient global cerebral ischemia differentially affects cortex, striatum and hippocampus in Bilateral Common Carotid Arterial occlusion (BCCAo) mouse model'. *J Chem Neuroanat*, 92 pp. 1-15.

Walz, R., Amaral, O. B., Rockenbach, I. C., Roesler, R., Izquierdo, I., Cavalheiro, E. A., Martins, V. R. & Brentani, R. R. (1999) 'Increased sensitivity to seizures in mice lacking cellular prion protein'. *Epilepsia*, 40 (12), pp. 1679-1682.

Walz, W. (2012) 'The Impact of Extracellular Potassium Accumulation in Stroke', *Metal Ion in Stroke.* pp. 363-372.

Wang, C., Shimizu-Okabe, C., Watanabe, K., Okabe, A., Matsuzaki, H., Ogawa, T., Mori, N., Fukuda, A. & Sato, K. (2002) 'Developmental changes in KCC1, KCC2, and NKCC1 mRNA expressions in the rat brain'. *Brain Res Dev Brain Res*, 139 (1), pp. 59-66.

Wang, G. J., Randall, R. D. & Thayer, S. A. (1994) 'Glutamate-induced intracellular acidification of cultured hippocampal neurons demonstrates altered energy metabolism resulting from Ca2+ loads'. *J Neurophysiol*, 72 (6), pp. 2563-2569.

Wang, L., Chiamvimonvat, N. & Duff, H. J. (1993) 'Interaction between selected sodium and potassium channel blockers in guinea pig papillary muscle'. *J Pharmacol Exp Ther*, 264 (3), pp. 1056-1062.

Wang, M., Song, J., Xiao, W., Yang, L., Yuan, J., Wang, W., Yu, Z. & Xie, M. (2012) 'Changes in lipid-sensitive two-pore domain potassium channel TREK-1 expression and its involvement in astrogliosis following cerebral ischemia in rats'. *J Mol Neurosci*, 46 (2), pp. 384-392.

Wang, Y., Liu, G., Hong, D., Chen, F., Ji, X. & Cao, G. (2016) 'White matter injury in ischemic stroke'. *Prog Neurobiol*, 141 pp. 45-60.

Watanabe, M. & Fukuda, A. (2015) 'Development and regulation of chloride homeostasis in the central nervous system'. *Front Cell Neurosci*, 9 pp. 371.

Waxman, S. G., Craner, M. J. & Black, J. A. (2004) 'Na+ channel expression along axons in multiple sclerosis and its models'. *Trends Pharmacol Sci*, 25 (11), pp. 584-591.

Wei, J., Huang, N. C. & Quast, M. J. (1997) 'Hydroxyl radical formation in hyperglycemic rats during middle cerebral artery occlusion/reperfusion'. *Free Radic Biol Med*, 23 (7), pp. 986-995.

Wei, L., Yu, S. P., Gottron, F., Snider, B. J., Zipfel, G. J. & Choi, D. W. (2003) 'Potassium channel blockers attenuate hypoxia- and ischemia-induced neuronal death in vitro and in vivo'. *Stroke*, 34 (5), pp. 1281-1286.

Weiser, T. (2005) 'AMPA receptor antagonists for the treatment of stroke'. *Curr Drug Targets CNS Neurol Disord*, 4 (2), pp. 153-159.

Weiser, T. & Wienrich, M. (1996) 'The effects of copper ions on glutamate receptors in cultured rat cortical neurons'. *Brain Res*, 742 (1-2), pp. 211-218.

Wen, Q. & Chklovskii, D. B. (2005) 'Segregation of the brain into gray and white matter: a design minimizing conduction delays'. *PLoS Comput Biol*, 1 (7), pp. e78.

Werner, P., Pitt, D. & Raine, C. S. (2001) 'Multiple sclerosis: altered glutamate homeostasis in lesions correlates with oligodendrocyte and axonal damage'. *Ann Neurol*, 50 (2), pp. 169-180.

Werth, J. L. & Thayer, S. A. (1994) 'Mitochondria buffer physiological calcium loads in cultured rat dorsal root ganglion neurons'. *J Neurosci*, 14 (1), pp. 348-356.

Witalison, E. E., Thompson, P. R. & Hofseth, L. J. (2015) 'Protein Arginine Deiminases and Associated Citrullination: Physiological Functions and Diseases Associated with Dysregulation'. *Curr Drug Targets*, 16 (7), pp. 700-710.

Wolman, M. (1968) 'Histochemistry of demyelination and myelination'. *J Histochem Cytochem*, 16 (12), pp. 803-807.

Wong, E. H., Kemp, J. A., Priestley, T., Knight, A. R., Woodruff, G. N. & Iversen, L. L. (1986) 'The anticonvulsant MK-801 is a potent N-methyl-D-aspartate antagonist'. *Proc Natl Acad Sci U S A*, 83 (18), pp. 7104-7108.

Wood, D. D., Bilbao, J. M., O'Connors, P. & Moscarello, M. A. (1996) 'Acute multiple sclerosis (Marburg type) is associated with developmentally immature myelin basic protein'. *Ann Neurol*, 40 (1), pp. 18-24.

Wood, D. D. & Moscarello, M. A. (1989) 'The isolation, characterization, and lipid-aggregating properties of a citrulline containing myelin basic protein'. *J Biol Chem*, 264 (9), pp. 5121-5127.

Woodruff, G. N., Foster, A. C., Gill, R., Kemp, J. A., Wong, E. H. & Iversen, L. L. (1987) 'The interaction between MK-801 and receptors for N-methyl-D-aspartate: functional consequences'. *Neuropharmacology*, 26 (7B), pp. 903-909.

Wright, S. H. (2004) 'Generation of resting membrane potential'. *Adv Physiol Educ*, 28 (1-4), pp. 139-142.

Wu, Z., Xu, H., He, Y., Yang, G., Liao, C., Gao, W., Liang, M. & He, X. (2013) 'Antisense oligodeoxynucleotides targeting connexin43 reduce cerebral astrocytosis and edema in a rat model of traumatic brain injury'. *Neurol Res*, 35 (3), pp. 255-262.

Yang, G. Y., Chen, S. F., Kinouchi, H., Chan, P. H. & Weinstein, P. R. (1992) 'Edema, cation content, and ATPase activity after middle cerebral artery occlusion in rats'. *Stroke*, 23 (9), pp. 1331-1336.

Yin, X., Kidd, G. J., Ohno, N., Perkins, G. A., Ellisman, M. H., Bastian, C., Brunet, S., Baltan, S. & Trapp, B. D. (2016) 'Proteolipid protein-deficient myelin promotes axonal mitochondrial dysfunction via altered metabolic coupling'. *J Cell Biol*, 215 (4), pp. 531-542.

You, H., Tsutsui, S., Hameed, S., Kannanayakal, T. J., Chen, L., Xia, P., Engbers, J. D., Lipton, S. A., Stys, P. K. & Zamponi, G. W. (2012) 'Abeta neurotoxicity depends on interactions between copper ions, prion protein, and N-methyl-D-aspartate receptors'. *Proc Natl Acad Sci U S A*, 109 (5), pp. 1737-1742.

Young, K. M., Psachoulia, K., Tripathi, R. B., Dunn, S. J., Cossell, L., Attwell, D., Tohyama, K. & Richardson, W. D. (2013) 'Oligodendrocyte dynamics in the healthy adult CNS: evidence for myelin remodeling'. *Neuron*, 77 (5), pp. 873-885.

Zambonin, J. L., Zhao, C., Ohno, N., Campbell, G. R., Engeham, S., Ziabreva, I., Schwarz, N., Lee, S. E., Frischer, J. M., Turnbull, D. M., Trapp, B. D., Lassmann, H., Franklin, R. J. & Mahad, D. J. (2011) 'Increased mitochondrial content in remyelinated axons: implications for multiple sclerosis'. *Brain*, 134 (Pt 7), pp. 1901-1913.

Zendedel, A., Beyer, C. & Kipp, M. (2013) 'Cuprizone-induced demyelination as a tool to study remyelination and axonal protection'. *J Mol Neurosci*, 51 (2), pp. 567-572.

Zhao, Q., Chen, A., Wang, X., Zhang, Z., Zhao, Y., Huang, Y., Ren, S. & Zhu, Y. (2018) 'Protective effects of dehydrocostuslactone on rat hippocampal slice injury induced by oxygenglucose deprivation/reoxygenation'. *Int J Mol Med*, 42 (2), pp. 1190-1198.

Zhou, J., Wen, Y., She, L., Sui, Y. N., Liu, L., Richards, L. J. & Poo, M. M. (2013) 'Axon position within the corpus callosum determines contralateral cortical projection'. *Proc Natl Acad Sci U S A*, 110 (29), pp. E2714-2723.

Zhu, X., Bergles, D. E. & Nishiyama, A. (2008) 'NG2 cells generate both oligodendrocytes and gray matter astrocytes'. *Development*, 135 (1), pp. 145-157.